The bovine teat canal: Its role in pathogen recognition and defence of the mammary gland

A thesis submitted in fulfilment

of the requirements for the degree

of

Doctor of Philosophy in Biological Sciences

at

The University of Waikato

by

Grant Alan Smolenski

THE UNIVERSITY OF
WAIKATO
Te Whare Wānanga o Waikato

agresearch

The University of Waikato

2018

For Shelley

Matthew and Jackson

&

For my Mum and Dad

Abstract

The bovine mammary gland is remarkable in that it produces over three litres of milk daily as an exocrine secretion, which passes through the teat into the external environment. Despite this substantial volume of fluid flow and that milk is one of the most nutritional mediums in which microorganisms can thrive, for the most part, this process occurs without colonisation of pathogens in the interior of the gland. Nevertheless, mastitis, when it does occur, is a significant dairy management problem. The major factor restricting ingress of pathogens into the gland has been assumed by most researchers in the field to be the length and diameter of the teat canal and the tightness of the teat sphincter. However, it has become increasingly clear in recent years that epithelial tissues have considerable innate immune functionality that contributes significantly to host defence. The presence of innate immune components within the teat end tissues has been only very superficially described to date. The presence of antimicrobial activity in the protein fraction of the teat canal lining has been previously demonstrated, as well as the presence of immune cells within some teat-end tissues, however, a detailed investigation into the identity of these proteins and cell types has not been undertaken.

The aims of this thesis are to firstly, characterise the protein component of the teat canal lining (Chapter 3) and secondly, identify key immune-related cells in healthy lactating dairy cows (Chapter 4). A third aim is to assess changes in the cell population and immune-related factors that occur within teat-end tissues during mammary involution (Chapter 5). The fourth and final aim is to begin to characterise the immediate localised inflammatory response within teat-end tissues to the presence of mastitis-causing pathogens (Chapter 6), a question that has never been previously addressed. The approach used to address these aims were to (i) apply proteomics methodologies to the characterisation of the proteins within the teat canal lining, and (ii) examination of teat-end tissues by fluorescence immunohistochemistry using antibodies directed against known immune cell markers.

The results revealed that aside from the major keratin proteins, the teat canal lining contained several other proteins and protein families (e.g. the S100 and serpin families) that differed from that of the cornified layer of the surrounding teat skin (Chapter 3). Immunofluorescent analysis revealed that there were substantial differences in the density and distribution of immune cells between the teat-end tissues. The Fürstenberg's rosette is especially rich in antigen-presenting cells (Chapter 4). Drying-off of the udder (mammary involution) was associated with an increase in some immune cell types in the teat sinus, and an increased abundance of some antimicrobial proteins in the teat canal lining, but relatively few and minor additional changes (Chapter 5). The introduction of pathogens into the teat canal resulted in similar changes in the abundance of teat canal lining proteins, but no obvious changes in localised immune cell abundance or distribution after 24 hours exposure (Chapter 6).

The presence of specific antimicrobial proteins in the teat canal lining, and the presence of immune cells within the Fürstenberg's rosette and teat sinus epithelia demonstrate that these tissues play an active role in host defence. Thus, the research presented in this thesis has laid the foundation for a more complete understanding of host-defence functionality in the teat. This has implications for devising novel approaches to reducing susceptibility to mastitis in dairy cows.

Keywords:

Teat Canal; Fürstenberg's rosette; Innate Immunity; Host defence; Mastitis; Proteomics; Mass Spectrometry; Immunohistochemistry.

Acknowledgements

First and foremost, a huge thank you to my two main supervisors, Dr Tom Wheeler and Dr Ray Cursons for their support, guidance, and patience, throughout the course of this PhD. Their doors were always open, and they were always ready to discuss ideas, research findings and provide encouragement.

I would like to thank Dr Steve Bird, Dr Jane Lacy-Hulbert, Professor Vic Arcus and Dr Brad Hine, for being part of my thesis committee. Their insight and suggestions have been extremely helpful, and I appreciate their contributions to this work. I would also like to express gratitude for the financial support provided to me by a University of Waikato Doctoral Scholarship, AgResearch PhD Studentship and a Humphrey M Russell Award.

I have been fortunate to have worked with many colleagues who were very helpful and accommodating throughout this research project. In particular, I would like to thank Marita for her support, advice, and various reality checks while drinking a decent bottle of wine. I would also like to thank Dr Stefan Clerens and his team at Lincoln for allowing me the use of the mass spectrometers during the holiday periods. I am indebted to Ali, Adrian and Mônica for sharing their experience in immunohistochemical techniques and for teaching me the art of fluorescent microscopy. Thank you Rita for your proof-reading and advice. Many others in the laboratory and office made Dairy Science an enjoyable workplace environment, and I would like to thank you all.

I am also grateful for the kind gift of the S100A7 polyclonal antibody from Professor Helga Sauerwein from the University of Bonn and samples of several monoclonal antibodies and immunohistochemical advice from Dr Constantin Constantinoiu from James Cook University.

Finally, to my sons, Matthew and Jackson, who after the many years of lab work and writing during the evenings and weekends, will now get their father back to play with. However, most of all a big thank you goes to Shelley for her understanding and incredible support and love. I could not have done this without you.

Publications and Presentations

The following papers were published and presented as a result of this work:

Peer reviewed publications:

Smolenski, G. A., Cursons, R. T., Hine, B. C., & Wheeler, T. T. (2015). Keratin and S100 calcium-binding proteins are major constituents of the bovine teat canal lining. *Veterinary Research*, *46*(1), 113.
DOI: 10.1186/s13567-015-0227-7

Oral presentations:

Proteomic analysis of the bovine teat canal under microbial challenge.
NZSBMB/NZMS Joint Conference Wellington, NZ 2014

Characterisation of innate immune cells in the teat canal of dairy cattle.
NZASI Joint Conference Palmerston North, NZ 2014

Additional publications by the author, which have been cited in the thesis:

Smolenski, G., Wieliczko, R., Pryor, S., Broadhurst, M., Wheeler, T., & Haigh, B. (2011). The abundance of milk cathelicidin proteins during bovine mastitis. *Veterinary Immunology and Immunopathology*, *143*(1), 125-130.
DOI: org/10.1016/j.vetimm.2011.06.034

Wheeler, T., Ledgard, A., Smolenski, G., Backmann, E., McDonald, R., & Lee, R.-F. (2012). Innate immune proteins as biomarkers for mastitis and endometritis. *Proceedings of the 5th Australasian Dairy Science Symposium*. pp294-297 http://www.adssymposium.com.au/inewsfiles/ADSS_Final_Proceedings.pdf.

Wheeler, T. T., G. A. Smolenski, D. P. Harris, S. K. Gupta, B. J. Haigh, M. K. Broadhurst, A. J. Molenaar, and Stelwagen, K. (2012) Host-defence-related proteins in cows' milk. *Animal*, *6*(no. 3), 415-422.

Smolenski, G. A., Broadhurst, M. K., Stelwagen, K., Haigh, B. J., & Wheeler, T. T. (2014). Host defence related responses in bovine milk during an experimentally induced *Streptococcus uberis* infection. *Proteome Science*, *12*(19), 1-14.
DOI: 10.1186/1477-5956-12-19

Boggs, I., Hine, B., Smolenski, G., Hettinga, K., Zhang, L., & Wheeler, T. T. (2015). Changes in the repertoire of bovine milk proteins during mammary involution. *EuPA Open Proteomics*, *9*, 65-75.
DOI: org/10.1016/j.euprot.2015.09.001

Table of Contents

List of Figures:

List of Tables

List of Abbreviations

1D	one-dimensional
2D	two-dimensional
2-DE	two-dimensional electrophoresis
APC	antigen-presenting cell
BSA	bovine serum albumin
CB	cuboidal
CCB	colloidal Coomassie blue
CD	cluster of differentiation
cfu	colony forming units
CHAPS	3-[(3-cholamidopropyl)-dimethylammonio]-1-propane sulfonate
CID	collision induced dissociation
CM	columnar
CNS	coagulase-negative *Staphylococci*
CV	coefficient of variation
d	day
DAB	diaminobenzidine
DAPI	4',6-diamidino-2-phenylindole hydrochloride
DTT	dithiothreitol
E. coli	*Escherichia coli*
ECL	enhanced chemiluminescence
ELISA	enzyme-linked immunosorbent assay
FFPE	formaldehyde-fixed paraffin embedded
FR	Fürstenberg's rosette
g	gram
γδ	gamma-delta

GeLC	sodium dodecyl sulfate-polyacrylamide gel electrophoresis followed by liquid chromatography-tandem mass spectrometry
h	hour
H&E	Gill's haematoxylin and eosin
HIER	heat-induced epitope retrieval
HPLC	high-performance liquid chromatography
HRP	horseradish peroxidase
IEF	isoelectric focussing
IFN	interferon
IHC	immunohistochemical
IF	immunofluorescence
IL	interleukin
IPG	immobilised pH gradient
K	keratin
kDa	kilodalton
KLH	keyhole limpet hemocyanin
kVh	kilo volt hours
LC-ESI-Q/TOF	liquid chromatography electrospray ionisation quadrupole time-of-flight
µ	micro ($x10^{-6}$)
m	milli ($x10^{-3}$)
mA	milliamps
MALT	mucosa-associated lymphoid tissues
MBS	maleimidobenzoyl-N-hydroxysulfosuccinimide
MHC	major histocompatibility complex
min	minute
MQ-H_2O	Milli-Q 'ultrapure' type-1 water
MS	mass spectrometry

MS/MS	tandem mass spectrometry
MW	molecular weight
NCBI	National Center for Biotechnology Information
NG	no growth
NSAF	normalised spectral abundance factor
PBS	phosphate buffered saline
REML	restricted maximum likelihood
RT	room temperature
S. aureus	*Staphylococcus aureus*
S. uberis	*Streptococcus uberis*
SCC	somatic cell counts
SD	standard deviation
SDS	sodium dodecyl sulfate
SDS-PAGE	SDS-Polyacrylamide gel electrophoresis
SEM	standard error of the mean
ST	stromal tissue
TBS	tris buffered saline
TBST	tris buffered saline + tween-20
TCL	teat canal lining
TCR	T cell receptor
TLR	toll-like receptor
TNF-α	tumour necrosis factor alpha
Tris	2-Amino-2-hydroxymethyl-propane-1,3-diol
V	voltage
v/v	volume per volume
w/v	weight per volume

1. Host-defence properties of the bovine teat canal

1.1. Introduction

The environment surrounding the teat of a cow contains a diverse array of microorganisms, yet the incidence of intramammary infections remains relatively low. In order to reach the interior of the mammary gland, bacteria must first negotiate passage through the teat canal. As a result, the teat canal serves as the first line of defence protecting the mammary gland against new infections manifesting as mastitis.

The anatomical and physical barriers provided by the teat canal have been previously investigated and described (Forbes, 1968; Seykora & McDaniel, 1985; Van der Merwe, 1985; Capuco *et al.*, 1992; Lacy-Hulbert & Hillerton, 1995; Paulrud, 2005). However, to date, inadequate attention has been ascribed to the biochemical and cellular defence mechanisms provided by the teat canal and associated teat-end tissues. A robust defence system is expected in the teat canal as comparable tissues such as the external skin layer and other mucosal tissues are protected by robust defence mechanisms consisting of antimicrobial barriers and an array of epithelial-associated immune cells.

It is very likely that similar cutaneous defence mechanisms exist in the teat canal and associated teat-end tissues and that these systems play a critical role in protecting the mammary gland from infection as are the physical barriers. For that reason, the aim of this thesis is two-fold. The first aim is to identify the protein component of the teat canal lining and identify innate immune cells residing in the teat canal and teat-end tissues. The second aim of this research aims to see how these protein and cellular components respond to physiological and environmental challenges such as involution and infection, respectively.

To introduce the current state of knowledge pertaining to host-defence by the teat canal, this chapter will provide a brief overview of the anatomical features of the teat canal and associated teat-end tissues along with the known physical barriers preventing bacterial penetration into the mammary gland. This will be followed by a summary of epithelial immunity and the role of the mucosal immune system. The

chapter will conclude with an analysis of the current literature, reviewing the induction of innate immune genes in the region of the teat canal, followed by the hypothesis and aims of my PhD research program.

1.2. Anatomical and histological aspects of the bovine teat canal and teat-end tissues

The bovine teat (*papilla mammae*) is a long cylindrical appendage that hangs perpendicular to each gland at the base of the udder. The primary function of the teat is to allow the controlled exit of milk from the upper mammary gland to the suckling calf. The internal structure of the teat consists of a large sinus cavity and a short, but highly structured, channel located at the distal end of the teat; known as the teat canal (*ductus papillaris*). The junction between the two structures is known as the Fürstenberg's rosette and is where the stratified epithelium, surrounding the teat canal, transitions to the bilayered epithelium lining the teat sinus (Figure 1.1).

Because the terminology, as observed in the literature is not consistent, the following definitions are offered to clarify their use in this thesis:

- Teat canal lining – Formed from the *stratum corneum* of fully differentiated teat canal keratinocytes. It is often referred to as 'keratin'.
- Gland cistern – The main milk collection area of the udder.
- Teat sinus – The large cavity enclosed entirely within the teat appendage. It is sometimes referred to as the teat cistern.
- Fürstenberg's rosette – The folds of epithelium located between the teat sinus and the teat canal.
- Teat canal – The small duct leading from the teat sinus to the teat orifice. It has previously been called the streak canal, teat duct or papillary duct.

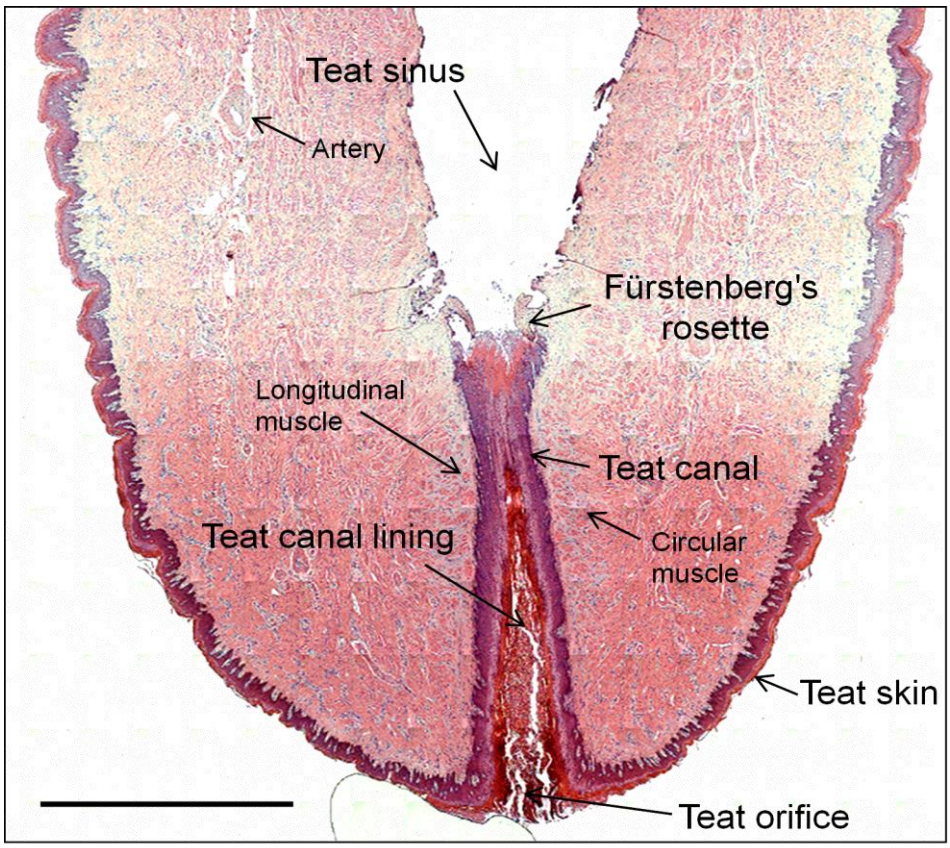

Figure 1.1: Composite light micrograph of a sagittal section of the bovine teat-end showing the internal structures in relation to the teat canal.
The stratified squamous epithelium of the teat canal abruptly transitions to the bilayered epithelium of the teat sinus at the Fürstenberg's rosette. The inner lining of the teat canal completely occludes the teat canal lumen. Haematoxylin and eosin (H&E) stain; composite of multiple photos (x100) taken individually and tiled together. Scale bar = 5 mm.

1.2.1. Morphological structure of the bovine teat canal

The teat canal is formed through invagination of the skin epithelium, which occurs after the development of the mammary bud, *in utero* (Paulrud, 2005). Intrinsically, it is a cylindrical-shaped cavity consisting of slightly spiralling longitudinal folds of stratified squamous epithelium that run the length of the teat canal (Giesecke *et al.*, 1972; Van der Merwe, 1985). These longitudinal folds allow the teat canal to stretch and expand when milk is released from the upper reservoirs of the gland cistern during milking (Figure 1.2).

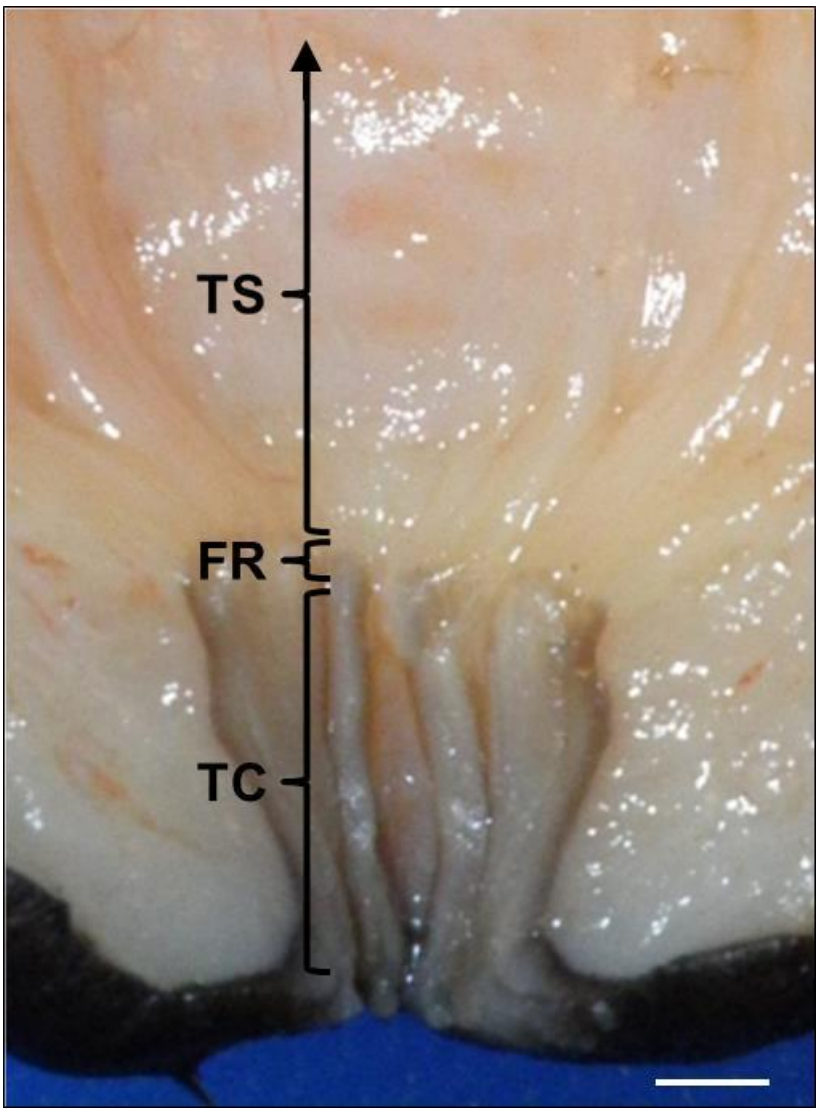

Figure 1.2: Sagittal photograph of the teat-end unilaterally dissected to reveal the internal structures of the teat canal.
Note the longitudinal folds observed in the teat canal. TC, teat canal; FR, Fürstenberg's rosette; and TS, teat sinus. Scale bar = 1 mm.

The teat canal extends from the teat orifice (distal end of the teat) through to the teat sinus, proximally terminating at the region known as Fürstenberg's rosette. In nature, the total length of the teat canal can vary from 3 to 18 mm in size depending on the cow's breed and its stage of lactation (Paulrud, 2005). In some animals, rear teat canals have been found to be slightly longer (3 %, $p < 0.01$) than teat canals located at the front of the udder (Paulrud & Rasmussen, 2004).

Teat canal epidermis:

The basic architecture of the teat canal epidermis has similarities to that of the teat skin and has been described previously in several publications (Fürstenberg, 1868; Mańkowski, 1903; Venzke, 1940; Adams *et al.*, 1961; Williams, 1984; Paulrud, 2005). Like the skin, the teat canal epithelium is composed of two distinct layers, the outer epidermis and the adjacent dermal layer. The epithelial layer of the teat canal is formed from a dense layer of stratified squamous epithelium which is thicker than the equivalent epithelial layer of teat skin. The organisation of the bovine teat canal and teat skin epithelial layers was originally described by Fürstenberg (1868) and Mańkowski (1903). Since then the architecture and cellular components of mammalian skin have been extensively characterised and have been the subject of many detailed reviews (Matoltsy, 1976; Williams, 1984; Urmacher, 1990; Kanitakis, 2002; Bos & Luiten, 2009; Goodwin, 2011; Menon *et al.*, 2012; Tay *et al.*, 2014). What they have found is that in addition to its function as a protective barrier to external insults, the skin can be considered an immune organ. As well as the keratinocytes of the epithelial layer, the epidermis contains a dynamic organisation of interacting immune cells that can sense pathogens and tissue damage in the cutaneous environment. The interplay between signalling mediators such as cytokines produced by these cells determines the extent of the immune response in maintaining skin immune homoeostasis. The activation of inflammatory defence mechanisms such as antimicrobial protein release and the influx of effector cells is constantly being used to meet the various challenges.

Keratinocytes are the major cell type found in stratified squamous epidermis. Both the skin and teat canal epithelia can be subdivided into six distinct layers (or *strata*), relating to stages of increasing maturation. This process is better known as keratinization (Watt, 1989). Beginning from the innermost basal layer of the epidermis out to the external epithelial surface, layers of teat canal epithelium were originally identified as the *stratum germinativum* (*stratum basale*), *stratum spinosum*, *stratum granulosum*, *stratum lucidum*, *stratum corneum* and *stratum mortificatum* (Mańkowski, 1903). These cell layers can be seen in the transverse section of the teat canal epithelium in Figure 1.3.

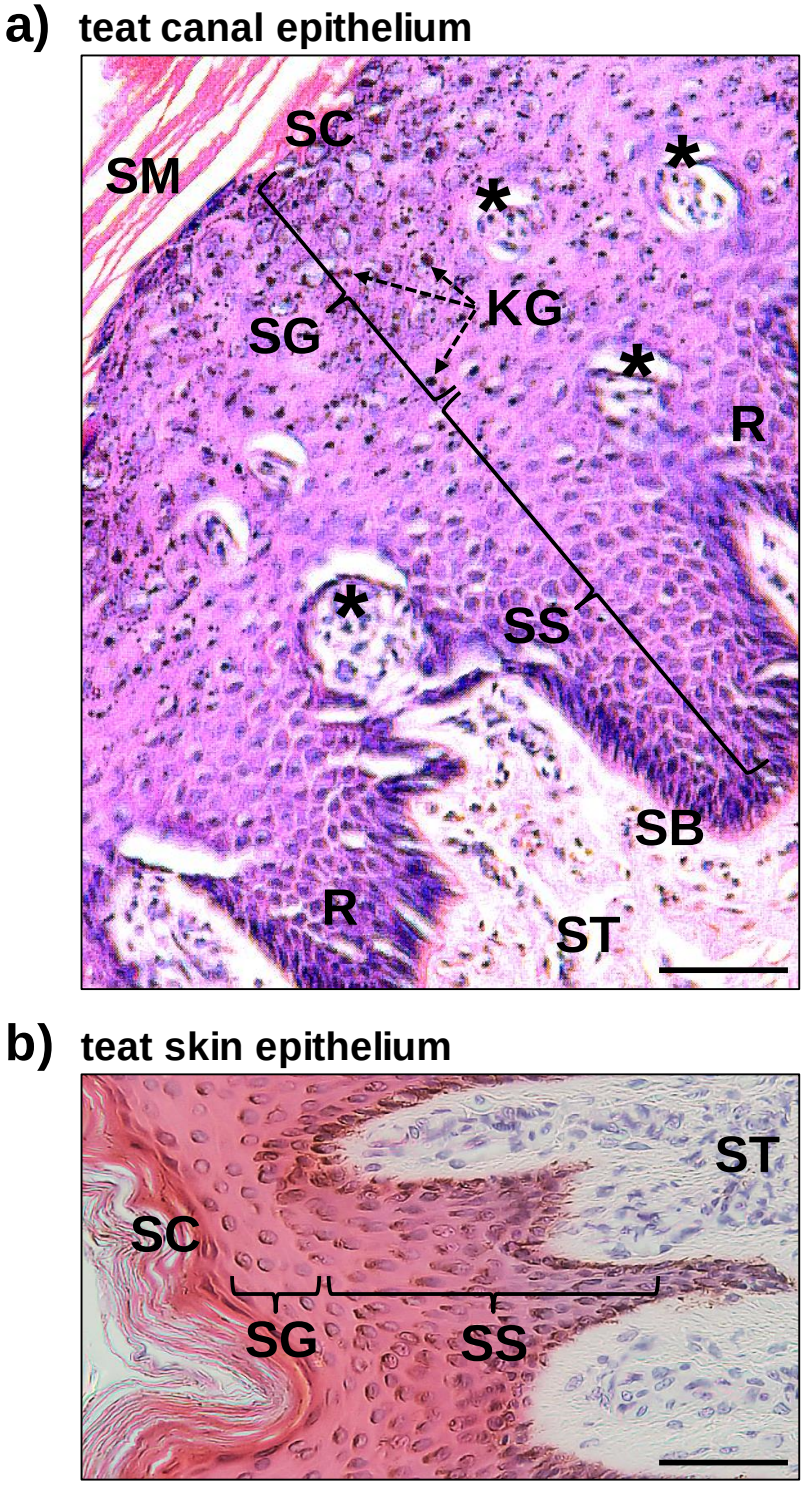

Figure 1.3: Low-power micrograph of transverse sections of the teat canal epithelium and teat skin epithelium.
(a) The different strata of the teat canal epithelia are labelled: SB, *stratum basale*; SS, *stratum spinosum*; SG, *stratum granulosum*; SC, *stratum corneum*; SM, *stratum mortificatum*. Structures of the epithelia such as keratohyalin granules (KG, dashed arrow), rete ridges (R), and Marksäulchen (asterisk) are also highlighted as well as the subepithelial connective tissue of the stroma (ST). (b) The width of the teat skin *stratum spinosum* and *stratum granulosum* is much less than in the teat canal. Section thickness 7 µm; stained with H&E. Magnification: 200x, Scale bar = 50 µm.

The basal layer cells of the *stratum germinativum* consist of a single layer of germinal cells that are short-columnar to cuboidal in shape. They form a continuous lining between the extracellular matrix of the dermal layer and the keratinocytes of the epidermal layer. Visually, they have an enlarged nucleus with prominent nucleoli and basophilic cytoplasm. Mitosis of these germinal cells generates daughter cells to replenish the basal cell population and to produce the spinal keratinocytes of the *stratum spinosum*. Melanocytes are observed to be present in both the basal and lower *spinosum* layers with dendrites containing melanin extending upwards between the keratinocytes (Obland, 1958).

Like the teat skin, the *stratum spinosum* of the teat canal epithelium is the thickest layer of the epidermis consisting of multiple layers of polyhedral shaped cells. These keratinocytes still have some meiotic activity as their nuclei contain prominent nucleoli and cytoplasmic basophilia. When observed under higher magnification these cells appear to be joined by short projections between adjacent keratinocytes making them look prickly; thus the name *spinosum* which means "little spine" (Menon & Elias, 2001). These projections are keratin filaments, called tonofibrils, converging into the desmosomes that result in enhanced linking between the neighbouring keratinocytes to form a strong net-like structure.

As the keratinocytes of the *stratum spinosum* migrate further into the epithelial layer, they develop into the cells of the *stratum granulosum*. In the teat canal, the *stratum granulosum* can be at least five times thicker than that observed in the teat skin (Figure 1.3) (Chandler *et al.*, 1969). Instead of four or five layers of flattened granulated cells, the *stratum granulosum* of the teat canal epithelium can be up to twenty cells thick. For the most part, these cells still retain their nuclei, but the cytoplasm is populated with dense, irregularly shaped basophilic granules, rich in histidine- and cysteine-rich proteins, known as keratohyalin granules (McAleer & Irvine, 2013). Keratohyalin granules also produce small lamellar bodies, which contain lipids and enzymes (Gonzalez *et al.*, 1976). These lamellar bodies fuse with the plasma membrane and are discharged into the intercellular space between the cells to act as a seal aiding in the waterproofing and protection of the epithelial layer. At the outermost aspect of the *stratum granulosum*, the keratinocytes undergo an abrupt terminal differentiation. This process is a result of organelle

membrane rupture and dissolution leading to cell death and the formation of the *stratum lucidum*, which are flattened cells devoid of nuclei, and the cornified layer known as the *stratum corneum* (Candi *et al.*, 2005).

The *stratum corneum* is the superficial layer of the epidermis. It is composed of multiple layers of flattened keratinocytes called corneocytes. These corneocytes are stacked irregularly on top of each other and are devoid of nuclei and cytoplasmic organelles. The cell husks are rich in high molecular weight keratin filaments and are encased in an extracellular lipid matrix. The *stratum mortificatum* is the site of desquamation where the dry, flat, scaly cells are shed from the superficial epithelial surface. In the teat canal epithelium, this cell layer is constantly being removed from the teat canal by wash-out during milk let-down.

Rete ridges:

The boundary between the epidermis and dermis of the teat canal has an undulating appearance with regular extensions projecting into the papillary dermis (Figure 1.3). These epithelial processes are known as "rete ridges" due to their interwoven nature amongst the papillary dermis (Hibbs & Clark, 1959). In the teat canal epithelium, the rete ridges appear wider and are more elongated than their skin counterparts. The function of rete ridges in the epidermis seems to be three-fold. Firstly, they increase the surface area of contact between the epithelium and the dermis allowing greater transfer of nutrients to the epithelial cells (Elgharably *et al.*, 2013). Secondly, they provide mechanical stability and resistance to shearing forces for the epithelial surface (van Zuijlen *et al.*, 2002), and thirdly they provide protective niches for the keratinocyte stem cells which are located at the base of the primary rete ridges (Xiong *et al.*, 2013). The primary rete ridges are the deepest epithelial extensions into the underlying connective tissue as opposed to the shorter extensions observed between the dermal papillae (Figure 1.3b).

Marksäulchen:

A distinct feature of the teat canal epithelium is the presence of circular vesicle-like structures emanating from the supra-papillary plate between the rete ridges throughout the teat canal epithelium (labelled with an asterisk in Figure 1.3). These structures were first observed by Fürstenberg in 1868 and were then later labelled as Marksäulchen by Mańkowski in 1903. Translated from German, Marksäulchen means 'spots of small columns'.

Although their function is not entirely understood, these structures have been suggested to provide the teat canal epithelium with increased elasticity (Mańkowski, 1903; Forbes, 1968). Small nucleated cells of unknown identity appear to reside within the Marksäulchen suggesting other unspecified functions for these structures.

Dermis:

The dermis or stromal tissue underlying the teat canal epidermis consists of supporting connective tissue containing an extracellular matrix of collagen bundles, elastic fibres, fibroblasts and various types of leukocytes (Kolarsick *et al.*, 2011). It can be subdivided into two distinct regions: an upper papillary dermis and a lower reticular dermis. Within each teat, an extensive network of vascular, lymphatic and nervous system cells run parallel to the long axis of the teat canal (Williams, 1984). Additionally, the dermal layer of the teat also contains a multi-spiralled, net-like, integrated musculo-elastic network of cells that facilitates the opening and closing of the teat canal (Van der Merwe, 1985) (Figure 1.4). Further information on mammalian dermal function can be obtained from the following reviews and publications (Daly, 1982; Urmacher, 1990; Bennett, 2011; Kolarsick *et al.*, 2011).

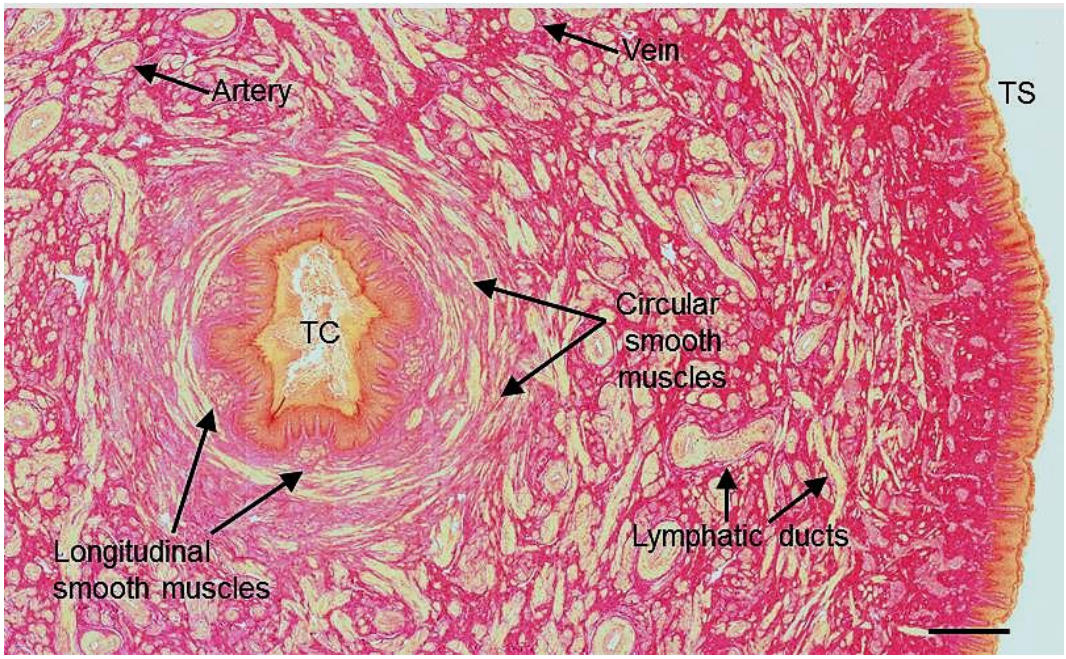

Figure 1.4: Composite light micrograph of a transverse section of the bovine teat showing the internal connective tissue structures in relation to the teat canal and teat skin.
Encircling the teat canal in the reticular layer of the dermis are bundles of longitudinal smooth muscle positioned either side of circularly oriented smooth muscle. Further, into the hypodermis, an extensive network of blood and lymphatic vessels can be observed. Weigert Van Gieson stain; composite of multiple photos (x100) taken individually and tiled together. TC, teat canal; TS, teat skin. Section thickness 7 µm. Scale bar = 1 mm

1.2.2. Teat sinus

The teat sinus is the large milk-holding cavity within the teat. The teat sinus is connected to the mammary gland cistern, separated by a dense ring of connective tissue called the annular (cricoid) fold (Turner, 1952). Towards the teat-end, the teat sinus narrows to form the region of epithelial tissue known as the Fürstenberg's rosette. This region covers the opening into the teat canal and is where the epithelia of the teat sinus connect and transition into the epithelia of the teat canal (Venzke, 1940).

Visual inspection of the teat sinus epithelium reveals numerous vertical and horizontal ridges running the length and breadth of the teat sinus converging at the Fürstenberg's rosette (Figure 1.2). Observations of the teat sinus epithelium and subepithelial connective tissue under the light microscope reveal a thin double layer of epithelial cells (Figure 1.5a). The epithelial cells are usually cuboidal or columnar in shape, and the majority of cells in the subepithelial connective tissue appear to be a mixture of fibroblasts (elongated nuclei) and leukocytes (circular nuclei clustered in the apex of each epithelial fold) (Nickerson & Pankey, 1983).

The lumen of the teat sinus has an undulating appearance that gives rise to several branches that run deep into the connective tissue. The epithelial cells making up these branches and the adjacent epithelium contain numerous small secondary folds that appear capable of a considerable degree of distension. Encircling the teat sinus, in the reticular layer of the dermis, are condensed bundles of longitudinally orientated smooth muscle positioned either side of circularly orientated bundles of smooth muscle (Figure 1.5b). The longitudinal muscle bundles provide structural support to the teat sinus cavity, whereas the circularly orientated smooth muscle (more commonly known as the sphincter muscle) is responsible for the opening and closing of the teat canal during milking (Venzke, 1940).

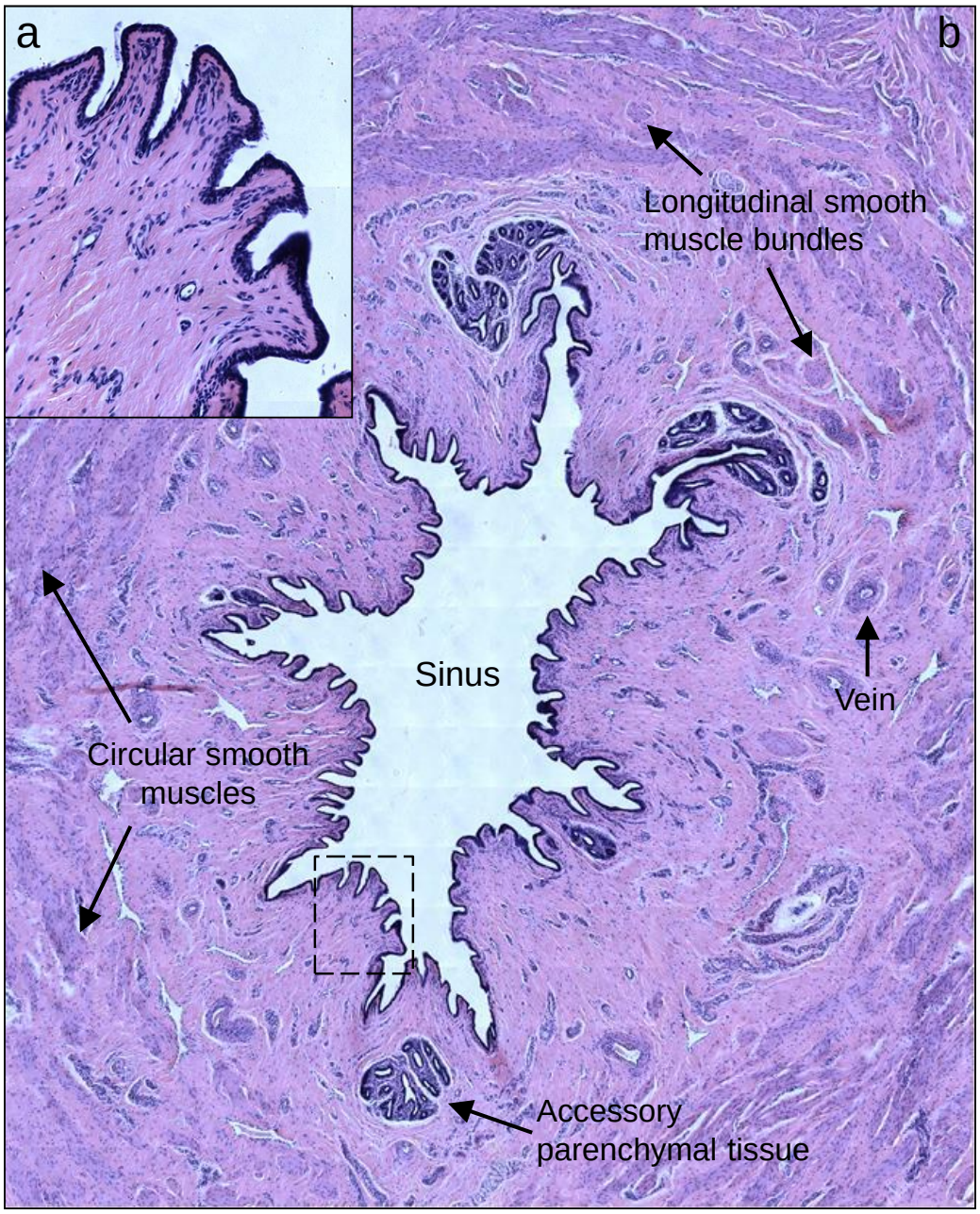

Figure 1.5: Composite light micrograph of a transverse section of the bovine teat sinus.
(a) Insert shows the undulated appearance of the thin epithelial bilayer of the teat sinus. Note the accumulation of leukocytes in the apex of each of the epithelial folds. (b) Multiple branches run deep into the connective tissue from the sinus lumen to allow for stretch and constriction during milking or suckling. The lumen is surrounded by circularly oriented smooth muscle and occasional longitudinal smooth muscle bundles. The position of insert (a) is indicated by a box with dashed lines. Toluidine Blue stain; composite of multiple photos (x100) taken individually and tiled together. Section thickness 7 µm.

1.2.3. Fürstenberg's rosette

The region of tissue known as the Fürstenberg's rosette begins at the proximal end of the teat canal (nearest to the teat sinus) where the stratified squamous epithelium transitions into the thinner double-layered columnar epithelium found in the teat sinus cavity (Figure 1.1). This structure was first described by Fürstenberg, where he noticed the appearance of longitudinal folds of mucosal epithelium that restricted the passage of milk through the teat canal (Fürstenberg, 1868). When a cross section of the teat sinus is examined under low magnification, the epithelial folds covering the closed teat canal resemble the petal arrangement or rosette of a flower; henceforth this tissue formation is known as the Fürstenberg's rosette.

The number of epithelial folds is variable between cows and have been referred to as mucosal folds in the literature (Vesterinen *et al.*, 2015). As shown in the cross-section of Fürstenberg's rosette in Figure 1.6, the mucosal folds can be separated into primary mucosal folds and branches of secondary mucosal folds. Cows with larger teat sinus cavities, and as a consequence wider rosettes are more likely to have more mucosal folds (Vesterinen *et al.*, 2015). One of the functions of the Fürstenberg's rosette is to act as a valve, retaining milk in the teat. As the teat canal closes, with a slight corkscrew motion due to muscle contraction (Van der Merwe, 1985), the mucosal epithelium twists together and overlaps. The downward pressure exerted from milk filling the teat sinus then causes the mucosal epithelium to smooth out covering and blocking the exit of the teat sinus (Reece, 2013).

Besides acting as a seal for the retention of milk, the Fürstenberg's rosette also appears to have a host-defence function. Firstly, it presents a physical barrier to the passage of bacteria into the mammary gland. Secondly, there is evidence that the folds of mucosal epithelium also play a role in the detection of bacteria and bacterial antigens. A number of published studies have reported significant numbers of leukocytes in the subepithelial connective tissue of the Fürstenberg's rosette. These cells accumulate in the finger-like projections of the mucosal epithelium and interact with the epithelial bilayer (Venzke, 1940; Adams *et al.*, 1961; Nickerson & Pankey, 1984; Wynn *et al.*, 2013; Okabe & Medzhitov, 2014).

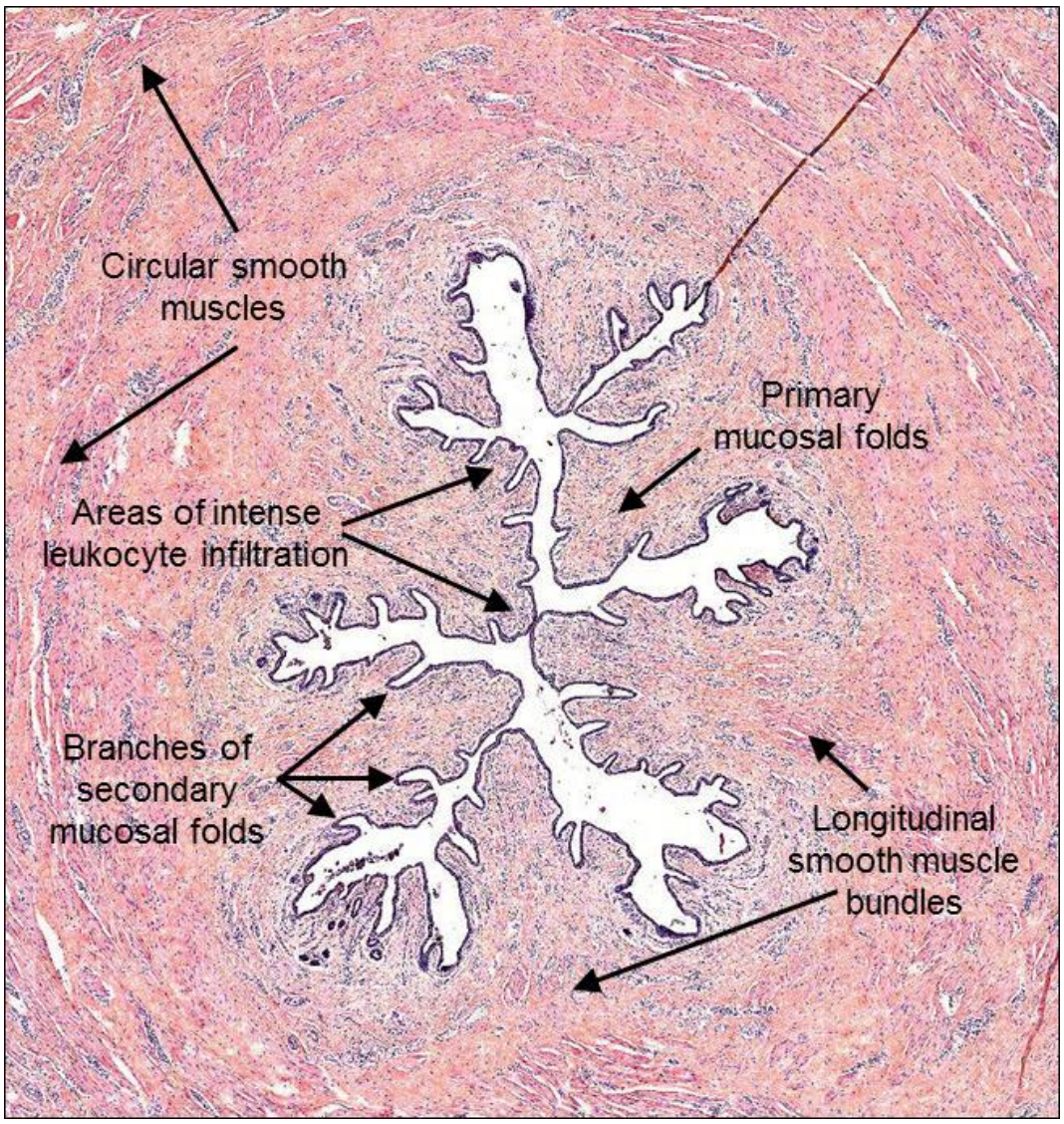

Figure 1.6: Composite light micrograph of a transverse section of the Fürstenberg's rosette. Multiple branches of primary and secondary epithelial folds stretch into the surrounding connective tissue. Each branch is bordered by considerable leukocyte infiltration stemming from numerous blood vessels in the reticular and papillary dermis. Encircling the lumen of the Fürstenberg's rosette are bundles of longitudinal smooth muscle and circularly oriented smooth muscle similar to the teat canal. H & E stain; composite of multiple photos (x100) taken individually and tiled together. Section thickness 7 µm.

These past studies have relied almost entirely on visual and histologic examination of the tissue and have highlighted the presence of lymphocytes, plasma cells and polymorphic leukocytes (PMNs) such as neutrophils. However, the full repertoire of innate immune cells in the Fürstenberg's rosette is yet to be evaluated.

1.2.4. Immune cell identification in the teat-end tissues

Light microscopy has been the primary tool used for immune cell identification in teat-end tissues in past studies. Limitations of this technique have restricted the ability of researchers to confidently identify the many different immune cell types that may be present in the teat-end tissues. One reason for this is that they share very similar morphological and biochemical features. Also, most immune cell types can exist as multiple phenotypes with each subset performing quite different immune functions (Mosmann & Sad, 1996; Liu, 2001; Mueller *et al.*, 2013). The differences between these cell phenotypes are usually elucidated by staining of their cell surface markers (Vignali *et al.*, 2008) therefore requiring more precise techniques and reagents for their identification.

Historically the characterisation of bovine immune cells has been hampered due to the lack of appropriate reagents to identify individual cell types. However, there are now a number of specific antibody reagents currently available that allow for a more precise identification and characterisation of several bovine immune cell populations.

1.3. Physical barrier functions of the teat canal

The anatomical and physiological barrier properties of the teat canal provide a significant physical barrier to microbial infiltration. This barrier is maintained by firstly, the ability to close the teat canal lumen tightly between milkings' and secondly, the ability to rapidly regenerate the teat canal lining which helps to seal the lumen of the teat canal and assists in the entrapment of foreign bodies such as bacteria. In addition, it is thought that the mechanical washing forces generated by peak milk flow are sufficient to remove most of the microbes that are bound to the outer layer of the teat canal lining (Capuco *et al.*, 1990).

1.3.1. Teat canal closure

Teat canal closure is an active process that is controlled by the spiralling integrated network of circular smooth muscle and elastic fibres encircling the teat canal and lower teat sinus (Van der Merwe, 1985). This process is under the influence of the sympathetic nervous system which acts to tighten and increase the muscle tension (tone) during the inter-milking period and relax the muscle tone of the teat during milk let-down. After milking, the teat canal takes approximately two hours to fully close again (Schultze & Bright, 1983). Directly after milking, the diameter of the teat canal is at its greatest, and the potential penetrability of the teat canal by pathogenic bacteria is at its highest.

As the teat canal closes, the mucosal epithelium of the Fürstenberg's rosette overlay each other and act as a one-way valve to prevent the release of milk from the teat sinus. This muscular process of closing and constricting the teat canal is often described in terms of the teat canal sphincter, which was originally described by Christ in 1905 (Christ, 1905). This process of closing at the Fürstenberg's rosette also aids in preventing the entry of microbes into the teat sinus from the teat canal (Van der Merwe, 1985).

1.3.2. Teat canal lining

The teat canal lining acts as a physical barrier to invading microorganisms through a variety of different mechanisms. These include the occlusion of the teat canal lumen, adsorption of bacteria to the teat canal lining, and elimination of bacteria and detritus by the removal of the outer most layer of teat canal lining during milking on a daily basis. Furthermore, during the dry period, the 'keratin plug' that forms from the desiccation of the teat canal lining also prevents ingress of bacteria into the mammary gland.

The teat canal lining is derived from fully differentiated teat canal keratinocytes and constitutes the *stratum corneum* and *stratum mortificatum* layers of cellular material. The teat canal lining is known to be composed of aggregated intermediate keratin filaments, lipids, esterified fatty acids and non-esterified fatty acids (Oviedo-Boyso *et al.*, 2007). The amount of lining produced by the teat canal is directly influenced by the length of the teat canal and its internal diameter (Kemper-

Krämer, 1983). Regeneration of the teat canal lining is rapid. If the outer layer of the teat canal lining is completely removed, it only takes two and a half days to be fully replaced (Capuco *et al.*, 1990). Removal of the teat canal lining increases susceptibility to bacterial infections (Murphy, 1959; Capuco *et al.*, 1992; Lacy-Hulbert & Hillerton, 1995). Furthermore, when bacteria are placed further up into the teat canal infection rates increased (Prasad & Newbould, 1968).

1.3.3. Teat canal keratin plug

At the end of lactation, dairy cows go through a drying-off period that enables the milk producing tissues of the mammary gland to undergo active involution, that enables repair and rejuvenation for the next lactation cycle (Hurley, 1987). During the early stages of this dry period, the udder is vulnerable to infection by mastitis causing pathogens (Cousins *et al.*, 1980). Natural protection from intramammary infections is provided through the formation of a teat canal keratin plug which acts as a physical barrier to infection in each teat (Capuco *et al.*, 1992).

Correct development of the keratin plug completely occludes the lumen of the teat canal preventing the upward movement of invading microorganisms. However, the time taken to form the keratin plug and close the teat canal after drying-off varies among cows (Williamson *et al.*, 1995). In most cases, the keratin plug takes a couple of weeks to form (Comalli *et al.*, 1984) but for some cows the keratin plug fails to become established and the teat canal remains open; dramatically increasing the likelihood of intramammary infection (Williamson *et al.*, 1995).

To minimise the prevalence of infection during the drying-off period, many dairy farmers in New Zealand follow the dry cow strategy as outlined by DairyNZ (https://www.dairynz.co.nz). This includes the use of antibiotic dry cow therapy and the use of intramammary teat sealants. Studies utilising these mastitis management tools have shown a significant reduction in infection during the onset of involution and the incidence of new intramammary infections during the dry period.

1.3.4. Beyond the physical barrier of the teat canal

The effective barrier function of the teat canal to the passage of microorganisms into the mammary gland can be best illustrated by a series of previous studies where researchers attempted to establish intramammary infections by mimicking the natural infection process. In these studies intramammary infection rates only increased marginally, above those occurring naturally, after teats were either repetitively exposed to challenge suspensions containing large numbers of mastitis causing pathogens (Pankey *et al.*, 1985; Nickerson & Boddie, 1994) or when bacteria were inoculated half way up the teat canal (Newbould & Neave, 1965b; Prasad & Newbould, 1968). In contrast, by-passing the teat canal and inoculating low numbers of pathogenic bacteria directly into the teat sinus invariably lead to the establishment of an intramammary infection (Newbould & Neave, 1965a; Schukken *et al.*, 1999; Boehmer *et al.*, 2008; Smolenski *et al.*, 2014).

In these aforementioned studies, the physical barriers normally encountered by the bacteria were lessened; yet in many instances, intramammary infection still did not occur. One interpretation of these results is that other barriers are acting together to protect the mammary gland from infection.

The skin is known to be protected by a broad array of antimicrobial proteins and peptides that act to form a biochemical shield; thereby limiting microbial colonisation and infection (Schröder & Harder, 2006; Schauber & Gallo, 2008). As the teat canal shares many morphological similarities with the skin, it is therefore plausible that similar arrangements of constitutively expressed and inducible host-defence proteins are also found in the teat canal and are present in the teat canal lining where they play a role in epithelial host defence.

Although outside of the scope of this study, the microflora of the skin can also act in a harmonious relationship and contribute to skin health, much like that of the gut microflora (Cogen *et al.*, 2008). The teat canal and mammary gland are also populated by a diverse array of bacterial species (reviewed in (Rainard, 2017). It is possible that commensal bacteria could occupy desirable niches in the epithelial lining of the teat canal and mammary gland and actively suppress colonisation of incoming pathogens, through similar mechanisms observed in the gut and on the skin (Kamada *et al.*, 2013) thereby contributing to innate host-defence.

1.4. Epithelial innate immunity

The epithelial innate immune system comprises both cellular and biochemical mechanisms and rapidly responds to foreign antigens. Unlike the adaptive immune system, these mechanisms are usually less specific and do not exhibit a memory component following repeated exposures. The innate immune system of the skin functions to limit the ability of foreign invaders, such as bacteria, to colonise and multiply on the epithelial surface or in areas of the skin that may have recently been damaged.

The elements of the skin innate immune system consist of 1) physical barriers, such as the epithelium, 2) biochemical barriers, such as antimicrobial proteins/peptides, 3) resident immune cells such as macrophages, dendritic cells, and intra-epithelial lymphocytes, 4) infiltrating phagocytic cells such as neutrophils, and cytotoxic natural killer cells, and 5) signalling molecules such as cytokines and chemokines (Mogensen, 2009). Unlike the adaptive immune system, the innate immune system is not based on the recognition of specific antigens but rather senses non-self antigens with the aid of pattern recognition receptors which recognise pathogen-associated molecular patterns (PAMPs) (Ip *et al.*, 2009; Kumar *et al.*, 2011).

The architecture and location of the teat canal make it unique in respect to innate epithelial immunity. The stratified squamous epithelial structure of the teat canal closely resembles that of the skin and as such would be expected to contain many of the immune system elements that protect the skin from infection. However, unlike the skin, which is exposed to the external environment, the teat canal is an internal structure. It is, therefore, possible that elements that more closely resemble the mucosal immune system are also involved in host-defence of the teat canal. To date, there is limited knowledge as to which components contribute to the host-defence capability of the bovine teat canal and teat-end tissues. Evidence supporting innate immune function in the teat canal and teat-end tissues will be described in more detail later in Section 1.5.

The skin and mucosal immune systems consist of fundamental cellular elements that are involved in the immunosurveillance and protection of epithelial surfaces. Listed below are brief descriptions of the major innate immune cell types and structures that have been identified from studies of mammalian skin and mucosal immune systems. It is likely that some of these cellular elements will play a role in defence of the bovine teat canal and teat-end tissues. For this reason, the identification of some of these cells and their spatial localisation in the teat canal and teat-end tissues will be investigated as part of this PhD study.

1.4.1. Resident immune system cells of skin epithelium

There are many different cell types found in skin epithelium that are involved in the innate immune response to pathogens. These include keratinocytes, resident and trafficking immune system cells, endothelial cells of the skin microvasculature, and cells of the connective tissue such as fibroblasts and adipocytes. All of these cells can recognise structures that are conserved among microbial species through the expression of specialised pattern recognition receptors on the surface of the cell (Janeway, 1989; Kupper & Fuhlbrigge, 2004; Miller & Modlin, 2007). Pattern recognition receptor families are divided into four distinct classes. These include transmembrane proteins such as the Toll-like receptors (TLR) and C-type lectin receptors, as well as cytoplasmic proteins such as the retinoic acid-inducible gene-1-like receptors and nucleotide oligomerization domain-like (NOD-like) receptors (Mogensen, 2009; Kumar *et al.*, 2011).

Each cell type and related cell subsets have a distinct array of pattern recognition receptors, and as a consequence, they respond differently to sensed stimuli (Kumar *et al.*, 2011). The major immune cell types expected to play a role in the innate immune defence of the teat canal and teat-end tissues are further described below.

Keratinocytes:

Keratinocytes represent the major cell population in the stratified squamous epithelia of skin. Not only do they provide a structural barrier to potential pathogens, but they are also able to produce a variety of biochemical signals when compromised. Like human skin keratinocytes, bovine skin keratinocytes express up to 10 different Toll-like receptors (Menzies & Ingham, 2006; Nestle *et al.*, 2009). Activation of these receptors by microbial antigens results in increased production of antimicrobial proteins and proinflammatory signalling molecules that not only attract effector immune cells but also modulate their response depending on the type of pathogen challenge (Albanesi *et al.*, 2005; Nestle *et al.*, 2009).

Mammalian keratinocytes produce antimicrobial proteins and peptides, both constitutively and in response to microbial pathogens. These antimicrobial proteins have broad-spectrum activity against both Gram-positive and Gram-negative bacteria and are effective against some fungi and viruses (Brogden, 2005). They are also thought to play a role in controlling the growth of normal 'commensal' microflora (Boman, 2000). Antimicrobial proteins found to be constitutively expressed in human skin keratinocytes include β-defensin-1, demcidin, RNase7, and S100A7 (psoriasin) (Krisanaprakornkit *et al.*, 1998; Schittek *et al.*, 2001; Harder & Schroder, 2002; Gläser *et al.*, 2005). However, in response to bacterial stimuli skin keratinocytes increase expression of antimicrobial proteins such as bactericidal/permeability-increasing protein, cathelicidin (hCAP-18/LL-37), β-defensin-2, β-defensin-3, RNase7, and S100A7 (Schröder & Harder, 2006).

Investigations into antimicrobial proteins produced by bovine epithelial cells of the teat and mammary gland have been limited to a few investigations (Regenhard *et al.*, 2010; Rinaldi *et al.*, 2010; Tetens *et al.*, 2010; Whelehan *et al.*, 2011). In three of these studies, investigators used quantitative PCR to measure the expression of selected genes encoding antimicrobial proteins in various tissues of the teat. While quantitative PCR can provide evidence for a regional change in gene expression, this technique is limited by firstly, not being able to determine the cell type responsible for the expression of each antimicrobial protein, and secondly, an increase in gene expression does not always lead to an equivalent increase in protein abundance.

Constitutive expression of antimicrobial protein transcripts for β-defensin-1, -4, -10, lingual antimicrobial peptide (LAP), tracheal antimicrobial peptide (TAP) and S100A7 has been demonstrated in healthy tissue samples from the teat canal and Fürstenberg's rosette region (Tetens *et al.*, 2010). Conversely, in studies where microbial challenge of the teat has occurred, expression of antimicrobial protein transcripts encoding bactericidal/permeability-increasing protein, β-defensin-4, and β-defensin-5 were found to be significantly increased in infected versus healthy tissues (Rinaldi *et al.*, 2010; Whelehan *et al.*, 2011). The significance of these results from these studies will be described in more detail in Section 1.5.4.

Macrophages:

Macrophages are a ubiquitous and heterogeneous population of immune cells that are derived from myeloid progenitors found in the bone marrow, spleen and foetal liver (Stout & Suttles, 2004). Once in the circulating blood, newly formed macrophages, termed monocytes, are exposed to a wide variety of hormones, agonists and biochemical signalling molecules that influence their functional and phenotypic development (Stout & Suttles, 2004). These 'conditioned' monocytes selectively home to different tissues in the body under the influence of chemokines (Xuan *et al.*, 2015) and tissue-specific homing and cell adhesion factors (Okabe & Medzhitov, 2014) where they further differentiate into macrophage or dendritic cell populations. Macrophages are found in every tissue within the body where they play a role in development, homoeostasis and repair, as well as being potent immune regulators (Stefater *et al.*, 2011; Wynn *et al.*, 2013).

The skin of humans, rats and mice contain relatively few macrophages compared to other tissues such as lung alveoli, liver and thymus (Platt *et al.*, 1998; Koay *et al.*, 2002; Bilzer *et al.*, 2006). In the skin the majority of macrophages are observed in the reticular dermal layer, surrounding both sweat ducts and hair follicles (Flotte *et al.*, 1983; Zwadlo *et al.*, 1985). This localisation is not unexpected as these accessory ducts and shafts constitute major portals of entry for microbes. Tissue-resident macrophages surrounding these sites represent an important sentinel population of immune cells that are alert for signs of invading pathogens or tissue damage (Murray & Wynn, 2011).

Like many other innate immune cells, macrophages express a wide variety of pattern recognition receptors for the detection of microbial antigens. In addition, macrophages also express specialised cell-bound and secreted receptors for the binding and phagocytosis of pathogens. This process is enhanced by the recognition of pathogen-bound protein molecules and is known as opsonisation. The binding of complement fragments and different types of antibodies allow complement and Fc receptors on immune cells to bind to pathogens and assist in their internalisation and removal (Reynolds *et al.*, 1975; Rossi & Kiesel, 1977; Medzhitov & Janeway Jr, 1997; Aderem & Underhill, 1999). Macrophages are activated by cytokines (such as interferon-γ) and microbial stimuli to become efficient effector cells; upregulating opsonic receptors and producing high levels of pro-inflammatory mediators that alter the tissue microenvironment (Stout & Suttles, 2004).

In the bovine mammary gland, macrophages are a major cell type found in regular cisternal milk, dry-cow secretions and in surrounding mammary tissues (Jensen & Eberhart, 1975; Jensen & Eberhart, 1981; Paape *et al.*, 2002b). This would imply that macrophages play an important role in the mammary gland and surrounding teat tissue. However, there have been few studies describing the distribution and importance of different macrophage phenotypes in cattle including in the mammary gland (Düvel *et al.*, 2012); let alone described in the region of the teat-end tissues. Research investigating macrophage function in the mammalian mammary gland has focused, for the most part, on their effector and phagocytic capabilities (Politis *et al.*, 1992; Sordillo & Streicher, 2002; Rainard & Riollet, 2006) as well as their developmental and regenerative capabilities in mammary alveoli (Van Nguyen & Pollard, 2002; Gyorki *et al.*, 2009; Bussard & Smith, 2011).

Histological investigation of teat-end tissues has been limited. For example, Nickerson and Pankey reported observing monocytes located between the epithelial cells of the teat sinus and rosette epithelial bilayers (Nickerson & Pankey, 1983) and Van der Merwe observed dendritic-like macrophages in the epithelia of the teat canal using electron microscopy (Van der Merwe, 1985). More recently, Düvel and colleagues (2012) used immunohistochemical (IHC) markers to study macrophage populations in the bovine teat. However, this

research article specifically focused on macrophage populations in the reticular dermis, peripheral connective tissue and surrounding blood vessels of the teat, rather than in the papillary dermis or epithelial layer of the teat canal, Fürstenberg's rosette and teat sinus, which is the focus of this study.

Dendritic cells:

Dendritic cells play a central role in linking innate and adaptive immune responses. They are considered professional antigen-presenting cells due to their ability to engulf and process antigen, their constitutive expression of high levels of the major histocompatibility complex (MHC) class II protein and their ability to activate T cells using additional co-stimulatory molecules (Banchereau *et al.*, 2000). Dendritic cells are predominantly found in mucosal and epidermal tissues and as such are among the first innate immune cells to come in contact with pathogen antigens (Iwasaki, 2007).

In humans and mice, distinct dendritic cell subpopulations have been identified at individual epithelial and mucosal sites, with the distribution of these subpopulations varying amongst the different mucosal compartments (Fries & Griebel, 2011). More recently, bovine dendritic cell subpopulations from mucosal tissues have started to be defined through the use of specific cell surface markers (Fries *et al.*, 2011; Maxymiv *et al.*, 2012; González-Cano *et al.*, 2014). However, the ability to identify different bovine dendritic cell subsets is limited by the availability of suitable bovine specific or bovine cross-reactive antibody reagents.

In mammals, skin dendritic cells can be separated into two distinct cell populations: Langerhans cells and dermal dendritic cells, which are located in the epidermis and dermis of the epithelium, respectively. Both populations of dendritic cells capture and process antigens within the skin and then migrate to cutaneous lymph nodes via afferent lymph vesicles (Steinman *et al.*, 1995; Cumberbatch *et al.*, 2000). In the lymph tissue, they can present antigens via the MHC class I and MHC class II proteins to naïve $CD8^+$ and $CD4^+$ T lymphocytes, respectively (del Rio *et al.*, 2007) as well as B cells, thereby initiating an adaptive immune response (Belz *et al.*, 2002). Langerhans cells and dermal dendritic cells express distinct myeloid markers and have quite distinct functions; each population preferentially activating different arms of the acquired immune response (Klechevsky *et al.*, 2008).

Langerhans cells are found primarily in mammalian stratified squamous epithelia where they preferentially occupy a suprabasal position in the *stratum spinosum* (Romani *et al.*, 2012). In humans, they can be classified by their relatively high expression of MHC class I and class II molecules, CD1a, E-cadherin, CD11c, CD205/DEC-205, CD207/Langerin (Mizumoto & Takashima, 2004; Mathers & Larregina, 2006) and by the presence of intracellular organelles called Birbeck granules (Birbeck *et al.*, 1961).

Antibodies to the two most commonly used markers used to identify Langerhans cells in humans and mice, CD1a and CD207, are not yet available for cattle. As a result, Langerhans cells can only be putatively defined in cattle by their location in the epidermis along with the expression of markers for CD11c, MHC class II and CD205. This Langerhans cell identification is also aided by the absence of detectable CD14, CD36, CD206, and CD209 cell surface markers (Valladeau & Saeland, 2005).

Mast cells:

While mast cells are better known for their roles in the augmentation of pathological conditions such as asthma, allergic reactions and anaphylaxis (Abraham & John, 2010), they are also important components of the innate immune system. Mast cells are ubiquitously distributed throughout the body but are most frequently found in close proximity to epithelial layers of the skin, the respiratory and gastro-intestinal mucosa; areas where they are likely to encounter invading pathogens (Metcalfe *et al.*, 1997).

Mast cells can detect minute changes in their environment and communicate these changes rapidly to other nearby cells through the release of cytokines, chemokines, and preformed mediators (Suzuki *et al.*, 2008). As mast cells are the first tissue-resident immune cells capable of releasing preformed mediators, they therefore, have a major influence on determining the magnitude of the initial inflammatory response induced by pathogens (John & Abraham, 2013). In addition, mast cells can survive for prolonged periods after activation and are therefore important immune cells that can shape the outcome of the innate immune response reactions (Abraham & John, 2010).

Mast cells express a number of receptors, such as toll-like, complement, stem cell factor (CD117) and high-affinity Fc receptors, which allow them to recognise and react to a diverse range of stimuli (Marshall, 2004). When activated, mast cells rapidly release preformed mediators, such as histamine, heparin and tumour necrosis factor-alpha (TNF-α) as well as serine proteases such as tryptase and chymase (Marshall, 2004). Mast cells also produce eicosanoid lipid mediators such as prostaglandin D2, a chemoattractant for eosinophils, and the proinflammatory mediator's leukotriene B4 and C4 (Boyce, 2007).

The release of these biochemical molecules acts to recruit effector cells including neutrophils, macrophages, and lymphocytes to the site (Wedemeyer *et al.*, 2000). Additionally, the release of histamine amplifies the expression of TLRs and proinflammatory cytokines (Kobayashi *et al.*, 2009). Histamine, prostaglandin D2, TNF-α and the serine proteases have been shown to increase vascular permeability and to stimulate the expression of adhesion molecules on endothelial cells, such as ICAM-1 and E-selectin, that facilitate leukocyte trafficking into inflammatory sites (Williams & Morley, 1973; Klein *et al.*, 1989; Cairns & Walls, 1996; Lytinas *et al.*, 2003).

Such findings suggest that mast cells, present in the bovine teat-end tissues, may play an influential role in the signalling and trafficking of circulating leukocytes into the lumen of the teat sinus. However, to date, there have been no published studies investigating the role of mast cells in the extravasation of leukocytes into the bovine teat lumen during infection.

Gamma-delta T cells:

Gamma-delta T cells (γδ T cells) constitute a population of non-conventional or innate-like T cells in mammals. γδ T cells express the γδ T cell receptor (γδ TCR) instead of the classical αβ TCR found on conventional migratory T cells (Bonneville *et al.*, 2010). In humans and mice, γδ T cells comprise a small proportion (1-10 %) of the circulating and intestinal intraepithelial T cell population (Holderness *et al.*, 2013). However, in young cattle γδ T cells represent the major lymphocyte subset, representing up to 70 % of the circulating T cell population, decreasing to 5-15 % in older cattle (Davis *et al.*, 1996).

In mammalian species, γδ T cells are found to be enriched in epithelial-associated tissues and at sites of infection and inflammation (Goodman & Lefrancois, 1988; Itohara *et al.*, 1990). In the small intestines of humans, mice, chickens and cattle, γδ T cells comprise a significant proportion of the intraepithelial lymphocytes that are directly juxtaposed with epithelial cells (Goodman & Lefrancois, 1988; Hayday & Viney, 2000). Intraepithelial lymphocytes are usually found in the skin and mucosal epithelium and are found at high levels in mucosal epithelium of the gastro-intestinal tract. The study of intraepithelial lymphocytes has also been extended to other mammalian tissues such as the uterine and vaginal epithelia, tongue, lung, and mammary tissue (Itohara *et al.*, 1990).

γδ T cells possess both adaptive and innate immune features (Bonneville *et al.*, 2010). Not only are they able to use their γδ TCRs as pattern recognition receptors to recognise PAMPs but they are also able to act as antigen-presenting cells through expression of MHC class II molecules and, as such, can induce proliferation of $CD4^+$ αβ T cells (Cheng *et al.*, 2008). γδ T cells have an extensive array of effector functions that reflect their involvement in a diverse range of pathological processes. Like natural killer cells, γδ T cells possess cytotoxic effector molecules and can kill infected, activated or transformed cells (Oliaro *et al.*, 2005; Kabelitz *et al.*, 2007; Qin *et al.*, 2009). γδ T cells have also been shown to be involved in wound healing and can regulate the inflammatory responses stimulated by activated αβ T cells (Girardi, 2006; Toulon *et al.*, 2009).

To date, the presence of γδ T cells adjacent to the epithelia of the teat canal and teat-end tissues has not been confirmed in cattle. However, recent studies utilising bovine-specific monoclonal antibodies to the WC1 receptor of γδ T cells demonstrated that significant numbers of γδ T cells reside in the subepithelial dermis and also border the epithelial layer of skin removed from the tail and perineum of cattle (Constantinoiu *et al.*, 2010; Constantinoiu *et al.*, 2013).

Neutrophils:

Neutrophils are specialised killer cells and are essential components of the innate immune system's armoury against invading pathogenic bacteria. Typically, neutrophils are the first type of leukocyte recruited to sites of infection in response to host- and pathogen-derived chemotactic factors (Paape *et al.*, 2003).

The primary function of neutrophils is to trap, engulf and eliminate pathogens thereby preventing their growth and expansion (Smith, 1994; Brinkmann *et al.*, 2004). Neutrophils ingest invading microbes by a process known as phagocytosis (Hampton *et al.*, 1998). Once ingested, neutrophils kill invading pathogens via oxygen-dependent and oxygen-independent mechanisms (Brinkmann *et al.*, 2004; Segal, 2005). The oxygen-dependent mechanism, known as the "respiratory burst", results in the production of large quantities of hydroxyl and oxygen radicals to destroy pathogens (Hampton *et al.*, 1998; Segal, 2005). The oxygen-independent system uses several enzyme reactants such as peroxidases, lactoferrin, lysozyme and a variety of hydrolytic enzymes to produce a hostile, non-physiologic environment in the phagosome (Elsbach & Weiss, 1985; Spitznagel & Shafer, 1985).

In addition to oxidising agents, neutrophils also contain three different types of intracellular granules that contain various combinations of antimicrobial proteins and enzymes (Paape *et al.*, 2003). The azurophil, specific and gelatinase granules are formed at the various stages of neutrophil development and contain antimicrobial proteins such as α-defensins, β-defensins, cathelicidins, lactoferrin and lysozyme (Borregaard *et al.*, 2007). Depending on the type of intracellular granule, these antimicrobial proteins can either be released into phagosomes, to assist in destroying ingested pathogens, or released into the surrounding environment to aid in the killing of extracellular pathogens (Kobayashi *et al.*, 2005).

Neutrophils are present in normal uninfected milk as part of a resident population of immune cells. In milk, normal somatic cell counts (SCC) range from between 20000 and 100000 cells/mL with neutrophils making up approximately 30 % of the total leukocyte population (Sarikaya *et al.*, 2004). However, in the matrix of milk, their ability to mount an effective defence against new infections appears to

be compromised. Reasons for this include: 1) their concentration in milk is too low for efficient phagocytosis, 2) a good proportion of them are nonviable or undergoing apoptosis, and 3) the ingestion of caseins and milk fat globules compromises their functional ability and accelerates premature cell death (Vangroenweghe *et al.*, 2001; Paape *et al.*, 2002a; Vangroenweghe *et al.*, 2002; Burton & Erskine, 2003; Burvenich *et al.*, 2003).

Phagocytosis of mastitis-causing bacteria is best performed when the microbes are coated in advance with opsonising proteins, such as complement, and antibodies, especially of the immunoglobulin IgG_2 subclass (Burton & Erskine, 2003). Peak milk IgG_2 concentrations can occur within 4 hours post-infection (Guidry *et al.*, 1983; Mackie & Logan, 1986), some 6 to 12 hours before peak neutrophil response (Paape *et al.*, 1974). This process facilitates effective targeting of microbes by neutrophils for phagocytic clearance of the infection. Dairy cattle with higher serum levels of IgG_2 and an effective inflammatory response had lower incidences of clinical mastitis (Wagter *et al.*, 2000).

Milking removes old and compromised neutrophils from the mammary gland. Under normal physiological conditions, low levels of replacement neutrophils usually enter the mammary gland via the alveoli, thereby maintaining a constant basal level of neutrophils (Paape *et al.*, 2002a; Burvenich *et al.*, 2003). During the initial stages of infection, however, the main entry point of neutrophils into the gland lumen appears to be in the teat-end tissues such as the Fürstenberg's rosette; (Nickerson & Pankey, 1983, 1984). This would make sense as neutrophil extravasation would occur proximity to the site of pathogen infiltration. In this instance, neutrophils rapidly migrate out of the vasculature into the surrounding tissues and milk resulting in increased SCC (Harmon & Heald, 1982; Nickerson & Pankey, 1984). In acute cases, where the infection has spread throughout the udder, rapid and substantial neutrophil extravasation occurs throughout the mammary gland tissue, including secretory alveoli, gland cistern epithelium and teat sinus epithelium (Harmon & Heald, 1982). The SCC of milk increases from tens of thousands into millions of cells per millilitre with neutrophils contributing to more than 95 % of the total leukocyte population (Kehrli & Shuster, 1994). It has been speculated that this prolonged mass migration of neutrophils into the gland, as well as the release of reactive oxygen species and proteolytic enzymes,

could result in permanent damage being caused to the secretory epithelial cells, resulting in decreased milk production (Harmon & Heald, 1982; Sordillo & Nickerson, 1988; Zhao & Lacasse, 2008).

1.4.2. Elements of the mucosal immune system

The tissues of the teat canal, Fürstenberg's rosette, and teat sinus are internally located within the bovine teat. While the teat canal has structural similarities to the external skin layer, the appearance of the cuboidal/columnar epithelial bilayer lining of the Fürstenberg's rosette, and teat sinus show more similarity to the mucosal linings of the eye, respiratory tract, intestinal tract and urogenital tract (McDermott & Bienenstock, 1979; Pudney & Anderson, 1995; McClellan, 1997; Campbell *et al.*, 1999; Sato & Kiyono, 2012). These epithelial tissues are susceptible to the invasion of pathogenic microorganisms and as such require an additional level of protection – known as the mucosal barrier. Our knowledge regarding mucosal defence mechanisms in the teat-end tissues is limited. However, earlier studies have identified antibody secreting plasma cells in the papillary stroma of the Fürstenberg's rosette and teat sinus (Nickerson & Pankey, 1983; Nickerson *et al.*, 1984; Collins *et al.*, 1986).

The mucosal immune system is characterised by a defined organisation of localised and specific immune elements that are designed to protect internal mucous membranes from microbial infection. In humans, it spans the mucosal surfaces of the oropharyngeal cavity, respiratory tract, gastrointestinal tract, and urogenital tract (Brandtzaeg, 1989; Cesta, 2006). The acinar regions of exocrine glands such as sweat glands, salivary glands and mammary glands are also protected by the mucosal immune system (Brandtzaeg *et al.*, 1999).

The mucosal immune system can be separated into inductive or effector sites based on their anatomical location, immune cell types, and functional properties of immune cells located within them (Brandtzaeg, 2009). Inductive sites resemble the structure of lymph nodes consisting of B cell follicles, intervening T cell zones and are characterised by the presence of antigen-presenting cells such as dendritic cells and macrophages (Brandtzaeg & Pabst, 2004). However, unlike lymph nodes, there are no afferent lymphatic ducts associated with these structures

(Brandtzaeg & Pabst, 2004). These inductive sites are called mucosa-associated lymphoid tissues (MALT).

Based on their anatomical localisation, organised MALT structures have been described in the oral and nasal cavities (nasopharyngeal-associated lymphoid tissue), respiratory tract (bronchus-associated lymphoid tissue), gastro-intestinal tract (gut-associated lymphoid tissue) and the appendix. The best studied of the inductive MALT sites are the gastro-intestinal and nasal structures which include the Peyer´s patches, isolated lymphoid follicles and tonsils, respectively (Wershil & Furuta, 2008; Jung *et al.*, 2010; Knoop & Newberry, 2012).

For the most part, the teat canal and teat-end tissues appear devoid of any organised MALT structures. This absence, however, is not unusual as other mucosal tissues, such as the vagina, mouth and cornea (Wang *et al.*, 2013), are also lacking in observable MALT structures and, as such, must rely on antigen uptake and transport into adjacent lymph nodes. Lymphoid follicle-like structures have been observed at the junction between the teat canal and the teat sinus in sheep (Mavrogianni *et al.*, 2007; Fragkou *et al.*, 2010) where they appear to be related to the age of the animal. The authors hypothesised that they were more likely to be the remnants of previous multiple infections. In dairy cows, isolated lymphoid-like structures have been observed in the epithelial folds of Fürstenberg's rosette (Nickerson & Pankey, 1983). In another report, two out of 39 teats examined by Collins and colleagues identified some areas of densely packed leukocytes surrounded by tightly packed lymphocytes in the subepithelial tissue of Fürstenberg's rosette (Collins *et al.*, 1986). These researchers speculated that these structures were examples of germinal centres.

If these structures are indeed MALT-like germinal centres, then we would expect them to be present in the teat sinus and Fürstenberg's rosette regions of the teat of every animal examined. However, in the study by Collins and colleagues (1986), they were only found in 5 % of the teats that were analysed. It is possible that these structures are the remnants of a prior infection, suggesting they may be transient. However, the true nature of these structures remains unknown.

Specialised epithelial M-cells in MALT sample antigens from mucosal surfaces via a follicle-associated epithelium (Neutra *et al.*, 2001). However, to date,

follicle-associated epithelia covering the lymphoid-like structures found in Fürstenberg's rosette has not been reported. A recent investigation of this tissue using histological and IHC techniques observed pinocytotic uptake of ferritin from the luminal surface through the epithelium, adjacent to the lymphoid-like aggregates (Aştı *et al.*, 2011). The authors suggested that these specialised areas had ultrastructural features like that of M-cells and that they constituted the surface of follicle-associated epithelium in the Fürstenberg's rosette. If this interpretation is correct, one would also expect to observe dendritic cells in basolateral pockets beneath the M-cells where they can take up transferred antigens. To date it is unknown if dendritic cells exist in the Fürstenberg's rosette where they are associated with epithelia, consistent with follicle-associated epithelium.

The *lamina propria* is a thin layer of loose connective tissue that lies directly beneath a thin layer of epithelial cells. Together with the mucin layer (gel forming glycoproteins produced by secretory epithelial cells), these three layers constitute the mucous membrane (Brandtzaeg, 2009). A wide variety of immune cells are located in the mucosal membrane. However, B-cells, antigen-presenting cells, macrophages and $CD4^+$ T cells tend to be the dominate cells present. Furthermore, the mucosal epithelium contains many intraepithelial lymphocytes (Hayday *et al.*, 2001). Intraepithelial lymphocytes have been extensively characterised in the intestines of both rodents and man (Cerf-Bensussan & Guy-Grand, 1991; Lundqvist *et al.*, 1995; Beagley & Husband, 1998; Hayday *et al.*, 2001; Hamada *et al.*, 2002). They comprise a heterogeneous cell population of specialised T cells and natural killer cells that protect the host tissue from infection (Hayday *et al.*, 2001).

In humans, the majority of intraepithelial lymphocytes express the αβ T cell receptor (TCR) with only about 10 % of intraepithelial lymphocytes in healthy individuals expressing the γδ TCR (Spencer *et al.*, 1989). However, in cattle γδ T cells represent the major T cell subset of both circulating T cells and intraepithelial lymphocytes in young animals (Goodman & Lefrancois, 1988; Guzman *et al.*, 2011). Studies illustrating lymphocytes bordering the bovine teat canal and teat sinus epithelium are limited to only a few non-descriptive investigations (Nickerson & Pankey, 1983; Van der Merwe, 1985). The intraepithelial lymphocytes of the bovine teat may play a critical key role in immunosurveillance and localised defence of the teat-end tissues; however, they are also yet to be investigated.

1.4.3. Unique aspects of the ruminant mucosal immune system

In non-ruminant species, it has been demonstrated that oral immunisation leads to a generalised secretory IgA response in several external secretions (Craig & Cebra, 1971; Montgomery *et al.*, 1974; Weisz-Carrington *et al.*, 1979; Czerkinsky *et al.*, 1987). These findings have given rise to the concept of a common mucosal immune system in which antigen-sensitized IgA precursor B cells from inductive sites within the gastrointestinal tract migrate to other mucosal surfaces or secretions in the body, such as breast milk (Slade & Schwartz, 1987). However, the mammary glands of sheep and cattle do not appear to form part of the common mucosal immune system (Chang *et al.*, 1981; Sheldrake *et al.*, 1988). In these species, IgA and IgM are found at much lower concentrations in mammary secretions relative to the level of IgG, which is in contrast to many non-ruminant species (Watson & Lascelles, 1973). Certainly, during colostrogenesis, significant amounts of IgG_1 are selectively transferred from the blood into colostrum in ruminants suggesting an important role for IgG_1 in protecting the young from disease early in life (Brandon *et al.*, 1971).

This aspect of the ruminant immune system has significant implications for the trafficking of antibody secreting cells between mucosal sites and is one of the likely reasons why it has proven very difficult to protect the mammary gland using vaccination, especially when administered via a route other than intramammarily (Chang *et al.*, 1981). It is also possible that this unique arrangement may lead to unconventional mucosal organisation in the ruminant mammary gland.

1.5. Evidence for innate immune function in the teat canal

There is emerging evidence to suggest that the role of the teat canal in host defence against pathogens is more than the provision of a physical barrier. The immune function of humoral components found in milk has been extensively reported elsewhere (Korhonen *et al.*, 2000; Valenti & Antonini, 2005; Hettinga *et al.*, 2011; Wheeler *et al.*, 2012b) and will only be discussed briefly here. Rather, this section will focus on reviewing evidence for cellular-based immunity in the teat-end tissues and the presence of compounds with antimicrobial activity in the teat canal lining.

1.5.1. Contribution of antimicrobial components from milk

Antimicrobial compounds represent a minor protein component of milk and may act independently or in concert with immune cells to restrict the growth of bacteria. These proteins include lactoferrin, lysozyme, lactoperoxidase, complement, soluble pattern recognition receptors, acute phase proteins and immunoglobulins of various isotypes. Many of their immune-related functions have been previously described in several excellent review articles (Reiter, 1978; van Hooijdonk *et al.*, 2000; Rainard, 2003; Jenssen & Hancock, 2009; Stelwagen *et al.*, 2009) but not necessarily in the context of their role in the teat canal. This is not surprising as bacteria residing in the teat canal would only be exposed to the proteins in milk during the act of milking. It is possible that opsonins such as complement C3, IgG_2 and soluble CD14 can bind to the outer surface of the bacteria during milking, thereby facilitating improved recognition and phagocytosis by macrophages and neutrophils. However, there is currently no evidence in the literature to support this notion.

1.5.2. Cellular immunity in the teat-end tissue region

Although the innate defence mechanisms of the skin and mucosal immune systems have been well documented (See Section 1.4 for reviews), there is very little direct information identifying the different types of immune cells residing within the teat canal epithelium and adjacent teat-end tissues, their potential function at that site and the role they may play in immune defence. To date, evidence to support the presence of immune cells in the teat canal and teat-end tissues has been limited to examination by light microscopes. The use of fluorescence IHC has yet to be applied to these tissue samples, primarily due to the unavailability of suitable antibody reagents. More recently, specific antibodies are now commercially available, allowing immunohistology techniques to be used to identify immune cell populations in the bovine teat tissues.

Venzke (1940) and Adams and colleagues (1961), were some of the first researchers to investigate cellular immunity in the teat-end tissues. Both research groups observed numerous subepithelial lymphocytes in the dermal layer of the bovine teat sinus and reported that the infiltration of lymphocytes appeared to

increase in number approaching the Fürstenberg's rosette region of the teat (Venzke, 1940; Adams *et al.*, 1961). These initial results were later confirmed in several studies by Nickerson, who also observed plasma cells in the subepithelial connective tissue of the teat (Nickerson & Pankey, 1983; Nickerson *et al.*, 1984). Plasma cells were also identified as the predominant cell type in the dermal layer of Fürstenberg's rosette and were seen to interact with the epithelial lining (Nickerson *et al.*, 1984). From these studies, it was concluded that the Fürstenberg's rosette region was important for the detection of bacterial antigens and the subsequent recruitment of immune effector cells. A subsequent study by the same authors focused on the migration of neutrophils into milk during the initial stages of infection (Nickerson & Pankey, 1984). In this study, they established that the infiltration and migration of neutrophils into the teat sinus lumen occurs predominantly through the tissues surrounding the Fürstenberg's rosette. Preferential infiltration of neutrophils at this site is logical for a number of reasons. Firstly, it provides the first point of contact beyond the teat canal for antigen detection; secondly, the epithelial bilayer is thin allowing for relatively easy epithelial transmigration into the lumen from the connective tissue; thirdly, there is an abundance of blood vessels and capillaries adjacent to the teat-end tissues to facilitate the migration of large numbers of neutrophils to the site, and lastly, substantial ongoing neutrophil transmigration through the alveolar tissue is thought to cause mechanical and chemical damage to both the secretory and ductal cell layers (Akers & Nickerson, 2011).

Evidence that the teat canal epithelium contains antigen-presenting cells was first provided by Van der Merwe (1985), who used electron microscopy to identify cell types (Van der Merwe, 1985). Here he was able to identify some dendritic macrophage cells within the teat canal epithelium that contained structures similar to the Birbeck granules of Langerhans cells. However, these granules were not present in all of the dendritic macrophages observed. Birbeck granule expression is lost on Langerhans cell activation (Weiss *et al.*, 2005), so it is possible that these cells were Langerhans cells that had already captured and processed antigens and were in the process of migrating to afferent lymph nodes.

1.5.3. Antimicrobial constituents within the teat canal lining

Investigations into the bacteriostatic or bactericidal properties of the teat canal lining have yielded conflicting results. Where the teat canal lining is the only source of carbon and energy, mastitis causing bacteria such as *Staphylococcus* and *Streptococcus* species were able to survive and eventually grow under *in vitro* conditions (Forbes, 1970; Murdough *et al.*, 1991). However, when these bacteria were tested against purified components of the teat canal lining, growth inhibition and even killing of the bacteria were observed (Adams & Rickard, 1963; Hibbitt *et al.*, 1969; Hogan *et al.*, 1986; Senft *et al.*, 1990) possibly suggesting a concentration effect.

The lipid component of the teat canal lining is approximately 3-5 % of wet weight (Hogan *et al.*, 1986; Bitman *et al.*, 1988; Bitman *et al.*, 1991). Long-chain fatty acids (defined as C_{12} and larger) make up over 70 % of the total fatty acid content of the teat canal lining, and the growth of mastitis causing pathogens, such as *Staphylococcus aureus* (*S. aureus*), *Staphylococcus hyicus* (*S. hyicus*), *Streptococcus agalactiae* (*S. agalactiae*) and *Corynebacterium bovis* (*C. bovis*) has been shown to be inhibited by long-chain fatty acids (Butcher *et al.*, 1976; Heczko *et al.*, 1979; Hogan *et al.*, 1987). Esterified and nonesterified fatty acids isolated from the teat canal lining were confirmed to be bacteriostatic to *S. agalactiae* (Adams & Rickard, 1963). The most potent of these fatty acids being myristic acid (C_{14}) followed by palmitoleic acid (C_{16}), and linoleic acid (C_{18}), respectively.

Proteins with antimicrobial properties have been purified from the teat canal lining previously. In two separate experiments, cationic proteins with antimicrobial activity against both *S. aureus* and *S. agalactiae* were purified from the teat canal lining (Hibbitt *et al.*, 1969; Senft *et al.*, 1990). In addition, anionic proteins also isolated from the teat canal lining were found to exhibit bacteriostatic activity. Following these studies, there has been no further reference made to these proteins in the literature and, as a result, the identity of these cationic and anionic proteins remains unknown.

Collins and colleagues used histochemical methods to show that xanthine oxidase was present in the stratified epithelium of the teat canal and the teat canal lining (Collins *et al.*, 1988). Xanthine oxidase has been shown to generate reactive-

oxygen species, superoxide anions and hydrogen peroxide (Granger *et al.*, 1981; Martin *et al.*, 2004) which play a role in microbial defence. Also, xanthine oxidase has been shown to produce reactive-nitrogen species such as nitric oxide. Hydrogen peroxide and nitric oxide react together to form peroxynitrite – a powerful oxidising agent which has potent antimicrobial properties (Godber *et al.*, 2000a; Godber *et al.*, 2000b). Therefore, it is possible that xanthine oxidase could contribute to host-defence in the teat canal through the production of these reactive-oxygen and reactive-nitrogen species.

1.5.4. Spatial and temporal studies of innate immune gene expression

Several research groups have recently reported the expression of key innate immune effector molecules, in the bovine teat-end tissues (Rinaldi *et al.*, 2010; Tetens *et al.*, 2010; Whelehan *et al.*, 2011).

Tetens and colleagues investigated the spatial expression pattern of six different antimicrobial proteins in healthy udder tissue. They observed relatively high levels of constitutive S100A7 expression in tissue collected from the teat canal and Fürstenberg's rosette. These findings were in contrast to the results of Regenhard and colleagues (2010), who observed expression of S100A7 on the skin surface but failed to detect S100A7 expression in normal teat canal and teat sinus tissues. Furthermore, five different bovine β-defensin proteins were detected in the teat-end tissues, with bovine β-defensin-10 constitutively expressed at relatively high levels in the teat canal tissue (Tetens *et al.*, 2010).

Both Rinaldi and colleagues (2010) and Whelehan and colleagues (2011) investigated the upregulation of effector molecules during the initial stages of experimental bacterial intramammary infection. Because of the different pathogens used in each study (*E. coli* and *S. aureus*, respectively), the identification of different target genes, and the differences in sampling times (12 h and 24 h compared to 48 h, respectively) a direct comparison of the results from these two experiments is challenging. However, for both experiments, genes encoding pro- and anti-inflammatory signalling molecules were upregulated in

tissue collected from the teat sinus along with genes encoding a number of antimicrobial proteins.

Rinaldi and colleagues (2010) reported significant upregulation in the expression of chemokine CCL20 and inducible nitric oxide synthase (NOS2) transcripts in tissues obtained from the Fürstenberg's rosette region. CCL20 acts as a chemoattractant for immature dendritic cells, effector/memory T cells and B cells (Schutyser *et al.*, 2003). It is known to play a role in mediating migration of these cell-types towards skin and mucosal surfaces under homeostatic and inflammatory conditions. Many cell types involved directly or indirectly in host-defence can synthesise nitric oxide, which is toxic to bacteria and parasites (Green *et al.*, 1990; Seguin *et al.*, 1994; Brunelli *et al.*, 1995). These include fibroblasts, endothelial and epithelial cells, neutrophils, macrophages, dendritic cells, natural killer cells, eosinophils and mast cells (Wallace & Miller, 2000; Coleman, 2002). In phagocytes, nitric oxide is a component of phagosomes and secretory granules where it plays a role in microbial degradation. In other cell types, it can be released into the external environment where it can react with other biochemical molecules or act as a signalling molecule (Palmer *et al.*, 1987).

The anti-inflammatory cytokines IL-10 and IL-17 and the pro-inflammatory cytokine interferon-γ (IFN-γ) were significantly up-regulated in response to infusion of *S. aureus* into the mammary gland and remained elevated after 48 hours post challenge (Whelehan *et al.*, 2011). The anti-inflammatory action of IL-10 prevents excessive tissue damage as a result of overproduction of IFN-γ and TNF-α (Couper *et al.*, 2008). IL-17 expression is predominantly restricted to skin and mucosal tissues. Recent studies have shown that γδ T cells produce significant amounts of IL-17 during infection (Hamada *et al.*, 2008; Martin *et al.*, 2009). Production of IL-17 aids in maintaining epithelial barrier integrity as well as promoting the release of antimicrobial proteins from epithelial cells (Cua & Tato, 2010). IFN-γ is produced by many different immune cell types including classical and unconventional T cells, macrophages, dendritic cells and B cells. IFN-γ is involved in the regulation of antigen presentation, control of Th1 and Th2 polarisation, chemokine secretion and immune cell activation (Schroder *et al.*, 2004).

1.6. Aims of the study

The teat canal and associated teat-end tissues are the first regions of the mammary gland to encounter mastitis causing pathogens. However, to date many of the innate immune proteins and cells that enable the teat canal to function as an effective gatekeeper to the mammary gland have yet to be characterised.

A review of the literature suggests that the teat canal, Fürstenberg's rosette and teat sinus all have the cellular mechanisms required to respond to bacterial antigens during the initial stages of mammary infection. However, there is a clear lack of knowledge regarding the identity of these immune cells, their ability to act as antigen-presenting cells and what role they play in immunosurveillance. Furthermore, the protein component of the teat canal lining – which is the primary physical barrier to the passage of bacteria up the teat canal, has yet to be determined.

As the teat canal is constantly exposed to bacteria on a daily basis, we expect that these tissues are protected by a structured arrangement of innate immune cells and proteins.

Therefore, we hypothesise that - ***the bovine teat canal and associated teat-end tissues play an important role in the immune surveillance and defence of the bovine mammary gland.*** This hypothesis is based on the expectation that the teat canal and teat sinus epithelial surfaces have a host-defence function that is similar to skin and mucosal surfaces found in other mammalian tissues.

By identifying the immune cells present in the teat canal and teat-end tissues and improving our knowledge of the underlying molecular events preventing infection of the mammary gland, this study may help us to understand why some animals are more resistant to intramammary infections than others. This knowledge could subsequently be applied to the development of novel tools and animal management practices to minimise the impact of mastitis within the dairy industry.

To address this hypothesis the following aims for the study were developed:

1. Characterise the protein component of the teat canal lining from healthy lactating dairy cows using protein separation technologies and tandem mass spectrometry (Chapter 3). This analysis will identify proteins from the surface of the teat canal lining that may play a role in protecting the mammary gland from infection by suppressing the growth and viability of bacteria and preventing their colonisation.

2. Identify key immune-related cells positioned along the length of the teat canal and associated teat-end tissues using fluorescent IHC techniques (Chapter 4). This investigation will use anti-bovine monoclonal antibodies to identify innate immune cells adjacent to the epithelial lining with potential immune surveillance and effector capabilities. Immune cells of interest include dendritic cells, macrophages, mast cells, T cells, γδ T cells, B-cells, and neutrophils.

3. Assess changes in the cell population and expression of immune-related factors that occur in the teat canal and associated teat-end tissues during mammary involution (Chapter 5). This section of work will identify changes in immune cell populations and the repertoire of proteins in the teat canal lining occurring during the onset of early involution.

4. Characterise the localised immune response induced in the teat canal and associated teat-end tissues in response to challenge by mastitis causing bacteria (Chapter 6). This analysis will examine the temporal response of the resident immune cells to a localised bacterial infection of the teat canal as well as investigate changes in the expression of teat canal lining proteins with potential host-defence capabilities.

2. Materials and Methods

This chapter contains the materials used and describes the methodologies employed within this thesis. Specialised methods or variations of these general methods are described further in their respective results chapters. All procedures, unless otherwise stated, were performed at ambient room temperature (RT).

2.1. Materials

2.1.1. Chemicals, reagents and enzymes

All common chemicals and reagents used in this thesis were of analytical grade or higher and were acquired from BDH (Radnor, PA, United States of America), Bio-rad (Hercules, CA, USA), GE Healthcare (GE Healthcare Life Sciences, Auckland, New Zealand), Fisher Scientific (Fisher Scientific, Loughborough, United Kingdom), Merck KGaA (Darmstadt, Germany), Life Technologies Inc. (Carlsbad, CA, USA), Roche Diagnostics New Zealand Ltd. (Auckland, NZ), Sigma-Aldrich (St. Louis, MO, USA) and Thermo Fisher Scientific New Zealand Ltd. (North Shore City, NZ).

All other chemicals and reagents, specialised equipment, commercially available kits are detailed in the relevant Methods Sections, as are the enzymes used which were purchased from Sigma-Aldrich, Merck and Promega Corporation (Madison, WI, USA). Solutions were made using Milli-Q 'ultrapure' type-1 water (MQ-H_2O) unless otherwise stated.

2.1.2. Antibodies

Antibodies cross-reactive with bovine proteins were purchased from multiple sources, gifted from collaborators or were developed "in-house" (Section 2.2.9). Primary monoclonal antibodies are listed in Table 2.1, primary polyclonal antibodies are listed in Table 2.2, and all secondary antibodies are listed in Table 2.3.

Table 2.1: Mouse monoclonal antibodies used to characterise bovine immune and epithelial cells

Antigen specificity	Catalogue # /Clone	Protein concentration	Ig[a] Isotype	Cellular expression	IF dilution used[b]	WB dilution used[c]	Source[d]	References
WC1 T cell receptor	ILA-29	1 mg/mL	IgG_1	γδ T cells	1:30	1:500	WSU	(Wijngaard *et al.*, 1992)
CD3	MM1A	1 mg/mL	IgG_1	T cells	1:400	1:5000	WSU	(Davis & Hamilton, 2006)
CD4	CACT138A	1 mg/mL	IgG_1	T helper cells	1:25	1:250	WSU	(Howard *et al.*, 1991)
CD8	BAQ111A	1 mg/mL	IgM	cytotoxic T cells	1:20	1:200	WSU	(Howard *et al.*, 1991)
CD11c	BAQ153A	0.3 mg/mL	IgM	dendritic cells, monocytes, macrophages, neutrophils	1:100	1:1000	WSU	(Naessens & Hopkins, 1996)
CD14	MM61A	1 mg/mL	IgG_1	monocytes, macrophages, dendritic cells, B cells	1:30	1:250	WSU	(Mosaad *et al.*, 2006)
MHC Class II antigen	IL-A21	1 mg/mL	IgG2a	dendritic cells, macrophages, B cells, activated T cells	1:50	1:500	WSU	(Taylor *et al.*, 1993)
CD205	IL-A53A	1 mg/mL	IgG_1	dendritic cells	1:30	1:500	WSU	(Gliddon *et al.*, 2004)
B cells	GB26A	1 mg/mL	IgM	B cells	1:100	1:1000	WSU	(Davis *et al.*, 2000)
Unknown	CH138A	1 mg/mL	IgM	granulocytes	1:200	1:2000	WSU	(Keresztes *et al.*, 1996; Naessens *et al.*, 1996)
Cytokeratin 18	Ab668	1 mg/mL	IgG_1	epithelial cells	1:100	1:1000	Abcam	(Goossens *et al.*, 2010)

a) Ig, Immunoglobulin; b) Dilution of antibody used for fluorescence IHC; c) Dilution of antibody used for Western blotting;

d) WSU, Washington State University Monoclonal Antibody Centre

Table 2.2: Polyclonal antibodies used for Western blotting and IHC of cryosections

Protein specificity	Catalogue # or clone	Concentration	Dilution (WB)[a]	Dilution (Fr)[b]	Host	Species	Epitope specificity	Source
Lactoferrin	JWT	4.8 mg/mL	1:60000	1:2000	Rabbit	Bovine	Full length purified bovine lactoferrin	Agresearch Ltd
Transferrin	T-6265	21.5 mg/mL	1:5000	1:200	Goat	Human	Full length purified human transferrin	Sigma-Aldrich
RNase7	Red	2.4 mg/mL	1:5000		Rabbit	Bovine	RPGNMTPAQWFETQHVQPSPQGC	Agresearch Ltd
PAUF	B1401	2.2 mg/mL	1:5000	1:200	Rabbit	Bovine	c-GQHKLLGISSIGFDWDYPIVR	Agresearch Ltd
S100A7	K6	51.5 mg/mL	1:150000	1:5000	Rabbit	Bovine	recombinant bovine S100A7	University of Bonn, Germany
S100A8	A8	2.5 mg/mL	1:5000	1:200	Rabbit	Bovine	C-MLTDLECAINS	Agresearch Ltd
S100A9	A9Black	3.1 mg/mL	1:5000	1:200	Rabbit	Bovine	C-MEDKMSQMESSIETI	Agresearch Ltd
S100A12	A12TailRB	2.6 mg/mL	1:10000	1:500	Rabbit	Bovine	C-VSRVLKTAHIDIHKE	Agresearch Ltd
pan-cathelicidin	A14	3.2 mg/mL	1:30000		Rabbit	Bovine	CNEQSSEPNIYRLLELDQ	Agresearch Ltd
CG-39	K22	1.5 mg/mL	1:5000		Rabbit	Bovine	recombinant bovine CG-39	Agresearch Ltd
β-defensin (LAP)	J26	2.6 mg/mL	1:5000		Rabbit	Bovine	VPIRCPGNLRQIGT	Agresearch Ltd
CD207	orb6287	1.0 mg/mL		1:50	Rabbit	Human	PKTWYSAEQFC	Biorbyt
c-kit (CD117)	A4502	8.2 mg/mL	1:1000	1:100	Rabbit	Human	TASSSQPLLVHDDV-C	Dako
GAPDH	TRK5G4-6C5	4.4 mg/mL	1:10000		Mouse	Rabbit	Full length purified rabbit GAPDH	Research Diagnostics Inc
Actin	A2066	0.5 mg/mL	1:5000		Rabbit	Bovine	SGPSIVHRKCF	Sigma-Aldrich
Serpin B3/B4	ab47726	1.0 mg/mL	1:10000		Rabbit	Bovine	synthetic peptide based on the amino-terminal end of human serpinB3	Abcam

a) WB, Western blotting; b) Fr, frozen cryosections.

Table 2.3: Secondary antibodies for Western blotting and IHC

Antibody specificity	Format	Catalogue # Clone	Isotype	Dilution used (WB)[a]	Dilution used (IHC)[b]	Dilution used (IF)[c]	Source
Goat anti-rabbit	HRP	A6154	IgG	1:20000	1:1000		Sigma-Aldrich
Rabbit anti-mouse	HRP	A9044	IgG	1:20000	1:1000		Sigma-Aldrich
Rabbit anti-goat	HRP	A5420	IgG	1:20000	1:1000		Sigma-Aldrich
Goat anti-mouse	Alexa Fluor 488nm	A21042	IgG (H+L)			1:1000	Life Technologies
Goat anti-mouse	Alexa Fluor 488nm	A11029	IgM			1:1000	Life Technologies
Goat anti-rabbit	Alexa Fluor 488nm	A31627	IgG			1:1000	Life Technologies
Goat anti-mouse	Alexa Fluor 546nm	A21123	IgG (H+L)			1:1000	Life Technologies
Goat anti-mouse	Alexa Fluor 594nm	A11032	IgG			1:1000	Life Technologies
Goat anti-mouse	Alexa Fluor 594nm	A21135	IgG2a			1:1000	Life Technologies
Goat anti-rabbit	Alexa Fluor 594nm	A11012	IgG			1:1000	Life Technologies
Goat anti-mouse	Alexa Fluor 594nm	A21044	IgM			1:1000	Life Technologies
Donkey anti-goat	Alexa Fluor 568nm	A-11057	IgG (H+L)			1:1000	Life Technologies

a) WB, Western blotting; b) IHC, paraffin-embedded immunohistochemistry; c) IF, immunofluorescent histochemistry.

2.1.3. Bacterial strains

Field strains of bacteria were isolated from clinical cases of mastitis from the Waikato region of New Zealand and were kindly provided by John Williamson and Dr Jane Lacy-Hulbert from DairyNZ, Hamilton, NZ.

Streptococcus uberis (*S. uberis*) strain SR115 was isolated from a dairy farm near Morrinsville, NZ and was confirmed as Gram-positive, catalase-negative, cocci that can cleave esculin.

Staphylococcus aureus (*S. aureus*) strain LY7111SA and *Escherichia coli* (*E. coli*) strain LY3286EC were both isolated from DairyNZ's Lye Farm, Hamilton, NZ. *S. aureus* LY7111SA was confirmed as Gram-positive, catalase-positive, cocci that were mildly haemolytic on blood agar and coagulase positive within 4-18 h. *E. coli* LY3286EC was confirmed as a Gram-negative, rod-shaped bacterium.

2.1.4. Experimental animals

Dairy cattle used in this study were from an AgResearch commercial/research dairy farm (250ha), located south of Hamilton. The cows were from a high producing (>26,000 kg milk solids/annum) Holstein-Friesian (~65 %) and Holstein-Friesian/Jersey (~35 %) crossbred herd of mixed age, consisting of ~900 milking cows. The cows were predominantly pasture-fed (ryegrass and white clover) but supplemented with grass silage as required.

Both experimental trials were conducted in early autumn (April – May) on late-lactating cows identified to be culled from the farm.

2.1.5. Ethics approval

Experimental animal procedures were approved by the Ruakura Animal Ethics Committee (Agresearch Ltd, Hamilton, New Zealand) and the University of Waikato Animal Ethics Committee (University of Waikato, Hamilton, New Zealand) in accordance with the guidelines of the Animal Welfare Act, 1999; for the use of animals in research, testing and teaching.

2.1.6. Normal sera

Normal sera were used in all IHC procedures to reduce the non-specific binding of secondary antibodies. The species used was dependent on the animal source of the secondary antibody. All goat, rabbit and mouse serum were sourced 'in-house' from the clotted blood of non-immunised animals.

2.2. Methods

2.2.1. Tissue collection

At the conclusion of each trial, cows were killed by captive bolt and exsanguination at the Ruakura abattoir. For each cow, the entire mammary gland was removed post-mortem, and the teats were collected from each udder quarter. Contralateral forequarter and hindquarter teats from each udder were randomly selected for proteomic studies. The TCL from these teats were collected as described in Section 2.2.2. One of the remaining two contralateral teats was processed for histological analyses, as described in Section 2.2.15. The remaining teat was dissected along the sagittal plane, from the teat sinus through the teat canal to the teat orifice, for frozen sectioning as described in Section 2.2.18. For these tissue samples, excess material was removed, and segments of the teat-end tissue were immediately snap-frozen in liquid nitrogen for future histological processing.

Tissue samples (2 cm^2 sections) of the gland sinus and alveolar tissue were collected from randomly selected animals for comparative analyses. Lymphoid tissues from the super mammary lymph node and Peyer's patch were collected to act as positive control tissues for the optimisation of IHC methods. All tissue samples were either fixed in paraformaldehyde or snap-frozen in liquid nitrogen as described in Sections 2.2.15 and 2.2.18, respectively.

2.2.2. Collection of teat canal lining and teat skin

Teat ends were unilaterally dissected along the sagittal plane from the teat sinus through one-half of the teat canal to the teat orifice. The skin surface of each teat was gently cleaned with sterile water to remove dirt and faeces. The teat canal was opened up, and the sebum-like material present on the inner surface of the teat canal was removed by gently scraping a clean scalpel blade over the exposed surface of the canal, resulting in an accumulation of the lining material on the blade (Figure 2.1). There was no washing of the teat canal lining, and it was collected unsullied.

After removal of the TCL samples, the teats were snap-frozen in liquid nitrogen to solidify the teat tissue. Slivers of the frozen epithelial layer of the external surface of the teat were cut using a clean scalpel blade to provide samples of skin epithelium. The TCL and teat skin samples were transferred to individual pre-weighted 1.5 mL tubes and immediately frozen in liquid nitrogen before being stored at –80 °C for subsequent analyses.

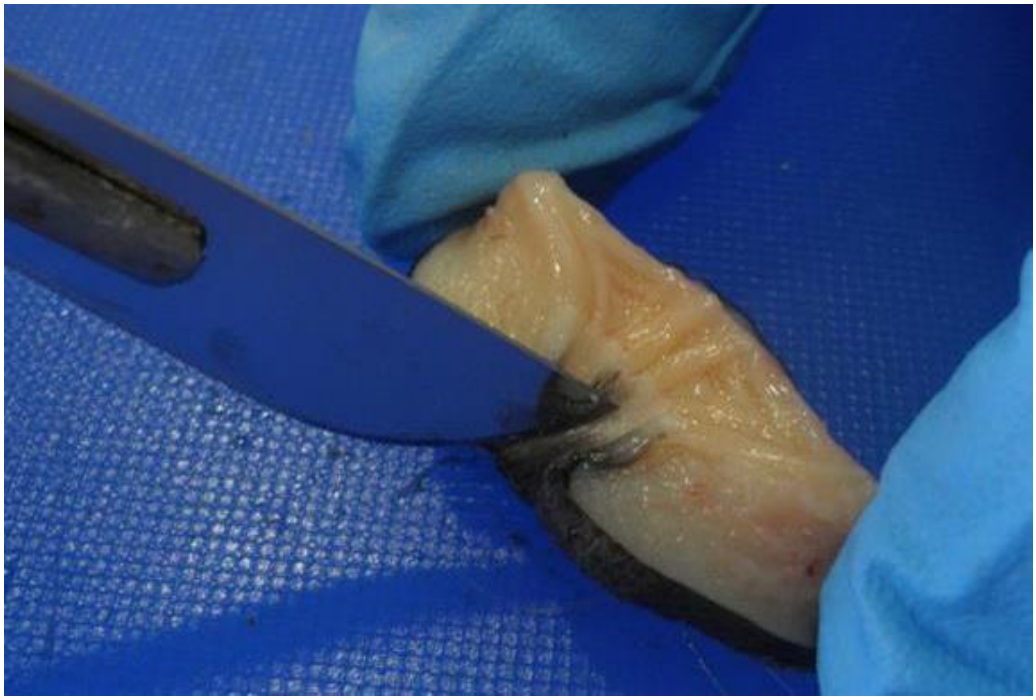

Figure 2.1: Collection of teat canal lining from a dissected teat by scalpel scraping.
The unilaterally dissected teat canal was spread wide so that the scalpel blade could be run over the epithelial surface of the teat canal lumen to collect the soft TCL. Care was taken not to disrupt the stratified squamous epithelial layer of the teat canal.

2.2.3. Milk sampling

2.2.3.1. Aseptic milk collection procedure

Milk samples for bacteriology were collected aseptically to determine the infection status of the gland.

Before milk collection, the teats were cleaned of all dirt using a 70 % (*v/v*) ethanol spray and Mediwipes (Sulco Limited, Auckland, NZ). Afterwards, the teat orifice was again sprayed with 70 % (*v/v*) ethanol and then meticulously cleaned with a new Mediwipe. Before sampling, the fore-milk was hand-stripped out to remove excess somatic cells residing in the teat sinus as well as to remove any bacterial flora residing in the teat canal. Two successive strips of milk (~ 3 mL) were collected into gamma-sterilised sample vials. Sample vials were capped immediately and labelled with the cow tag number and the quarter position. All sample vials were stored on ice for transportation and plated out within six hours of collection for bacteriological analyses. At all times clean gloves were used with both teats and gloves constantly sprayed with 70 % (*v/v*) ethanol to reduce the potential for cross-contamination.

2.2.3.2. Collection of milk from dissected udders

After the removal of each teat from the udder, a sterile 25 mL serological pipette was immediately inserted into the open cavity and milk was withdrawn before it could be contaminated with blood from the open wound. Milk (~ 2 mL) was then transferred into gamma-sterilised containers for bacteriology analyses. A 1 mL aliquot of milk was also collected for protein analyses.

2.2.3.3. Somatic cell count

Somatic cell count (SCC) was determined on 25 mL of milk using an automated, fluorescent, microscopic somatic cell counter (Fossomatic, Foss Electric, Hillerød, Denmark; operated by LIC, Hamilton, NZ).

2.2.4. Microbiological procedures

2.2.4.1. Sterilisation of liquid solutions

The following buffers and solutions were sterilised by autoclaving for 15 minutes.at 121 °C.

i. Sterile milk: 9.9 mL pasteurised trim milk.
ii. ¼ Ringer's solution: One salt tablet (Oxoid Microbiological Products) of Ringer's solution was dissolved in 500 mL MQ-H_2O + 0.5 g proteose-peptone (Gibco).
iii. Brain heart infusion broth (3.7 % *w/v*): Add 14.8 g brain heart infusion extract to 400 mL MQ-H_2O. Heat gently to mix before autoclaving.
iv. 0.85 % (*w/v*) Saline solution: Add 4.25 g NaCl to 500 mL MQ-H_2O.
v. 80 % (*v/v*) Glycerol solution: Add 10 mL MQ-H_2O to 40 mL glycerol.

2.2.4.2. Bacteriological assessment of quarter milk samples

Aseptically collected milk samples were examined microbiologically following the recommendations of the National Mastitis Council (Hogan, 1999). In brief, 10 µL of each milk sample was spread onto the surface of one-half of a Tryptic Soy agar plate containing 5 % sheep blood and 0.1 % esculin (*w/v*) (Fort Richard Laboratories, NZ; #1134). The plates were examined following 48 h incubation at 37 °C in aerobic conditions. Plates without visible colonies were deemed negative for bacterial growth and mastitis-associated pathogens. Plates with three or more colony types were considered contaminated, and aseptic milk samples were repeated from these cows. Bacterial colonies were provisionally identified based on colony morphology, appearance and haemolysis. Putative *S. aureus* colonies were differentiated from CNS colonies by the rabbit plasma coagulase test. *S. uberis* was identified by its morphology and ability to hydrolyse esculin.

Samples negative for bacterial growth were labelled NG; for no-growth. Bacterial growth of 1 to 10, 11 to 50 and more than 50 colonies was defined as +, ++, and +++, respectively.

2.2.4.3. Detection of bacteria in the teat sinus

Bacterial specimens were collected from the sinus cavity of dissected teat ends from 14-day involuted cattle. The specimens were obtained by introducing and pivoting a cotton swab 360° onto the sinus wall of a freshly dissected teat. The specimen swab was then placed back into its sterile transport container and labelled with both the cow tag number and the quarter position.

The bacterial load of the teat sinus was assessed using the same method previously described for "*Bacteriological assessment of quarter milk samples*" with a few minor changes. In brief, 20 µL of sterile 0.85 % (*w/v*) saline solution was placed on one-half of a trypticase soy agar plate containing 5 % sheep blood and 0.1 % (*v/v*) esculin. Individual specimen swabs were then placed onto the saline solution, and the swab rotated and swiped evenly across the half-plate to allow the transfer of bacteria onto the plate. The plates were examined following 48 h incubation at 37 °C in aerobic conditions and the bacterial colonies provisionally identified as before. Putative *S. aureus* colonies were further characterised using the rabbit plasma coagulase test.

2.2.4.4. Rabbit plasma coagulase test

To differentiate *S. aureus* species from CNS species, a tube coagulase test was performed using rabbit plasma. Coagulase is an enzyme produced by *S. aureus* that converts soluble fibrinogen in plasma to insoluble fibrin.

To perform the test, individual colonies of putative *Staphylococcus* species were picked from the agar plates, and a suspension was made with 0.5 mL rabbit plasma containing EDTA (Becton, Dickinson and Company, USA; #240827) in glass tubes (12 mm in diameter). The mixtures were incubated at 37 °C for 24 h. Controls using 50 µL of sterile 0.85 % (*w/v*) saline solution were included in each test. A positive test was recorded only when a visible coagulum mass was produced. Readings were recorded as negative, +, ++, +++, or ++++. A + recording indicates just perceptible coagulum, while ++++ represents a solid coagulated mass.

2.2.4.5. Growth conditions for stock solutions of bacteria

Five-millilitre aliquots of sterile 3.7 % (*w/v*) brain heart infusion broth (Oxoid, Basingstoke, UK) were inoculated with single colonies of *S. uberis* SR115, *S. aureus* LY7111SA, and *E. coli* LY3286EC for 24 h at 37 °C with gentle shaking. A 1 mL aliquot from each culture was then used to inoculate 49 mL of fresh brain heart infusion broth media, pre-warmed to 37 °C. The inoculums were incubated with gentle shaking until late exponential phase (OD_{600} of 0.6 - 0.8) was reached.

Parallel 50 mL cultures of the three bacteria were also inoculated at the same time so that a growth curve of OD_{600} verses time could be constructed. When late exponential phase was reached, the growth of the bacteria was stopped by placing the flask on ice and 0.5 mL aliquots taken for glycerol stocks.

2.2.4.6. Glycerol stocks

Glycerol stocks for long-term storage of bacteria were made by the addition of 0.5 mL of bacterial culture to 0.5 mL sterile 80 % (*v/v*) glycerol. Stocks were stored at -80 °C until required.

2.2.4.7. Preparation of cultures for teat canal infusion

The live bacterial cultures were prepared as follows: A stock solution (1 mL) of each bacterial culture was removed from storage at -80 °C and incubated at 37 °C for one hour. Bacteria were pelleted for 5 minutes at 3,000 x g and resuspended in 1 mL of one-quarter strength Ringer's solution (28 mM NaCl, 1.4 mM KCl, 0.6 mM $CaCl_2$, 0.6 mM $NaHCO_3$) containing 0.1 % (*w/v*) proteose-peptone. A 0.1 mL aliquot of each culture was then diluted 100-fold into sterile skim milk (9.9 mL) and incubated at 37 °C overnight (~16 h).

Ten-fold serial dilutions of the skim milk inoculum were prepared to 10^{-8} in sterile 0.85 % (*w/v*) saline. Bacterial counts were determined by spotting 10 µL of the serial dilutions (10^{-5} to 10^{-8} for *E. coli* and *S. aureus*; 10^{-4} to 10^{-7} for *S. uberis*) onto 0.5 % blood agar plates in triplicate and incubating them at 37 °C for 24 h (Figure 2.2). The average colony forming units per mL (cfu/mL) of each stock dilution was calculated and used to prepare each inoculum for the challenge trial. The objective was to obtain approximately 1.25 x10^6 cfu/mL for both the *S. uberis* and *S. aureus* inoculums, and 2.5 x 10^8 cfu/mL for the *E. coli* inoculum.

2.2.4.8. Bacterial inoculation of teat canals

Thirty-two quarters from eight cows were challenged by teat canal inoculation. Inoculations occurred two hours after morning milking using sterile Newbould inoculators (Newbould and Neave, 1965) (Figure 2.3). For each cow, individual teats were inoculated with two µL of sterile milk (Control), *S. aureus* (SA), *E. coli* (EC), or *S. uberis* (SU).

After morning milking the teat ends were sprayed with 70 % (*v/v*) ethanol and cleaned thoroughly using Mediwipes. Five minutes before inoculation, the teat orifice was given another clean to make sure that no contaminating material was still present. A total volume of 2 µL of bacterial solution was carefully loaded into the circular recess at the tip of each inoculator and gently inserted into the teat canal up to the shoulder of the rod. The inoculator was rotated 360° to deposit the bacteria evenly midway up the teat canal at a depth of approximately 4 mm. Once all cows were inoculated, temperature data loggers were inserted into the vaginal cavity to measure core body temperature over the 24 h period (See Section 2.2.5).

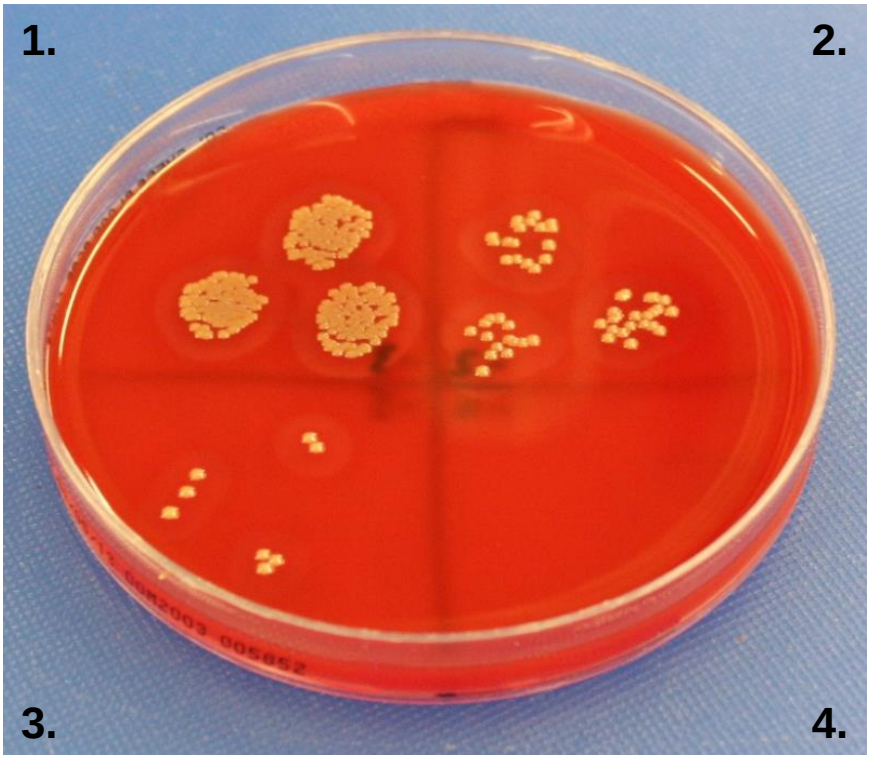

Figure 2.2: Ten-fold serial dilutions of *S. aureus* milk inoculum prepared to 10^{-7}.
Ten microliters of inoculum were diluted in 0.85 % saline and spotted in triplicate onto 0.5 % (*v/v*) blood agar plates. 1.) 1 x 10^{-5}, 2.) 1 x 10^{-6}, 3.) 1x10^{-7}, 4.) 1 x 10^{-8} dilutions. After incubation at 37 °C for 24 h, the colonies can be counted and the average cfu/mL of each stock dilution determined. **Note:** a small amount of haemolysis of the blood agar is visible surrounding each colony.

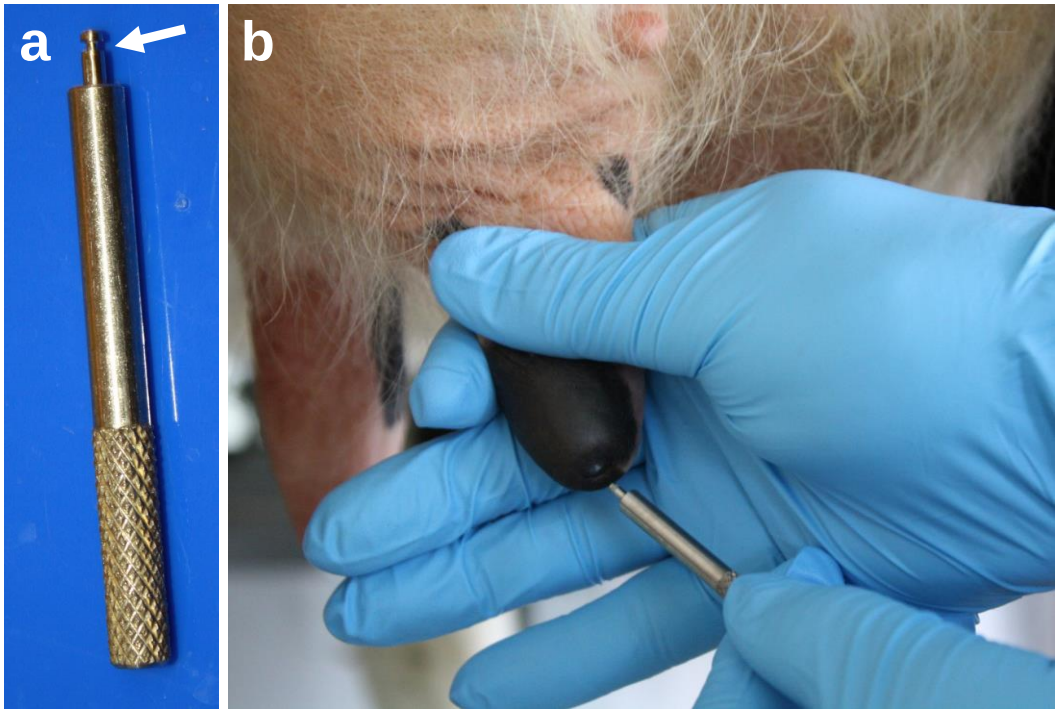

Figure 2.3: Bacterial inoculation of the teat canal using a Newbould inoculator.
(a) The stainless-steel rod is approximately 5 cm long and 4 mm in diameter. The head of the rod reduces to 2 mm in diameter for a distance of 6 mm. A recess 1 mm wide and 0.5 mm deep, 4 mm from the base of the head allowed for 2 µL of inoculum to be held in the recess of the inoculator. The 1 mm cap at the top of the rod held the inoculum in place and reduced the likelihood of bacteria from the inoculum being introduced further than 4 mm. The shoulder of the rod prevented the instrument from being inserted more than 6 mm into the teat canal. (b) Inoculation of the teat canal was performed by inserting the rod into the teat orifice, rotating the rod 360° and withdrawing the instrument to leave a film of inoculum along the inner lining of the teat canal epithelium.

2.2.4.9. Growth inhibition assays

Protein solutions were tested on their ability to inhibit the growth of bacteria using a plate growth inhibition assay.

A 1 mL glycerol stock solution of bacteria was incubated at 37 °C for one hour. The solution was vortexed briefly, and 100 µL of bacteria suspension was added to 4.9 mL BHI Broth and incubated at 37 °C overnight (~16 h). The bacterial solution was diluted 1:10, by adding 400 µL of broth to 3.6 mL 0.85 % (*w/v*) sterile saline solution. A 50 µL aliquot of the diluted bacteria solution was added to Petri-dishes containing Nutrient agar (Fort Richard Laboratories, NZ; #1240) and spread around uniformly so that the bacteria could grow into an even lawn.

The ability of various protein solutions to inhibit the growth of the bacteria was examined by spotting three 10 µL serial dilutions of the protein solution onto quarters of the dish. In the fourth quarter, a 10 µL sample of buffer solution was spotted to act as a negative control. On separate dishes, 10 µL of positive control samples were spotted. These included 0.001 % (*v/v*) Pen/Strep antibiotic mixture (Life Technologies; #15140-122) and a panel of human and bovine cathelicidin peptides; 0.5 µM LL-37 peptide, 0.5 µM bac5-linier peptide, 0.5 µM bac5-dimer peptide, and 0.5 µM bac4 peptide. The Petri-dishes were then incubated for 24 h at 37 °C, and growth inhibition was demonstrated by a clear zone in the bacterial lawn.

2.2.5. pH measurements

The pH of the teat canal lining was measured by using a pH meter (Laqua Twin compact pH33 meter; Horiba, Kyoto, Japan) calibrated at pH 4.0 and pH 7.0. Each sample of teat canal lining was placed on the sensor pad and flattened to cover the whole sensor. After each reading, the sensor pad was washed with Milli-Q water and carefully dried with a soft tissue.

2.2.6. Temperature data loggers

Directly after milking and approximately 90 minutes before teat canal inoculation, temperature loggers were inserted in the vaginal cavity to measure the core body temperature (for each group, n = 4). Vaginal temperatures were recorded at 10-minute intervals using a microprocessor-controlled temperature logger (Minilog 8-bit data logger; Vemco Ltd., Canada) for 24 to 30 h. Approximately one hour before slaughter, the temperature loggers were removed. Data were downloaded from each logger using a Minilog-PC interface and Minilog software and converted to Excel™ format for data analyses (Figure 2.4).

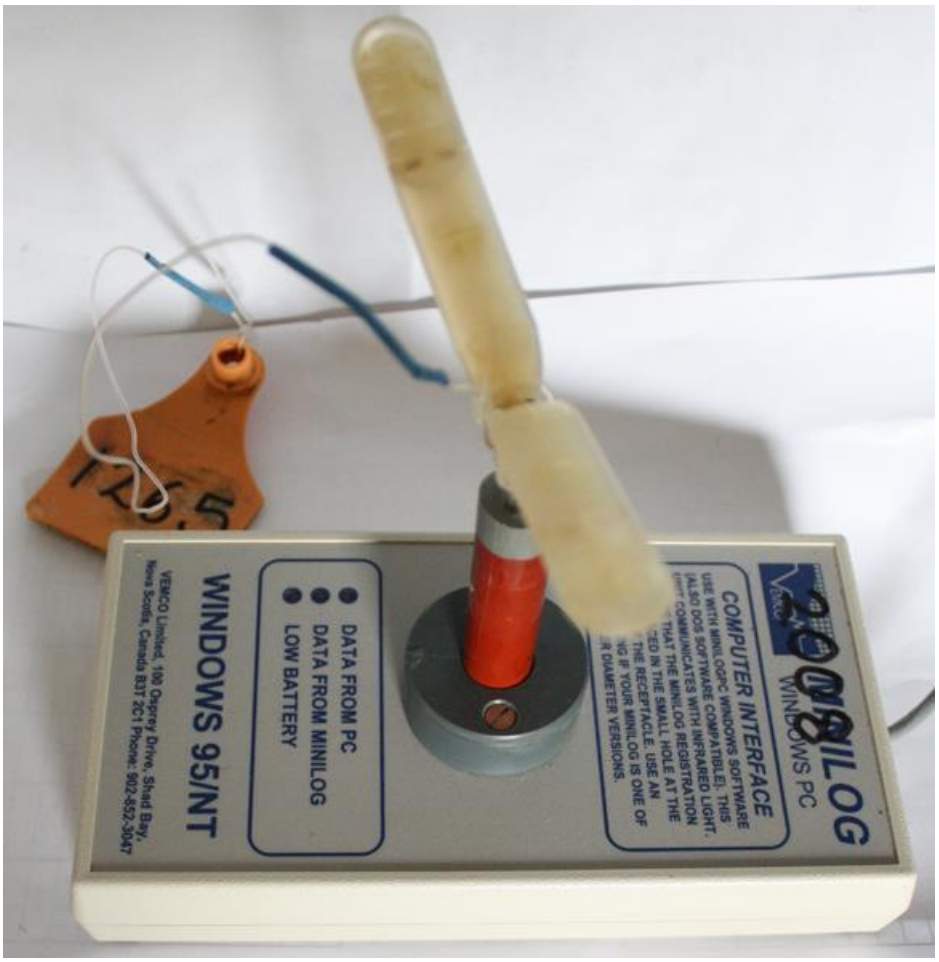

Figure 2.4: Vemco minilog 8-bit data logger.
Vaginal temperatures, recorded at 10-minute intervals during the 24 h trial period was downloaded and converted to Excel format for data analyses.

2.2.7. Protein estimation

Protein estimation was performed using two different dye-binding methods.

2.2.7.1. Bradford protein assay

Total protein concentration in milk was measured using the Bradford protein assay as per the manufacturer's instructions (Bio-rad; #500-0006). The standard curve was generated using 0, 3, 6, 9, 12, 15 and 18 µg/mL bovine serum albumin (BSA) calibration standards, prepared from a 1 mg/mL standard solution. The absorbance of the unknown protein samples was measured at 595 nm (Shimadzu; UV-160A) and their concentrations calculated from the calibration curve. Each sample was measured in triplicate using two different sample volumes.

2.2.7.2. 2D-Quant protein assay

The protein concentration of teat epidermal and teat canal keratin samples that had been solubilised in 2D lysis buffer (Section 2.2.8) was measured using the 2-D Quant kit (GE Healthcare; #80-6483-56) according to the manufacturer's instructions. Briefly, the standard curve was prepared using 0, 10, 20, 30, 40 and 50 µg of BSA prepared from a 2 mg/mL standard solution provided by the kit. The absorbance of the unknown protein samples was measured at 480 nm (Shimadzu; UV-160A) and their concentrations calculated from the calibration curve. Each sample was measured in triplicate.

2.2.8. SDS-polyacrylamide gel electrophoresis (SDS-PAGE)

SDS-PAGE was performed according to the basic principles developed by Laemmli (1970). Milk, supernatant and lysate samples were made to 2 mg/mL using 3x Laemmli sample buffer (187 mM Tris; pH 6.8, 30 % (*v/v*) glycerol, 15 % (*v/v*) β-mercaptoethanol, 6 % (*w/v*) SDS, plus a couple of grains of bromophenol blue) whereas proteins extracted from TCL using 2D sample buffer (See Section 2.2.8) were made to 1 mg/mL. All samples were fully denatured by boiling for 3 minutes in a heated water bath. Following heat treatment, samples were vortexed for 30 sec and centrifuged for 5 minutes at 12,000 x g, to pellet any insoluble material.

Protein samples were loaded into wells (maximum of 25 µL) of pre-cast Criterion-XT Bis-Tris 12 % acrylamide gels (Bio-rad; #345-0118). Samples were separated on the gels using the 2-(N-morpholino) ethanesulfonic acid (XT MES, Bio-rad; #161-0796) running buffer system run at a constant voltage of 100 V for two hours. SeeBlue Plus2 prestained protein standards (Life Technologies; #LC5928) were run on all SDS-polyacrylamide gels for molecular weight determination. After electrophoresis, gels were washed in two changes of gel fixing solution (50 % (*v/v*) methanol, 2 % (*v/v*) phosphoric acid) prior to overnight staining with colloidal Coomassie blue (CCB) (17 % (*w/v*) $(NH_4)_2SO_4$, 2 % (*v/v*) phosphoric acid, 0.06 % (*w/v*) Coomassie G-250). Digital images of the gels were captured using a GS-800 calibrated densitometer (Bio-rad) and processed with Quantity One 1-D software package (v4.6.6, Bio-rad).

2.2.9. Two-dimensional electrophoresis (2-DE)

Proteins solubilised from the teat canal lining and teat skin were subjected to two-dimensional electrophoresis (2-DE) as follows:

2.2.9.1. Sample preparation

A portion of each individual TCL and skin scraping sample (See Section 2.2.2) was resuspended in 2D lysis buffer (50 mM Tris, pH 8.0; 8 M urea, 3 M thiourea, 65 mM dithiothreitol (DTT), 0.1 % SDS, 4 % (*w/v*) 3-[(3-cholamidopropyl)-dimethylammonio]-1-propane sulfonate (CHAPS)) to achieve a final tissue:buffer ratio of 25 mg of sample (wet weight)/mL of lysis buffer. The samples were shaken vigorously for one hour at RT and incubated in a sonicating water bath (Fisher Scientific, Model FS-9) for 15 minutes. After a second round of shaking and sonication, the lysates were then centrifuged for 15 minutes at 14,000 x g to sediment any insoluble material. The protein concentration of the supernatant was determined using a 2-D Quant protein assay kit (See Section 2.2.6).

2.2.9.2. Isoelectric focusing (IEF) of proteins

An equal amount of protein from each of the individual cows in each sample group was pooled to create a sample with enough protein for 2-DE analyses. Up to 12 strips could be focused in a single run.

Aliquots of pooled sample containing 350 µg of protein was made up to 125 µl with urea sample buffer (50 mM Tris, pH 8.0; 8 M urea, 3 M thiourea, 65 mM DTT, 65 mM CHAPS) and then mixed with 225 µl of rehydration buffer (8 M urea, 6 mM DTT, 2 % (*w/v*) CHAPS, 2 % (*v/v*) immobilized pH gradient (IPG) buffer (GE Healthcare; #17-6004-40) plus a few crystals of Orange-G). The sample solution (350 µl) was evenly applied lengthwise into a lane of a rehydration tray (Bio-rad; #165-4041), and an 18-cm, pH 3-11, non-linear, IPG DryStrip (GE Healthcare; #17-6003-76) was lowered, gel-side down, on top of the sample. The tray was wrapped in Gladwrap to prevent dehydration and left overnight at RT for the DryStrips to passively absorb the protein solution.

After rehydration, the IPG DryStrips were transferred to a PROTEAN II IEF cell (Bio-rad; #165-4000) and laid, gel-side down, on top of 'wetted' wicks that covered both the anode and cathode electrodes. The strips were then covered with mineral oil, and IEF was carried out for a total of 90 kVh using the ramping protocol listed in Table 2.4. In all cases, the current was limited to ≤50 μA/strip.

Table 2.4: PROTEAN II focusing protocol for isoelectric focusing of IPG strip

Step	Time (min)	Voltage (V)	RAMP	Vh
1	10	500	rapid	83
2	80	500	rapid	750
3	60	1000	rapid	1,600
4	60	2500	rapid	3,700
5	1040	5000	rapid	89,200
6	20	100	linear	90,006
7	30	100	linear	90,056

After IEF was completed, the IPG strips were removed from the tray and equilibrated for 20 minutes in 2D-equilibration buffer (6 M urea, 50 mM Tris-HCl (pH 6.8), 2 % (*w/v*) SDS, 30 % (*v/v*) glycerol) containing 0.25 % (*w/v*) DTT, and then for another 20 minutes in 2D-equilibration buffer containing 2.5 % (*w/v*) iodoacetamide.

2.2.9.3. Large format SDS-PAGE

Following separation of proteins in the first dimension, the second dimension is performed using large format SDS-PAGE where proteins were separated according to their molecular weights. All gel incubations in solutions were carried out with gentle agitation on an orbital shaker in sealed containers.

The IPG strip was laid on top of a discontinuous 14 % T/2.7 % C Tris-glycine SDS-PAGE gel (1.0 x 180 x 180 mm) with a 4 % T/2.7 % C stacking gel (1.0 x 15 x 180 mm). Electrophoresis was carried out at a constant current of 25 mA/gel, for the first 90 minutes, and 35 mA/gel after that until the bromophenol blue dye front was one cm from the bottom of the gel. Molecular weight determination

was performed by loading 10 µL of Broad Range molecular weight standards (Bio-rad, #161-0317) in a well on one side of the large format gel.

After completion of second-dimension electrophoresis, the gels were washed in three changes of gel fixing solution to remove all contaminants. The gels were covered with CCB staining solution for overnight staining. Gels were destained firstly in 10 % (v/v) methanol for two hours and then in two changes of 5 % (v/v) methanol for a further four hours.

Gel image acquisition and analyses

CCB stained 2-DE gels were scanned using a GS-800 calibrated densitometer (Bio-rad) at a pixel resolution of 63.5 µm and the images were processed using Quantity One (Bio-Rad). Spot matching and quantification were performed using the PDQuest (v8.0.1) Advanced 2-D software package (Bio-Rad).

Before analyses, each gel was cropped to a dimension of 185 mm x 156 mm to enable consistent spot processing across all sample gels. Gel images were warped, and spot centres were determined by Gaussian modelling using the automated 'Spot Detection Wizard'. The individual quantity of resolved spots was normalised using the local regression model LOESS. The program identified matched and unmatched spots from all gels in the match-set. Landmark spots were manually defined, and spot editing was performed to increase the correlation between the different 2-DE gels. All detected spots were inspected for quality and accurate alignment in the match-set. Spots incorrectly matched were manually re-matched.

Quantitative analysis tools within PDQuest were used to find spots that differed between gels from each sample group. Match-sets were constructed from triplicate gels and were analysed as two groups in Chapters 3 & 5; Group A was the control group consisting of normal lactating TCL whereas Group B was either the teat skin (Chapter 3) or TCL from d14 involuted cattle (Chapter 5). For the challenge studies in Chapter 6, TCL samples were analysed in four groups; control TCL (A), *S. aureus* (B), *E. coli* (C) and *S. uberis* (D). The analysis tool "outside limits" was used, and ±2.0-fold change was set as the lower limit.

Statistical analyses of the relative abundance of each matched protein spot, between replicate groups, was performed by using Student's two-tailed *t*-test. Proteins displaying quantitative differences with a *p*-value of ≤0.05 were considered statistically significant, and protein spots with an intensity of 30 or greater were further analysed by MS/MS.

2.2.10. Antibody development and purification

Rabbit polyclonal antibodies to bovine RNase7 and bovine pancreatic adenocarcinoma upregulated factor (PAUF) were produced in New Zealand White Rabbits for use in this thesis. Inoculations and blood collection were performed under animal ethics approval by Ric Broadhurst (Small Animal Colony, AgResearch, Ruakura, NZ).

The entire amino acid sequence for bovine RNase7-like protein (DAA25514.1) and bovine PAUF-like protein (DAA15702.1) was obtained from the National Center for Biotechnology Information (NCBI). Synthetic peptides were synthesised by AusPep Proprietary Ltd. based on their location within the complete protein sequence, charge, hydrophobicity and polarity. The following peptide sequences were synthesised:

Protein	**Amino acid sequence**	**Amino acid number**
RNase7	RPGNMTPAQWFETQHVQPSPQGC	28 – 50
PAUF	C-GQHKLLGISSIGFDWDYPIVR	135 – 155

To facilitate conjugation to carrier proteins, the PAUF peptide was synthesised with an additional cysteine residue at the amino-terminus.

Synthetic peptides were activated and coupled to the amino groups of keyhole limpet hemocyanin (KLH, Sigma-Aldrich; #H7017) and ovalbumin (Sigma-Aldrich; #A5503) using the ester maleimidobenzoyl-N-hydroxysulfosuccinimide (MBS, Sigma-Aldrich; #M278) by the following methods:

2.2.10.1. Activation of carrier proteins

KLH and ovalbumin were made up to 10 mg/mL in 150 µL and 50 µL of phosphate buffered saline (PBS) (0.14 % (*w/v*) NaH_2PO_4, 0.57 % (*w/v*) Na_2HPO_4 and 0.9 % (*w/v*) NaCl, pH 7.4), respectively. Protein solutions were aliquoted into separate 1.5 mL microfuge tubes. Five milligrams of MBS was dissolved in 250 µL of dimethylformamide (DMF, Sigma-Aldrich; #D8654). To KLH, 20 µL of MBS was added and to ovalbumin 6.6 µL of MBS was added in dropwise fashion with gentle mixing between each drop. The solutions were left for 30 minutes with occasional mixing. Two 1 mL G-10 Sephadex columns (GE Healthcare) were equilibrated with PBS, and the activated-KLH and activated-ovalbumin samples were added to the tops of each column. Fifteen fractions of 0.5 mL were collected for each protein by the addition of 7.5 mL PBS in 0.5 mL aliquots. Fractions containing the eluted proteins were determined using the Bradford protein assay and pooled together (~3.5 mL total volume).

2.2.10.2. Coupling of peptide to activated carrier proteins

Lyophilised synthetic peptide was dissolved in 300 µL of PBS at 10 nM final concentration. The peptide solution (150 µL) was added to the pooled activated-KLH fraction, and 50 µL of peptide solution to the pooled activated-ovalbumin fraction and the samples left to mix for three hours. The remaining peptide solution (100 µL) was stored for use as an antibody blocking reagent if required.

The protein solutions were dialysed against three 2 L changes of PBS at 4 °C overnight to remove any uncoupled peptide. The protein content of each solution was determined using the Bradford protein assay. The peptide-KLH conjugate solution was divided into two lots with aliquots of 1 x 200 µg, and at least three aliquots of 100 µg for rabbit inoculations.

2.2.10.3. Inoculation of rabbits

The peptide-KLH conjugate (200 µg/rabbit) was emulsified in an equal volume of Freund's complete adjuvant and injected subcutaneously at multiple sites into two NZ white rabbits by Ric Broadhurst (AgResearch Ltd). Two weeks after the initial inoculation, the rabbits were inoculated again using 100 µg/rabbit of peptide-KLH conjugate emulsified in an equal volume of Freund's incomplete adjuvant. Two more subsequent boosts were given at intervals of two weeks. A week after the final boost, a test bleed was performed to gauge antigen reactivity. If the reactivity of the sera was high enough, the rabbits were bleed-out for the harvesting of the serum.

Rabbit blood was collected in 10 mL glass Vacutainer blood collection tubes (Becton Dickinson and Company, NJ, USA; #366430) and allowed to stand at RT for three hours to allow clot formation to occur. The tubes were centrifuged for 10 minutes at 200 x g, at 4 °C and the serum layer carefully transferred to 50 mL centrifuge tubes (Fisher Scientific; #LBSCN8CT50). The centrifuge tubes were then spun at 200 x g for a further 5 minutes to remove any remaining red blood cells. The serum was then aliquoted into 12 mL storage tubes and kept at -80 °C until required.

2.2.10.4. Purification of serum immunoglobulins

Immunoglobulins were partially purified from the rabbit antiserum using ammonium sulphate precipitation and protein A agarose (Sigma-Aldrich; #P9424).

Whole serum (~10 mL) was diluted two-fold with 100 mM Tris, pH 8.0. The serum solution was slowly made up to 50 % (*w/v*) $(NH_4)_2SO_4$ saturation and left to stand on ice for one hour. The precipitated protein containing immunoglobulins was centrifuged at 1,100 x g for 5 minutes at 4 °C and the supernatant removed. The protein pellet was re-solubilised in 4 mL of 100 mM Tris, pH 8.0 and loaded onto five mL of protein A-agarose beads packed in a 10 mL Poly-Prep chromatography column (Bio-rad; #731-1550). The column was washed with 20 mL of 100 mM Tris, pH 8.0 and immunoglobulins were eluted

with 10 mL of 100 mM Glycine, pH 3.0. The eluate was collected in 0.5 mL fractions into 100 µL of 1 M Tris, pH 8.0. Each fraction was mixed immediately, stored on ice and the protein concentration determined by the Bradford protein assay. Fractions containing immunoglobulins were pooled and dialysed at 4 °C overnight against two 3 L changes of 10 mM Tris, pH 7.8 containing 1 mM phenyl-methanesulfonyl fluoride (PMSF, Sigma-Aldrich; #P7625). After dialysis, the protein concentration of the pooled antibody solution was determined, and aliquots stored at -80 °C.

The concentration of the Protein-A purified primary antibody to be used in experimental procedures was optimised by using half-log serial dilutions (e.g., 1:300, 1:1000, 1:3000, 1:10,000, 1:30,000, 1:100,000) on milk or tissue lysate samples known to contain the protein of interest, as well as on the ovalbumin-peptide conjugated protein (50 ng/lane). These samples were all separated by SDS-PAGE and analysed by Western blotting analyses. The dilution of the secondary antibody and the amount of protein (e.g., from 0.5 - 30 µg protein/lane) were also optimised across a smaller primary antibody dilution range.

2.2.11. Western blotting

Primary and secondary antibodies and concentrations used for Western blotting experiments are listed in Table 2.2 and Table 2.3 respectively. All polyclonal and monoclonal antibodies were stored as aliquots at -20 °C while antibodies in use were stored at 4 °C.

Proteins separated by SDS-PAGE were transferred from the gel onto BioTrace NT nitrocellulose membrane (Pall Corporation, FL, USA; # P/N66485) using the Trans-Blot Cell (Bio-rad; #170-4070) wet blotting system. Electroblotting of proteins were conducted in electroblot transfer solution (10 mM CAPS, pH 11; 10 % *(v/v)* methanol) at 15 V overnight (or at 45 V for 3 h). Alternatively, the semi-dry transfer was performed using the iBlot Dry Blotting system (Life Technologies; #ib21001) for 7 minutes according to the manufacturer's instructions. Following transfer, the membranes were stained with 0.1 % (*w/v*) Ponceau S (Sigma-Aldrich; #P3504) made up with 1 % (*v/v*) acetic acid for 2 minutes and then rinsed in MQ-H_2O until protein bands were clearly defined.

Membranes were scanned using a GS-800 densitometer and images digitised using Quantity One 1-D software.

Membranes were blocked in skim milk blocking solution (4 % (*w/v*) non-fat skim milk powder, 50 mM Tris; pH 7.5, 150 mM NaCl, 0.1 % (v/v) Tween-20) for 2 h and then washed in three changes of Tris-buffered saline (TBS) (50 mM Tris; pH 7.5, 150 mM NaCl) for 3 minutes each before membranes were incubated with primary antibody diluted in TBST/BSA (TBS plus 0.1 % (*v/v*) Tween-20 and 0.1 % (*w/v*) BSA) at 4 °C overnight. The membranes were washed in TBS and reprobed for 2 h with 50ng/mL goat anti-rabbit immunoglobulin conjugated to horseradish peroxidase (GAR, Sigma-Aldrich). The blots were visualised using enhanced chemiluminescence (ECL) as previously described (Broadhurst *et al.*, 2015). The chemiluminescent signal was visualised by exposure to X Omat AR film (Eastman Kodak Company, NJ, USA), or by using a ChemiDoc XRS imager (Bio-rad). Developed films were scanned on a GS-800 densitometer, and the intensity of immunoreactive bands was quantified using Quantity One 1-D software.

2.2.12. In-gel tryptic digestion

2.2.12.1. 2-DE protein spots

Protein spots from 2-DE gels were manually excised as gel pieces of approximately 1 mm^2 and transferred into 0.5 mL Protein Lo-bind tubes (Eppendorf AG, Hamburg, Germany; #022431064). The gel pieces were destained overnight with three changes of wash buffer (50 mM NH_4HCO_3/ 50 % (*v/v*) acetonitrile) followed by a wash in 100 % acetonitrile for 2 minutes. The clear gel pieces were then dried for 10 minutes in a rotary Speed-Vac concentrator (Thermo Scientific; RVT400). Each gel piece was then rehydrated with 15 µL of digest solution (50 mM NH_4HCO_3, pH 7.8; 10 % acetonitrile) containing 50 ng/mL sequencing grade modified trypsin (Promega, Madison, USA; #V5111). After incubating the tubes for 30 minutes on ice, an additional 20 µL of digest solution was added to cover the gel pieces and the mixture was incubated for a minimum of 20 h at 37 °C. The protein digests were sonicated for 10 minutes in an ultrasonic water bath and the supernatant from each tube was transferred to a

new 0.5 mL Protein Lo-bind tube using a 200 µL gel loading tip (Biorad, #2239917); which was kept in the tube for subsequent transfers. Peptides remaining in each gel were recovered by sonicating the gel pieces for 10 minutes with 50 µL of fresh extraction buffer consisting of 0.1 % (*v/v*) trifluoroacetic acid in 50 % (*v/v*) acetonitrile. After recovering the buffer, a second extraction was performed with the same buffer followed by a wash with 20 µL of 100 % acetonitrile for 2 minutes. The four supernatants were combined, lyophilised and reconstituted in 50 µL of MS loading buffer consisting of 0.2 % (*v/v*) formic acid for tandem mass spectrometry (MS/MS) analyses.

2.2.12.2. 1D gel slices (GeLC-MS/MS)

The peptide extraction from 1D gel slices was essentially the same method used as for the peptide extraction from 2-DE protein spots. Modifications included a four-fold increase in buffer volume for each step, use of 1.5 mL Protein Lo-bind tubes (Eppendorf AG; #022431081), and the reduction and alkylation of the proteins before digestion.

For GeLC-MS/MS analyses the entire lane was excised from the gel and separated into 10 gel slices based on the molecular mass of the SeeBlue Plus2 markers. Each gel slice was then cut into multiple slivers of approximately 1 mm in width to assist in the destaining, digestion and extraction of the tryptic peptides (Figure 2.5).

Proteins in the 1D gel slices were reduced by treatment with 150 µL 10 mM DTT for 30 minutes at 56 °C. The 1D gel pieces were dehydrated with 100 % acetonitrile, dried in a rotary Speed-Vac concentrator, and alkylation was performed with 150 µL 55 mM iodoacetamide in 50 mM ammonium bicarbonate for one hour in the dark. Gel pieces were once again dehydrated with 100 % acetonitrile and dried in a rotary Speed-Vac concentrator before peptide extraction as essentially described previously in Section 2.2.12.1.

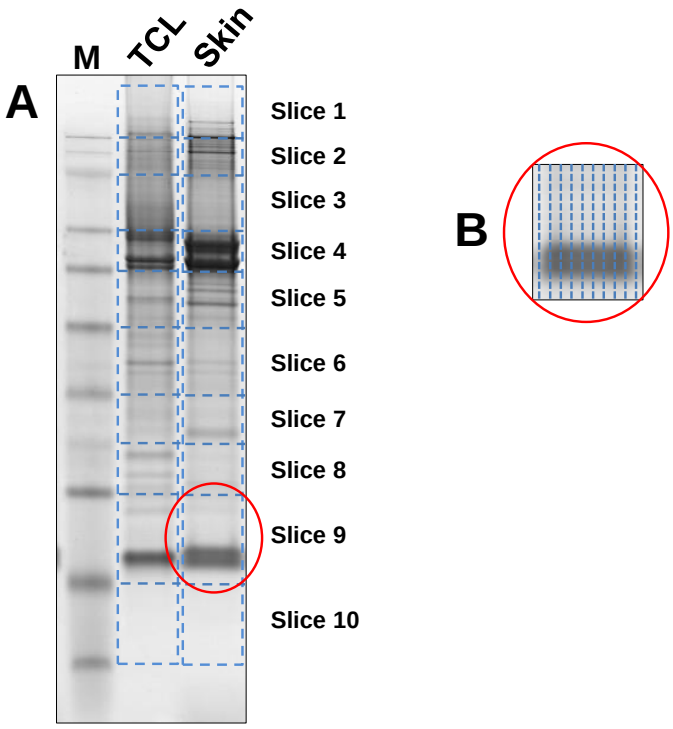

Figure 2.5: SDS-PAGE separation of teat canal lining and teat skin protein extracts.
(A) Individual lanes were cut into ten separate slices based on the position of the SeeBlue Plus2 molecular weight markers (M). (B) Each gel slice was further divided into multiple slivers, as indicated, for efficient removal of Coomassie stain, reduction, alkylation and tryptic digestion.

2.2.13. GeLC-MS/MS analyses

For GeLC-MS/MS analyses the peptides in each fraction were reconstituted in 300 µL of MS loading buffer. Due to the low amount of protein observed in slices 1 and 10 for both the TCL and teat skin extracts, slices 1 & 2 were combined as were slices 9 & 10, respectively for peptide identification. Each of these fractions was reconstituted in 150 µL of MS loading buffer resulting in a total of eight 150 µL fractions for each GeLC analyses set.

2.2.14. LC-ESI-Q/TOF mass spectrometry

All protein digests were analysed by nano liquid chromatography electrospray ionisation quadrupole time-of-flight (LC-ESI-Q/TOF) tandem mass spectrometry (MS/MS) using a nano-Advance UHPLC (Bruker-Daltonics, Bremen, Germany) coupled to a maXis high definition ultra-high resolution Q/TOF mass spectrometer (Bruker-Daltonics) located at the Lincoln campus, AgResearch Ltd. For each sample, 5 µL was loaded on a Magic C18AQ nano trap column (5 µm particle, 100 µm x 100 mm, 200 Å; Bruker-Michrom, Bremen, Germany) at a flow rate of 5000 nL/minute for 5 minutes in mobile phase solvent A (0.2 % formic acid in MQ-H_2O). The trap-column was then switched in-line with the analytical column (Intensity C18P, 1.8 µm particle, 100 µm x 150 mm, 100Å; Bruker-Michrom) heated to 50 °C. Peptides were eluted from the trap column to the analytical column at a flow rate of 800 nL/minute, with the introduction of mobile phase solvent B (0.2 % formic acid in 99.8 % acetonitrile), using the reverse phase gradient listed in Table 2.5. The eluent from the analytical column was introduced directly into the maXis using a captive spray nano-ESI source (Bruker-Daltonics). The instrument was set up to perform collision-induced dissociation (CID) on selected precursor ions. A mass/charge (*m/z*) range of 300–1250 Da was used for data-dependent precursor scanning. The three most intense precursor ions in each MS scan were selected for CID fragmentation and MS/MS analyses. Dynamic exclusion was enabled for 0.2 minutes after a repeat count of 2.

Table 2.5: Gradient-elution programme for reverse-phase HPLC

Step	Time (min)	Solvent A (%)	Solvent B (%)
isocratic hold	0	98	2
	5	98	2
elution gradient	25	55	45
wash	26	5	95
	29	5	95
equilibration	30	98	2
	35	98	2

2.2.15. Data analyses

2.2.15.1. Protein identification

The raw MS data were deconvoluted using the Compass DataAnalysis software (v4.0 SP5, Bruker-Daltonics) software package and peak lists were imported into the ProteinScape (v3.1.3, Bruker-Daltonics) Bioinformatics Platform for data analyses. Peak lists were queried against a target-decoy version of the *Bos taurus* NCBI non-redundant database (release date, Jan. 22, 2014) using the Mascot search engine (v2.3; Matrix Science, London, UK). For protein identification, the MS and MS/MS error tolerances were set to ±10 ppm and ±0.05 Da, respectively, with one missed tryptic cleavage allowed. Carbamidomethylation of cysteine was included as a fixed modification and N-terminal ammonia-loss, deamidation of asparagine and glutamine, phosphorylation of serine and threonine, and oxidation of methionine set as variable modifications. Search results were compiled and analysed by ProteinScape, and peptide identifications were accepted if the Mascot ion score was ≥25 with a false discovery rate (FDR) limited to 5 %. All proteins with low numbers of identified peptides (< 5) were manually interpreted to eliminate any potential false positives.

2.2.15.2. Label-free quantification

Mascot generic files (MGF) were converted to DAT files using the Mascot export function. Scaffold Q+ (v4.3.0, Proteome Software Inc, OR, USA) was used to verify MS/MS peptide identifications by Mascot using the X!Tandem database searching program (Searle, 2010). Peptide identifications were accepted if they could be established at greater than 95.0 % probability as specified by the PeptideProphet algorithm (Keller *et al.*, 2002). Protein identifications, with a minimum of 2 identified peptides, were accepted if they could be established at greater than 99.9 % probability, as specified by the ProteinProphet algorithm (Nesvizhskii *et al.*, 2003). The FDR was calculated by searching a "target-decoy" database. The decoy database consisted of the target database sequences concatenated to a separate database made up of the target sequences in the reverse order.

For label-free quantification by spectral counting (SpC), data were normalised across each set of biological samples. Fold change (Fc) was determined using average normalised total raw spectra whereas fold change and relative protein quantification was determined using 'built-in' algorithms for determining the average exponentially modified protein abundance index (emPAI) or averaged Normalised Spectral Abundance Factor (NSAF). For the data to be considered valid, a minimum of 5 SpC must be observed in at least one of the biological samples. Both unpaired and paired *t*-tests were used to determine the significant difference (p-value < 0.05) between the late-lactating and involution experimental groups and between the control and treatment samples, respectively.

Fold change was defined as the ratio of the averaged experimental values over the averaged control values. Where the average value for the divisor (control values) was zero, half the minimal SpC (0.5) was used as a replacement for the fold calculations. Where the average value of both the numerator and the divisor were zero, a fold change of 1.0 was recorded. Proteins with significant changes and had SpC that were at least twice the control values were considered as up-regulated proteins. Similarly, those values with a two-fold decrease were regarded as down-regulated proteins. In some cases, proteins in the biological replicates were highly variable. Values that were not deemed significant but had an average five-fold change in SpC (i.e., p-value ≥ 0.05, Fc ≥ 5 or ≤ 0.2) were tentatively added to the significance list.

2.2.16. Peptidomic analyses

2.2.16.1. Solubilisation of teat canal lining

Frozen teat canal lining samples were pooled together and mixed with MQ-water at a ratio of 125 mg/mL in a Protein Lo-bind tube. The samples were vortexed for 5 minutes and then sonicated for a further 10 minutes in a sonicating water bath. The suspension was then subjected to sonication (four 15-s pulses at 30 % power) using a Vibra-Cell probe-tip sonicator (VC 50T, Sonics & Materials, CT, USA) operating at a frequency of 25 kHz. In between sonication, the sample was placed on ice for 1 minute to reduce unwanted heating. The resulting emulsion was centrifuged at

12,000 x g for 10 minutes and the supernatant, containing released proteins and peptides, was assayed for total protein concentration and stored at -20 °C.

2.2.16.2. Organic solvent precipitation

Endogenous peptides were extracted from 200 µL of teat canal lining supernatant by methanol/chloroform precipitation (Wessel & Flügge, 1984). To 200 µL of teat canal lining extract, 800 µL of methanol was added and mixed well. Chloroform (200 µL) was added and mixed with the methanol solution. To the organic solvent mix, 600 µL of Milli-Q water was added, vortexed briefly, and then spun at 12,000 x g for 1 minute. Approximately 800 µL of the peptide-rich aqueous phase (top layer) was collected, lyophilised and then made back up to 1 mL with 2 % acetonitrile/0.1 % formic acid for solid-phase extraction.

2.2.16.3. Solid phase extraction

Oasis hydrophobic/lipophilic balance (HLB) cartridges (1cc, 10mg HLB; Waters, MA, USA) were conditioned with 1 mL methanol, equilibrated with 1 mL 75 % acetonitrile/0.1 % formic acid and then washed with 5 mL of 2 % acetonitrile/0.1 % formic acid. One millilitre of sample was loaded onto the HLB cartridge and drawn through the resin at a flow rate of ~0.5 mL/minute. The cartridge was then washed with three 1 mL washes of 2 % acetonitrile/0.1 % formic acid. The peptides were eluted firstly with 600 µL of 15 % acetonitrile/0.1 % formic acid, and then secondly with 600 µL of 60 % acetonitrile/0.1 % formic acid. The combined peptide-enriched eluate was then lyophilised. For LC-ESI-Q/TOF MS/MS analyses the peptide-enriched sample was reconstituted with 50 µL of 2 % acetonitrile/0.1 % formic acid and processed as described previously in Section 2.2.14.

2.2.16.4. Peptide identification

Data analyses were performed as previously described in Section 2.2.15 with the following modifications. No enzyme was selected, and no missed cleavages were allowed. The peptides were not alkylated, so the fixed modification of cysteine carbamidomethylation was also excluded. All other variable modifications remained the same as previously listed.

2.2.17. Histological processing

2.2.17.1. Tissue fixing

Teat and alveolar tissue samples, collected as described in Section 2.2.1., were quickly washed in PBS and fixed for 48 h, at RT, in PBS containing 4 % (*w/v*) paraformaldehyde (Fisher BioReagents, NJ, USA) to prevent post-mortem decay and to provide mechanical stability for processing and sectioning. For whole teat ends to be cut in the transverse orientation, 1-2 mm of the distal portion of the teat (teat orifice) was removed using a razor blade so that the fixing solution could penetrate through the connective tissue, into the teat. After 24 h the old fixing solution was replaced, and after 48 h the fixing solution was exchanged with 70 % (*v/v*) ethanol for long-term storage of the tissue samples.

2.2.17.2. Tissue processing

Before processing, mammary and teat samples were dissected into slices approximately 3 mm thick and stored in Histosette tissue processing cassettes (Simport, QC, Canada; #M490) in 70 % (*v/v*) ethanol. For sagittal sectioning of the teat-end tissue, two facing vertical slices were made through the connective tissue directly adjacent to the teat canal with a razor blade. The tissue section containing the uncut teat canal (~3mm thick) was trimmed to fit into a Histosette cassette. Teat-end tissues for transverse sectioning were separated into three 2 – 3 mm spherical segments encompassing teat canal, Fürstenberg's rosette and the teat sinus. The orientation of each segment into the Histosette cassettes meant that for segments 1 and 2, the segments would be positioned into the paraffin wax block with the distal face (teat canal) available for sectioning. Segment 1 contained the teat orifice and distal end of the teat canal. Segment 2 contained the proximal end of the teat canal, all of Fürstenberg's rosette and the distal end of the teat sinus and was sectioned in that order. For slice 3 (teat sinus) the opposite orientation was used so that proximal face was available for sectioning.

Automated processing of tissues through graded alcohols and xylene was performed overnight in a Leica Jung TP1050 vacuum tissue processor (Leica Microsystems, Milton Keynes, UK) using the schedule listed in Table 2.6.

Processed tissues were positioned in the orientation mentioned above and then set in liquid paraffin wax using a Histo-Centre II-N embedding station (Thermolyne Corp., USA). Tissue blocks were stored at RT until required.

2.2.17.3. Tissue sectioning

Formalin-fixed, paraffin-embedded (FFPE) tissues were serially sectioned at a thickness of 7 μm using a microtome (Leica Microsystems), floated on a water bath set to 50 °C and mounted on Polysine coated glass slides (ThermoScientific; #LBSP4981). The slides were dried at 50 °C overnight and stored at RT before staining to visualise tissue, and cell morphology (Section 2.2.15) or IHC was performed to visualise the location of a particular protein of interest (See Section 2.2.16).

Table 2.6: Automated programme for paraffin fixation of tissue samples

Step	Stage	Reagent	% (*v/v*)	Temp (°C)	Time (min)
1	Dehydration	Ethanol	70	Ambient	60
2	Dehydration	Ethanol	70	Ambient	60
3	Dehydration	Ethanol	95	Ambient	60
4	Dehydration	Ethanol	95	Ambient	60
5	Dehydration	Ethanol	100	Ambient	60
6	Dehydration	Ethanol	100	Ambient	60
7	Dehydration	Ethanol	100	Ambient	60
8	Clearing	Xylene	100	Ambient	30
9	Clearing	Xylene	100	Ambient	45
10	Clearing	Xylene	100	Ambient	45
11	Infiltration	Paraffin wax		60	60
12	Infiltration	Paraffin wax		60	120
13	Infiltration	Paraffin wax		60	120

2.2.18. Staining of paraffin embedded tissues

2.2.18.1. Haematoxylin and eosin (H&E) staining

Gross histological analyses of tissues were performed on sections stained with Gill's haematoxylin and eosin. Slides were dewaxed by immersion in two washes of xylene for 5 minutes each, and then tissues rehydrated by immersion in a series of decreasing concentrations of alcohol as follows: 100 % ethanol (2 x 2 minutes), 95 % (*v/v*) ethanol (2 minutes) and 75 % (*v/v*) ethanol (1 minute) followed by rinsing under running tap water (2 minutes). The slides were immersed in Gill's haematoxylin (0.4 % (*w/v*) haematoxylin, 1.85 M sodium iodate, 53 mM aluminium sulphate, 25 % (*v/v*) ethylene glycol, 4 % (*v/v*) glacial acetic acid) for 2 minutes to stain the nuclei blue/black. Slides were washed under running tap water for 2 minutes before being placed in Scott's tap water (24 mM sodium bicarbonate, 81 mM magnesium sulphate) for a further 2 minutes to allow the blue dye to develop. Slides were then rinsed under running tap water (2 minutes) to remove salts. Cytoplasmic components were stained pink/red by immersing the slides in eosin solution (1 % (*w/v*) eosin, 2 % (*v/v*) acetic acid) for 1 minute 20 sec followed by rinsing under running tap water for 2 minutes. Tissues were dehydrated in ascending concentrations of alcohol as follows: 70 % (*v/v*) ethanol for 10 sec, 95 % (*v/v*) ethanol for 30 sec, and 100 % ethanol for 2 x 2 minutes followed by clearing in three changes of xylene for 1 minute each. Tissues sections were immediately mounted under a glass coverslip (LabServ, ThermoFisher, USA) using DePeX mounting medium (DPX; BDH Laboratory Supplies).

2.2.18.2. Toluidine Blue staining

Paraffin-embedded tissue sections were dewaxed in xylene and taken through graded alcohols as previously described for H&E staining. Frozen sections were fixed in in ice-cold ethanol for 8 minutes and then washed with distilled water. Sections were stained for 2 minutes in a solution of freshly filtered Toluidine blue staining solution (0.02 % (*w/v*) Toluidine blue, 0.008 % (*w/v*) sodium acetate, 100 mM acetic acid, pH 4.0). Sections were rinsed in distilled water, air dried and mounted in DPX mounting medium and covered with a glass coverslip.

2.2.18.3. Weigert Van Gieson staining

Tissue sections were stained for collagen and elastin using the Weigert Van Geison staining protocol as described in (Gray, 1954). Briefly, paraffin-embedded tissue sections were dewaxed in xylene and taken through graded alcohols as previously described for H&E staining and washed in PBS. Tissue sections were then stained for 5 minutes in Weigert's iron haematoxylin solution and rinsed well in running water. Van Giesons staining solution was added to the sections for 10 minutes, and the slides were quickly rinsed under running water for 10 s, 90 % ethanol/2 % picric acid for 30 s and 100 % ethanol/2 % picric acid for 1 minute. The tissue sections were dehydrated in two washes of 100 % ethanol for 1 minute each before two 5 minutes washes in xylene. Dehydrated sections were immediately mounted in DPX mounting medium and covered with a glass coverslip.

2.2.19. Immunohistochemistry (IHC)

Paraffin-embedded tissue sections were dewaxed in xylene and taken through graded alcohols as previously described for H&E staining. Antigen retrieval was performed by heat-induced epitope retrieval (HIER) in low-pH citrate buffer, pH 6.0 or high-pH Tris/EDTA buffer, pH 9.0 using the techniques and protocols published at IHC-world.com (http://www.ihcworld.com/epitope_retrieval.htm). Alternatively, antigen retrieval was performed by pre-treatment of the tissue sections with TPCK-modified trypsin (Sigma-Aldrich; #T1425) or proteinase K (Merck; #1245680010).

Optimisation of the IHC procedure was performed on control tissues such as Peyer's patch, super mammary lymph node and teat skin using a 4 x 4 matrix optimising scenario (See Table 2.7). To protect the sections from drying out, all incubation procedures were carried out in a humidified chamber at RT except for the incubation of primary antibody which was performed at 4 °C overnight.

Table 2.7: 4x4 matrix for antigen retrieval optimisation

Primary Antibody Dilution	1:30	1:100	1:300	Negative Control
Enzyme	A	B	C	D
HIER pH 6.0	E	F	G	H
HIER pH 9.0	I	J	K	L
No pre-treatment	M	N	O	P

After antigen retrieval, tissues sections were circled with a PAP pen (Zymed Laboratories Ltd., CA, USA) and blocked for endogenous peroxidase and alkaline phosphatase activity (Dako, CA, USA; Dual Endogenous Enzyme Block; #S2003) for 10 minutes and washed in TBST for 5 minutes. Protein blocking was performed by incubating each section with 2.5 % (*w/v*) BSA in TBST for two hours. Primary antibodies (See Tables 2.1 and 2.2) were diluted in antibody amplifying buffer (StressMarq Biosciences, Canada: #SKC-902) containing 3 % (*v/v*) goat serum and were used to cover one of the two tissue sections on each slide. The other section was covered with an equivalent concentration of rabbit or mouse non-immune serum to act as a negative control. Sections were incubated in a humidified chamber at 4 °C overnight. The sections were washed in TBST (3 x 5 minutes) and incubated with anti-rabbit and anti-mouse immunoglobulins conjugated to horseradish peroxidase (Sigma-Aldrich) (Table 2.3) for one hour. After washing off any unbound antibody (TBST, 3 x 5 minutes) the reactions were developed with a solution of freshly prepared, metal enhanced, diaminobenzidine (DAB) (Roche; #11718096001) and 0.01 % (*v/v*) H_2O_2 following the manufacturer's instructions. Developed sections were counterstained with Gill's haematoxylin, dehydrated and mounted in DPX with a glass coverslip as described previously.

2.2.20. Immunofluorescence (IF) staining

Snap-frozen tissue samples were thawed to -5 °C and cut into transverse sections exposing cross-sections of the teat canal, teat skin, Fürstenberg's rosette, and teat sinus. Each section was placed into 1 cm^2 tinfoil boats, partially filled with Tissue-Tek O.C.T. compound embedding medium (Sakura Finetek, CA, USA;

#4583). The tinfoil boats containing the tissue sections were then filled with OCT compound and snap-frozen in liquid nitrogen before being stored at -80 °C.

2.2.20.1. Cryosectioning of teat tissue

All cryosectioning was performed by microtome in a Leica CM1850 UV cryostat (Leica Microsystems). The temperature of the cooling chamber was set to -23 °C before the commencement of tissue handling and the blocks of prepared tissue were equilibrated to this temperature. Blocks of frozen tissue were mounted on a cryostat chuck, and serial 5 μm thick sections of tissue were then cut and transferred to Polysine glass microscope slides (Thermo Scientific). Slides were allowed to air-dry overnight and stored at -20 °C for up to 1 month. Each slide contained two sections; one for antibody examination and the other to act as a negative control with non-immune serum (Figure 2.6).

Non-immune serum was chosen to act as a negative control because immunising peptides used to generate the mouse monoclonal antibodies were not available. Antibodies can be neutralised by incubating them in excess peptide, thereby blocking the binding sites from recognising protein epitopes present on/in the cell.

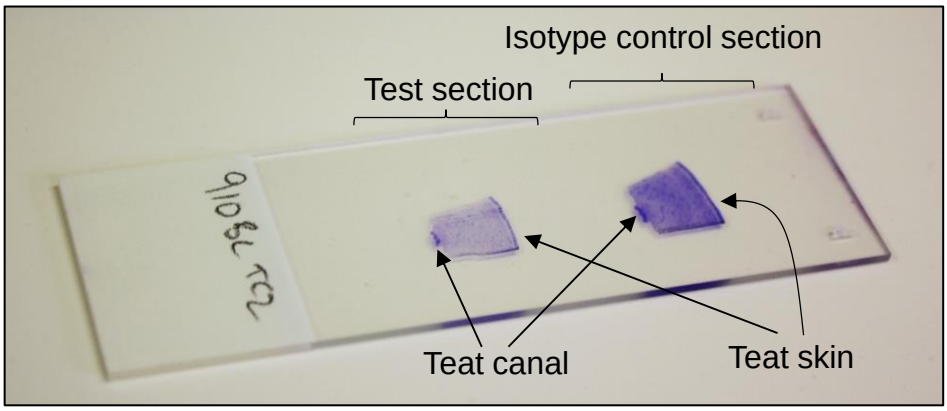

Figure 2.6: Photograph of cryosection setup on a Polysine coated glass slide.
Two serial transverse cryosections of teat canal tissue from cow #910 are shown. Each cryosection contains both teat canal and teat skin tissue. The top right-hand section is used for isotype control staining, and the lower left-hand section is used for antibody staining. Cryosections visualised by Toluidine blue staining.

2.2.20.2. Fixation and immunostaining

Stored tissue cryosections were immediately fixed in ice-cold ethanol for eight minutes and then washed three times in TBS for 10 minutes each on an orbital shaker. If the primary antibody epitopes were intracellular antigens, the tissues were subjected to permeabilisation by washing with TBST, instead of TBS, for the same period. After marking each tissue boundary with a Pap-Pen, blocking solution consisting of 10 % (*v/v*) goat serum in TBS or TBST was applied to each section and the tissue sections incubated for two hours in a humidified chamber.

Primary antibodies were diluted in antibody amplifying buffer containing 3 % (*v/v*) goat serum and were used to cover one of the two tissue sections on each slide. The other section was covered with an equivalent concentration of rabbit non-immune serum to act as a negative control. Sections were incubated in a humidified chamber at 4 °C overnight. The primary antibody solution was removed, and the slides were washed three times with TBST, and then reprobed with the appropriate Alexa Fluor-conjugated secondary antibody for two hours. All incubations from this point onwards were performed in the dark to preserve fluorescence. The slides were washed three times in TBS for 10 minutes each and the sections stained for 2 minutes with 0.4 µM diamidinophenylindole (DAPI) hydrochloride in TBS to visualise nuclei before mounting with fluorescent mounting medium (Dako; #S3023).

2.2.20.3. Fluorescent image acquisition and processing

Fluorescent images were examined and photographed using a Leica DMI 6000B inverted Fluorescence and Light microscope (Leica Microsystems) equipped with a DFC300 FX digital colour CCD camera (Leica Microsystems). The excitation/emission filters for Alexa-Fluor 488 were 480/527 nm, and those for Alexa-Fluor 594 were 620/700 nm. DAPI exposure times ranged from 40 – 100 ms while exposure time to antibodies ranged from 450 to 3000 ms. Images were adjusted to match for contrast, and brightness using Coral Paint Shop Pro Photo XI and DAPI and Alexa Fluor images of each slide were merged using SPOT advance software (version 4.6.4.3, Diagnostic Instruments).

2.2.20.4. Semi-quantitative analyses of immunofluorescent intensity

The signal intensity of cells expressing the MHC class II and CH138A antigens were obtained semi-quantitatively using a multiplicative 'Quickscore' method (Detre *et al.*, 1995). Briefly, the Quickscore analyses take into account the proportion of positively stained cells (termed category A and assigned scores from 1 to 6) as well as the intensity of the signal (termed category B, and scores from 0 to 3). The two values are then multiplied to arrive at a Quickscore that can range from 0 to 18 as follows:

Quickscore = Category A *x* Category B

For category A, assigned scores were broken down as follows: (1 = no staining, 2 = ≤ 3 % total staining, 3 = 3-10 % total staining, 4 = 10-33 % total staining, 5 = 33-67 % total staining and 6 = 67-100 % total staining) and for category B; (0 = no staining, 1 = weak staining, 2 = moderate staining, 3 = strong staining). The result for each region of tissue was then classified as strongly positive (++++) if the Quickscore was greater than 16, moderately positive (+++) if the Quickscore was between 16 and 12, mildly positive (++) if the Quickscore was between 12 and 6, weakly positive (+) if the Quickscore was between 1 and 6, and negative (-) if the score was 0.

2.2.20.5. Quantitative analyses of epithelial-bound immune cells

For relative abundance counts, innate immune cells were stained for the appropriate cell surface markers, and the total number of positively stained cells associated with the basal layer of the teat canal and teat skin or located within the epithelial bilayer of the Fürstenberg's rosette and teat sinus were manually counted. The exception to this was CD11c which is expressed by cells within the epithelium, including the teat canal and teat skin.

For each field of view, regions that were counted contained similar amounts of tissue and cells. The average number of positive cells was calculated from 7 randomly selected, non-overlapping fields of view per slide at 200 x magnification for each cow in the study. Each study group consisted of teat-end tissues from late-lactating (n = 6), involution (n = 7), and experimentally

challenged cows (n = 4). The quantitative data are expressed as the average number of cells (± SEM) derived from the average positive cell counts from each cow in each study group.

2.2.21. Statistical Analyses

All data values are presented as mean values ± standard deviation (SD) or standard error of the mean (SEM). Differences between groups were assessed using the paired and unpaired two-tailed Students *t*-test. Data were logarithmically transformed when required, to stabilise the variance and a geometric mean was derived. The transform $x \rightarrow \log (1 + x)$ was applied to normalise all protein expression values. Restricted Maximum Likelihood (REML) analyses were performed using Genstat 16 (VSN International, Hemel Hempstead, UK) to estimate the within- and between-animal variation of S100 proteins. The *p*-values for REML analyses were derived using the modified F-statistic, and the threshold level for statistical significance was set at $p < 0.05$. Significant differences were determined at $p < 0.05$*, $p < 0.01$**, $p < 0.001$***.

2.2.21.1. Power Analyses

The minimum number of cows required to detect a statistical significance in each trial was determined by Power Analyses. To detect a mean shift of 2 standard deviations or more in the mean values from the experimental groups from the mean values observed in the control group, a minimum of 6 cows was required for each trial (80 % power, two sample two-tailed *t*-test, 5 % significance level).

3. Proteomic analysis of the bovine teat canal lining

Limited information regarding the composition of the soft cerumen-like material lining the teat canal is currently available. This is quite surprising given that the teat canal lining provides an important physical and biochemical barrier to the passage of bacteria up the teat canal. Modern protein separation and identification technologies now offer the capacity to identify and quantify thousands of proteins simultaneously in a range of complex biological samples. Identifying the proteins that compose the teat canal lining will improve our understanding of the host-defence functionality of the teat canal.

In this chapter, the teat canal linings collected from six healthy lactating dairy cattle were analysed and proteins characterised using SDS-PAGE, two-dimensional gel electrophoresis (2-DE) and mass spectrometry (MS). For a selection of proteins, their identification was validated by Western blot analysis and localisation within the epithelial tissue confirmed using IHC. In addition, the teat canal lining protein repertoire was compared with that of the external teat skin epithelium highlighting similarities and differences between the protein composition of these two tissues.

3.1. Experimental design:

The udder health of 28 late-lactation dairy cows was evaluated by SCC and microbiological analysis. From this evaluation, 13 cows were identified which had a SCC $\leq$ 200,000 cells/mL in all quarters and the quarter milk showed no signs of bacterial infection. Six of the 13 cows were randomly selected for sampling, and their details are provided in Table 3.1. Teat canal lining collected from contralateral hindquarter and forequarter teats, from all six cows, were processed to extract solubilised proteins (n = 12). On the day of sampling, the infection status of each quarter sampled was confirmed using SCC and microbiological analysis. Due to the limited amount of sample collected from each teat, an equal amount of teat canal lining protein from both quarters of each cow were pooled together for 2-DE analysis. Likewise, an equal amount of solubilised teat skin epithelium protein from each cow were also pooled together

for 2-DE analysis. The experiment was designed to compare the 2-DE and GeLC-MS/MS protein profiles of the teat canal lining and teat skin proteins and to determine the biological variation of identified proteins among individual animals.

Table 3.1: Details of cows enrolled in lactation trial

Cow #	Age	Gestation status	Days in milk	Daily Yield (L)[a]	SCC (x10^3 cells/mL)[b]
5	4	Pregnant	244	14.4	117
390	3	Empty	281	15.9	11
452	4	Empty	215	15.4	141
872	7	Empty	232	11.2	48
910	3	Pregnant	282	10.6	131
1048	3	Pregnant	286	13.1	70
Average ± SD	*4.0 ± 1.5*		*257 ± 30*	*13.4 ± 2.2*	*86.3 ± 51.6*

a) Daily yield of milk in Litres (L).

b) Bulk somatic cell count (SCC) determined from milk collected from each cow.

3.2. Extraction of teat canal lining and teat skin proteins

Teat canal lining proteins from 11 uninfected teats and epithelial teat skin proteins from six individual cows were extracted using the 2D lysis buffer as described in Section 2.2.2. The teat canal lining sample collected from the left hindquarter (BL) teat of cow #452 was not included in the study due to the high SCC value and presence of bacteria from the quarter milk sample evaluated on the day of sample collection. The total 'wet weight' of teat canal lining collected from each teat is summarised in Table 3.2. The average amount of total protein extracted out of the individual teat canal lining and teat skin samples was 14.8 % and 12 % of the original sample weight, respectively. The amount of teat canal lining collected and the quantity of protein extracted from individual teat canal lining samples were similar to that reported previously (Senft *et al.*, 1990).

Approximately 350 µg of total protein collected from teats from both quarters of each cow (teat canal lining, n = 11; teat skin, n = 6) were combined to create pooled teat canal lining and pooled teat skin samples for 2-DE and GeLC-MS/MS analysis.

Table 3.2: Amount of solubilised protein obtained from teat canal lining

Cow#/ Quarter	SCC ($x10^3$ cells/mL)	TCL (mg wet weight)	Total yield of protein (mg)	% (mg wet weight)	pH
5/FR	47	12.8	1.935	15.1	5.75
5/BL	46	10.5	1.272	12.1	5.78
390/FL	54	9.9	1.184	12.0	6.08
390/BR	21	11.5	1.424	12.4	6.02
452/FR	70	12.7	2.105	16.6	5.89
452/BL[a]	6437	*n.d.*	*n.d.*	*n.d.*	*n.d.*
872/FR	34	14.8	2.435	16.5	5.92
872/BL	64	16.8	3.080	18.3	5.86
910/FR	125	11.7	1.735	14.8	5.78
910/BL	32	12.9	1.990	15.4	5.82
1048/FR	24	18.3	2.874	15.7	6.06
1048/BL	13	16.3	2.275	14.0	6.01
Average ± SD	*48 ± 31*	*13.3 ± 2.6*	*5 ± 0.6*	*14.8 ± 2.0*	*5.91 ± 0.1*

a) TCL (teat canal lining) from the left hindquarter teat of cow #452 was not collected due to the SCC being outside of the parameters for this study.
FR; right forequarter, FL; left forequarter, BR; right hindquarter, BL; left hindquarter.
pH was measured from the total mass of collected wet weight TCL as set out in the Methods.

3.3. 2-DE profiling of pooled teat canal lining

Triplicate 2-DE gel analysis was performed on 350 µg of the pooled teat canal lining sample to verify the reproducibility of the 2-DE results (Figure 3.1). 2-DE revealed a complex pattern of protein spots dominated by two clusters of proteins of relatively high abundance. The main cluster contained many resolvable protein spots between 50 to 70 kDa with a p*I* ranging from 4.5 to 9.5. These proteins were estimated to constitute 51 % of the total resolvable protein in the sample by densitometry. The second cluster of proteins comprised 27 protein spots of between 7 to 21 kDa with a p*I* ranging from 4.5 to 6.5 (boxed in Figure 3.2). In total, these 27 protein spots represented an estimated 19 % of the total resolvable protein in the sample by 2-DE and were the second most abundant group of proteins in the teat canal lining.

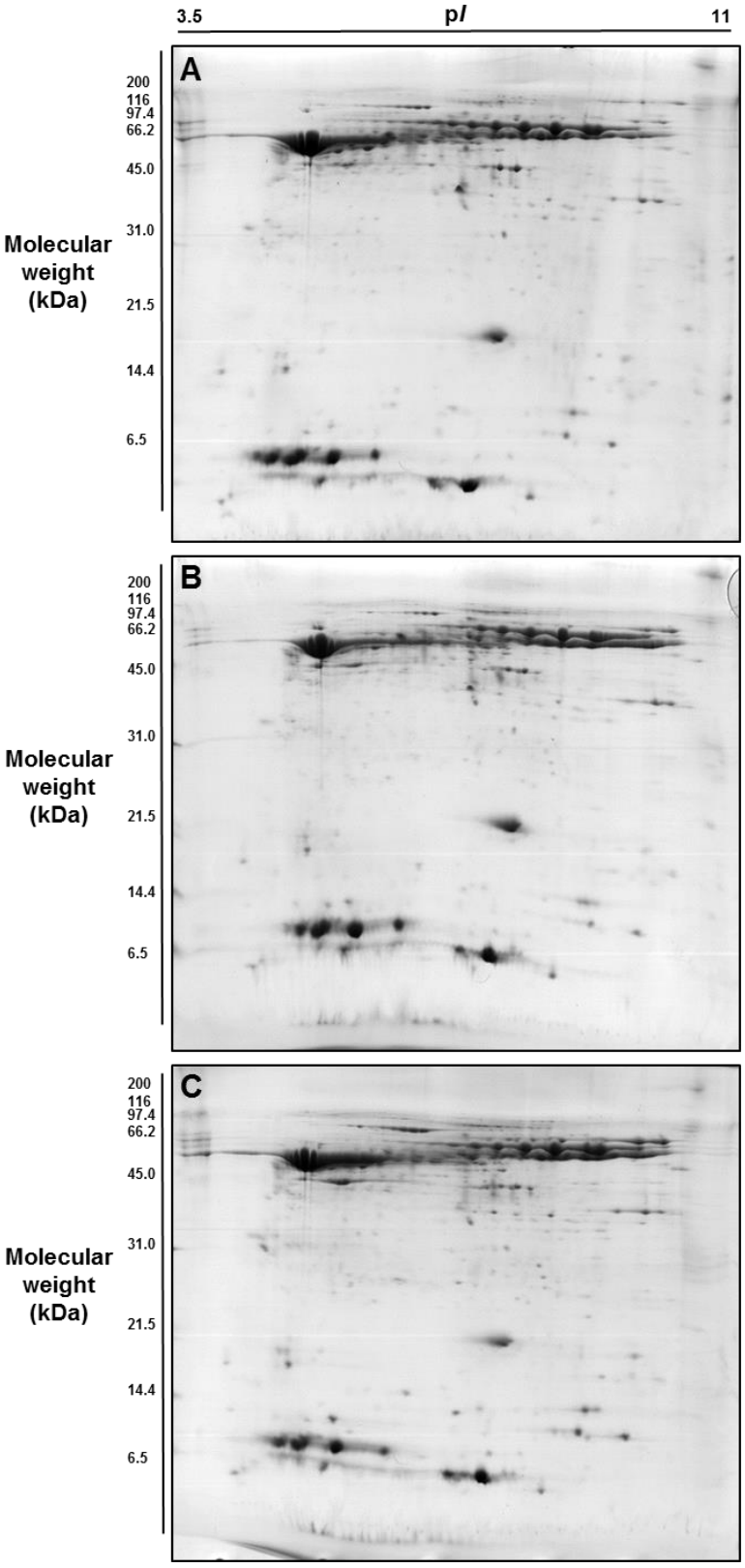

Figure 3.1: Colloidal Coomassie blue stained triplicate 2-DE gels (pH 3-11) of pooled bovine teat canal lining extract.
Gels show 350 µg of solubilised protein separated by IEF and 14 % SDS-PAGE (A-C).

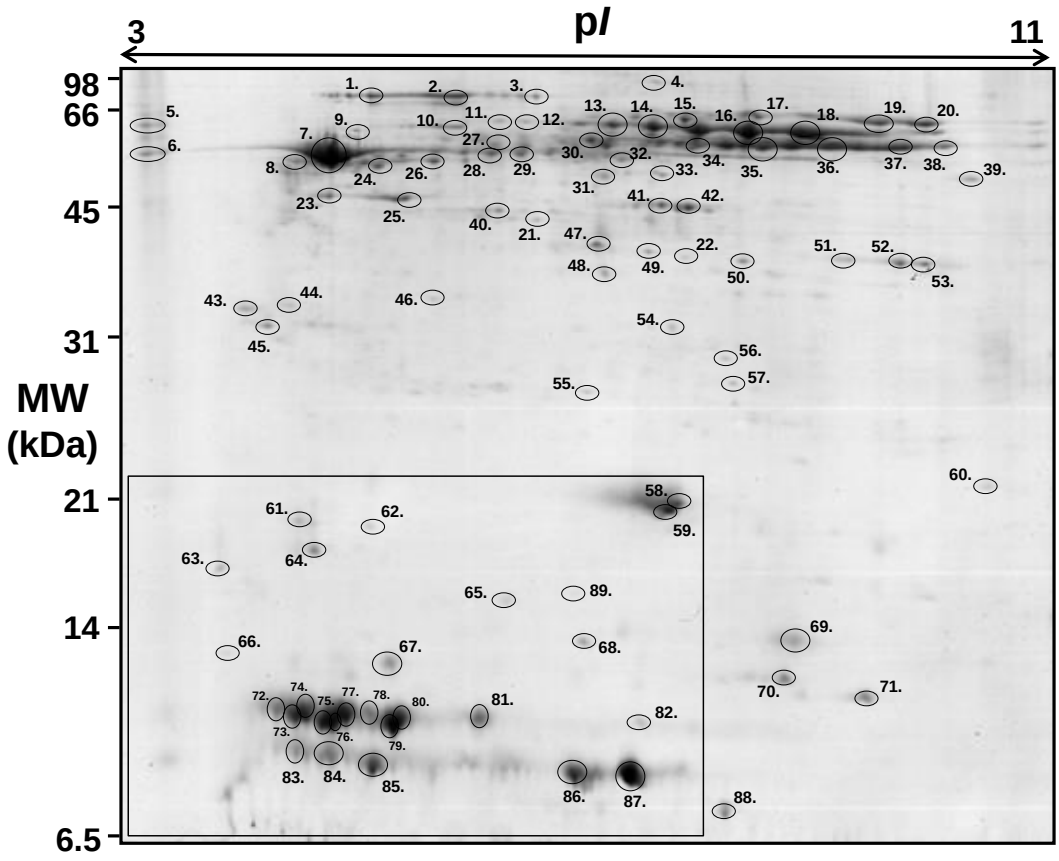

Figure 3.2: Representative 2-DE reference map of 350 µg pooled bovine teat canal lining from healthy lactating cows.
The identified proteins are indicated by circles and numbers, and the names are listed in Table 3.3. The boxed area includes a group of abundant low molecular weight proteins.

PDQuest was used to match spots between the colloidal Coomassie-stained triplicate gels. A total of 496, 477 and 458 protein spots were identified for gels A, B and C, respectively (Figure 3.1). PDQuest matched 437 of these protein spots between all three gels. Only 46 spots remained unmatched between at least two of the replicates representing an average match rate of 94 %. Protein spots were selected for MS identification on the basis of high intensity, location and resolution in the 2-DE gels. In total, 89 spots were manually excised, digested by trypsin and characterised by nano LC-ESI-Q/TOF MS/MS. The 89 protein spots analysed are indicated on the 2-DE reference map with their corresponding spot identification number (Figure 3.2). The identity of all 89 protein spots was confirmed and resulted in the identification of 46 unique proteins (Table 3.3). More detailed information derived from the protein searches for each of the 89 protein spots from Figure 3.2 is listed in Supplementary data Table A1. For some protein spots, multiple proteins were identified, especially in the major cluster of high molecular weight proteins. Of the 89 protein spots excised and identified by MS more than two-thirds of them (68.5 %) belonged to three different protein groups. These were the keratin, S100 and serpin (serine protease inhibitor) families of proteins. Identified proteins in each of these three groups are indicated in Figure 3.3.

Thirty-six of the 89 2-DE spots were identified by MS as cytokeratins. Cytokeratins are filament-forming proteins present in epithelial cells that are essential for normal cell structure, development and function. However, since 2006, they have simply been called keratins (K) (Schweizer *et al.*, 2006). The types of keratin proteins identified in the teat canal lining included the primary (cell-type defining) keratins (K1, K3, K4, K5, K10 and K14) as well as the secondary keratins (K6A, K6C, K17, and K79). The acidic type I keratins (K10, K14 and K17) were resolved as single, tight clusters of proteins between pH 4.8 to 5.3 on the 2-DE gel. K10 was by far the most abundant type I acidic keratin resolved. This is consistent with previous observations that K10 is the main type I keratin of keratinizing cells of the epidermis and other cornifying stratified epithelia (Coulombe & Omary, 2002). The type II intermediate forming keratin proteins (K1, K3, K4, K5, K6 isoforms, and K79) were observed as a horizontal

string of protein spots spread over the width of the gel; suggesting extensive post-translational modification of these proteins (Figure 3.3). This isoform heterogeneity has been previously observed among the keratins and was attributed to variable phosphorylation of the keratin proteins (Franke *et al.*, 1981). Type II keratin 59 kDa component IV (NP_001244333) and predicted keratin 6A (XP_884760) represent the same protein in the NCBI non-redundant database. For simplicity and continuity, these two proteins will be identified in this thesis as keratin 6C (K6C) as they are translated from the keratin 6C gene sequence (KRT6C).

Eighteen of the protein spots were identified by MS as belonging to six different members of the S100 family of calcium-binding proteins and are visible in the boxed cluster highlighted in Figure 3.2. These include S100A12 (calgranulin C), S100A11 (calgizzarin), S100A9 (calgranulin B), S100A8 (calgranulin A), S100A7 (psoriasin) and a predicted S100A7-like protein (S100A7L). Similar to the keratin proteins, many of the S100 proteins were also present as strings of horizontal spots, suggesting that they may also be post-translationally modified. The two most abundant S100 proteins identified were S100A7 and the S100A7L protein, represented in the gels as strings of four and six spots, respectively (Figure 3.3).

The third most abundant class of proteins identified in the 2-DE gel was the serpin clade B family of proteins. Serpins constitute a large family of related proteins, the majority of which are serine protease inhibitors. A cluster of nine protein spots were resolved between 38 to 46 kDa with a p*I* ranging from 5.8 to 8.0. These included multiple spots for serpin-B3, serpin-B3-like, serpin-B4 and serpin-B4-like. A serpin-B4-like protein was identified from spot #4, however, in contrast to the other serpin protein spots, its position on the 2-DE gel did not correspond to its theoretical mass and p*I* (observed: 91 kDa/6.6, versus theoretical: 61 kDa/9.1).

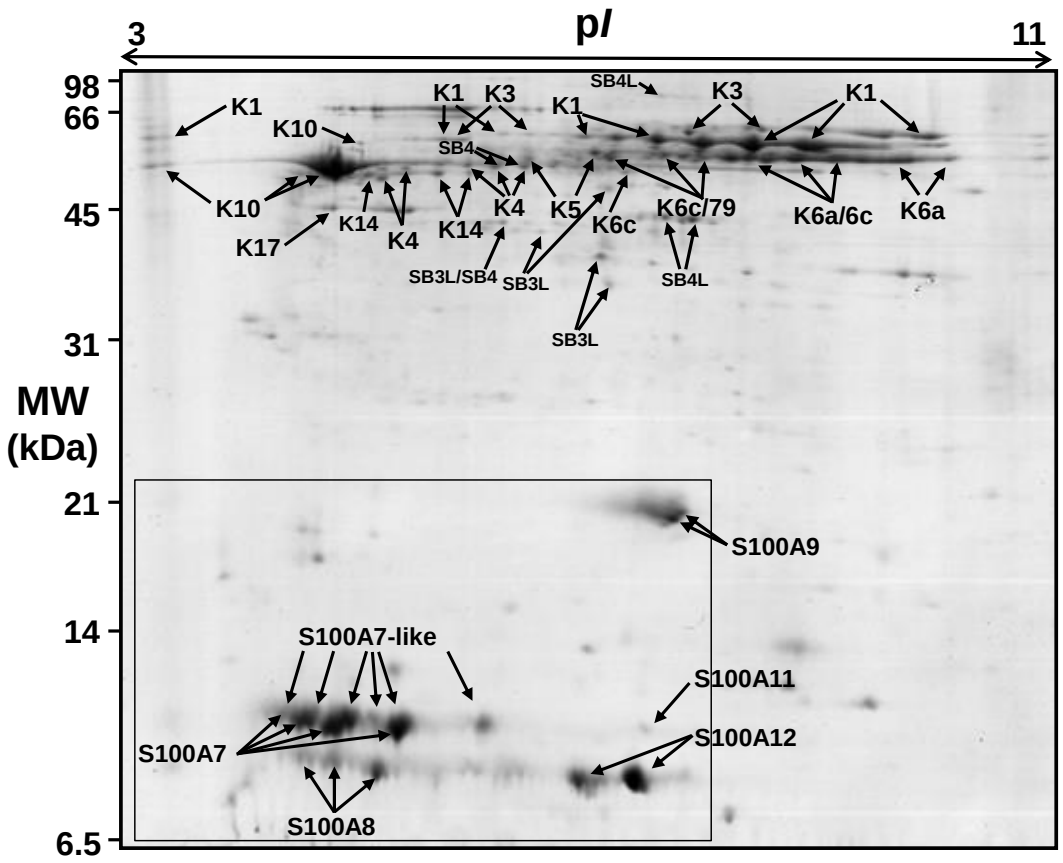

Figure 3.3: 2-DE protein spots identified as keratin, S100 and serpins in pooled bovine teat canal lining.

Thirty-six protein spots corresponding to identified keratin proteins, 18 S100 protein spots (enclosed in box), and 10 serpin protein spots are indicated by arrows. Keratin abbreviations are (K1), keratin type II cytoskeletal 1; (K3), keratin type II cytoskeletal 3; (K4), keratin type II cytoskeletal 4; (K5), keratin type II cytoskeletal 5; (K6A), keratin type II cytoskeletal 6A; (K6C), keratin type II cytoskeletal 6C; (K10), keratin type I cytoskeletal 10; (K14), keratin type I cytoskeletal 14; (K17), keratin type I cytoskeletal 17; (K79), keratin type II cytoskeletal 79. Serpin abbreviations are SB3L, serpin-B3-like; SB4, serpin-B4; SB4L, serpin-B4-like.

Table 3.3: Unique teat canal lining proteins separated by 2-DE and identified using nano LC-ESI-Q/TOF MS/MS

#	Identified protein	NCBI accession code	Spot #
1	14-3-3 protein sigma	gi|57163961	45
2	alpha S1 casein, partial	gi|159793209	43
3	annexin A2	gi|73586982	22, 50
4	annexin I	gi|74	49
5	aspartic peptidase, retroviral-like 1	gi|358414487	65
6	beta-actin	gi|313507212	25
7	beta-lactoglobulin	gi|49259423	61, 62
8	calmodulin	gi|640294	63
9	calmodulin-like 5	gi|148234364	66
10	caspase-14	gi|329663440	44, 64
11	EEF1A1 protein	gi|86827651	38
12	fatty acid-binding protein, adipocyte	gi|27805811	67
13	fatty acid-binding protein, epidermal	gi|27805805	69
14	galectin-7	gi|119910404	68, 89
15	gasdermin-A	gi|118151260	54
16	glyceraldehyde-3-phosphate dehydrogenase	gi|77404273	51, 52, 53
17	hemoglobin, subunit alpha	gi|576142	71
18	hemoglobin, subunit beta	gi|27819608	70
19	heat shock cognate 71 kDa protein	gi|148887198	1
20	heat shock protein beta-1	gi|71037405	55
21	keratin, type II cytoskeletal 1	gi|297474460	5, 10, 11, 12, 13, 14, 15, 16, 17, 18, 19, 20, 29, 30, 46
22	keratin, type II cytoskeletal 3	gi|358421417	10, 11, 12, 15, 17
23	keratin, type II cytoskeletal 4	gi|148356276	24, 26, 27, 28, 29, 30, 34, 35
24	keratin, type II cytoskeletal 5	gi|296487899	27, 28, 29, 30
25	keratin, type II cytoskeletal 6A	gi|134085706	28, 29, 30, 32, 33, 34, 35, 36, 37
26	keratin, type II cytoskeletal 6C	gi|76617862	32, 34, 35, 36, 37
27	keratin, type I cytoskeletal 10	gi|296476308	6, 7, 8, 9,
28	keratin, type I cytoskeletal 14	gi|262118301	26
29	keratin, type I cytoskeletal 17	gi|160395544	23
30	keratin, type II cytoskeletal 79	gi|115496454	28, 30, 32, 33, 34, 35, 36, 37
31	non-specific cytotoxic cell receptor protein 1 homolog	gi|76641449	60
32	phosphoglycerate mutase 1	gi|77404217	56

Table 3.3 continued

33	S100A7	gi|27807077	72, 73, 75, 76, 79, 81
34	S100A7-like	gi|76612440	72, 74, 77, 78, 80, 81
35	S100A8	gi|165973998	83, 84, 85
36	S100A9	gi|114052490	58, 59
37	S100A11	gi|296489536	82
38	S100A12	gi|27807183	86, 87
39	serine (or cysteine) proteinase inhibitor, clade B (ovalbumin), member 4-like	gi|296473654	4
40	Serpin-B3-like	gi|359079289	21, 31, 40, 47
41	Serpin-B3-like	gi|119916469	48
42	Serpin-B4	gi|358420938	28, 29, 40
43	Serpin-B4-like	gi|119923094	41, 42
44	serum albumin precursor	gi|30794280	2, 3
45	triosephosphate isomerase	gi|61888856	57
46	ubiquitin	gi|290560476	88

3.4. Identification of a previously uncharacterised S100A7-like protein

The two most abundant S100 proteins identified in the teat canal lining, by 2-DE, were S100A7 and the previously uncharacterised S100A7L protein. S100A7 and S100A7L were represented in the gels as strings of four and six spots, respectively (Figure 3.3). The S100A7L protein sequence is present in the NCBI non-redundant database as a predicted protein sequence (XP_875693.1, accession number gi|76612440) derived from automated *Bos taurus* genomic sequencing.

MS analysis of individual 2-DE spots confirmed the identity of both proteins. Due to their small mass, theoretical fragmentation by trypsin only resulted in the generation of six tryptic peptides for both proteins (Table 3.4) with 86.1 % sequence coverage. Many more than the six theoretical peptides were detected as a result of variable biological and processing modifications. These modifications included phosphorylation, oxidation and deamination of specific amino acid residues. Modifications that would influence the p*I* of the proteins and support the observation of multiple isoforms in the 2-DE gels include phosphorylation of

serine and threonine residues as well as the oxidation of lysine and arginine residues. A re-examination of the peptide sequence identifications and their corresponding variable modifications found that serine residue #2 in the large N-terminal peptide (Met^{1}-Lys^{19}) was phosphorylated and that lysine residue #38 was oxidised and uncleaved by trypsin (Arg^{35}-Lys^{49}). The full extent of the S100A7/A7L modifications and what effect they may have on function was not examined further as this was outside the scope of the current research project.

Table 3.4: List of theoretical tryptic fragments for S100A7 and S100A7L

S100A7 pI 5.22 Monoisotopic mass: 11536.60; 86.1 % sequence coverage

Mass $[M+H]^+$	Position	Modifications	Peptide sequence
2175.1114	1-19		MSSSQLEQAITDLINLFHK
1114.4898	20-29		YSGSDDTIEK
645.3566	30-34		EDLLR
1411.6310	38-49	Carbamidomethyl: 47	DNFPNFLGACEK
1128.5571	53-61		DYLSNIFEK
3517.6077	70-101	Carbamidomethyl: 96	IDFSEFLSLLADIATDYHNHSHGAQLCSGGNQ

S100A7L pI 5.47 Monoisotopic mass: 11596.70; 86.1 % sequence coverage

Mass $[M+H]^+$	Position	Modification(s)	Peptide sequence
2205.1372	1-19		MSGFQLEQAITDLINLFHK
1114.4898	20-29		YSGSDDTIEK
645.3566	30-34		EDLLR
1455.6573	38-49	Carbamidomethyl: 47	ENFPNFLSACEK
1142.5728	53-61		QYLSDIFEK
3517.6077	70-101	Carbamidomethyl: 96	IDFSEFLSLLADIATDYHNHSHGAQLCSGGNQ

Monoisotopic masses were calculated using the PeptideMass prediction tool via the ExPASy website (http://web.expasy.org/peptide_mass/). The only modification included was the fixed modification of cysteine carbamidomethylation. Unique amino acids in the diagnostic peptides for each protein are highlighted in red.

The S100A7 and S100A7L protein share 91 % sequence homology and have similar molecular weights and p*I* values (Figure 3.4). To date, antibodies are not available to differentiate between the two S100A7 proteins in a complex mixture, leaving identification by MS as the only current diagnostic tool. Three of the six tryptic peptides identified were unique to each S100A7 protein enabling identification of the two proteins to be confirmed. The N-terminal peptide (Met^{1}-Lys^{19}) was the largest of these diagnostic peptides. It was observed in multiple charge states and, for S100A7, was phosphorylated on serine residue #2. However, for both proteins, this peptide was not consistently observed during analysis suggesting that it is altered by other unknown modifications. The two other diagnostic peptides, Asp^{38}-Lys^{49} and Gly^{51}-Lys^{61} for S100A7 and Glu^{38}-Lys^{49} and Gln^{53}-Lys^{61} for S100A7L, respectively, were present in all protein spots analysed. The MS/MS fragmentation spectra for each of these two diagnostic peptides for S100A7 and S100A7L are shown in Supplementary data Figures A2 and A3, respectively.

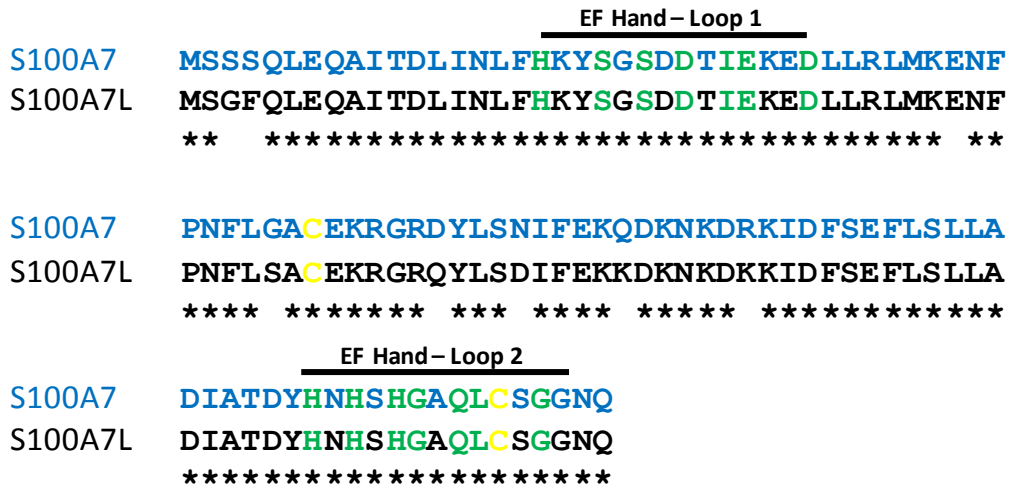

Figure 3.4: Sequence alignment of the bovine S100A7 and the predicted protein S100A7L. S100A7L (XP_875693) shows 91 % sequence identity compared to S100A7 (NP_777021.1). Identical amino acid residues between the two proteins are indicated with an asterisk. Conserved cysteine residues are highlighted in yellow. The predicted EF-hand motifs for both proteins are marked above the sequences, and amino acids directly involved in calcium binding are coloured green.

3.5. Comparison of the protein profiles between the teat canal lining and the cornified layer of the teat skin

As part of this study, the protein profiles of two different forms of *stratum corneum* derived from keratinized bovine teat stratified squamous epithelia were compared. Based on their dissimilar locations on the teat (internal versus external) and physical conformation (malleable versus ridged), differences in the protein profiles of the teat canal lining and the cornified layer of the external teat skin was expected. While these differences may reflect the expression of different combinations of keratin proteins (as observed in nail and hair compared to the skin), we hypothesised they could also reflect the different function that each tissue provides in host-defence of the mammary gland.

3.5.1. Individual protein analysis by 1D SDS-PAGE:

The protein profile of the teat canal lining and teat skin epithelium was first examined by 1D SDS-PAGE (Figure 3.5). Six teat canal lining protein preparations, one from each of the six cows, were compared to the six teat skin protein preparations, extracted from the equivalent teat. Densitometry measurements of the separated proteins from each lane across both gels, representing both sample types, verified that an equal loading of protein was applied to each lane. The 1D SDS-PAGE banding pattern was found to be highly reproducible within the teat canal lining protein samples and within the teat skin protein samples, respectively. However, although a relatively similar overall protein pattern was observed within a sample type, there were several noticeable differences observed between the two groups of samples. There was a 1.5-fold increase in the relative abundance of proteins located between 50 and 60 kDa in the teat skin samples as compared to the teat canal lining samples. In the teat skin, these protein bands represented 78% of the solubilised protein whereas in the teat canal lining they represented only 53% (solid arrow; $p < 8.9 \times 10^{-6}$). Based on the previous 2-DE analysis of the pooled teat canal lining proteins, the majority of proteins located in this cluster were expected to be keratin proteins. A protein band at approximately 45 kDa was barely visible (dashed arrowed) and a further protein band at approximately 18 kDa absent in the teat skin samples

(asterisk) compared to the teat canal lining samples. MS analysis of these two protein bands from the 1D SDS-PAGE gel verified their identity as serpin-B4-like protein and S100A9, respectively.

The protein band located at approximately 7 kDa was approximately two-fold more abundant in the teat canal lining than the corresponding band in the teat skin samples (solid arrow; $p < 1.5 \times 10^{-4}$). The broad fuzzy appearance of the band suggested that a number of proteins with similar molecular weights were present. This was confirmed by MS analysis where S100A7, S100A7L, S100A8 and S100A12 were identified in the teat canal lining 7 kDa protein band but only S100A7, S100A8 and S100A12 were identified in the teat skin 7 kDa protein band.

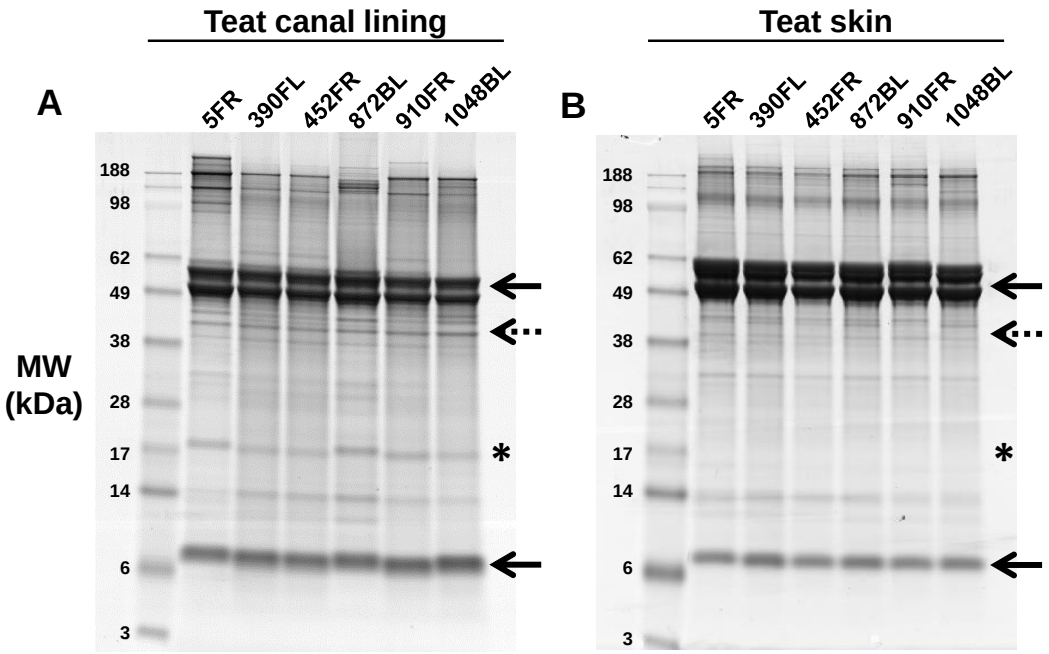

Figure 3.5: 1D SDS-PAGE protein separation of teat canal lining and teat skin epithelium. Each lane on the gel represents approximately 10 µg of solubilised protein that has been collected from a particular teat (6 individual cows per gel). Bands of interest are indicated with arrows and asterisks. Teat canal lining (A). Teat skin epithelium (B).

3.5.2. 2-DE analysis of pooled teat canal lining and pooled teat skin samples:

Triplicate 2-DE gels of pooled teat skin extract (350 µg each) were generated (Figure 3.6) and the protein profile compared to that observed for the pooled teat canal lining described in Section 3.3.2. PDQuest was used to generate a teat canal lining analysis set and a teat skin analysis set from triplicate gels for protein spot quantification and statistical validation.

The teat canal lining analysis set and teat skin analysis set matched 437 and 504 individual proteins spots, respectively. Between the two analysis sets, 386 spots were matched across all six gels. A total of 43 protein spots, with an intensity value of 30 or greater, and which were significantly altered in relative abundance between the two analysis sets (> two-fold; $p < 0.05$), are identified in Figure 3.7. The 43 protein spots excised for MS/MS identification are listed in Table 3.5. Eighteen different proteins were identified from the 43 protein spots, with several spots representing isomeric forms of the same protein. The 43 proteins identified and the statistical data derived from PDQuest are listed in Supplementary data Table A2.

Thirty-two protein spots were found to be higher in abundance in the teat canal lining analysis set compared to the teat skin analysis set. Seventeen of these proteins were identified as keratin proteins, including K1, K3, K4, K5 and K6A. A further ten proteins were identified as S100 proteins, including S100A7, S100A7L, S100A8, S100A9 and S100A12. The remaining five proteins were identified as two forms of serpin-B4-like, two subunits of haemoglobin and caspase 14.

Seven of the 11 protein spots found to be less abundant in the teat canal lining analysis set, compared to the teat skin analysis set, were identified as keratin proteins. These included K10 and several isomeric forms of K1 and K3. Of the four non-keratin proteins identified, three of them (calmodulin-like 5, 14-3-3 sigma and galectin-7) have been previously implicated in the regulation of keratinocyte differentiation and apoptosis (Bernerd *et al.*, 1999; Méhul *et al.*, 2001; Raj *et al.*, 2006). A single protein spot of S100A7 was found to be five-fold more abundant in the teat skin analysis set than in the teat canal lining analysis set, suggesting a change in the post-translational modification of S100A7 between the two tissues.

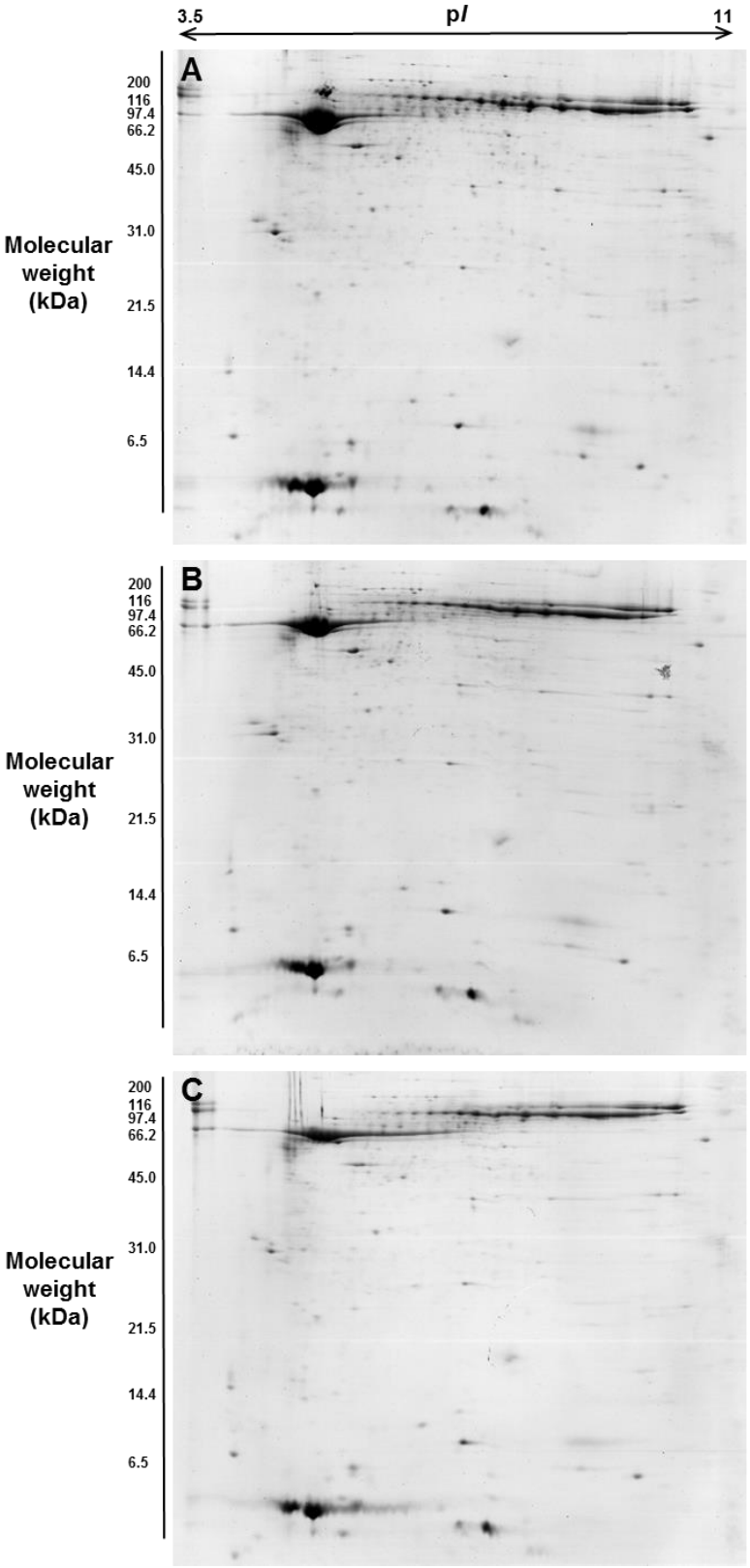

Figure 3.6: Colloidal Coomassie blue stained triplicate 2-DE gels (pH 3-11) of pooled bovine teat skin extract.
Gels show 350 µg of solubilised protein separated by IEF and 14 % SDS-PAGE.

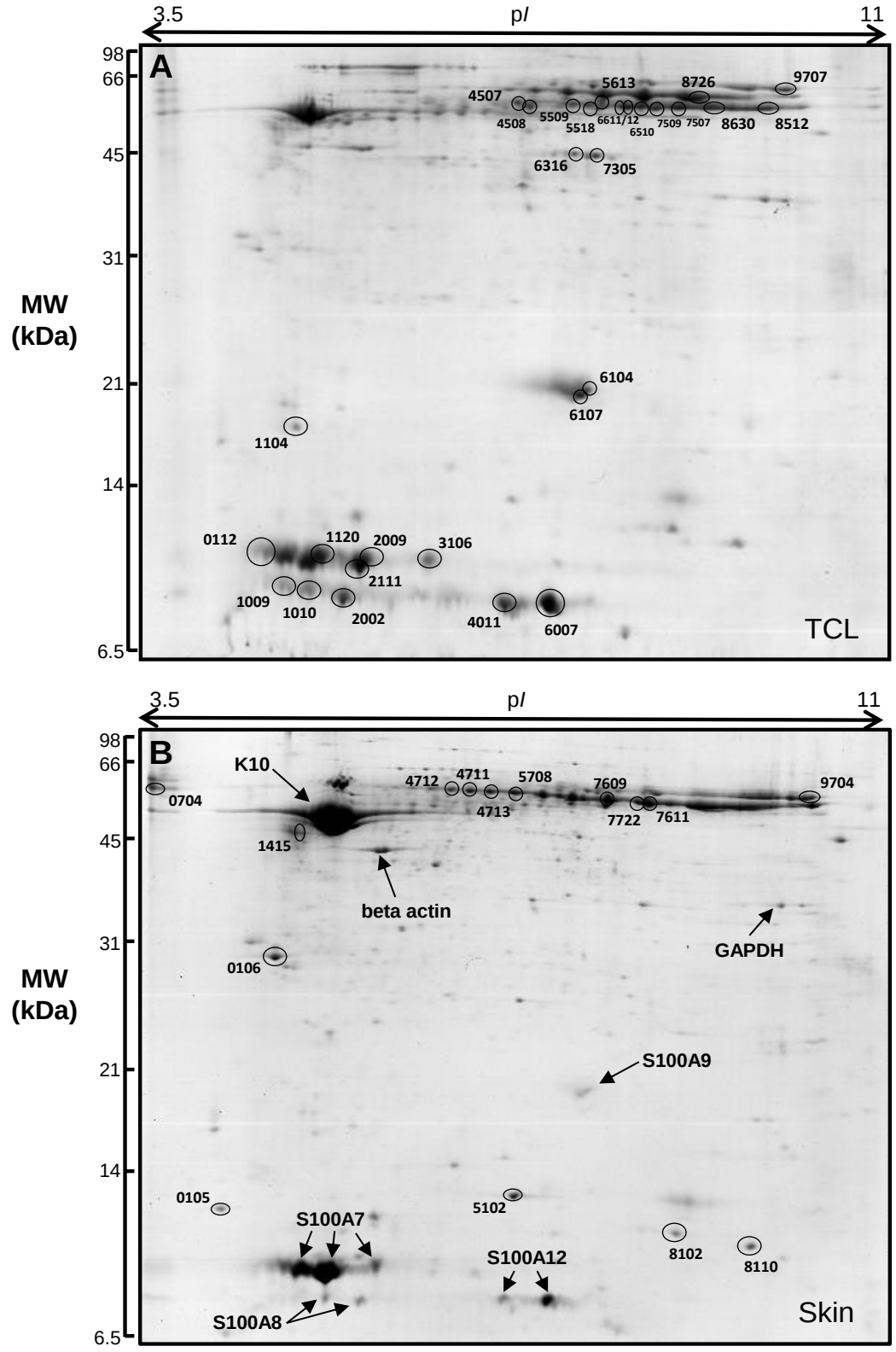

Figure 3.7: Representative 2-DE reference maps of pooled bovine teat canal lining (A) and pooled bovine teat skin (B).
Proteins with significantly different abundance ($p < 0.05$) between the two sample groups are circled. Each protein is annotated with its SSP number, given by PDQuest software and are listed in Supplementary data Table A2. Several proteins not significantly altered in the teat skin reference map are also labelled.

Table 3.5: Proteins identified as having altered abundance across teat canal lining and teat skin samples (≥2-fold altered in abundance ($p < 0.05$)).

SSP	Identified protein	Fold change	*p*-value
7507	keratin, type II cytoskeletal 6A	157.7	0.016
5518	keratin, type II cytoskeletal 4	109.83	0.048
6611	keratin, type II cytoskeletal 6A	64.82	0.035
6510	keratin, type II cytoskeletal 6A	59.4	0.022
2009	S100A7-like	38.61	0.005
7509	keratin, type II cytoskeletal 6A	38.5	0.008
3106	S100A7-like	33.62	0.001
7305	serpin-B4-like	23.56	0.003
8512	keratin, type II cytoskeletal 6A	22.2	0.001
8630	keratin, type II cytoskeletal 6A	21.5	0.026
1009	S100A8	17.95	0.049
6316	Serpin-B4-like	17.5	0.024
5509	keratin, type II cytoskeletal 5	12.84	0.009
4507	keratin, type II cytoskeletal 4	9.68	0.018
6104	S100A9	8.82	0.007
7611	keratin, type II cytoskeletal 1	7.73	0.040
4508	keratin, type II cytoskeletal 5	6.74	0.035
6612	keratin, type II cytoskeletal 6A	6.62	0.024
2002	S100A8	6.37	0.043
1104	caspase-14	5.8	0.046
8102	hemoglobin subunit beta	5.78	0.008
1120	S100A7-like	3.91	0.034
4011	S100A12	3.71	0.001
7609	keratin, type II cytoskeletal 1	3.44	0.012
6107	S100A9	2.98	0.014
7722	keratin, type II cytoskeletal 3	2.75	0.001
8726	keratin, type II cytoskeletal 1	2.65	0.014
1010	S100A8	2.6	0.038
5613	keratin, type II cytoskeletal 5	2.46	0.021
6007	S100A12	2.27	0.043
9704	keratin, type II cytoskeletal 1	2.01	0.048
8110	hemoglobin subunit alpha	2.00	0.028
5708	keratin, type II cytoskeletal 1	0.36	0.031
9707	keratin, type II cytoskeletal 1	0.26	0.013
112	S100A7	0.21	0.014
1415	keratin, type I cytoskeletal 10	0.17	0.011
5102	galectin-7	0.16	0.001
105	calmodulin-like 5	0.13	0.012
106	14-3-3 protein sigma	0.11	0.003
4713	keratin, type II cytoskeletal 1	0.10	0.032
4712	keratin, type II cytoskeletal 3	0.06	0.016
4711	keratin, type II cytoskeletal 1	0.05	3.9E-04
704	keratin, type I cytoskeletal 10	0.04	0.036

3.6. GeLC-MS/MS analysis of teat canal lining and cornified layer of the teat skin

Large format 2-DE analysis is limited by the amount of protein that is required for separation, resolution of proteins and gel-to-gel variability. Therefore, the pooled teat canal lining and pooled teat skin samples were subjected to an alternative simpler method for resolving and identifying proteins. This method, which uses 1D SDS-PAGE-separation and analysis by nano-LC-MS/MS, is called GeLC-MS/MS.

For comparative GeLC-MS/MS analysis between the proteins extracted from the teat canal lining and teat skin tissue samples, the two pooled samples used for 2-DE analysis were separated and analysed in triplicate to create three technical replicates for each pooled sample. The teat canal lining and teat skin pools consisted of the same six protein samples from each tissue as previously shown in Figure 3.5. Preparative SDS-PAGE gels, resolving 25 µg/lane of pooled teat canal lining sample (n = 3) and pooled teat skin sample (n = 3), were run for GeLC-MS/MS analysis (Figure 3.8). A total of 48 fractions were subjected to MS/MS analysis resulting in the generation of 34,540 fragment spectra for the teat canal lining technical replicates and 35,297 fragment spectra for the teat skin technical replicates. These spectra were submitted to a Mascot database search using the identification criteria described in Section 2.2.13 at a false discovery rate of 5 %. This analysis resulted in the identification of 73 different teat canal lining proteins and 76 different teat skin proteins. For this analysis, peptides were required to be identified in at least two of the three technical repeats with at least one technical repeat consisting of 2 or more peptides. For simplicity of presentation, the 73 teat canal lining proteins and 76 teat skin proteins are shown in Table 3.6 organised in family or functional groups (i.e. keratins, S100 proteins, cytoskeletal proteins, serum proteins, enzyme inhibitors, proteins involved in apoptosis, cellular proteins, and major milk proteins). Forty-two of the 46 proteins (91 %) identified from 2-DE spots were also identified by GeLC-MS/MS. The four proteins that were not identified by this method were retroviral-like aspartic peptidase, calmodulin, phosphoglycerate mutase, and non-specific

cytotoxic cell receptor protein-1 homolog. All four proteins were present as small, faint spots on the 2-DE gels and are likely to be below the detection level of the GeLC-MS/MS method.

When the two protein lists were combined a total of 103 unique proteins were identified (Table 3.5). Among the more prominent proteins (i.e. proteins with ≥ 5 unique peptides), nine proteins were found to be exclusive to the teat canal lining proteome, and ten proteins were exclusive to the teat skin proteome. Of the unique proteins, 45 proteins were commonly identified in all six technical replicates across both tissue types. These proteins constitute the primary protein set generated by fully differentiated teat stratified squamous epithelium.

In the teat canal lining, three of the nine exclusive proteins identified were keratin proteins that are known to be involved in keratinocyte hyperproliferation (K17, K6C) and keratinocyte migration (K79) (Leigh *et al.*, 1995; Veniaminova *et al.*, 2013). Four other exclusive proteins were identified as serine protease inhibitors (serpin-B3-like isoforms and serpin-B4), and a further two proteins (GAPDH and nucleoside diphosphate kinase B) are involved in energy production.

Of the ten proteins exclusive to the teat skin, four were keratin proteins (K15, K19, K27 and K73) and another four were cytoskeletal proteins (desmocollin, desmoglein, epiplakin and plakophilin) that interact with the keratin intermediate filament networks and assist in cell to cell adhesion. Two cell signalling regulators, 14-3-3 epsilon and 14-3-3 zeta, were also found to be distinct to the teat skin proteome. Comparison of the less prominent proteins (i.e. proteins with 4 or less unique peptides) is more uncertain as the technical error could have contributed to the observed quantitative differences between the two sample groups.

In both the teat canal lining and teat skin analysis there was an absence of extracellular matrix proteins, such as collagen and elastin. This suggests that minimal contamination from the underlying dermal layer proteins occurred during the scraping and collection of both types of tissue samples.

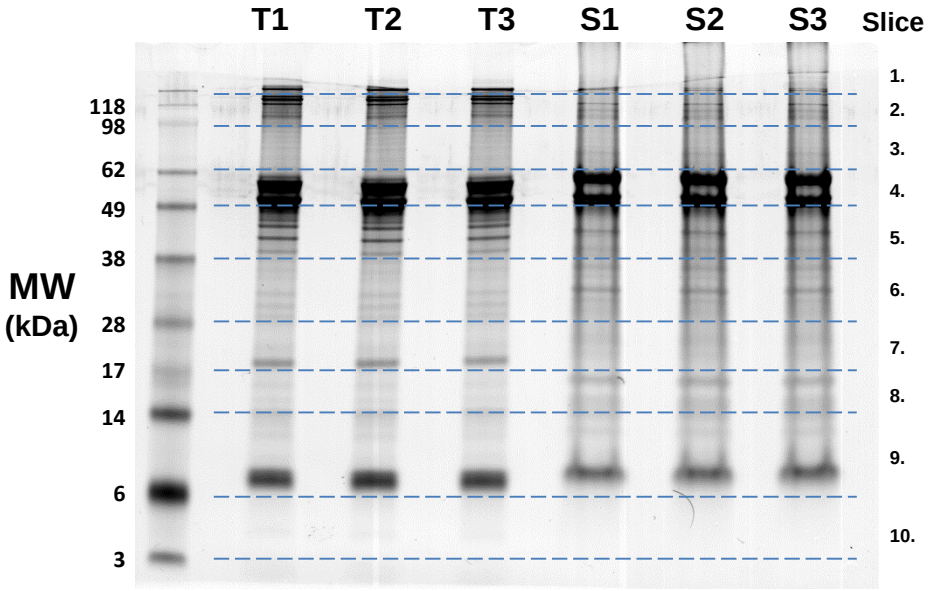

Figure 3.8: 1D SDS-PAGE of pooled teat canal lining technical replicates and pooled teat skin technical replicates.
Each lane was cut into 10 gel slices based on the molecular mass of the SeeBlue Plus2 markers and processed individually for in-gel tryptic digestion. T, teat canal lining; S, teat skin.

Table 3.6: Summary of pooled teat canal lining and pooled teat skin proteins identified by GeLC-MS/MS.

Identified proteins (species)	Accession number[a]	TCL[b]			Teat skin		
		R1[c]	R2	R3	R1	R2	R3
Keratins							
keratin, type I cytoskeletal 10	gi|296476308	54	52	48	68	59	61
keratin, type II cytoskeletal 1	gi|358421409	50	48	54	53	54	60
keratin, type II cytoskeletal 6A	gi|296487872	43	39	41	15	12	15
keratin, type II cytoskeletal 6C	gi|383872577	41	39	42			
keratin, type I cytoskeletal 14	gi|262118301	37	36	38	36	26	38
keratin, type II cytoskeletal 5	gi|146186887	35	36	38	29	26	29
keratin, type II cytoskeletal 3	gi|358421417	35	34	35	36	32	38
keratin, type II cytoskeletal 4	gi|148356276	35	34	36	10	9	10
keratin, type II cytoskeletal 79	gi|115496454	35	36	35			
keratin, type I cytoskeletal 17	gi|157427776	29	23	31			
keratin, type II cytoskeletal 2 epidermal	gi|119892108	13	13	16	37	38	41
keratin, type II cytoskeletal 2 oral	gi|358421415	7	10	7	6	6	6
keratin, type II cytoskeletal 73	gi|162287381				8	9	8
keratin, type I cytoskeletal 27	gi|115494902				3	2	6
keratin, type I cytoskeletal 19	gi|62751472				2	7	2
keratin, type I cytoskeletal 15	gi|195539527				18	15	17
Cytoskeletal proteins							
profilaggrin-like	gi|296489626	19	18	21	10	6	11
filaggrin	gi|358411311	14	16	15	0	4	5
junction plakoglobin	gi|51591897	11	9	12	21	19	19
desmoplakin	gi|300797856	7	5	7	47	55	52
hornerin	gi|528942932	5	5	7	5	3	2
vimentin	gi|289450	3	2	3			
tubulin alpha-1B chain (*Mus musculus*)	gi|34740335	2	1	2	2	2	2
repetin	gi|297472686	2	2	4			
alpha-actinin-2	gi|296472241	0	2	1			
epiplakin	gi|528914337				14	10	12
desmocollin	gi|162971				6	4	5
desmoglein	gi|436062				5	7	4
plakophilin-1	gi|27806479				4	2	5
alpha-actinin 1	gi|145286437				3	3	2
S100 calcium-binding proteins							
S100A12	gi|27807183	11	11	9	9	10	10
S100A7	gi|27807077	7	7	10	8	10	8
S100A8	gi|165973998	6	7	6	5	5	5
S100A7-like	gi|76612440	6	7	5	5	7	5
S100A9	gi|114052490	16	13	18	4	5	4
S100A11	gi|296489536	2	0	2			
S100A14	gi|118601864	2	0	2			
S100A2	gi|77735683	2	1	2			

Table 3.6 continued.

Major milk proteins							
beta-lactoglobulin	gi|162748	7	8	6	4	5	5
alpha-S2-casein precursor	gi|27806963	4	5	5	2	2	3
alpha-S1 casein, partial	gi|159793187	3	2	3	2	3	2
beta-casein	gi|119388700	2	4	3	2	2	2
casein para kappaA	gi|229416				0	1	2
Cellular proteins							
14-3-3 protein epsilon (*homo sapiens*)	gi|5803225				4	5	6
14-3-3 protein sigma (*ovis aries*)	gi|57163961	5	4	5	14	18	18
14-3-3 protein zeta	gi|253706				9	10	12
ADP-ribosylation factor 3	gi|296487799				2	2	2
AHNAK nucleoprotein 2	gi|296475271				2	2	2
annexin A1	gi|74	10	8	11	5	2	4
annexin A2	gi|73586982	4	2	2	2	3	1
annexin A8	gi|27806317	2	0	1	2	3	4
annexin V=CaBP33 isoform	gi|260137				4	2	3
beta-actin	gi|168177284	5	6	5	5	6	4
calmodulin-like 5	gi|148234364				0	2	2
cofilin-1 (*sus scrofa*)	gi|51592135				3	2	2
cyclophilin I	gi|7767529	3	1	0	3	4	4
elongation factor 1 alpha	gi|28189681				4	3	4
elongation factor 2	gi|115497900				3	3	4
fatty acid-binding protein, adipocyte	gi|296480594	5	3	5	6	6	6
fatty acid-binding protein, epidermal	gi|296480537	3	0	4	9	9	9
F-box only protein 50	gi|76641449	1	2	1			
gamma-glutamylcyclotransferase	gi|83035087				2	0	2
glutathione S-transferase P	gi|29135329				2	1	1
glyceraldehyde-3-phosphate dehydrogenase	gi|89573947	6	6	5			
heat shock 27kDa protein 1	gi|61553385	4	2	5	5	5	5
heat shock cognate protein ATPase domain, K71m Mutant	gi|157831588	0	2	1			
histone H2A type 1	gi|529004004	3	0	3	6	7	7
histone H2B	gi|229329	2	1	1	2	2	3
lactate dehydrogenase-A	gi|217590	3	3	4	3	0	1
L-lactate dehydrogenase B chain	gi|27806561	2	1	2			
malate dehydrogenase, cytoplasmic	gi|77736203	5	3	6	3	3	3
malate dehydrogenase 2, mitochondrial	gi|89574145				2	2	2
nucleoside diphosphate kinase B	gi|296488274	5	4	4			
pancreatic adenocarcinoma upregulated factor-like (PAUF)	gi|296473587	4	4	3			
peroxiredoxin-1	gi|27806081	1	1	3	4	5	4
peroxiredoxin-2	gi|27807469				2	3	3
profilin	gi|253723066				3	3	0

Table 3.6 continued

protein DJ-1	gi|62751849	2	1	0			
purine nucleoside phosphorylase, chain A	gi|157834116				2	2	3
rab-10 (*mus musculus*)	gi|7710086				2	2	2
ras-related protein Rab-11A isoform X1	gi|528962105				2	2	0
retroviral-like aspartic protease 1	gi|358414487				2	1	1
ribosomal protein L12	gi|28189683				3	1	2
thioredoxin	gi|296484386	1	0	2	2	2	2
transitional endoplasmic reticulum ATPase isoform 3 (*canis lupus familiaris*)	gi|73971210	2	2	3	2	3	2
triosephosphate isomerase	gi|61888856				2	1	0
tyrosine 3/tryptophan 5 - monooxygenase activation protein, zeta polypeptide-like	gi|296475944	2	2	3			
ubiquitin	gi|290560476	3	2	4	3	3	2
Serum proteins							
serum albumin	gi|367460260	21	19	21	3	1	1
hemoglobin, subunit beta	gi|27819608	10	9	11	13	14	12
hemoglobin, subunit alpha	gi|576142	7	5	7	5	5	4
apolipoprotein A-I precursor	gi|162678	3	0	2			
IgM heavy chain constant region	gi|2232299	3	1	2			
Apoptosis							
caspase-14	gi|329663440	15	13	11	2	0	2
galectin-7	gi|119910404	2	3	2	6	8	6
gasdermin 1	gi|296476376	1	2	3			
cornulin	gi|300796748	1	0	2			
Enzyme inhibitors							
serpin-B3-like	gi|119916473	19	17	16			
serpin-B3-like	gi|119916469	18	16	19			
serpin-B3-like	gi|359079289	18	18	19			
serine (or cysteine) proteinase inhibitor, clade B (ovalbumin), member 4	gi|332205893	14	12	15			
serpin-B12	gi|297464091	1	2	0			
cystatin-A	gi|268607697	3	1	3			

a) gene index accession number from NCBI; b) TCL, teat canal lining; c) technical replicates 1-3

3.7. The consequence of sample pooling on assessing biological variability

Sample pooling removes the ability to assess between animal variation and to determine the influence that individual variations in protein abundance have on biological characteristics; however, sample pooling is suitable when the characteristics of the population are of more interest than that of the individual. It is also an attractive option when insufficient biological sample is available from individuals for analysis.

To assess biological variation of proteins from individual teat canal lining and teat skin samples, preparative SDS-PAGE gels resolving 25 µg/lane of teat canal lining proteins (n = 6) and teat skin proteins (n = 6) were run for GeLC-MS/MS analysis. The individual samples consisted of the same six biological samples that were also used to make up the pooled samples for GeLC-MS/MS analysis in Section 3.6 and are presented as 10 µg loadings in Figure 3.5. From the 12 separate lanes, a total of 120 gel slices were excised, and 96 fractions were subjected to MS/MS analysis resulting in the generation of over 100,000 fragment spectra (Supplementary data Table A3 & A4). These spectra were submitted to Mascot resulting in 8585 peptide assignments (8.3 %) from the bovine non-redundant database. A total of 154 distinct proteins with 2 or more unique peptides present in at least one of the 12 biological samples were identified by this analysis. All 154 distinct proteins identified are listed in Supplementary data Table A5. From this list, 117 proteins were identified in teat canal lining, and 130 proteins were identified in teat skin. Ninety-three of these proteins were common to both tissue samples, with 24 proteins exclusive to the teat canal lining samples and 37 proteins exclusive to the teat skin samples. Of the 154 distinct proteins detected, 39 proteins appeared in all 12 samples representing 25.3 % of the total identifiable proteins. These 39 proteins are listed in Table 3.7 along with the average peptide count of the six biological replicates for the teat canal lining and teat skin, respectively.

Table 3.7: Proteins identified in all 12 GeLC-MS/MS samples from teat canal lining and teat skin

		Average peptide count		
Identified proteins (species)	**Accession number**	**TCL**	**Teat skin**	**Fold change**
Keratins				
keratin, type II cytoskeletal 1	gi|358421409	43	61	1.4
keratin, type I cytoskeletal 10	gi|27805977	44	57	1.3
keratin, type II cytoskeletal 2 epidermal	gi|119892108	6	49	8.2
keratin, type II cytoskeletal 2 oral	gi|358421415	11	9	0.8
keratin, type II cytoskeletal 3	gi|358421417	29	41	1.4
keratin, type II cytoskeletal 4	gi|148356276	33	12	0.4
keratin, type II cytoskeletal 5	gi|296487899	33	41	1.2
keratin, type II cytoskeletal 6A	gi|134085706	39	18	0.5
keratin, type I cytoskeletal 14	gi|262118301	34	43	1.3
Cytoskeleton				
desmoplakin	gi|300797856	6	61	10.2
hornerin	gi|528942932	6	5	0.8
junction plakoglobin	gi|109658166	9	24	2.7
filaggrin	gi|359063845	18	10	0.6
profilaggrin-like	gi|296489626	20	12	0.6
tubulin alpha-1B chain (*Mus musculus*)	gi|34740335	2	2	1.0
Major milk proteins				
alpha-S1-casein precursor	gi|30794348	7	7	1.0
beta-casein precursor	gi|162797	4	4	1.0
beta-lactoglobulin	gi|2194088	9	6	0.7
S100 calcium-binding proteins				
S100A7	gi|27807077	6	7	1.2
S100A7-like	gi|528901741	4	4	1.0
S100A8	gi|165973998	4	4	1.0
S100A9	gi|114052490	12	5	0.4
S100A12	gi|27807183	10	11	1.1
Cellular proteins				
actin, beta	gi|148744172	7	7	1.0
annexin A1	gi|73853762	10	3	0.3
annexin A2	gi|73586982	3	2	0.7
ubiquitin	gi|51701999	5	5	1.0
fatty acid-binding protein, epidermal	gi|27805805	6	8	1.3
heat shock 27kDa protein 1	gi|61553385	3	7	2.3
L-lactate dehydrogenase A chain	gi|27806559	3	4	1.3
malate dehydrogenase, cytoplasmic	gi|77736203	3	2	0.7
thioredoxin	gi|296484386	1	2	2.0
transitional endoplasmic reticulum ATPase isoform 3 (*canis lupus familiaris*)	gi|73971210	2	3	1.5
Serum proteins				
serum albumin	gi|367460260	15	2	0.1
hemoglobin subunit alpha	gi|116812902	7	7	1.0
hemoglobin subunit beta	gi|27819608	11	15	1.4
Apoptosis				
caspase-14	gi|329663440	10	2	0.2
gasdermin 1	gi|296476376	4	1	0.3

Fold change is calculated from average peptide counts with the teat canal lining as the denominator.

Triplicate GeLC-MS/MS analysis of the pooled technical replicates identified 45 proteins inclusive to both teat canal lining and teat skin data sets (Table 3.6); six more than the individual biological replicates. These additional six proteins included annexin A8, 14-3-3 sigma protein, fatty acid-binding protein (adipocyte), cyclophilin I, kappa-casein and alpha-S2-casein. Due to individual sample variation, these proteins were not detected in all 12 cows, however, they were still sufficiently abundant in individual samples to be detected in the pooled samples.

Alternatively, the GeLC-MS/MS analysis on the individual biological replicate samples also identified 44 more unique teat canal lining proteins and 54 more unique teat skin proteins than their respective pooled replicate samples. Most of these proteins were identified by only a few peptide hits suggesting that their abundance is on the edge of the MS detection limit for analysis. By pooling the samples together, these proteins are therefore further diluted, with the average peptide count in the pooled sample below the minimum threshold for identification (i.e. 2 unique precursor ions in a single MS/MS run).

Using 2-DE, the S100 family of proteins appeared to be more abundant in the teat canal lining than in the teat skin. S100 proteins are known to play a role in host-defence and therefore, their abundance in the teat canal lining where they may play a role in the growth inhibition or killing of pathogenic microorganisms is not unexpected. PDQuest analysis of the replicate gel sets demonstrated that in the six cows sampled, the relative abundances of S100A7L, S100A8, S100A9 and S100A12 in the pooled teat canal lining was significantly higher compared to that of the pooled teat skin (See Table 3.4 for fold change and *p*-values). However, results from the GeLC-MS/MS analysis were less clear. Although a two-fold increase in the average peptide count for S100A9 was observed in the teat canal lining relative to the teat skin, in agreement with the 2-DE results, the same average peptide count or a slightly increased average peptide count was observed in the teat skin relative to the teat canal lining for the other four S100 proteins which is in contrast to the 2-DE results. While providing an initial guide, peptide count is not an accurate proxy for relative abundance. Instead, accurate quantification is reliant on established immunological methodologies such as Western blotting or ELISA, requiring an antibody specific to the protein of interest.

3.8. Validation of proteomic results by Western blot analysis

Western blot analysis was performed on six individual teat canal lining and six matching teat skin samples, on proteins of interest, to confirm the MS identifications and to verify the quantitative differences observed by 2-DE and GeLC-MS/MS. These proteins comprised, β-actin, GAPDH, S100A7/A7L, S100A8, S100A9, S100A12, serpins B3/B4 and lactoferrin. Several proteins with proven innate immune function that are known to be expressed by keratinocytes, but were not identified by GeLC-MS/MS, were also examined. These included β-defensin-LAP (lingual antimicrobial protein), cathelicidin and RNase7. The S100A7 and S100A7L proteins were not assessed independently, as antibodies specifically recognising each protein were not available. Therefore, quantitative values presented here for the S100A7 and S100A7L proteins are a sum of both S100 proteins.

A comparison of protein preparations from the teat canal lining and teat skin of individual cows showed that the relative abundance of S100A8, S100A9, S100A12 and serpins B3/B4 were higher in the teat canal lining samples (Figure 3.9). A significant increase in protein abundance of 1.6-fold, 11-fold, 4.2-fold and 80-fold in the teat canal lining was calculated for S100A8, S100A9, S100A12, and serpins B3/B4, respectively. Among the S100 proteins, S100A8 and S100A12 appeared the most variable among the six teat canal lining samples. Results suggested the relative abundance of S100A7/A7L in the teat canal lining and the teat skin samples was similar (p = 0.696). No chemiluminescent signal was observed in the Western blots for cathelicidin, lactoferrin, β-defensin and RNase7. This confirmed the findings of the GeLC-MS/MS analysis which failed to detect these proteins in the normal lactating teat canal lining or teat skin epithelium, at the examined loadings. The abundance of β-actin was found to be variable between the teat canal lining and teat skin samples, and GAPDH was only detected in two of the six teat skin samples after extended exposure. These results were also in agreement with the findings of GeLC-MS/MS analysis.

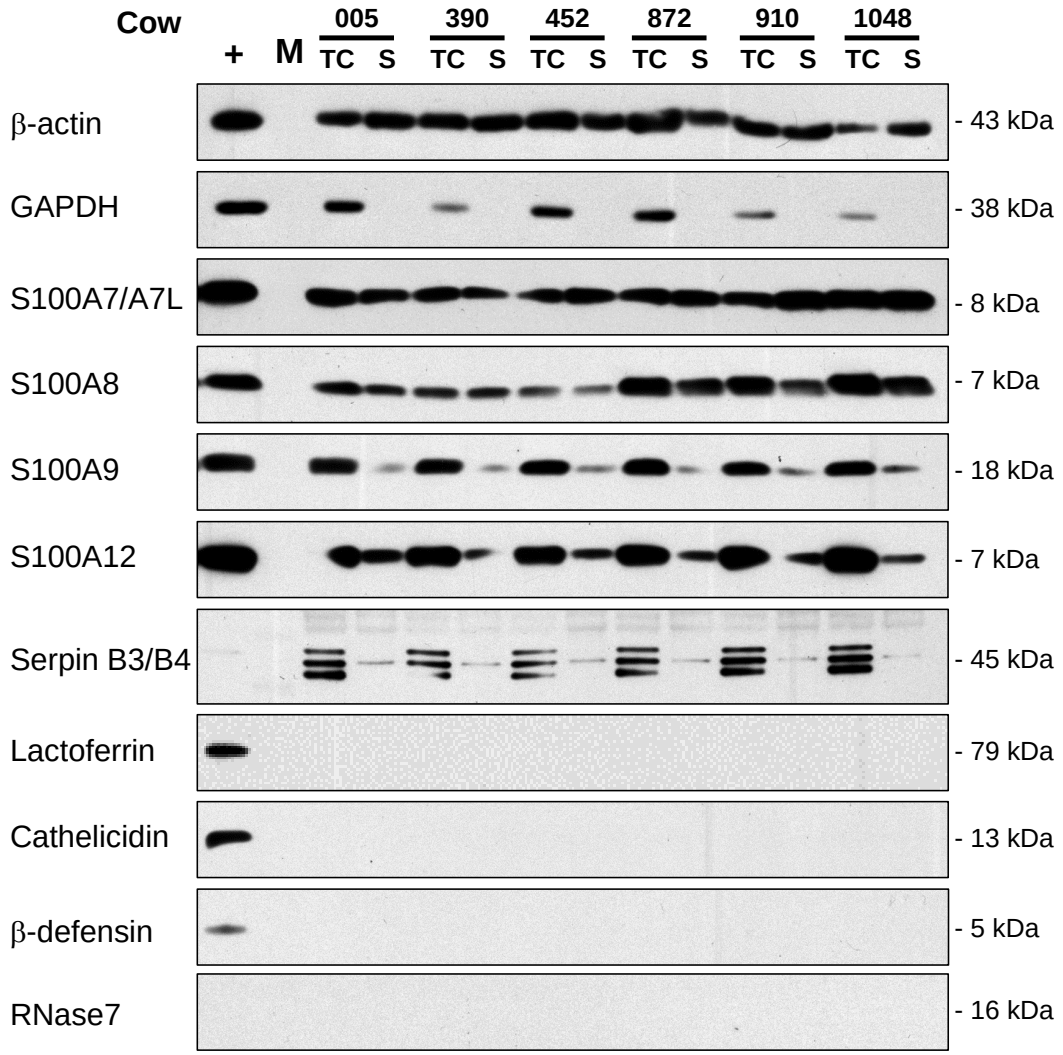

Figure 3.9: Validation of relative protein abundance by Western blot analysis.
A side-by-side comparison of the Western blot data of β-actin, GAPDH, S100A7/A7L, S100A8, S100A9, S100A12, serpins B3/B4, lactoferrin, cathelicidin, β-defensin, and RNase7 for teat canal lining and teat skin from six individual cows. **Note:** the positive control for RNase7 was the ovalbumin conjugated peptide which ran at ~40 kDa and is not shown at 16 kDa. Due to lactoferrin being the most abundant minor milk protein in skim milk, the lactoferrin blot was blocked with 2 % polyvinylpyrrolidone 25 in TBST/BSA to eliminate any non-specific background signal. +, positive control; M, molecular weight marker; TC, teat canal lining; S, teat skin.

3.9. Individual variation in the abundance of S100 proteins in the teat canal lining

The variability in the abundance of S100 proteins observed in the teat canal lining of individual cows was investigated further by Western blot analysis on the full set of teat canal lining samples (n = 11). As teat canal lining samples were collected from two different teats from the same cow, this enabled the within-cow biological variability of S100 protein abundance to be assessed along with the between-cow variability.

The relative abundance of each S100 protein in the 11 teat canal lining samples collected was determined by reference to a four-point standard curve. The standard curve was produced from serial two-fold dilutions of a positive control sample (teat skin for S100A7; neutrophil lysate for S100A8, S100A9, and S100A12) run on the same gel. All samples were run in triplicate with each triplicate run on an independent gel. For each anti-S100 antibody, an optimised protein loading was determined. The amount of teat canal lining and teat skin protein loaded per lane for S100A7/A7L, S100A8, S100A9 and S100A12 was 0.8 µg, 10 µg, 10 µg and 4 µg, respectively.

Previous results had suggested that the occurrence of the 'housekeeping proteins' GAPDH and β-actin was quite variable in the teat canal lining and teat skin samples (Figure 3.9), and therefore, could not be used to normalise for loading and gel-to-gel variation. To overcome this problem, an equivalently loaded gel was stained with CCB and subjected to densitometry to verify equal protein loading. This method of verification has been previously described (Aldridge *et al.*, 2008).

Representative images of Western blot analyses are shown in Figure 3.10, and the mean abundance ± SD of each S100 protein in each teat canal lining sample was determined after quantitative chemiluminescence analysis. The data is shown in a parallel coordinate plot in Figure 3.11. A coefficient of variation (CV) of less than 7 % (technical variation) was obtained for the replicated samples analysed. The variability observed among the samples for each of the S100 proteins was significantly greater than the variation due to technical factors. A 2.2-fold, 4.2-fold,

2.4-fold and 2.4-fold range in protein abundance was detected in teal canal lining samples for S100A7/A7L, S100A8, S100A9 and S100A12 proteins with coefficients of variation of 14.6 %, 39 %, 15.3 % and 20 %, respectively. These values, which are up to 5-fold greater than the technical variation, indicate that there was significant biological variation among teats from an individual cow and between teats on different cows. The variance in abundance of S100A8 was almost twice that of the other S100 proteins. Estimates of the within-cow and between-cow variation in S100 protein abundance using REML suggested that no significant difference exists within or between cows for the S100A7/A7L, S100A9 and S100A12 proteins. However, for S100A8, analysis suggested significant within-cow (CV = 24.8%) and between-cow (CV = 39.0%) variation exists.

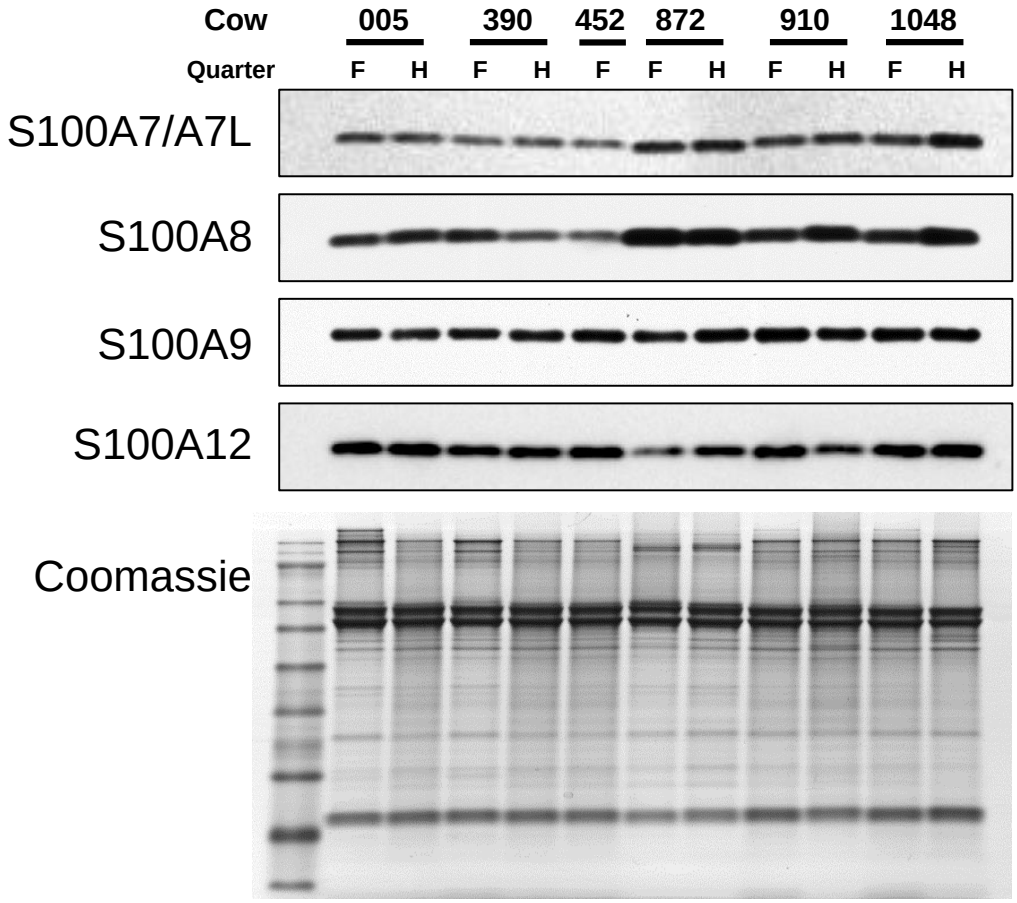

Figure 3.10: Western blotting analysis of S100 proteins from the teat canal lining of six individual cows.
Proteins extracted from the TCL of six individual cows were subjected to SDS–PAGE followed by Western blot analysis. Samples were collected from a forequarter (F) and hindquarter (H) teat from each cow except for cow 452. The blots were probed with antibodies specific for bovine S100A7/A7L, S100A8, S100A9, and S100A12. A replicate gel loaded with 10 µg of total protein was stained with Coomassie blue G-250 (bottom panel) to demonstrate equivalent loading.

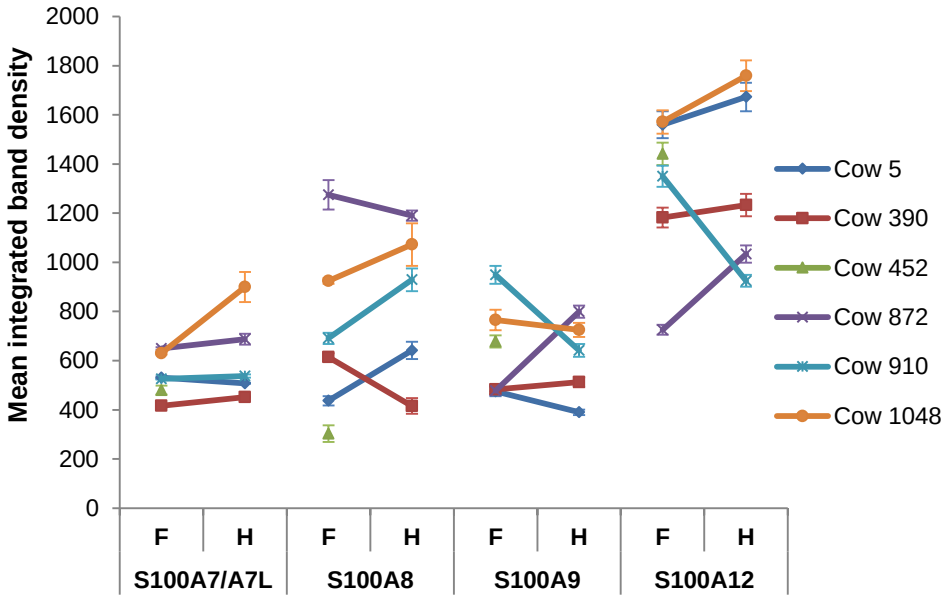

Figure 3.11: Abundance of S100 proteins in teat canal lining from individual teats.
Teat canal lining proteins were subjected to quantitative Western blotting using internal standards. Chemiluminescence signal was captured by a CCD camera and densitometry performed on the images. The mean untransformed integrated density values for each S100 protein in each teat canal are presented in the parallel coordinate plot with S100 proteins measured from forequarter (F) and hindquarter (H) teats from the same cow horizontally linked. Error bars represent the standard deviation of triplicate analyses.

3.10. Localisation of S100 proteins in the teat canal

S100 proteins have been previously identified in normal mammalian skin (Eckert *et al.*, 2004), in neutrophils isolated from human blood (Lominadze *et al.*, 2005) and in milk from cows with mastitis (Wheeler *et al.*, 2012a). To determine if the S100 proteins found in the teat canal lining were locally produced by the teat canal epithelium or originating from cells in milk, IHC analysis of frozen teat canal sections was performed.

Indirect immunofluorescence (IF) revealed strong signals in the epidermal layer of the teat canal epithelium for S100A7/A7L, S100A8, S100A9, and S100A12 (Figure 3.12). The merged micrographs presented as Figure 3.12 are representative for all teat sections analysed for each of the four different anti-S100 antibodies. Most of the signal from all four S100 proteins was restricted to the epidermal layer in which keratinocytes are the predominant cell type. The signal

was concentrated in the cornified layer of the epidermis, but distinct patterns of expression within the epidermal layer were also observed for each of the S100 proteins. For example, S100A7/A7L signal occurred predominantly within the *stratum granulosum* (See arrowed in Figure 3.12a), whereas an intense signal for S100A8 and S100A9 was observed throughout the epithelial layer. The most concentrated signal for S100A9 and S100A12 was in the inter-papillar zones of the epithelium between the teat canal rete ridges (See arrowed in Figures 3.12c, d). S100A12 was also present in all epidermal layers; however, the signal in the lower spinous layer (Marked S in Figure 3.12d) was less intense than that observed for S100A8 and S100A9.

For S100A8, S100A9 and S100A12, IF signals were also observed in non-epithelial cells located directly beneath the basal cells of the epidermis and within the supra-papillary plate between the rete ridges (Figure 3.12b-d). These signals, however, were far weaker than the signals observed in the teat canal epithelium. Evidence of a weak signal was also apparent in cells observed to be inside the circular follicle-like structures that are present within the epidermal layer. These structures, which are not found in skin epithelium, are known as Marksäulchen (Marked M in Figure 3.12c). While their function in the teat canal epithelium is not completely understood these findings suggest that they may provide access for immune cells to the more highly differentiated areas of the teat canal epithelium and possibly the teat canal lining.

IF signals for all four S100 proteins were also observed in the teat skin (Figure 3.13a-d). Figure 3.13 is representative for all teats analysed and was performed on the same section of tissue as for the teat canal analysis. For S100A7/A7L, the signal appeared to be as strong in the teat skin as was observed in the teat canal epithelium and had a similar pattern of expression. S100A7/A7L was predominantly expressed within the *stratum granulosum* (Arrowed in Figure 3.13a) with the signal concentrating in the *stratum corneum*. The signal for both S100A8 and S100A9 was noticeably less intense in the teat skin sections as compared to the teat canal sections. However, a weak signal could still be observed in the basal keratinocytes and in some non-epithelial cells within the supra-papillary plate between the rete ridges (Figure 3.13c-d). The IF signal for

S100A12 appeared to be weaker than was observed in for the corresponding teat canal lining sections. The signal for S100A12 was observed in all keratinocyte cell layers, in non-epithelial cells located between the rete ridges and in cells lining endothelial cells of blood vessels (Figure 3.13d).

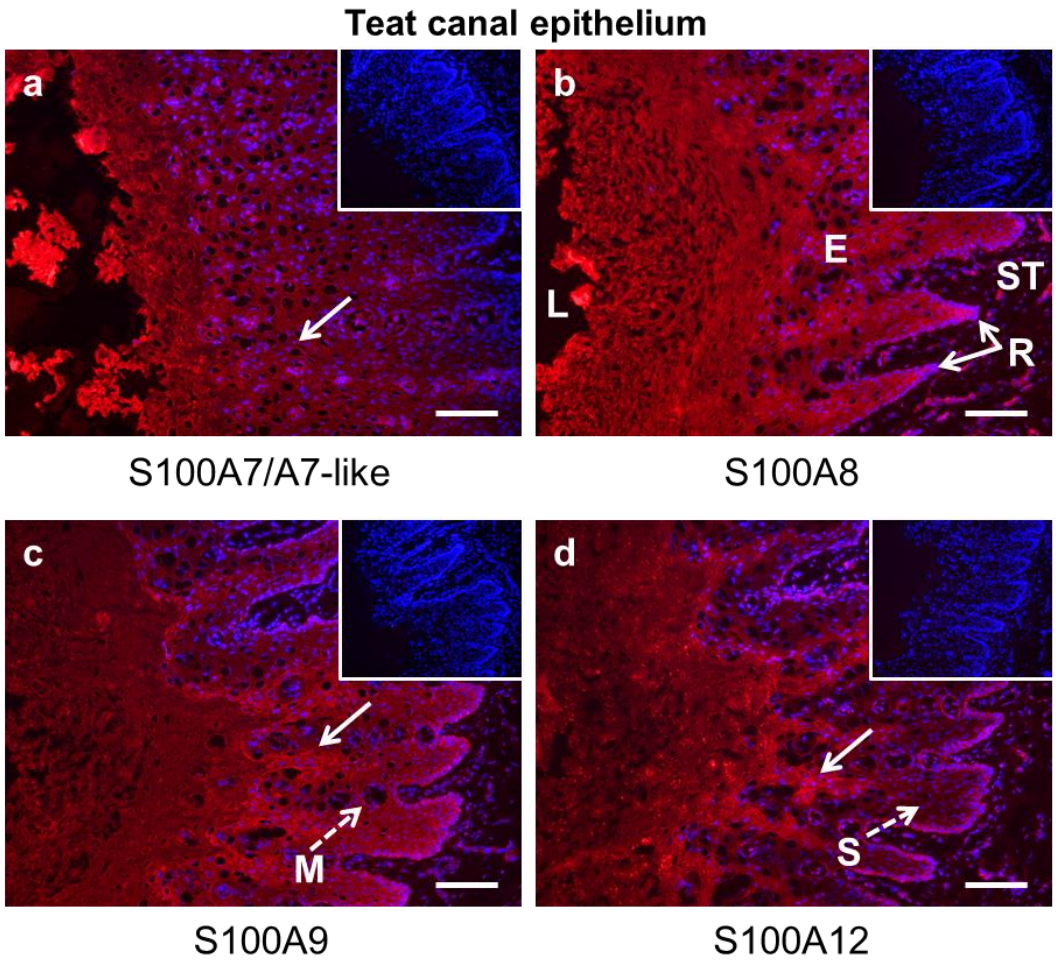

Figure 3.12: S100 proteins in bovine teat canal tissue.
Transverse teat canal cryosections were stained using indirect immunofluorescence for (a) S100A7/A7L, (b) S100A8, (c) S100A9 and (d) S100A12. Serial sections were probed with anti-S100 protein antibodies, and the signal detected with Alexa Fluor-594 labelled secondary antibodies (red signal). Each section was counterstained with DAPI (blue signal). Equivalent sections probed with non-specific IgG (isotype controls) are shown as inserts on the upper right-hand corner. All micrographs were exposed for the same length of time as the negative isotype controls. Strong S100A7/A7L signal was observed in the *stratum granulosum* of plate a (arrowed). Concentrated signal for S100A9 and S100A12 in the inter-papillary zones of the epithelium located between the teat canal rete ridges is indicated by a solid arrow in plates c and d. L, lumen; E, epidermis; ST, stromal tissue; M, Marksäulchen; R, rete ridges; S, *spinosum*. Scale bars in all panels are 100 µm.

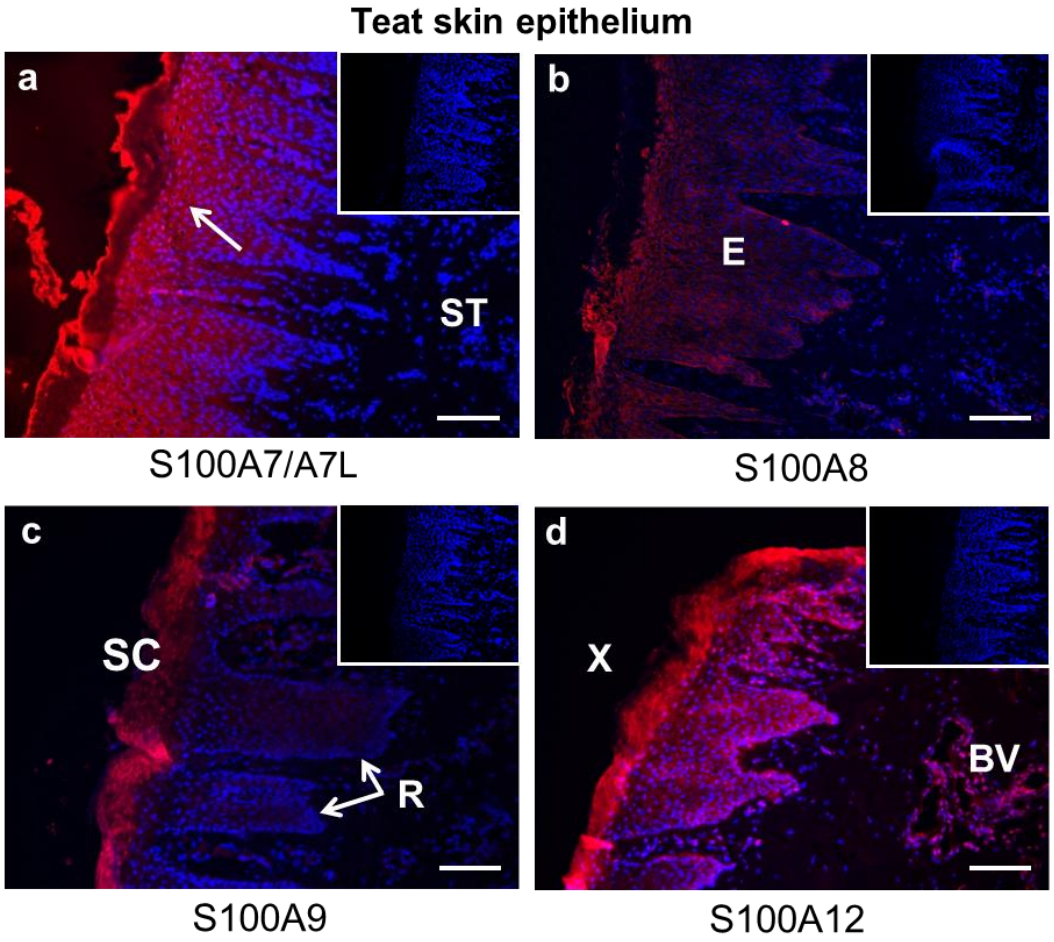

Figure 3.13: S100 proteins in bovine teat skin tissue.
Transverse teat cryosections were stained using indirect immunofluorescence for (a) S100A7/A7L, (b) S100A8, (c) S100A9 and (d) S100A12. Serial sections were probed with anti-S100 protein antibodies, and the signal detected with Alexa Fluor-594 labelled secondary antibodies (red signal). Each section was counterstained with DAPI (blue signal). Equivalent sections probed with non-specific IgG (isotype controls) are shown as inserts on the upper right-hand corner. All micrographs were exposed for the same length of time as the negative controls. Strong S100A7/A7L signal was observed in the upper *stratum granulosum* of plate a (arrowed). Absence of S100A9 signal was observed around the teat skin rete ridges in plate c (arrowed). X, external skin surface; E, epidermis; ST, stromal tissue; R, rete ridges; SC, *stratum corneum*; BV, blood vessels. Scale bars in all panels are 100 µm.

3.11. Identification of proteins of microbial origin

As previously discussed in Section 3.7., only a low percentage (8.3 %) of the total detected MS/MS spectra matched to peptides of bovine origin. This low percentage can be attributed to several experimental and computational factors. Firstly, not all ions selected for fragmentation are peptide ions (i.e. metabolite or carbohydrate molecules). Secondly, only a small number of peptides are selected for fragmentation giving rise to high-confidence identifications. Another contributing factor may be that some of the peptide fragmentation spectra do not match to proteins in the bovine database, but are from other biological species.

Recent analysis by a number of research groups have shown that both the milk and teat canals from otherwise healthy cows' are populated by a diverse array of commensal bacterial species (Gill *et al.*, 2006; Oikonomou *et al.*, 2012; Kuehn *et al.*, 2013; Oikonomou *et al.*, 2014; Falentin *et al.*, 2016). It is therefore plausible that some of the unidentified GeLC-MS/MS spectra could be attributed to the resident microflora of the teat canal.

To test this possibility, the combined teat canal lining MS/MS spectra from the three GeLC-MS/MS technical replicates (Section 3.7) were searched by Mascot against the bacterial subset of the NCBI database using the same protein identification parameters listed in Section 2.2.14.

Very few spectra were identified as bacterial proteins. In fact, only 458 spectra out the 49,737 teat canal lining spectra (0.92 %) matched to proteins in the bacterial database. Furthermore, of these 458 spectra, only 50 (0.1 %) were identified as proteins with 2 or more peptide matches at a false discovery rate of 5 %. These results indicate that although there might be a diverse population of microflora residing in the lining of the teat canal; proteins extracted from this population are negligible compared to the abundance of proteins from the teat canal lining itself.

3.12. Peptidomic analysis of the bovine teat canal lining

Peptidomic analysis of the soluble teat canal lining fraction was performed to determine if any keratin-derived antimicrobial peptides were present. A recent report by Tam and colleagues identified several human K6-derived C-terminal peptides with broad-spectrum antimicrobial activity against a range of bacteria, including *Pseudomonas aeruginosa*, *E. coli*, *Streptococcus pyogenes*, and *S. aureus* (Tam *et al.*, 2012). These antimicrobial peptides are glycine-rich with the bovine homolog of the most bactericidal keratin-derived antimicrobial peptide being composed of 30% glycine residues and sharing 70% similarity with the equivalent human peptide; (K6A bovine sequence; R.AIGCGFGSSGGGSSSTIK; A^{540}-K^{556}).

For both the bovine K6A (NP_001076979.1) and K6C (DAA29996.1) protein sequences, the N- and C-termini of the peptide fragment are flanked by theoretical trypsin cleavage sites (Arg-Ala and Lys-Tyr, respectively) (Figure 3.14A). This peptide, however, was not detected after tryptic fragmentation of these proteins and separation by SDS-PAGE and 2-DE (Figure 3.14b). In fact, there were very few C-terminal tryptic fragments identified suggesting that these proteins may have already been proteolytically processed before 2-DE and GeLC analysis. If that were the case, then it is possible that these K6A and K6C C-terminal fragments may be found in the soluble teat canal lining fraction where they could provide a similar host defence function as the human cornea and ocular derived peptides.

For this peptidomics investigation, 78 mg of teat canal lining from five individual teats was collected from five healthy late-lactating cows. The soluble fraction for each sample was extracted as previously described (See Section 2.2.15). An SDS-PAGE gel of each extract is shown in Figure 3.15. The major protein bands in this extract were identified as BSA, serpins B3-like and B4-like along with the S100 proteins A7, A8, A9 and A12. The extracts were pooled together, and the peptide fraction was obtained as previously described (See Section 2.2.15). LC-ESI-Q/TOF analysis of the enriched peptide fraction failed to identify any K6A or K6C peptide fragments but did identify several large glycine-rich N- and C-terminal keratin fragments from K5 and K79 (Table 3.8). These findings were unexpected since K6 and K6C are two of the more abundant keratins found in the teat canal lining.

A) Keratin 6A

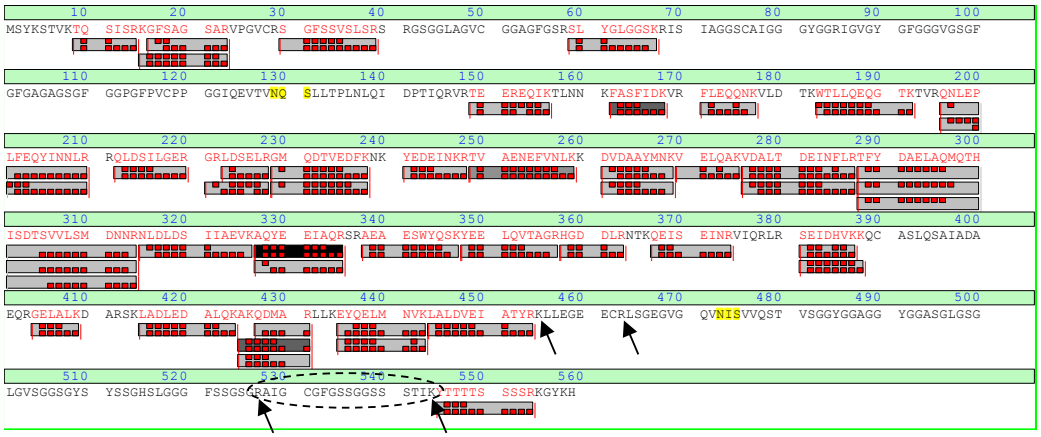

B) Keratin 6C

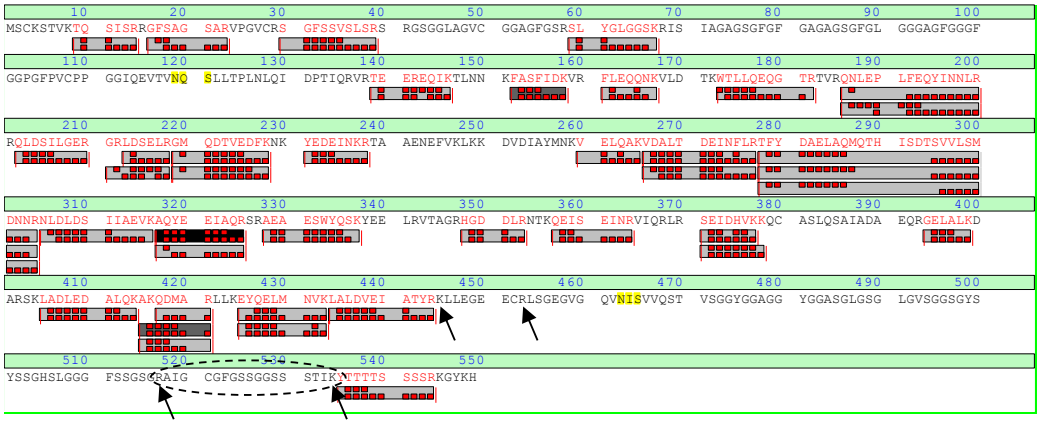

Figure 3.14: Sequence alignment of keratin 6A and keratin 6C tryptic peptides identified from teat canal lining.
Tryptic peptides were identified by GeLC analysis of the teat canal lining from a cow in late-lactation (Cow #005) and are mapped against the full keratin 6A (A) and keratin 6C (B) protein sequence. The matched sequence is highlighted in red, and the b and y ion MS/MS identifications are found in the grey boxes below each fragment. **Note:** for both keratins, there is an absence of tryptic fragments in the C-terminal region of the proteins. Depicted by arrows are four potential trypsin cleavage positions whose fragments were not detected by MS/MS analysis. The fragment highlighted by the dashed ellipse is homologous to the 17 amino acid sequence identified by Tam et al., 2012.

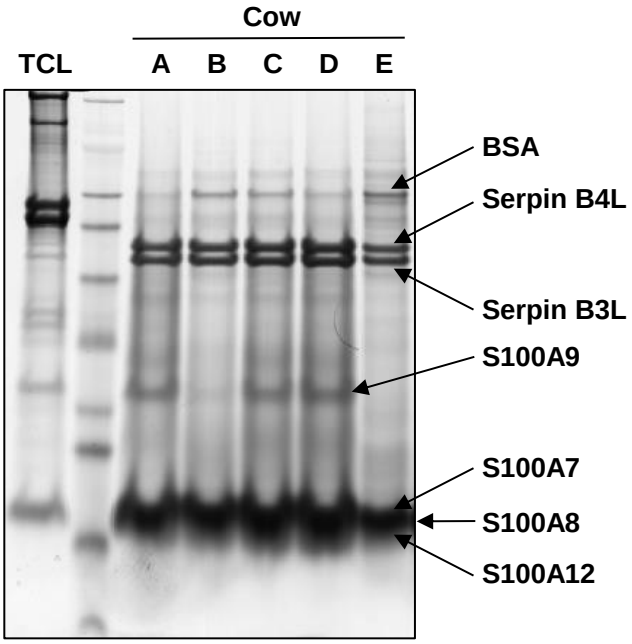

Figure 3.15: 1D SDS-PAGE separation of the soluble teat canal lining protein fraction.
Each lane represents approximately 10 µg of solubilised protein extract collected from an individual teat, each from a different cow; A-E). In comparison, lane 1 contains 10 µg of pooled teat canal lining (TCL) prior to soluble protein extraction. Major protein bands of interest were identified by LC-ESI MS/MS and are indicated with arrows.

Table 3.8: Identified keratin peptides from pooled solubilised teat canal lining

Peptide sequence	Position	Protein of origin	Accession #
R.SGGGGGGGFGRVSLGGAYGAGGFGSR.S	38 - 63	keratin, type II cytoskeletal 5	gi|296487899
Y.SSSSGGVGLGGGLSVGGSGFSASSGRSLGFGSGGGS.S	547 - 582		
Y.SSSSGGVGLGGGLSVGGSGFSASSGRSLGFGSGGGSS.S	547 - 583		
Y.SSSSGGVGLGGGLSVGGSGFSASSGRSLGFGSGGGSSSS.V	547 - 585		
Y.STKGAFSSSSASGGGGSQARTS.F	11-32	keratin, type II cytoskeletal 79	gi|115496454
Y.STKGAFSSSSASGGGGSQARTSF.S	11-33		

3.13. Does the soluble teat canal lining fraction have antimicrobial activity?

To examine the antimicrobial activity of the S100 proteins and keratin-derived peptides in teat canal lining soluble extracts, extract fractions were tested for their capacity to restrict the growth of three different mastitis causing bacteria (See Section 2.2.4).

The growth inhibition properties of the crude soluble protein extracts from five different cows against *E. coli* LY3286EC, *S. aureus* LY7111SA and *S. uberis* SR115 were examined using a plate growth inhibition assay. Due to the dilute nature of the crude extract, the maximum concentration that could be employed in the assay was 1 mg/mL of total protein. At this concentration, the results of the assay suggested that none of the crude soluble protein extracts (sample test plate A–E) inhibited the growth of the three bacterial strains.

On the positive control plate, the antibiotic Pen-Strep (Penicillin-Streptomycin; 0.0001 units) showed clear zones for all three bacterial strains. The human synthetic cathelicidin peptide LL-37 showed some initial inhibition of growth for *E. coli* and *S. uberis* (dashed ellipses on plates) but not for *S. aureus*. The bovine synthetic cathelicidin peptide bcath5L also showed some initial inhibition of growth for *S. uberis* only. However, growth of bacteria in these zones by 24 h would suggest that the initial inhibitory effect was easily overcome.

The low level of growth restriction observed using the synthetic peptides suggested the sensitivity of the assay may have been compromised, possibly due to sub-optimal *in-vitro* conditions for bacteriostatic/bactericidal activity. Bacteriostatic/ bactericidal activity can be influenced by conditions including pH, ionic strength of cofactor ions (i.e. Ca^{2+} Mn^{2+}, and Zn^{2+}) and peptide concentration.

More detailed optimisation of the assay may well establish an inhibitory effect for the synthetic peptides and crude soluble extract. However, as the assay failed to show any apparent growth inhibition and only low protein extract concentrations were achieved it was decided not to test for minimum inhibitory concentration (MIC) using a microbroth dilution assay.

3.14. Discussion

Once a bacterium enters the teat canal, it encounters the soft waxy cerumen-like material known as the teat canal lining. This lining is the end-product of keratinocyte differentiation and, as such, is comparable to the *stratum corneum* of the external skin. However, the physical appearance of the teat canal lining is very different to that of the *stratum corneum*. This disparity would suggest that there are compositional and functional differences between these two tissues and that these differences have an influence on the host defence mechanisms at play in each tissue.

The proteomic analysis confirmed the long-standing assumption that keratins are the predominant proteins found in the teat canal lining. Furthermore, major differences were identified in the keratin protein composition of the teat canal lining as compared to that of the external teat skin. In addition, analyses revealed that multiple members of the S100 calcium-binding protein and serpin family of proteins are also present in the teat canal lining at relatively high abundance. The potential role that these proteins may play in the host-defence capacity of the teat canal is discussed further below.

The keratin proteins identified by proteomic analysis are consistent with the known physiology of the teat canal lining and the external teat skin. Multiple primary acidic and basic keratins typical of stratified squamous epithelia (K1, K3, K4, K5, K10, and K14) were identified in both the teat canal lining and the teat skin. However, when comparing the proteome profiles between the two tissue types, several major differences were observed. The most obvious being the high abundance of the secondary keratins K6A and K6C as well as its intermediate filament binding partner K17 in the teat canal lining, as compared to teat skin, proteome along with the reduced expression of epidermal K2 and the absence of K15.

In human and mouse studies, the K6 isoforms and their binding partner K17 are not normally expressed at high levels in healthy skin epithelium (Dale *et al.*, 1990). However, they are observed to be upregulated in the skin during periods of

physiological stress such as wound-healing (Patel *et al.*, 2006), psoriasis (Thewes *et al.*, 1991) and in certain carcinomas (Moll *et al.*, 2008) where the epithelial cells are undergoing periods of rapid proliferation. The keratinocytes of the teat canal appear to be activated and in a state of hyper-proliferation. Evidence supporting this notion includes the rapid regeneration of the teat canal lining together with the high abundance of key indicators such as K6, K17, S100 proteins and serpins as well as the decrease in abundance of K15 (Waseem *et al.*, 1999).

Recent research by Tam and colleagues has provided evidence that peptide fragments of keratin 6A are antimicrobial (Tam *et al.*, 2012). Under physiological conditions, these keratin-derived antimicrobial peptides have been shown to be effective at killing mastitis-causing bacteria such as *E. coli*, *S. aureus* and *Pseudomonas aeruginosa*, suggesting that they may play an important role in preventing intra-mammary infection. In this study, however, no peptide fragments derived from keratin 6A or 6C were observed in the soluble fraction of the teat canal lining. This was surprising considering that the K6 proteins are some of the most abundant proteins in the teat canal lining. There may be several reasons for this including, i) that the peptide extraction method may not have been optimised for the enrichment of the keratin 6 fragments, ii) the fragments may have already interacted with bacteria in the teat canal and have been removed during the extraction process, and iii) the fragments were not present. However, several long glycine-rich keratin-derived fragments were identified from keratin 5 and keratin 79 suggesting that this protection mechanism may also exist in the teat canal lining. It is unknown if these K5 and K79 fragments are antimicrobial without isolating (or synthesising) them and testing for their antimicrobial properties. However, they do appear to have characteristics typical of other glycine-rich antimicrobial peptides as characterised by Tam *et al.*, 2012. Further studies are required to optimise peptide extraction methods, determine the concentration of these peptides in the teat canal lining as well as to determine if their antimicrobial activity extends to other mastitis-causing pathogens.

As keratins are the predominant proteins in the teat canal lining, it would be likely that these proteins, along with the lipid component, would be utilised by invading

bacteria as a carbon and energy source. Microbes produce a variety of endo- and exopeptidases to degrade complex matrixes into free amino acids for consumption. The ability to derive nutrients from the surrounding environment is considered one of the virulence factors of a microorganism (Travis *et al.*, 1995). However, keratin proteins are highly rigid, strongly cross-linked polypeptide structures that are difficult to break down (Gupta & Ramnani, 2006). To overcome this, some microbes produce keratinolytic enzymes which specialise in the degradation of keratin, several of which are known to cause mastitis. These include bacteria of the *Bacillus* species such as *B. cereus* and *B. subtilis*, as well as the opportunistic pathogen *P. aeruginosa* (Suh & Lee, 2001; Zambare *et al.*, 2007; Sharma & Gupta, 2010).

Keratinases have a broad temperature and pH activity range and are mainly serine or metalloproteases (Gupta & Ramnani, 2006). For the most part, keratinases tend to be alkaline proteases (pH > 7.0). The pH of the teat canal lining measured in this study ranged from pH 5.7 - 6.1. In this pH range, the degrading ability of the keratinolytic enzymes could be compromised. In addition, these enzymes and other serine proteases produced by bacteria are likely to be inhibited by the relatively high concentration of various serpin protease inhibitors found in the teat canal lining, thereby reducing their pathogenicity.

In normal human and mouse skin tissue, serpins are involved in controlling and regulating a number of serine proteases that are involved in the formation and desquamation of the cornified envelope (Magert *et al.*, 2005; Meyer-Hoffert, 2009). In this study, 2-DE and GeLC analysis revealed that serpins are expressed at low levels in normal teat skin when compared to the teat canal lining. This result is in agreement with previously published experimental results (Carlén *et al.*, 2005; Huang *et al.*, 2005; Mikesh *et al.*, 2013; Lundberg *et al.*, 2015). In the teat canal lining, however, the serpins constitute the third most abundant family of identified proteins. There is growing evidence of an important role for serpins in immune defence for plants (Yoo *et al.*, 2000), arthropods (Levashina *et al.*, 1999), insects (Park *et al.*, 2011b) and mammals (Aboud *et al.*, 2014). While some elements of their biological role in host-defence is unclear, their most obvious biological function in epithelial tissue is to protect the host tissue from bacterial

proteases. In this instance, some serpins have previously been shown to interact with microbial proteases such as proteinase K (Komiyama *et al.*, 1996) and subtilisin A (Dahlen *et al.*, 1997). Bacterial proteases are able to inhibit the local immune response by cleaving immunoglobulins (Kilian *et al.*, 1996), inactivating cytokines (Theander *et al.*, 1988; Hell *et al.*, 1993), and inhibiting complement (Lambris *et al.*, 2008) creating an environment suitable for colonisation and the establishment of infection. Reducing the protease activity of invading microorganism is therefore expected to diminish their pathogenicity by allowing other elements of the innate immune system more time to interact and eliminate the potential threat.

Serpins may also have anti-inflammatory properties, protecting the teat canal keratinocytes from the deleterious effects of neutrophil proteases. Neutrophils are key effector cells of the innate immune system and are the primary cells that infiltrate into sites of epidermal infection. Serine proteases released from neutrophils during degranulation include neutrophil elastase, cathepsin G and proteinase 3 (Faurschou & Borregaard, 2003). Considerable neutrophil infiltration has been previously observed in the teat sinus, and Fürstenberg's rosette region of the teat canal (Adams *et al.*, 1961; Nickerson & Pankey, 1983, 1984) and their action can inadvertently damage the host tissue causing scaring to the epithelial lining.

The presence of S100 proteins in the teat canal lining is consistent with earlier reports of S100 proteins being present in skin (Broome *et al.*, 2003) albeit during periods of physiological stress. However, the distinct 2-DE pattern of the abundance of the S100 proteins between the teat canal and the teat skin suggests that there are functional differences between the members of this protein family.

There is evidence that some S100 proteins contribute to epithelial host defence. In human skin and bovine teat skin, S100A7 is highly effective in killing *E. coli* and is moderately effective in killing other bacterial species (Gläser *et al.*, 2005; Regenhard *et al.*, 2009). Intracellular expression of the S100A8/A9 heterodimer complex calprotectin imparts epithelial cell resistance to bacterial invasion (Nisapakultorn *et al.*, 2001; Champaiboon *et al.*, 2009) as well as reducing

susceptibility to fungal infections (Eversole *et al.*, 1993). Broad spectrum antimicrobial activity has also been demonstrated for purified preparations of S100A7, S100A8, S100A9, and S100A12 at concentrations as low as 0.5 µmol/L (Steinbakk *et al.*, 1990; Murthy *et al.*, 1993; Gottsch *et al.*, 1999; Cole *et al.*, 2001; Regenhard *et al.*, 2009).

The S100 family of proteins have also been shown to be chemotactic to $CD4^+$ lymphocytes, capable of inducing monocyte trafficking (Donato, 2003), and able to facilitate the recruitment of immune cells to sites of infection (Chen & Nuñez, 2010). Calprotectin has been shown to interact with Toll-like receptor 4 (TLR4) (Ehrchen *et al.*, 2009), and all four S100 protein members are ligands for the receptor for advanced glycation end products (RAGE) (Foell *et al.*, 2007; Leclerc *et al.*, 2009) suggesting that they are also involved in pathogen recognition. Consistent with this notion, stimulation of mammary tissues with microbial pathogen-associated molecular patterns leads to up-regulation of S100 protein transcripts (Lind *et al.*, 2015).

Until now there has been no experimental evidence to show that the S100A7-like protein is expressed *in vivo* in the bovine mammary gland. The distinct 2-DE spot pattern and the detection of multiple peptides specific to this protein is a clear indication of its existence in the bovine teat. In the teat canal lining, it appears to be expressed at a similar abundance to S100A7. This is in contrast to the teat skin and other mammalian epithelial tissues where the S100A7-like protein has not been previously identified. Although the exact biological function of S100A7-like remains unclear, S100A7 has been shown to permeabilize bacterial membranes at low pH (Michalek *et al.*, 2009). The change in amino acid sequence and p*I* may provide S100A7-like with unique antimicrobial properties.

Because the two S100A7 proteins are so similar, standard protein purification methods are not able to separate the proteins. Cloning and recombinant expression of both S100A7 proteins provide an alternative method to generate pure preparations of each protein to allow the potency of these proteins against a range of mastitis-causing pathogens and experimental conditions to be assessed.

In this study, significant variability in the abundance of S100A8 both between cows and between teats from the same cow was observed. S100A8 has demonstrated antimicrobial activity in complex with S100A9, binding Zn^{2+} and Mn^{2+} ions (Sohnle *et al.*, 2000; Kehl-Fie *et al.*, 2011) which are necessary for bacterial growth. Therefore, it is possible that in cows producing less S100A8 the teat canal would be more susceptible to bacterial colonisation, resulting in an increased incidence of intramammary infections. Further studies will be required to establish the basal level of the S100 proteins in the teat canals of uninfected cows and to establish the variability of these proteins in a larger population of cows. The variation in S100 protein levels in the teat canal may be linked to mastitis susceptibility and as such there is potential for S100 protein levels, both basal or in response to infection, to be used as future biomarkers for mastitis resistance. However, extensive further studies involving the collection and analysis of large amounts of teat canal lining material from many cows will be required to validate the biomarker potential of the S100 protein family.

The distribution patterns of the S100 proteins observed in the teat canal lining appear similar to the abundance and distribution patterns previously reported in human skin during the inflammatory condition psoriasis (Broome *et al.*, 2003). Furthermore, the relatively high abundance of K6 and K17 in the teat canal lining compared with normal teat skin is like that observed for skin undergoing repair or proliferation. These observations suggest that the teat canal epithelium is in a hyper-proliferative state during lactation, even in the absence of infection. This high turnover of keratinocytes and the subsequent extensive cornification not only contributes to the physical barrier function of the teat canal but may also provide the teat canal lining with a constantly regenerating biochemical barrier to microbial infection.

Taken together, these results provide a number of insights into the biology of the teat canal and teat canal lining. It is possible that the high abundance of S100 proteins and serpins in combination with keratin derived peptides and bactericidal lipid molecules (Adams & Rickard, 1963; Hogan *et al.*, 1987; Drake *et al.*, 2008) could act in concert with each other to enhance their antimicrobial activity, limiting the passage of bacteria through the teat canal and into the mammary

gland. This generalised concept is depicted in Figure 3.16. To validate this concept, additional experimental evidence is required. Studies comparing the activities of the two isoforms of S100A7 proteins would allow functional differences to be examined. In addition, the binding ability of the S100 proteins to bacterial cell membranes and act as opsonins, needs to be studied under conditions that mimic the physiological conditions of the teat canal. Furthermore, studies aimed at identifying the full spectrum of keratin derived glycine-rich peptides in the teat canal lining should be undertaken. Such studies are expected to significantly improve our understanding of the immune mechanisms influencing resistance and susceptibility of dairy cattle to bacterial infection.

It is unlikely that the antimicrobial properties of the proteins, peptides and lipids found in the teat canal lining are all that is required for comprehensive host defence of the bovine mammary gland. The failure of the crude soluble protein extracts, by themselves, to limit the growth of bacteria provides some evidence supporting this notion. It is likely that additional host defence elements, such as innate immune cells, working in unison with the proteins, peptides and lipids of the teat canal lining are required to assist in protecting the mammary gland against infection.

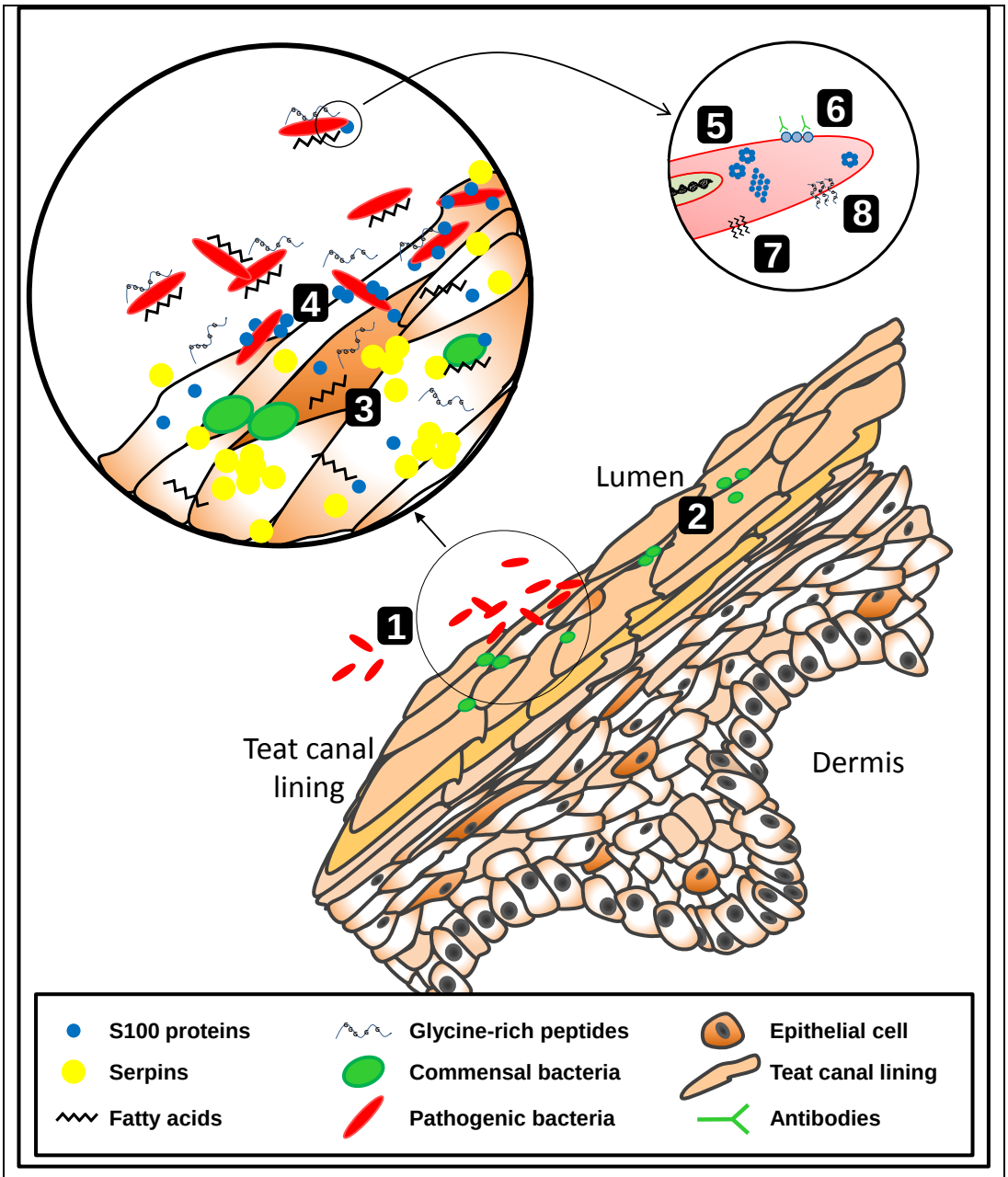

Figure 3.16: Possible host-defence roles for teat canal lining proteins identified through proteomic analysis.
The numbered processes are as follows: (1) bacteria enter the teat canal and are entrapped in the teat canal lining; (2) commensal bacteria occupy niche areas in the teat canal lining leaving less favourable areas for the bacteria to attach; (3) serpins prevent the proteolytic action of bacterial proteases reducing the availability of essential nutrients; (4) S100 proteins bind to the outer surface of the bacteria and exert antimicrobial activity through (5) disruption of the cell membrane and (6) opsonin activity; (7) long chain fatty acids can disrupt cell membranes and bind to receptors disrupting signal transduction; (8) molecular function of the glycine-rich peptides is unknown.

4. Characterisation of innate immune cells in the teat canal and teat-end tissues

Localised immune cells with antigen surveillance and effector capabilities are an essential element of mucosal epithelial surfaces such as the gastrointestinal, respiratory, and urogenital tracts as well as the external skin layer. These cells can detect antigens from microorganisms and coupled with pattern recognition receptors control the induction of the innate and adaptive immune responses.

The epithelial lining of the teat canal is morphologically similar to the epithelium of the external skin layer, and the internal lining of the teat sinus displays many structural similarities to mucosal epithelium. The innate immune elements of mammalian skin and mucosal epithelium have been extensively characterised (See Chapter 1). The teat canal and the teat sinus are the primary entry points for bacterial infiltration into the mammary gland of the cow. Because of this, it would be reasonable to presume that a robust host-defence system exists in the teat-end tissues.

Previous investigations into the types of immune cells present along the length of the bovine teat canal has been limited to histological observations of the teat tissues (Venzke, 1940; Adams *et al.*, 1961; Nickerson & Pankey, 1983, 1984). In more recent times, extensive characterisation of immune cell surface markers in human and murine tissues has assisted in understanding the spatial, temporal and interacting roles that these cells participate in; especially in the skin and mucosal epithelium. Unfortunately, not many of the monoclonal and polyclonal antibodies specific to human and murine antigens are cross-reactive with the analogous bovine cell surface markers.

There are some studies that have used cross-reactive antibodies raised against human, murine and other domestic farm animals to identify populations of immune cells in bovine tissues. For example, a recent study used monoclonal antibodies raised against human, ovine and porcine antigens to identify populations of bovine monocytes/macrophages in the subepithelial stromal tissue of bovine teats (Düvel *et al.*, 2012).

Monoclonal antibodies raised against bovine antigen targets are required as they will provide better target protein recognition than cross-reactive antibodies directed towards protein antigens from other species.

Over the past two decades, a number of antibodies raised against bovine antigens of several well-known immune cell surface markers have become available (http://vmp.vetmed.wsu.edu/resources/monoclonal-antibody-center). Therefore, the aim of this chapter was to use a panel of mouse monoclonal antibodies to bovine targets to detect specific lineage and maturation cell surface molecules on bovine immune cells within the teat tissue of normal uninfected late-lactating cows. This investigative research will allow the identification and characterisation of immune cell types in the epithelia and subepithelial stromal tissue and provide the means to compare the relative abundance of these cells within different teat-end microstructures, such as the teat canal, Fürstenberg's rosette and teat sinus.

4.1. Tissues analysed

Formaldehyde-fixed, paraffin-embedded (FFPE) and frozen (Fr) teat-end tissue sections of teat canal, Fürstenberg's rosette, teat sinus, and teat skin were obtained from the remaining pairs of contralateral teats not used for TCL analysis (See Chapter 3). These were sections of teat tissue obtained from normal uninfected late-lactating cows. The milk SCC for each quarter and the processing methods for each of the collected teats are listed in Table 4.1 and show that the quarters were free of infection.

Initially, the study was designed so that one of the pairs of teats was to be used for IHC analysis on FFPE tissue while the other teat was to be stored at -80 °C for potential real-time PCR analysis. Regrettably, the process of fixing the tissues in paraformaldehyde failed to generate any positive IHC signal that was specific to immune cells, when using diaminobenzidine (DAB) for staining (For more detail see Section 4.3). To overcome this problem, the remaining frozen teat tissues were processed by cryosectioning and analysed using IF detection. Antibodies that did not recognise antigen in the FFPE sections produced a positive signal on the unmodified cryosections. As a result of this observation, subsequent IHC

analysis was performed with each monoclonal (n = 10) and one polyclonal antibody (Table 4.2) using cryosectioning and IF detection.

Table 4.1: Tissues samples from uninfected lactating teats for IHC analysis

Cow#/Quarter	SCC ($x10^3$ cells/mL)	Tissue processing
5/FL	47	Fr and IF
5/BR	24	FFPE and IHC
390/FR	20	FFPE and IHC
390/BL	13	Fr and IF
452/FL	13	Fr and IF
452/BR*	3458	FFPE and IHC
872/FL	198	FFPE and IHC
872/BR	28	Fr and IF
910/FL	96	Fr and IF
910/BR	30	FFPE and IHC
1048/FL	136	FFPE and IHC
1048/BR	15	Fr and IF
Average ± SD	*56 ± 61*	

* Milk from mammary gland 452/BR was infected with *S. uberis*. Therefore teat 452/BR was not included in the study. Fr, Cryosections; IF, immunofluorescence; FFPE, formaldehyde-fixed paraffin-embedded; IHC, immunohistochemistry.

Table 4.2: List of bovine-specific mouse monoclonal and rabbit polyclonal antibodies used to detect immune cell types in teat-end tissues. (See Table 2.1 for more details)

Antigen Specificity	Cell type	Clone	Host
MHC class II	APC	IL-A21	Mouse
CD3	T cell	MM1A	Mouse
CD4	T cell	CACT138A	Mouse
CD8α	T cell	BAQ111A	Mouse
WC-1	γδ T cell	IL-A29	Mouse
B cells	B cells	GB26A	Mouse
CD205	APC	IL-A53A	Mouse
CD11c	APC	BAQ153A	Mouse
CD14	macrophages	MM61A	Mouse
unknown	granulocytes	CH138A	Mouse
c-kit (CD117)	mast cell	A4502	Rabbit

APC, antigen-presenting cell

4.2. Histological evaluation of the teat-end tissues

Histological analysis of formaldehyde fixed teat canal and teat skin sections, using Gill's haematoxylin and eosin staining (H&E), showed a stratified squamous epithelium whose cells varied in shape from columnar basal cells, polyhedral spinous cells to flattened granular cells (Figure 4.1a, b). The cells staining deep red to purple are presumed to be differentiating keratinocytes (labelled K in inserts in Figure 4.1a, b), due to their similar morphology with skin epithelium in which these cells have been previously identified (Urmacher, 1990). Similarly, the loose red staining cells are almost certain to be *stratum corneum*. The abundance of *stratum corneum* is far greater in the teat canal than the teat skin. Within the teat canal epithelium, but not the teat skin, numerous circular structures can be seen (labelled M in Figure 4.1a) which have previously been observed in bovine teat epithelium and named Marksäulchen (Mańkowski, 1903). These structures appeared to be aligned with the supra-papillary plate between the rete ridges (labelled R in Figure 4.1a), structures which are also observed in skin epithelium (Venus *et al.*, 2011). The Marksäulchen cells consist of small rounded nuclei with no cytoplasmic staining similar in appearance to the cells observed in the subepithelial stroma located between the rete ridges (Figure 4.2). These small

cells were more abundant in the areas between the rete ridges of the teat canal epithelium than between the rete ridges of the teat skin (dashed arrows in Figure 4.1a, b).

Similar histochemical analysis of the Fürstenberg's rosette and teat sinus FFPE sections revealed a simpler epithelium than that of the teat canal and teat skin (Figure 4.1c, d). The Fürstenberg's rosette and teat sinus epithelium consisted of a bilayer of epithelial cells that varied in shape from columnar to cuboidal (labelled CM and CB in Figure 4.1c, d). In some parts of the Fürstenberg's rosette epithelial bilayer large cells with clear areas of cytoplasm, presumably non-epithelial cells, were present between the two layers of epithelium (Arrowed in Figure 4.1c). These cells were rarely observed in the teat sinus tissues.

The apparent abundance of nuclei seen in the Fürstenberg's rosette stromal tissue was notably more than in the teat sinus stroma (labelled ST in Figure 4.1c, d). These nuclei were not only clustered directly adjacent to the epithelial bilayer of the Fürstenberg's rosette but also covered the breadth of stromal tissue making up the papillary dermis. In the teat sinus, small clusters of spherical nuclei were observed directly adjacent to the epithelial bilayer. Elongated nuclei, consistent in appearance with nuclei from fibroblasts, were observed as the major cell type in the remaining stromal tissue (Arrowed in Figure 4.1d). In the teat canal and Fürstenberg's rosette, the majority of cells appeared to be mononuclear in nature with only a small number of polymorphonuclear cells able to be distinguished at magnifications higher than that shown in Figure 4.1.

Overall, morphological analysis by light microscopy and H&E staining of the teat-end tissues are consistent with previous observations of the structure of the bovine teat canal, teat skin, Fürstenberg's rosette and teat sinus (Fürstenberg, 1868; Mańkowski, 1903; Venzke, 1940; Adams *et al.*, 1961; Paulrud, 2005). Due to their shape and size, the small nuclei observed in the stromal tissue, Marksäulchen and epithelial layer are likely to be various types of leukocytes. However, more specific identification methods are required to distinguish the different cell types better and potentially identify different subpopulations.

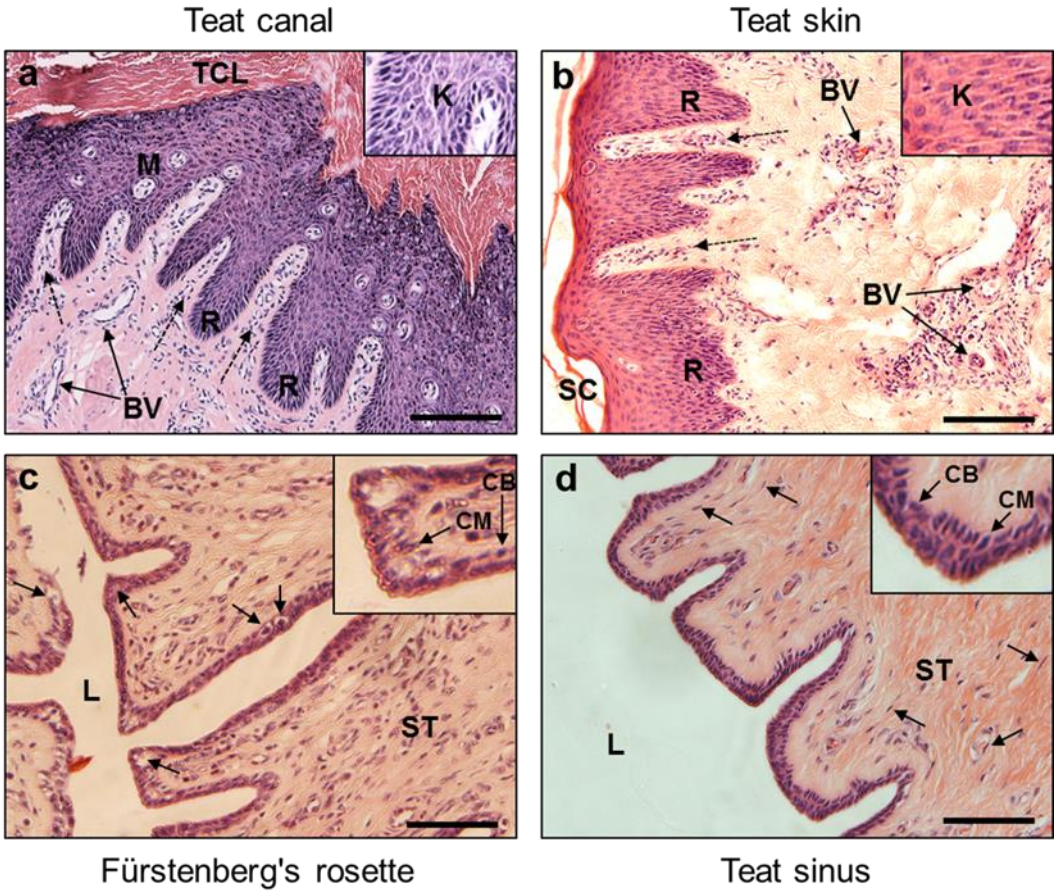

Figure 4.1: Low magnification view of epithelial cross-sections of formaldehyde fixed teat-end tissues.

a) Teat canal epithelium showing elongated rete ridges (R) with numerous nuclei grouped in the outermost papillary dermis (dashed arrows). Many circular Marksäulchen (M) are observed in the epithelium extending to the teat canal lining (TCL) along with blood vessels (BV). b) Teat skin epithelium showing similar abundance of nuclei surrounding BV and in the areas between the rete ridges. The *stratum corneum* (SC) of the skin is less dense than the equivalent layer in the teat canal. Keratinocytes (K) of the teat canal (a) and teat skin (b) epithelium are shown as inserts. c) Double layered epithelium of the Fürstenberg's rosette exhibiting both columnar (CM) and cuboidal (CB) morphology (see insert). Numerous nuclei can be seen in the stromal tissue (ST) underlying the epithelium. Larger non-epithelial cells can be observed embedded within the two layers of the epithelial bilayer (arrowed). d) Teat sinus epithelium illustrating multiple ridges or folds facing the sinus lumen (L), a double layered epithelium is also found with CM and CB morphology (see insert). **Note:** the reduced number of nuclei in the stromal tissue compared to the Fürstenberg's rosette. Arrowed are elongated nuclei, resembling nuclei found in fibroblasts. H&E staining. Section thickness: 7 µm. Scale bar = 100 µm (a, b), 50 µm (c, d).

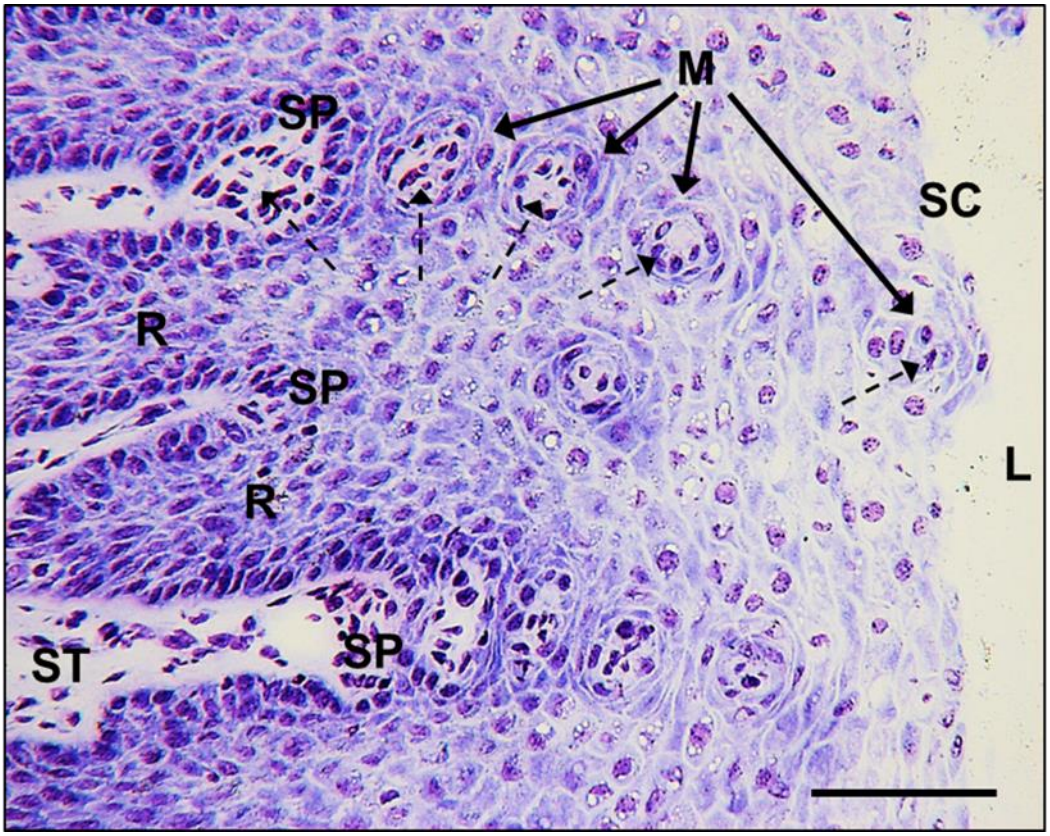

Figure 4.2: Teat canal Marksäulchen extending from the suprapapillary plate to the *stratum corneum*.
Representative transverse cryosection of bovine teat canal stained with Toluidine blue. Marksäulchen (M) structures occupy the entire depth of the teat canal epithelium, beginning at the suprapapillary plate (SP), between the rete ridges (R), and extending inwards towards the teat canal lumen (L). Within the Marksäulchen, darker staining nuclei are visible (dashed arrows) similar to those observed in the stromal tissue (ST). The Marksäulchen appear to diminish in size as they get closer to the teat canal lumen. The number of darker staining nuclei in these structures also appear to decrease closer to the *stratum corneum* (SC). Section thickness: 7 µm. Scale bar = 50 µm

4.3. IHC staining of formalin-fixed, paraffin-embedded tissue sections

Antibodies specific for distinct immune cell markers and proteins of interest were tested on FFPE tissue sections using heat-induced and enzymatic antigen retrieval methods as described in Section 2.2.17.

Polyclonal antibodies directed against S100A7, -A8, -A9 and -A12 were first tested on the FFPE tissue sections. These four antibodies were chosen because of the relatively high abundance of S100 protein in the teat canal lining (See Chapter 3). As judged by the intensity of the staining reaction using diaminobenzidine (DAB), good morphological features and clean background were observed in the teat canal epithelium for S100A7, -A8, -A9 and -A12, respectively. In comparison to the teat canal epithelium, staining of the teat skin epithelium was less intense for three of the four antibodies, the exception being S100A7 (*data not shown*). The DAB staining pattern was similar to the IF staining pattern for S100A7, -A8, -A9 and -A12 portrayed previously (See Figures 3.14 & 3.15).

Having established the method using the S100 antibodies, five different monoclonal antibodies were tested on FFPE prepared sections of teat tissue, Peyer's patch and super-mammary lymph node. These included MHC class II, CD3, CD8, C205, and CD14. Both the teat tissues and the positive control lymphoid tissues failed to produce well-defined cell staining for any of these five antibodies (*data not shown*). Further optimisation of heat-induced epitope retrieval and enzymatic antigen retrieval methods were still unsuccessful in producing a specific signal. Possible reasons for this are that the cell surface antigens are masked or have been modified during fixation. To circumvent these issues, testing of the same five antibodies was performed on super-mammary lymph node frozen sections. Four of the five different antibodies produced a specific signal (See Supplementary data B1). Because of this observation and for future consistency, all subsequent polyclonal and monoclonal based IHC was performed on frozen sections of tissue using indirect IF detection.

4.4. Expression of MHC class II in the teat-end tissues

The major histocompatibility complex (MHC) class II cell surface antigen is found on all types of antigen-presenting cells, such as dendritic cells, mononuclear phagocytes, some endothelial cells and B-cells, where its function is to present peptide antigens to T cells. The mouse monoclonal anti-bovine antibody, IL-A21, was employed in this study to identify cells in the teat-end tissues expressing high levels of the MHC class II cell surface antigen. This antibody had been used previously to identify antigen-presenting cells in bovine epithelial tissues (Taylor *et al.*, 1993; Constantinoiu *et al.*, 2010; Constantinoiu *et al.*, 2013).

Transverse cryosections of normal late-lactating teat canal, teat skin, Fürstenberg's rosette and teat sinus were subjected to IF staining using this antibody. MHC class II^+ signal was mostly localised to the subepithelial stromal tissue between the rete ridges in each of the six cows examined. Representative images from a single cow are shown (Figure 4.3a, b). Only very weak or no signal was observed within the epithelial layer in both the teat canal and the teat skin. The relatively intense signal surrounding the subepithelial nuclei formed quasi-filamentous processes (See insert in Figure 4.3b), consistent with the morphology of macrophages or dermal dendritic cells (Romani *et al.*, 2010; Guilliams *et al.*, 2014). However, to confirm their identity, other cell-type specific cell surface markers are needed. The IF signal was not detected using non-specific mouse immunoglobulin and using the same exposure time as for IL-A21 (Figure 4.3e-h).

As with the teat canal, the Fürstenberg's rosette tissue produced particularly intense MHC class II signals, in a subset of cells present in the uppermost layer of the epithelial bilayer; directly adjacent to the teat lumen (Figure 4.3c). Deeper within the secondary mucosal folds, positive staining cells were more intermittently spread. In some cases, a strong signal was associated with nuclei that appear to be located between the layers of epithelial cells. These cells seemed to distort the epithelial bilayer (Arrowed in Figure 4.4). A less intense signal was observed around the apical layer of cells in the bilayer (dashed arrows in Figure

4.4). This signal could be associated with the epithelial cells themselves or derived from other nearby antigen-presenting cells. The subepithelial region contained numerous MHC class II positive cells of varying shapes and sizes with both well-defined and indeterminate borders. Overall, the intensity of signal and proportion of positive staining cells suggests that the Fürstenberg's rosette is an important site of antigen recognition in the teat-end tissues.

In the teat sinus, MHC class II positive cells were predominantly restricted to a proportion of cells associated with the epithelial bilayer (Figure 4.3d) as is also the case in the Fürstenberg's rosette. These cells produced a particularly intense signal and appeared to be located between the two layers of epithelial cells (insert Figure 4.3d). Unlike the Fürstenberg's rosette, the stromal tissue of the teat sinus contained no intensely stained cells. Similar observations for MHC class II expression have been previously reported in tissues of the mammary gland, teat sinus and teat canal (Fitzpatrick *et al.*, 1992). However, this is the first time that MHC class II expression has been demonstrated within the Fürstenberg's rosette.

Table 4.3: **Quickscore summary of MHC class II signal intensity in the different late-lactating teat-end tissue regions.**

Cow#/Quarter	Teat canal	Teat skin	Fürstenberg's rosette	Teat Sinus
5/FL	++	++	+++	++
390/BL	++	++	+++	++
452/FL	++	++	+++	++
872/BR	++	++	+++	++
910/FL	++	++	+++	++
1048/BR	++	++	+++	++

The IF signal of labelled cells is subjectively graded as negative (-), weakly positive (+), mildly positive (++), moderately positive (+++), and strongly positive (++++).

Semi-quantification of the MHC class II signal associated with the epithelium of the teat canal, teat skin and teat-end tissues were performed using the Quickscore method (See Section 2.2.18). Due to the undefined nature of the MHC class II signal observed within the subepithelial region, grading of this signal was not performed. The average Quickscores from seven randomly selected, non-overlapping fields per slide at 200 x magnification were assessed for each of the four tissue regions from all six cows (Table 4.3).

The proportion of MHC class II positive cells adjacent to the epithelium was also assessed (Figure 4.5). Similar to the Quickscore analysis, seven randomly selected, non-adjacent fields per slide at 200 x magnification were calculated for each of the four tissue regions from all six cows (n = 42/tissue region). The fields examined contained a similar amount of tissue and cells for the teat skin, Fürstenberg's rosette or teat sinus. The teat canal sections contained slightly more cells due to the large area of densely packed stratified epithelium. The density of MHC class II positive cells was derived from the total number of DAPI stained epithelial nuclei in each field of view. This analysis demonstrated that the Fürstenberg's rosette, followed by the teat sinus contained the most epithelial-associated MHC class II expressing cells and that both the teat canal and teat skin epithelium contained the lowest number of these cells in the four tissue regions examined (Figure 4.5).

Overall, the observations using the IL-A21 antibody suggest that the teat canal lining, teat skin, Fürstenberg's rosette and teat sinus each have significant proportions of potential antigen-presenting cells, but that each tissue also has a distinct role. The results suggest that the epithelial lining of both the Fürstenberg's rosette and teat sinus are sites of active immune surveillance. The high proportion of intensely staining cells in Fürstenberg's rosette suggests that this tissue is a particularly active site for surveillance.

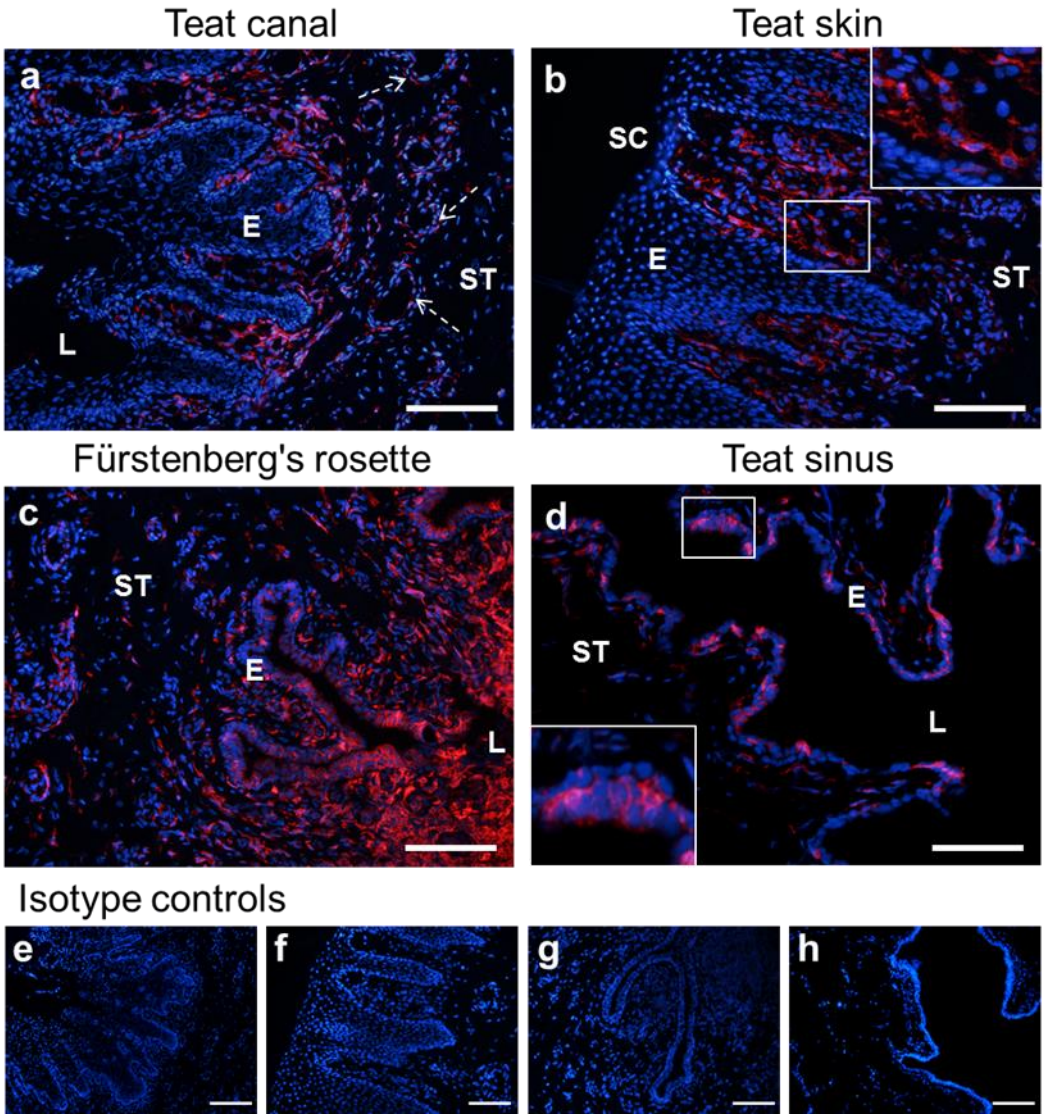

Figure 4.3: **Distribution of MHC class II positive cells in cryosections of the teat-end tissues**. Representative micrographs from Cow #005 of transverse cryosections of teat canal (a), teat skin (b), Fürstenberg's rosette (c), and teat sinus (d). Sections were probed with anti-MHC class II monoclonal antibody and bound antibody was detected with Alexa Fluor-594 IgG2a labelled secondary antibody (red signal) using fluorescence microscopy. Isotype matched control antibody shows negative staining for MHC class II (e-h). Each cryosection was counterstained with DAPI (blue signal). **Note:** for the teat canal and teat skin the majority of the MHC class II^+ cells were located in between the rete ridges underlying the epithelium whereas in the Fürstenberg's rosette and teat sinus, the MHC class II^+ cells were located within the epithelial bilayers. E, epidermis; SC, *stratum corneum*; ST, stromal tissue; L, lumen. Section thickness: 5 µm. Scale bar = 100 µm (a, b, e, f); 50 µm (c, d, g, h).

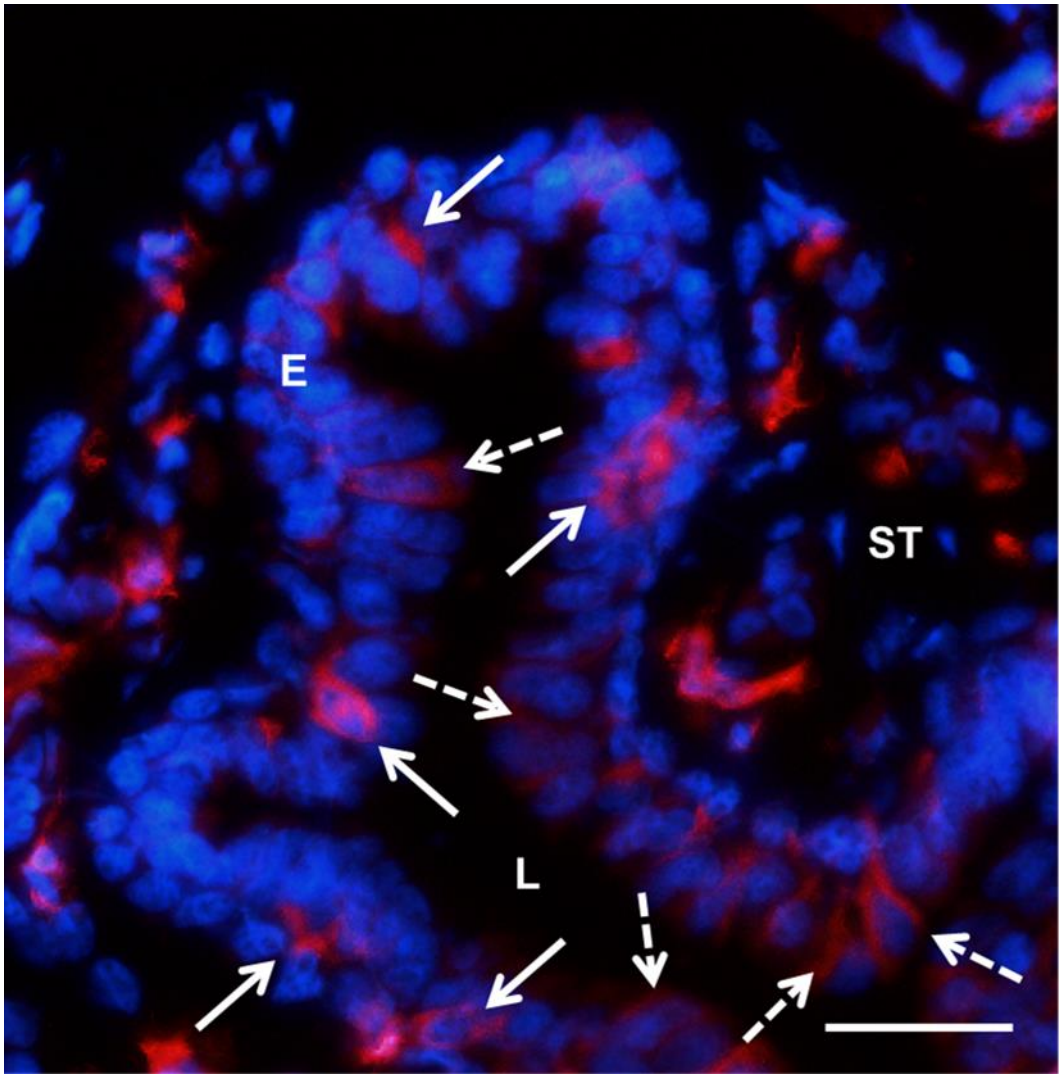

Figure 4.4: MHC class II positive cells located in the epithelial bilayer of the Fürstenberg's rosette.
Intense MHC class II signals (red staining) surrounding nuclei found between the two epithelial layers appear to correlate with deformation of the epithelial bilayer (indicated by arrows). In comparison, lower intensity, perinuclear staining was observed in the apical epithelial layer (indicated by dashed arrows). E, epidermis; ST, stromal tissue; L, lumen. Section thickness: 5 µm. Scale Bar = 25 µm.

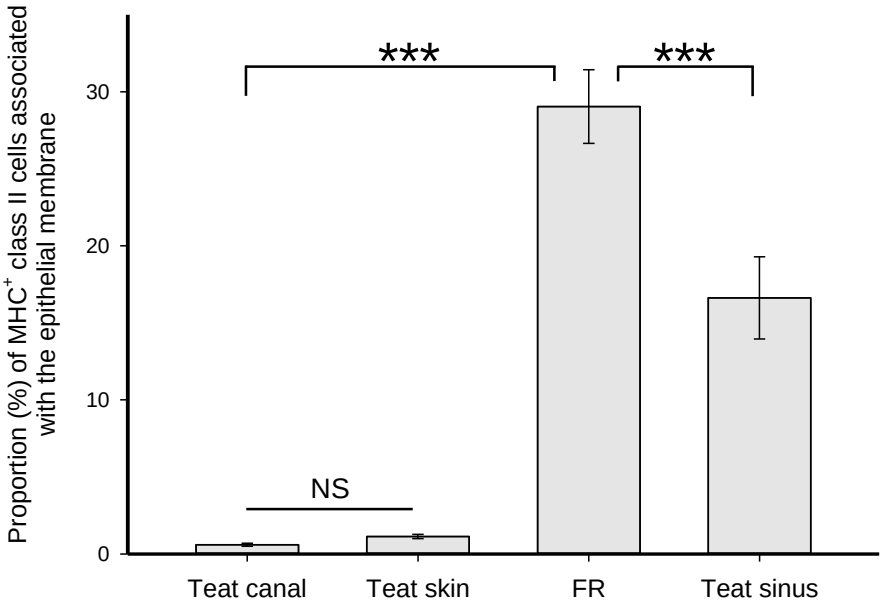

Figure 4.5: Semi-quantitative analysis of MHC class II positive cells associated with epithelial cells.
The relative density of positively stained MHC class II cells associated with epithelial cells was counted from seven nonadjacent fields per slide at 200 x magnification. The average density was derived by simple proportion of the total number of nuclei in each field of view. The results are cumulative data from all six cows (n = 6). FR, Fürstenberg's rosette. Error bar: ± SEM. The asterisk *** indicates $p < 0.001$; NS, not significant.

4.5. Distribution of T cell subsets present in the teat-end tissues

T cells or T lymphocytes represent a major immune cell population in mucosal epithelium (MacDonald, 2003; Montilla *et al.*, 2004). T cells can be distinguished from other lymphocyte subtypes, such as B cells and natural killer cells, by the presence of the T cell receptor on the cell surface. This receptor is responsible for recognising peptide antigens presented by MHC molecules. The T cell receptor associates non-covalently with the CD3 accessory complex, and this is a defining feature of the T cell lineage (Chetty & Gatter, 1994). Hence antibodies recognising the CD3 epitope are specific for cell surface markers for all T cells.

A subset of T cells, γδ T cells, are present in epithelial and mucosal tissues, such as the skin, intestines, lung, urinary and reproductive tracts (Girardi, 2006). These cells have a unique T cell receptor and can respond to a distinct set of antigens compared with the more common αβ T cells. The majority of bovine γδ T cells express a transmembrane scavenger receptor known as WC1 (Guzman *et al.*, 2011). While the role of this receptor has not been fully elucidated, a number of monoclonal antibodies have been raised against the WC1 receptor and have been used to define γδ T cell populations (Guzman *et al.*, 2011).

IF staining using the mouse anti-bovine monoclonal antibody MM1A was employed to identify $CD3^+$ cells in the teat-end tissues (Figure 4.6). For the teat canal and teat skin, there were very few positively stained cells observed, and those cells were predominantly associated with the basal and spinous cell layers of the epithelium (Figure 4.6a, b). In the Fürstenberg's rosette, the majority of $CD3^+$ T cells were localised in the subepithelial stromal tissue. However, a minor population of $CD3^+$ T cells were also detected in the epithelial bilayer (Figure 4.6c). In contrast to Fürstenberg's rosette tissue sections, almost all the CD3 signal in teat sinus sections was situated in the epithelial bilayer, with very little CD3 signal observed in the stromal tissue (Figure 4.6d).

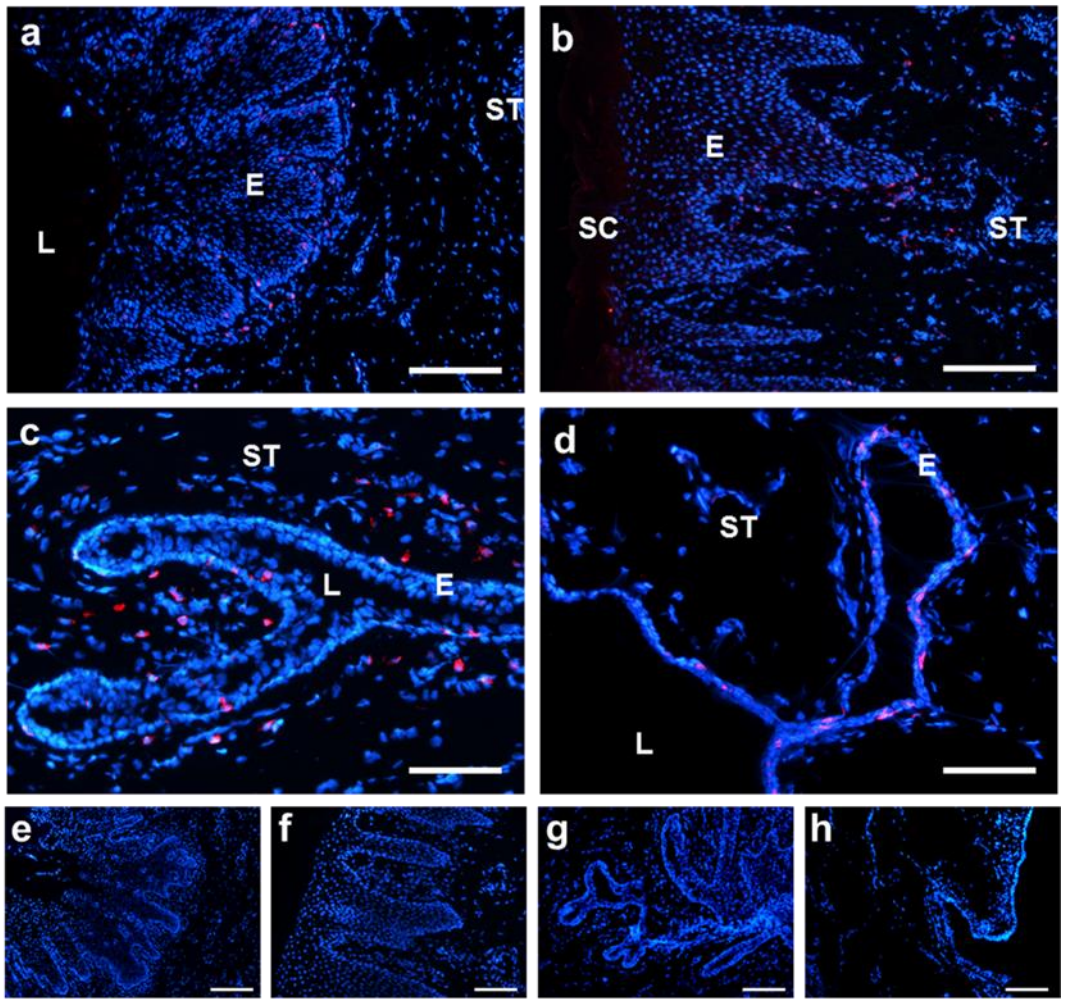

Figure 4.6: Identification of CD3 positive lymphocytes in teat-end tissues.
Representative immunofluorescence micrographs of transverse cryosections from Cow #1048. Cyrosections of teat canal (a), teat skin (b), Fürstenberg's rosette (c), and teat sinus (d) were probed with the anti-CD3 monoclonal antibody and the bound antibody detected with Alexa Fluor-594 IgG2a labelled secondary antibody (red signal). Each cryosection was counterstained with DAPI (blue signal). Isotype matched control antibody shows negative staining for CD3 (e-h). **Note:** for the teat canal, teat skin and teat sinus, the majority of the $CD3^+$ lymphocytes are associated with the epithelium whereas in the Fürstenberg's rosette the majority of $CD3^+$ lymphocytes are located in the stromal tissue. E, epidermis; SC, *stratum corneum*; ST, stromal tissue; L, lumen. Section thickness: 5 µm. Scale bar = 100 µm (a, b, e, f); 50 µm (c, d, g, h).

To better characterise the $CD3^+$ T cell population, serial cryosections of teat tissue were probed for CD4 (T-helper cell; CACT138A), CD8 (cytotoxic T cell; BAQ111A), and specialised γδ T cells expressing the γδ T cell receptor, as defined by the presence of the WC1 co-receptor molecule (γδ T cell; IL-A29). Unfortunately, dual-colour labelling could not be performed with sets of these antibodies as the immunoglobulin isotype of the CD3, CD4 and WC1 receptor monoclonal antibodies were all IgG_1.

To overcome this limitation, serial cryosections were individually probed for CD3 or with each of the T cell phenotype cell surface marker (CD4, CD8, and WC1). DAPI stained nuclei on each section were used to orientate the sections, and IF images of equivalent fields of view were compared. For all six cows, there were no detectable signals for $CD4^+$ or $CD8^+$ cells in any of the four different tissue locations. It is possible that other antibody clones, specific to bovine CD4 and CD8 markers, may have better distinguished these T cell phenotypes. In addition, other T cell types such as natural killer T cells and mucosal associated invariant T cells may be present in these tissues contributing to the observed CD3 signal.

The majority of $WC1^+$ cells appeared to colocalise with the $CD3^+$ cells located within the epithelium (Figure 4.7). Averaged cell counts from seven nonadjacent fields per slide, from all six cows at 200 x magnification, estimated that the $WC1^+$ γδ T cell populations are approximately 5 %, 15 %, 28 % and 35 % of the total $CD3^+$ T cell populations in the tissues surrounding the epithelium of the teat canal, teat skin, Fürstenberg's rosette, and teat sinus, respectively.

Statistical analysis using Students paired t-test showed that the proportion of $WC1^+$ γδ T cells located within the epithelial bilayers of the Fürstenberg's rosette ($p < 0.001$) and teat sinus ($p < 0.001$), were significantly higher than the mean total number of $WC1^+$ γδ T cells located within the stratified epithelium of the teat canal and teat skin. This analysis also demonstrated that there was no significant difference between the mean number of γδ T cells in the stratified epithelium of the teat canal and the teat skin ($p = 0.161$) (Figure 4.8).

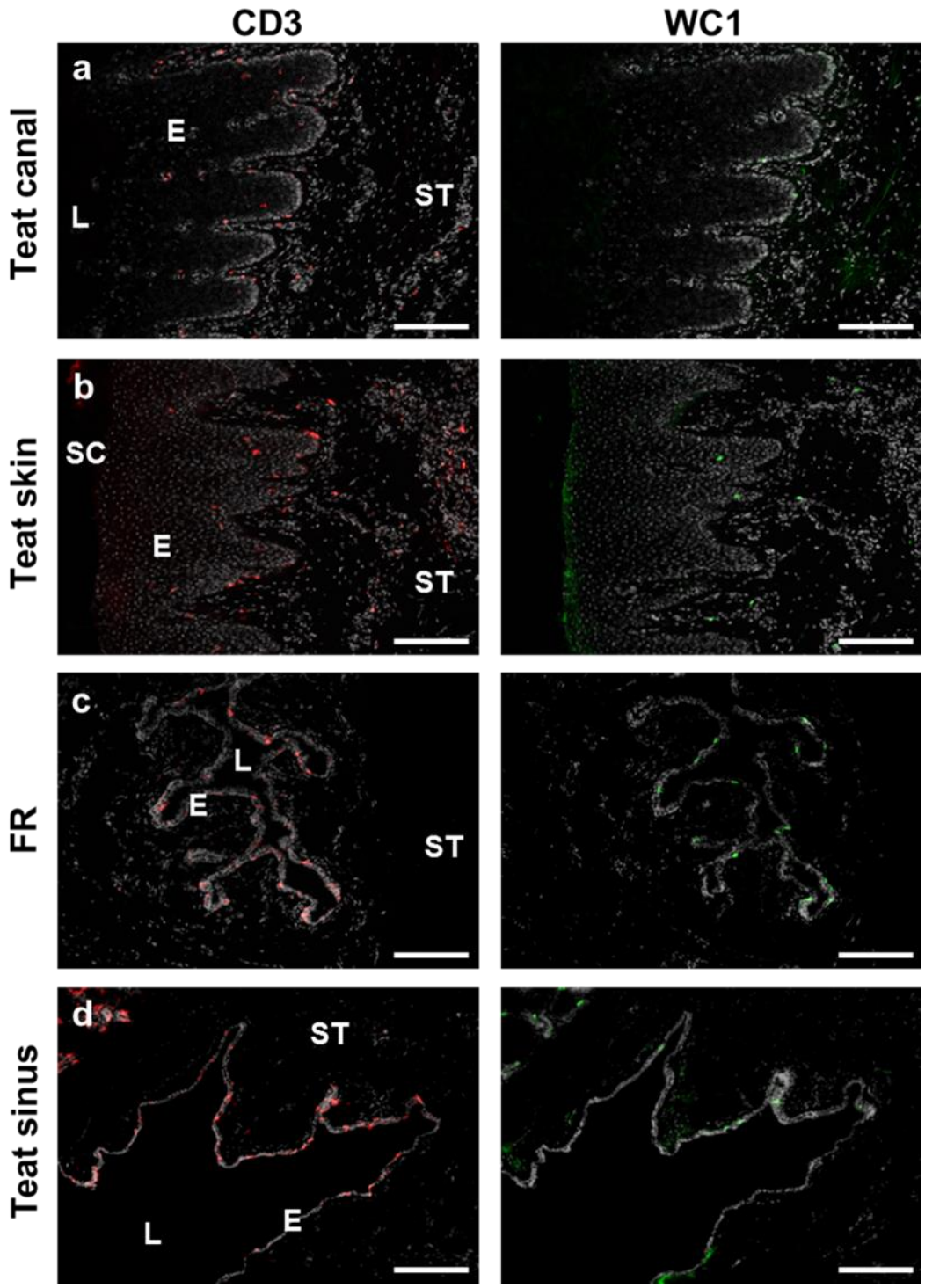

Figure 4.7: WC1$^+$ γδ T cells in the teat-end tissues.
Representative immunofluorescence micrographs of transverse cryosections from Cow #390. Serial sections of teat canal (a), teat skin (b), Fürstenberg's rosette (c), and teat sinus (d) were probed with anti-CD3 monoclonal antibody (Alexa-fluor 594 IgG; red signal) and anti-WC1 monoclonal antibody (Alexa-fluor 488 IgG; green signal). Each cryosection was counterstained with DAPI (grey signal). Greyscale was used for the DAPI signal to better display and compare the CD3 and WC1 signals. E, epidermis; SC, *stratum corneum*; ST, stromal tissue; L, lumen. Section thickness: 5 µm. Scale bar = 100 µm

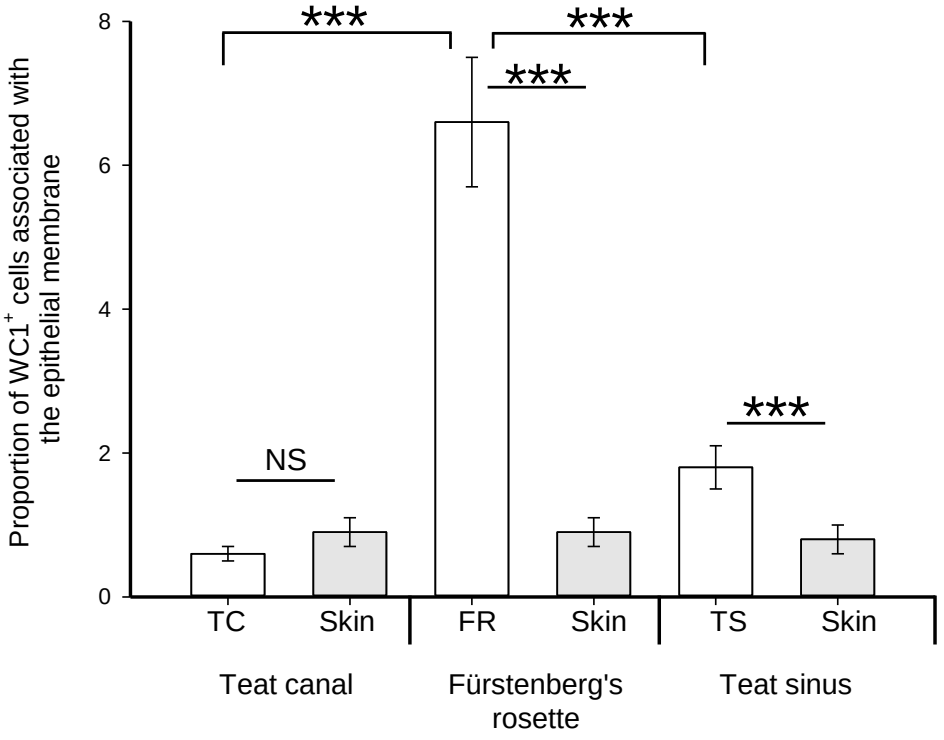

Figure 4.8: Semi-quantitative analysis of $WC1^+$ γδ T cells associated with epithelial cells in the teat-end tissues.
The numbers of positively stained WC1 expressing cells associated with epithelial cells were counted from seven nonadjacent fields per slide at 200 x magnification and then averaged. The results are cumulative data from all cows (n = 6). For each cryosection, the number of $WC1^+$ γδ T cells interacting with the skin epidermal layer were counted to act as an internal control for signal intensity and exposure time (grey bars). TC, teat canal; FR, Fürstenberg's rosette; TS, teat sinus. Error bar ± SEM. *** indicates $p < 0.001$; NS, not significant.

Previous studies have shown that bovine γδ T cells can express MHC class II molecules and act as antigen-presenting cells (Collins *et al.*, 1998). Colocalisation of two antigens in one cell is performed using dual IF labelling. This procedure is dependent on the primary antibody combination being different between animal species, Ig isotype, or Ig subclass and that the secondary antibody is specific to the primary antibody isotype.

In this experiment, dual IF staining was performed on $WC1^+$ cells using an IgG_1 isotype primary antibody and MHC class II^+ cells using an IgG2a isotype primary antibody from serial cryosections of the teat canal, teat skin, Fürstenberg's rosette, and teat sinus (Figure 4.9). Hardly any $WC1^+$ cells in the teat canal and teat skin sections showed MHC class II expression (Figure 4.9a, b). In contrast, MHC class II positive $WC1^+$ cells were evident within the epithelial bilayer in the

Fürstenberg's rosette and teat sinus cryosections (arrowed in Figure 4.9e, f). Sparsely scattered $WC1^+$ cells in the stromal tissue of the Fürstenberg's rosette and teat sinus appeared to be MHC class II negative (dashed arrow in Figure 4.9c, d).

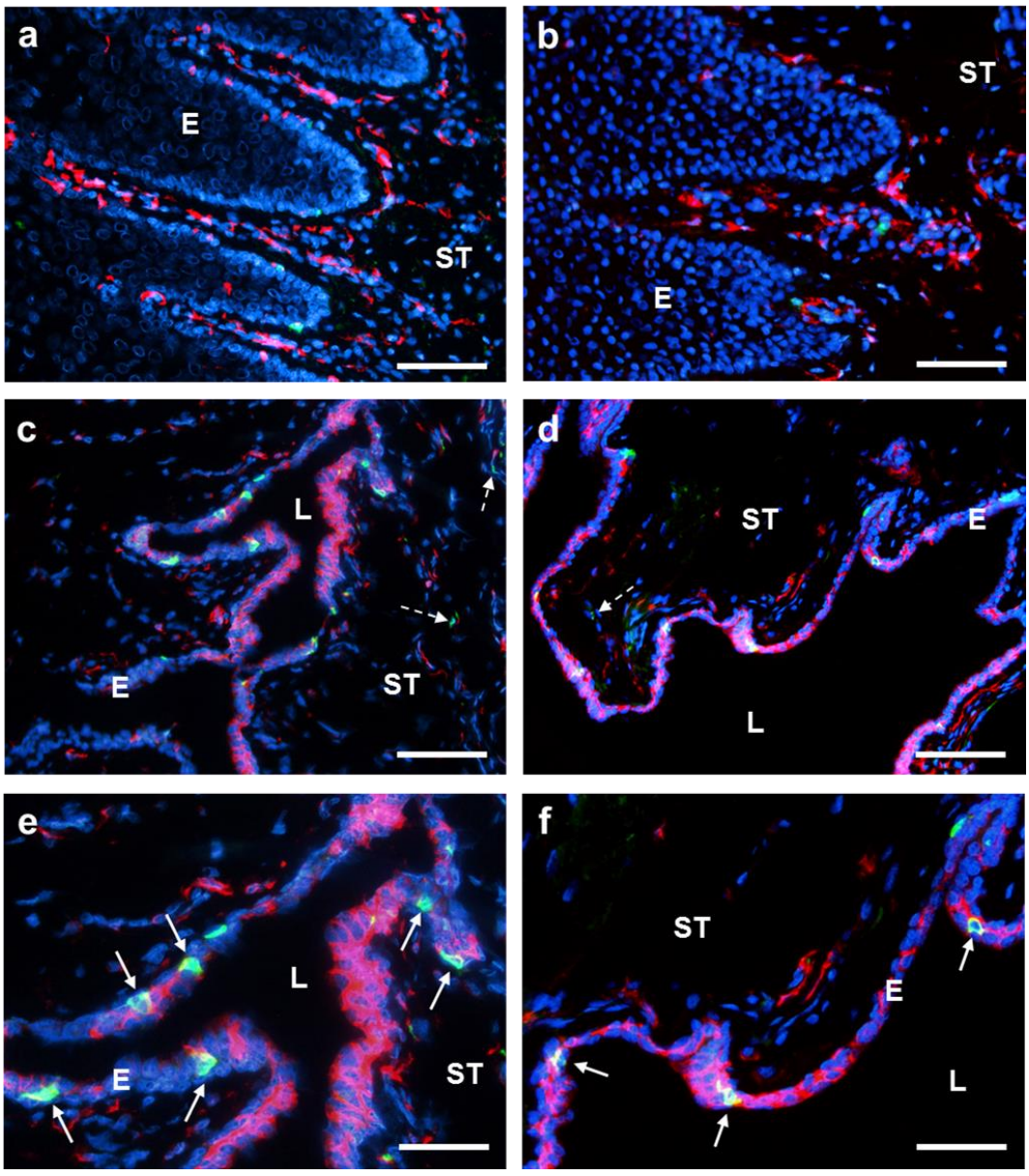

Figure 4.9: Epithelial bound $WC1^+$ γδ T cells co-expressing MHC class II.
Representative micrographs from Cow #872 of transverse cryosections of teat canal (a), teat skin (b), Fürstenberg's rosette (c, e), and teat sinus (d, f). The cryosections were probed with anti-MHC class II monoclonal antibody (Alexa-fluor 594 IgG2a; red signal) and anti-WC1 monoclonal antibody (Alexa-fluor 488 IgG; green signal) and counterstained with DAPI (blue signal). Cells expressing both MHC class II and WC1 antigen show up yellow and are indicated by arrows (e, f). E, epidermis; ST, stromal tissue; L, lumen. Section thickness: 5 µm. Scale bar = 50 µm (a-d); 25 µm (e, f).

4.6. Detection of B lymphocytes

B cells are lymphocytes of the adaptive immune system whose primary function is to make antibodies; however, they also have antigen-presenting capability and are able to release signalling molecules, such as IL-10, that modulate the inflammatory response (Mauri & Bosma, 2012). Upon activation by T-helper cells, B cells mature into either plasma B cells or memory B cells. The monoclonal antibody, GB26A, has been shown to be specific for B cells from animals of the order Artiodactyla (even-toed ungulates), which includes bovine, caprine, ovine and camelid members of the family. Presently, the epitope for GB26A is unknown and as such, has not been assigned to a human CD equivalent.

IF signals, indicating the presence of the B cell marker GB26A, were not observed in any of the teat canal, teat skin or teat sinus cryosections from all six cows examined. However, B cell immunostaining was detected in a cryosection of the Fürstenberg's rosette from a single cow. In this example, several $GB26A^+$ cells were observed in an area of increased cell density (Figure 4.10). Similar nodule-like structures have been observed previously in ovine Fürstenberg's rosette tissue sections where it was postulated that they arose as a result of a previous immune response to infection (Mavrogianni *et al.*, 2007).

Mature B cells such as plasma cells or memory cells were not detected in the teat-end tissues using immunostaining with GB26A. This is in contrast to previous reports where IgG_1- and IgA-producing plasma cell types were identified in tissues surrounding the Fürstenberg's rosette (Nickerson & Heald, 1982; Collins *et al.*, 1986; Aştı *et al.*, 2011), and to a lesser extent, the teat canal of uninfected mammary quarters (Doymaz *et al.*, 1988). Two possibilities for this observation are that there are very few, if any, B cells present in the teat-end tissues, and secondly, that the differentiated B cells present in these tissues may now not express the B cell antigen recognised by GB26A.

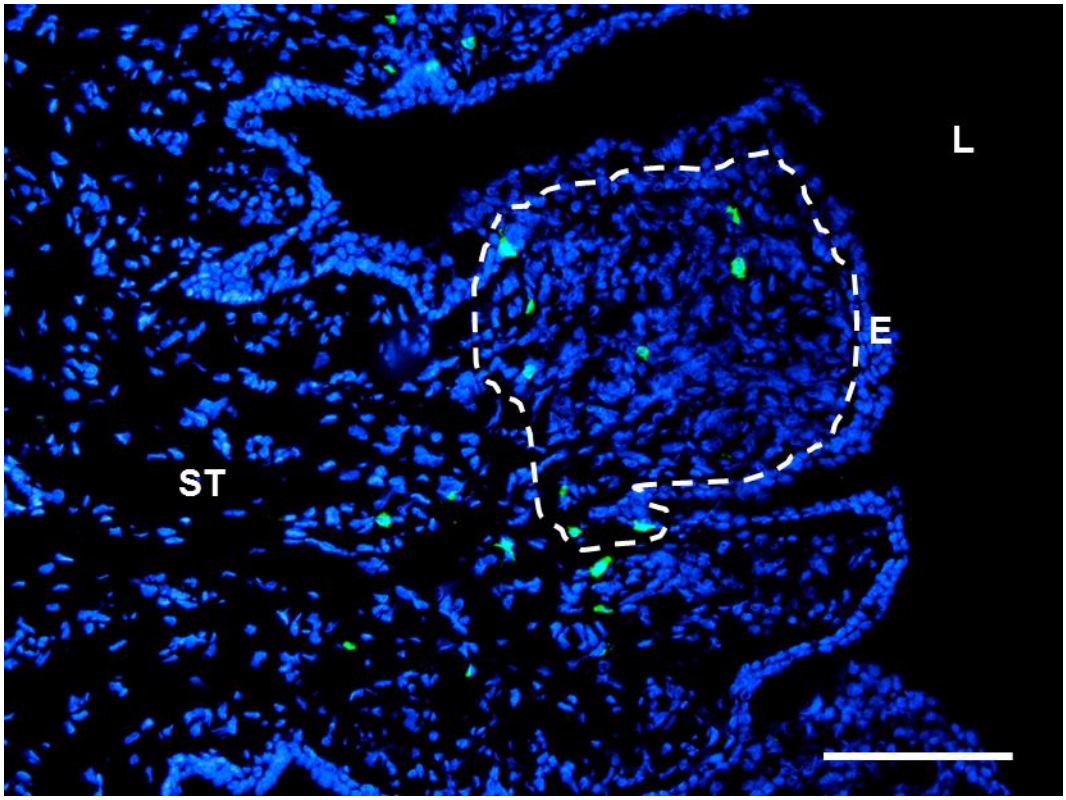

Figure 4.10: GB26A positive B cells in the Fürstenberg's rosette.
Micrograph from Cow #005 of a transverse cryosection from Fürstenberg's rosette. The cryosection was probed with anti-GB26A monoclonal antibody (Alexa-fluor 488 IgM; green signal) and counterstained with DAPI (blue signal). The dashed line surrounds an area of increased cell density. E, epidermis; ST, stromal tissue; L, lumen. Section thickness: 5 µm. Scale bar = 50 µm.

4.7. Detection of epithelial and dermal dendritic cells in the teat-end tissues

The two main types of dendritic cells found in non-inflamed human skin are epidermal Langerhans cells and dermal dendritic cells (Valladeau & Saeland, 2005). Langerhans cells are a unique subset of dendritic cells that populate the epidermal surfaces of the body. Specific cell markers that can distinguish Langerhans cells from other dendritic cell subsets include langerin (CD207) (Valladeau *et al.*, 2000), and high levels of expression of CD1a (Fithian *et al.*, 1981), and E-cadherin (Tang *et al.*, 1993). In contrast to Langerhans cells, dermal dendritic cell populations are made up of immature dendritic cells and macrophages. These two cell populations share many of the same cell surface markers making them difficult to distinguish. Recently, experiments using fluorescence IHC showed that human dermal dendritic cells express high levels of CD208 (DC-LAMP), CD83 and CD1 molecules, compared with macrophages, which express high levels of CD209 (DC-SIGN), CD14, CD68 and CD163 (Ochoa *et al.*, 2008).

Antibodies to the two most commonly used markers used to identify Langerhans cells in humans and mice, CD1a and CD207, are not yet available for cattle. Another of the Langerhans cell markers, E-cadherin, is expressed by most normal epithelial tissues (Takeichi, 1990) so cannot be used to identify bovine epithelial Langerhans cells. An anti-human polyclonal antibody to CD207 (orb6287) was tested for cross-species specificity on frozen cryosections of mouse skin, bovine teat canal and bovine teat skin samples. This antibody was reported to be cross-reactive to mouse CD207. A strong signal was observed in the epidermis of the mouse skin tissue (Figure 4.11a). The signal, however, appeared to be non-specific and did not distinguish individual Langerhans cells from the surrounding keratinocytes. This was unexpected as Langerhans cells and melanocytes are the next most abundant cell type in the stratified epithelium of skin behind keratinocytes (Nestle *et al.*, 2009). The signal in bovine teat canal and teat skin cryosections was diffuse and non-specific to any particular cell type (Figure 4.11b, c). As a result, other available cell surface markers were explored to identify

Langerhans cells in the bovine teat canal and skin epithelium. These included the already used MHC class II antibody and additional antibodies raised against epitopes of bovine CD205 and CD11c.

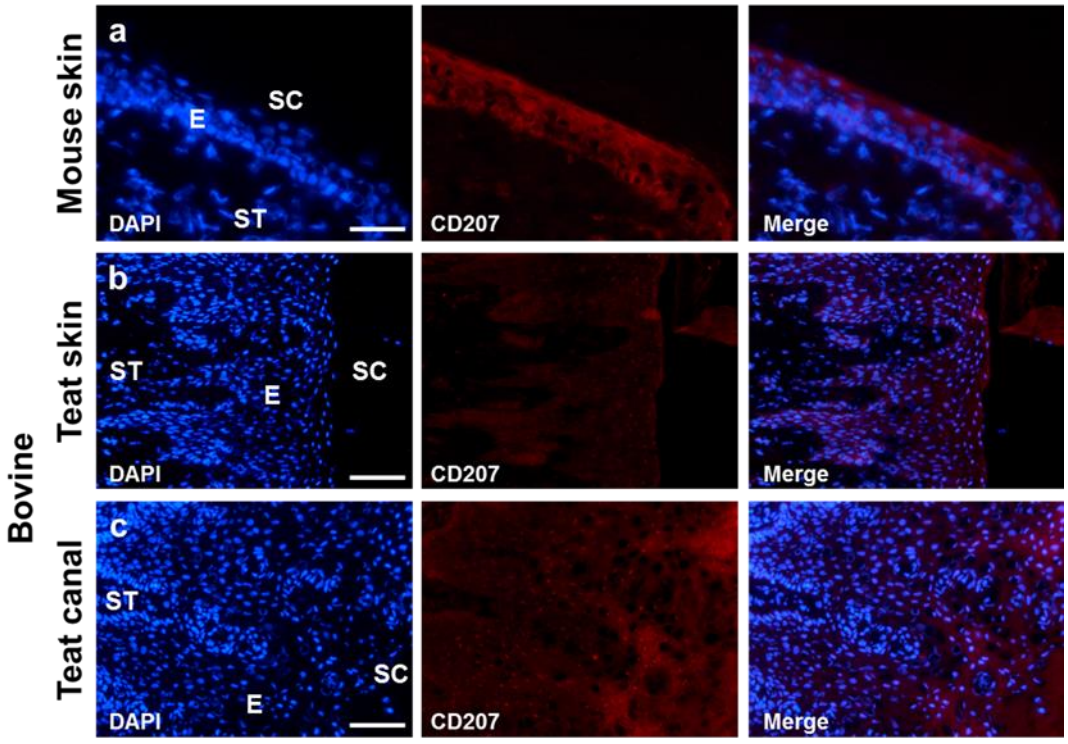

Figure 4.11: CD207 specific staining in mouse skin and bovine teat-end tissues.
Representative micrographs of a) Mouse skin, b) bovine teat skin and c) bovine teat canal epithelium probed with anti-human CD207 rabbit polyclonal antibody (Alexa-fluor 594 IgG; red signal). Nuclei were counterstained with DAPI (blue signal). E, epidermis; ST, stromal tissue; SC, *stratum corneum*. Section thickness: 5 µm. Scale bar = 50 µm (a); 100 µm (b, c).

CD205 is a C-type lectin belonging to the same family as the macrophage mannose receptor. Its function is to capture antigens and then transfer these antigens into specialised antigen-processing compartments for MHC class II presentation. In humans, CD205 is found at high levels on myeloid blood dendritic cells and monocytes. It is present at medium-to-low levels on human B cells, natural-killer cells, plasmatoid dendritic cells and some T cell subtypes (Inaba *et al.*, 1995). CD205 can also be observed on immature dendritic cells and Langerhans cells at low levels, but expression of CD205 on the cell surface increases markedly on cell activation and maturation (Figdor *et al.*, 2002; Butler *et al.*, 2007).

Signal for CD205 was detected in all tissues tested using the mouse monoclonal anti-bovine antibody. In the teat canal, only a few cells were observed to be expressing the CD205 receptor (Figure 4.12a). The most intense staining $CD205^+$ cells appear to be associated with the basal cells of the epithelium. Furthermore, CD205 signal was associated with certain cells that constituted the Marksäulchen structure (arrowed in Figure 4.12a, e). In contrast to the teat canal epithelium, a greater number of $CD205^+$ cells were observed within the spinous layer and adjacent to the basal cells of the teat skin epithelium (Figure 4.12b, f).

CD205 positive cells were more numerous in the Fürstenberg's rosette (Figure 4.12c, g) and teat sinus (Figure 4.12d, h) than in the squamous epithelial tissues of the teat canal (Figure 4.12a, e) and teat skin (Figure 4.12b, f). A good proportion of the $CD205^+$ cells in the Fürstenberg's rosette appeared to be associated with the epithelial bilayer (Figure 4.12c, g). The abundance and spatial localisation of the $CD205^+$ cells in the teat sinus sections were quite different from that observed in the Fürstenberg's rosette sections in that they appeared to be predominantly in the epithelial bilayer with very few $CD205^+$ cells in the stroma (Figure 4.12d, h).

CD11c is a leukocyte cell surface integrin molecule that is present at high levels in epithelial-associated human and mouse dendritic cells, such as the Langerhans cells. Furthermore, CD11c have also been found to be present at low levels on human and murine monocytes, granulocytes, and subsets of NK cells and B cells (Postigo *et al.*, 1991; Stacker & Springer, 1991; Aranami *et al.*, 2006).

Very little signal for CD11c was detected in teat canal cryosections using the mouse monoclonal anti-bovine antibody, BAQ153A (Figure 4.13a). In contrast, there was considerably more CD11c signal present throughout the teat skin epithelium (Figure 4.13b). Most of the $CD11c^+$ cells were localised within the *stratum spinosum* and lower *stratum granulosum* layers of the teat skin. In the Fürstenberg's rosette cryosections, the $CD11c^+$ cells were associated with the epithelial bilayer (Figure 4.13c) with no signal detected in the subepithelial stromal tissues. In the teat sinus, very few $CD11c^+$ cells were observed scattered in the stromal tissue, and practically none were detected in the epithelial bilayer (Figure 4.13d).

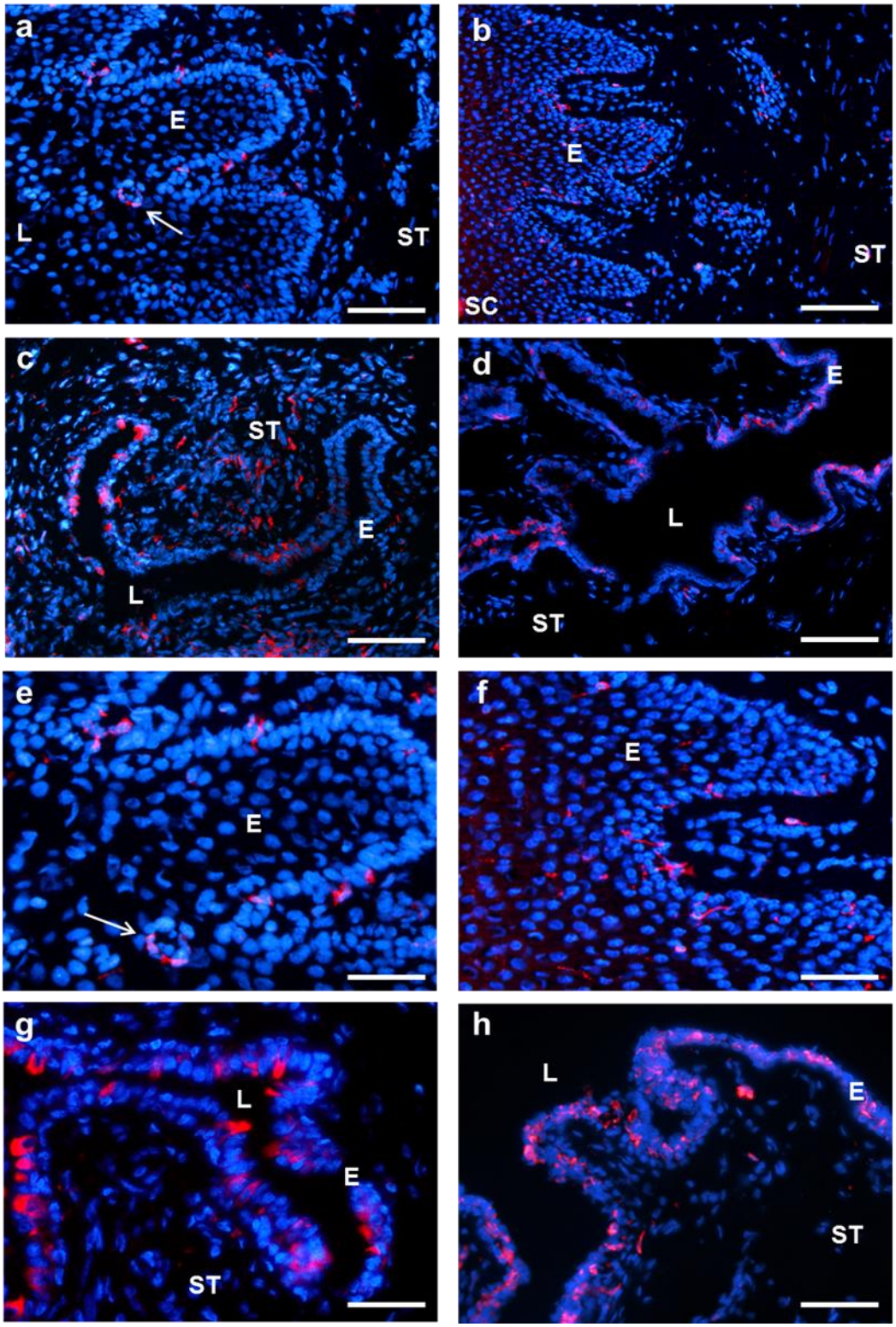

Figure 4.12: CD205 labelled cells in the teat-end tissues.
Representative micrographs from Cow #452 of transverse cryosections. Sections of teat canal (a, e), teat skin (b, f), Fürstenberg's rosette (c, g), and teat sinus (d, h) were probed with anti-CD205 monoclonal antibody (Alexa-fluor 594 IgG; red signal) and counterstained with DAPI (blue signal). E, epidermis; SC, *stratum corneum*; ST, stromal tissue; L, lumen. Section thickness: 5 µm. Scale bar = 50 µm (a-d); 25 µm (e-h).

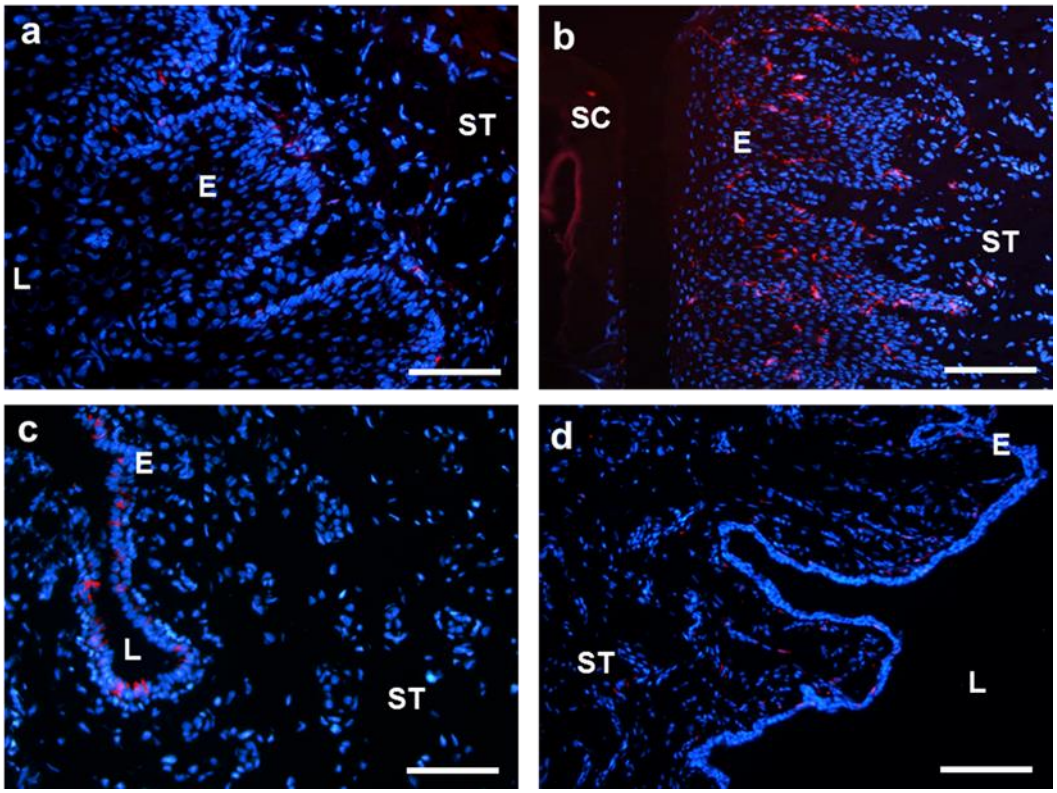

Figure 4.13: CD11c labelled cells in the teat-end tissues.
Representative micrographs from Cow #452 of transverse cryosections. Sections of teat canal (a), teat skin (b), Fürstenberg's rosette (c) and teat sinus (d) were probed with anti-CD11c monoclonal antibody (Alexa-fluor 594 IgM; red signal) and counterstained with DAPI (blue signal). E, epidermis; SC, *stratum corneum*; ST, stromal tissue; L, lumen. Section thickness: 5 µm. Scale bar = 50 µm (a-c), 100 µm (d).

From these results, it would appear that the $CD11c^+$ cells observed in the Fürstenberg's rosette co-localise with a population of CD205 expressing cells. To investigate this apparent characteristic, dual IF labelling was performed using antibodies to CD205 and CD11c. In the teat canal and teat skin cryosections, there was scarcely any co-expression observed (*data not shown*).

In the Fürstenberg's rosette, the majority of cells in the epithelial bilayer expressing CD205 also expressed CD11c (Figure 4.14). Cells expressing both markers appeared to be confined to the epithelial bilayer. There were no $CD11c^+$ cells observed in the stroma. A different pattern of expression was observed in sections from the teat sinus. Very few of the $CD205^+$ cells associated with the sinus bilayer co-expressed CD11c (*data not shown*). This result suggests that there may be a different population of $CD205^+$ cells in the bilayer of the teat sinus compared to the epithelial bilayer of Fürstenberg's rosette.

It is quite probable that the $CD205^+/CD11c^+$ subset of cells are dendritic cells, but other cell surface markers, specific to this cell type, are required to verify this. In addition, the identity of the $CD205^+/CD11c^-$ population of cells is currently unknown, however colocalisation with other lineage-specific cell markers, such as the macrophage marker CD14, might provide more insight into their identity.

In mice, CD205 is exclusively expressed by interdigitating dendritic cells, Langerhans cells and thymic epithelium, making it a definitive marker for mouse dendritic cells (Kraal *et al.*, 1986). However, in humans, CD205 is expressed in a variety of leukocytes at varying levels (Kato *et al.*, 2006). In cattle, the distribution and level of expression of CD205 have yet to be defined. However, results to date have shown that targeting of antigen by CD205 receptor results in a more efficient presentation to both MHC class I and II molecules (Bonifaz *et al.*, 2002; Birkholz *et al.*, 2010). Thus, CD205 is an integral cell surface receptor of 'professional' antigen-presenting cells such as dendritic cells.

To test this idea, dual IF labelling was performed to verify if the CD205 signal colocalised with MHC class II expressing cells. In the Fürstenberg's rosette, all of the $CD205^+$ cells in the epithelium also expressed high levels of MHC class II

(Fig. 4.15). However, none or very few of the MHC class II^+ cells in the stroma were positive for CD205. A similar pattern of staining was seen in the teat sinus sections from all six animals (*data not shown*).

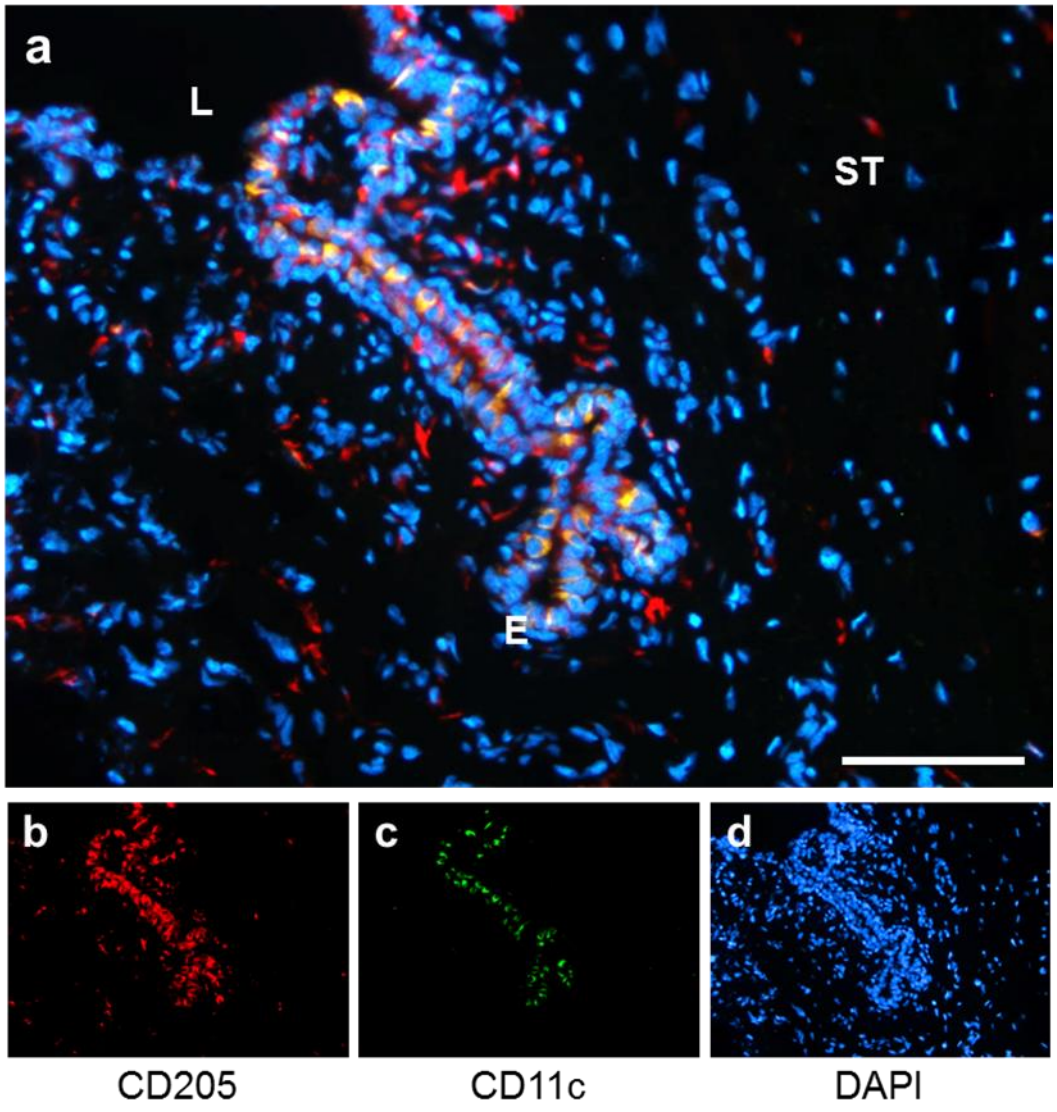

Figure 4.14: CD11c and CD205 positive cells in the Fürstenberg's rosette.
Representative micrograph from Cow #452 of a transverse cryosection from Fürstenberg's. The section was probed with anti-CD205 monoclonal antibody (b) (Alexa-fluor 594 IgG; red signal), anti-CD11c monoclonal antibody (c) (Alexa-fluor 488 IgM; green signal) and counterstained with DAPI (d), (blue signal). Cells expressing both CD205 and CD11c antigen show up yellow and are restricted to the epithelial bilayer (a). E, epidermis; ST, stromal tissue; L, lumen. Section thickness: 5 µm. Scale bar = 50 µm.

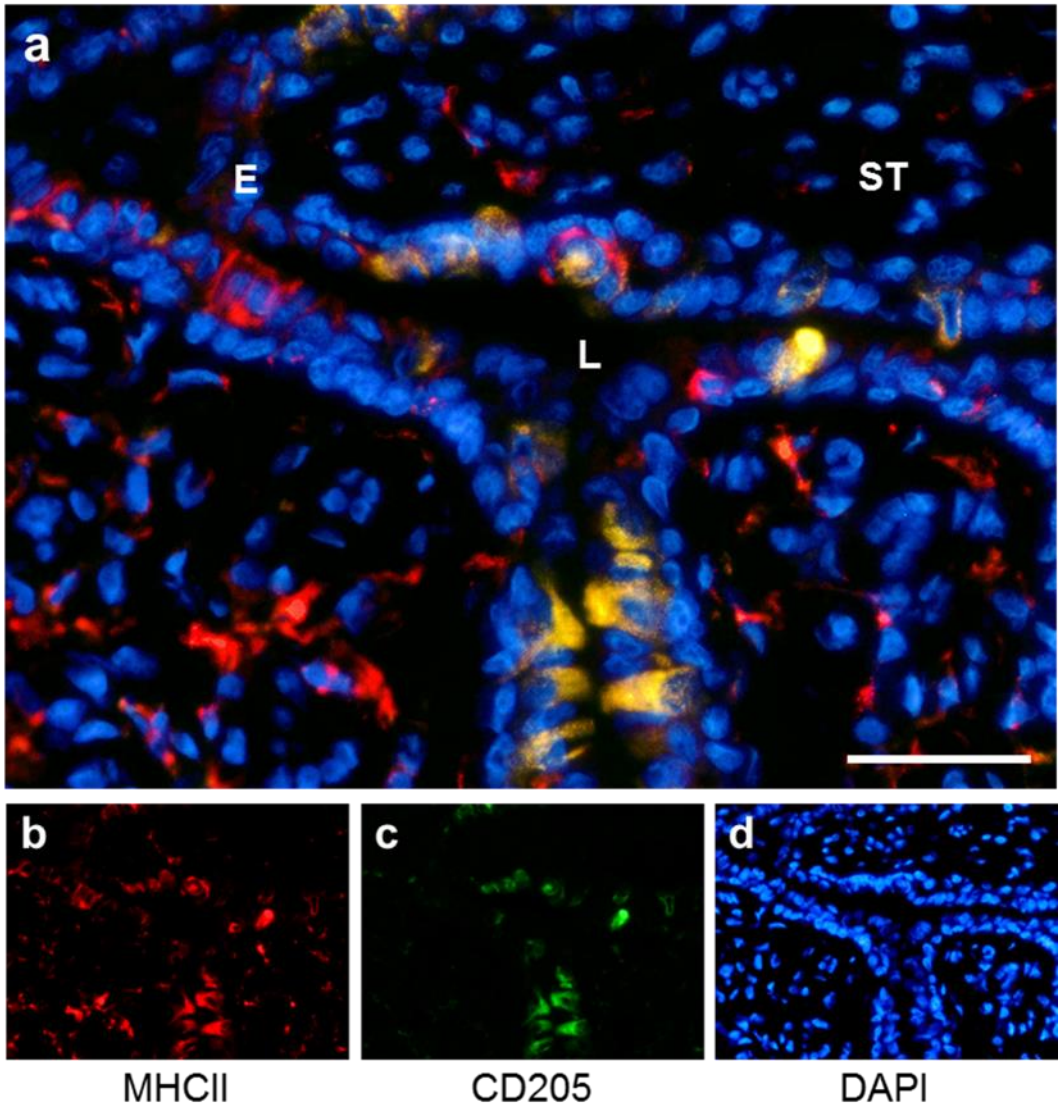

Figure 4.15: CD205 and MHC class II expressing cells in the Fürstenberg's rosette.
Micrographs from Cow #452 of a transverse cryosection from Fürstenberg's rosette. The cryosection was probed with anti-MHC class II monoclonal antibody (b) (Alexa-fluor 594 IgG2a; red signal), anti-CD205 monoclonal antibody (c) (Alexa-fluor 488 IgG; green signal) and counterstained with DAPI (d), (blue signal). Cells expressing both MHC class II and CD205 antigen show up yellow (a). E, epidermis; ST, stromal tissue; L, lumen. Section thickness: 5 µm. Scale bar = 25 µm.

4.8. Distribution of CD14 positive cells in the teat-end tissues

CD14, in complex with lipopolysaccharide-binding protein and toll-like receptor 4 (TLR4), act together as a cell surface receptor for the detection and binding of lipopolysaccharide. CD14 is highly expressed in macrophages; however, dendritic cells and neutrophils are also known to express low levels of the protein.

Macrophages have previously been found in the milk and tissues of healthy lactating and involuted bovine mammary glands, suggesting that they are part of the normal defence system of the mammary gland (Sordillo *et al.*, 1997; Dosogne *et al.*, 2003). Macrophages are active phagocytic cells that are capable of ingesting bacteria, cellular debris, and other milk components (Sordillo & Nickerson, 1988) and have also been shown to play a key role in antigen processing and presentation (Politis *et al.*, 1992). To determine whether the MHC class II and CD205 positive cells are macrophages, cryosections of teat-end tissues were probed with the anti-bovine CD14 monoclonal antibody MM61A.

The monoclonal antibody, MM61A, raised against the bovine CD14 epitope, is the only commercially available antibody specific for identifying bovine macrophages. Other more commonly used anti-macrophage antibodies, such as MAC387, were incompatible with the tissues in this study as they recognise the calprotectin (S100A8/A9 heterodimer) molecule which was shown to be highly expressed by the teat canal keratinocytes (See Chapter 3).

$CD14^+$ cells were located in the subepithelial stromal tissue regions of the teat canal, and teat skin cryosections (Figure 4.16a, b) with very little staining observed within the epithelium. In both of these tissues, the $CD14^+$ cells were located within the stromal tissue between the rete ridges (Arrowed in Figure 4.16a, b). It was not possible to distinguish between macrophages and dendritic cells in these sections, based on cell morphology alone (Figure 4.16e). In the Fürstenberg's rosette (Figure 4.16c, e) and teat sinus (Figure 4.16d, f), $CD14^+$ cells were predominantly found within the epithelial bilayers.

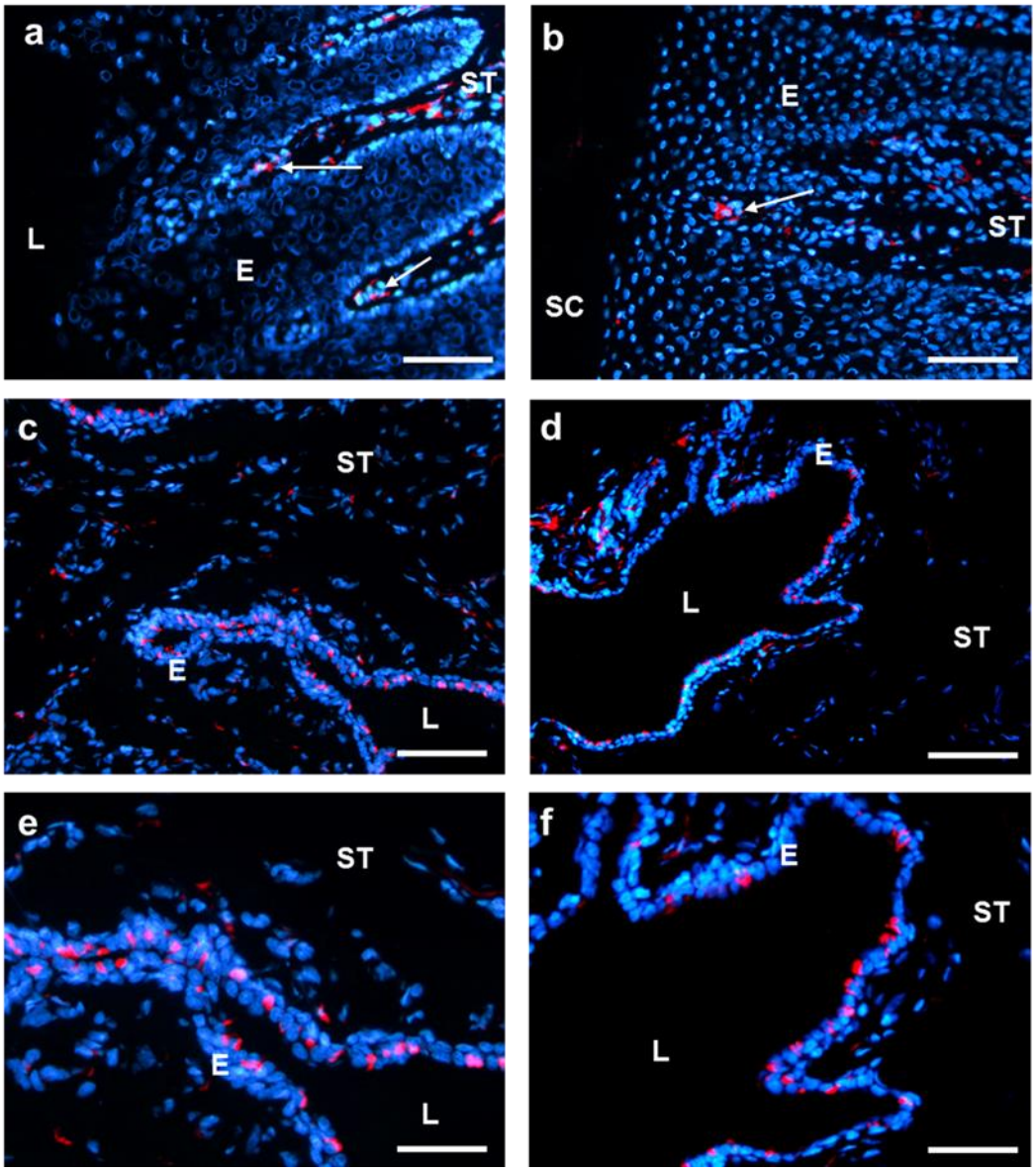

Figure 4.16: CD14 labelled cells in the teat-end tissues.
Representative micrographs from Cow #910 of transverse cryosections. Sections of teat canal (a), teat skin (b), Fürstenberg's rosette (c, e), and teat sinus (d, f) were probed with anti-CD14 monoclonal antibody (Alexa-fluor 594 IgG; red signal). Each cryosection was counterstained with DAPI (blue signal). E, epidermis; SC, *stratum corneum*; ST, stromal tissue; L, lumen. Section thickness: 5 µm. Scale bar = 50 µm (a-d), 25 µm (e, f).

Dual IF staining with CD14 and MHC class II monoclonal antibodies revealed that all the $CD14^+$/MHC class II^+ cells in the Fürstenberg's rosette were localised in the epithelial bilayer (Figure 4.17). Taking an average cell count from seven nonadjacent fields per slide, from all six cows at 200 x magnification, the dual-labelled cells comprised just over a quarter of the epithelial-bound MHC class II^+ cells (~27 ± 9 %).

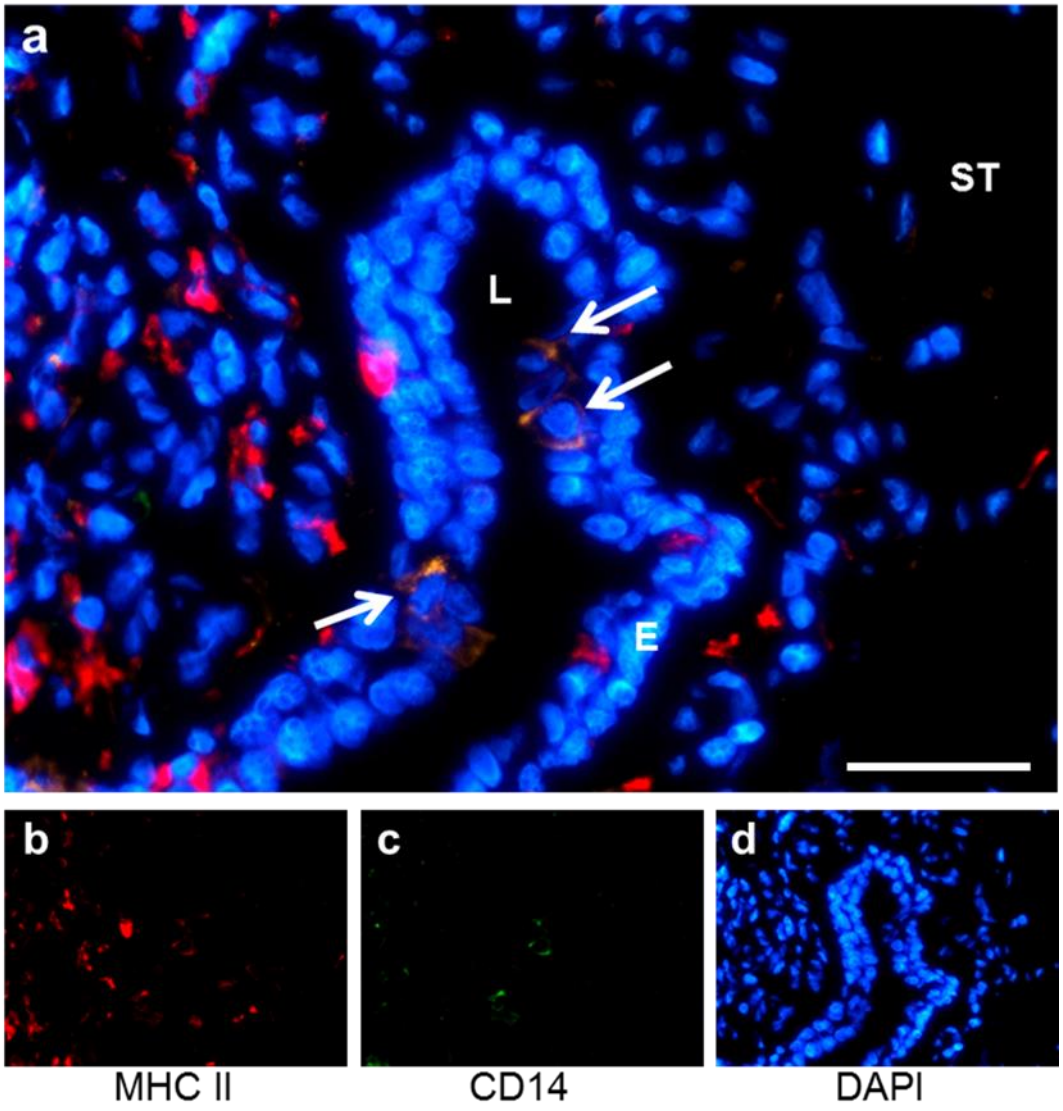

Figure 4.17: CD14 and MHC class II expressing cells in the Fürstenberg's rosette.
(a) Representative micrograph from Cow #910 of a transverse cryosection from Fürstenberg's rosette. The cryosection was probed with anti-MHC class II monoclonal antibody (b) (Alexa-fluor 594 IgG2a; red signal), anti-CD14 monoclonal antibody (c) (Alexa-fluor 488 IgG; green signal) and counterstained with DAPI (d), (blue signal). Cells expressing both MHC class II and CD14 antigen show up yellow (arrowed). E, epidermis; ST, stromal tissue; L, lumen. Section thickness: 5 µm. Scale bar = 25 µm.

Compared with the Fürstenberg's rosette, a similar analysis calculated that the $CD14^+$/MHC II^+ cells constituted approximately 41 ± 6 % of the total MHC class II^+ cells in the teat sinus epithelial bilayer (Figure 4.18). The increase in abundance of the $CD14^+$/MHC II^+ cells would suggest that they may play a more prominent surveillance role in the teat sinus region compared to the Fürstenberg's rosette of healthy late-lactating cows.

Additional experiments showed that cells bearing both CD14 and CD11c markers were not identified in any of the tissues from all the cows examined (*data not shown*).

4.9. Keratinocytes of the Fürstenberg's rosette and teat sinus epithelial bilayer also expressed MHC class II

The MHC class II positive cells within the epithelial bilayer of the Fürstenberg's rosette and teat sinus far exceed the total number of CD205, CD14, and WC1 positive cells, combined. This suggests that there are other yet unidentified cell types that express MHC class II.

Epithelial cells of the intestinal and respiratory mucosal systems constitutively express or can be induced to express MHC class II molecules (Panja *et al.*, 1993; Cunningham *et al.*, 1997; Hershberg *et al.*, 1997). In the intestine, antigen uptake generally occurs through modified epithelial cells (M cells) in the intestinal epithelium, which overlie organised lymphoid tissue such the Peyer's patches (Frey *et al.*, 1996). M cells facilitate the transport of large molecules without significant cellular processing to the underlying lymphoid tissue and innate immune cells (Kraehenbuhl & Neutra, 2000). Under high power magnification, they are histologically identified by their lack of a rigid brush border. Recently, keratin 18 (K18) has been identified as a specific marker for bovine intestinal M cells by IHC (Hondo *et al.*, 2011).

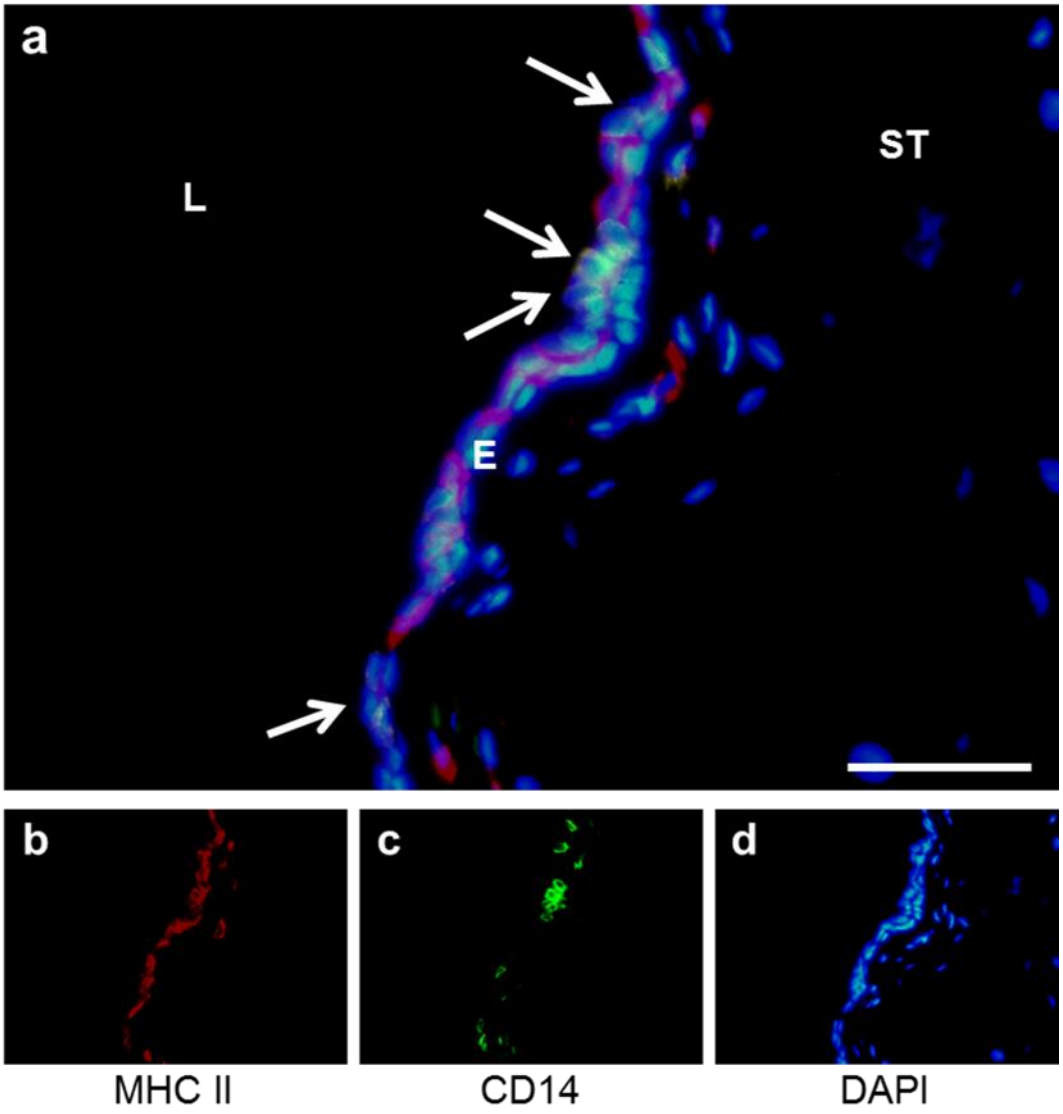

Figure 4.18: CD14 and MHC class II expressing cells in the teat sinus epithelial bilayer.
(a) Representative micrograph from Cow #910 of a transverse cryosection from Fürstenberg's rosette. The cryosection was probed using anti-MHC class II monoclonal antibody (b) (Alexa-fluor 594 IgG2a; red signal), anti-CD14 monoclonal antibody (c) (Alexa-fluor 488 IgG; green signal) and counterstained with DAPI (d), (blue signal). Cells expressing both MHC class II and CD14 antigen appear yellow (arrowed). E, epidermis; ST, stromal tissue; L, lumen. Section thickness: 5 µm. Scale bar = 25 µm.

To determine if the Fürstenberg's rosette and teat sinus epithelium contained areas that might be analogous to M cells, which express MHC class II proteins, teat-end cryosections were probed with both an anti-bovine K18 monoclonal antibody and MHC class II antibodies.

There were no cells expressing K18 in epithelia of the teat canal and teat skin cryosections (Figure 4.19a, b). In contrast, the apical layer of the Fürstenberg's rosette and teat sinus epithelial bilayer showed strong immuno-reactivity to K18 (Figure 4.19c-f). Dual IF staining demonstrated that the majority of the $K18^{+}$ cells were also positive for MHC class II in both the Fürstenberg's rosette (Figure 4.20) and teat sinus (Figure 4.21).

4.10. Detection of stem cell factor receptor (*c-kit*) on mast cells

Mast cells are a specialised type of granulocyte-derived within the myeloid cell lineage. Upon activation, Mast cells secrete a wide array of biologically active compounds such as histamine, heparin and tumour necrosis factor-alpha (TNF-α) (Metz *et al.*, 2008). These molecules affect blood vessel permeability and increase the influx of innate immune cells such as neutrophils and macrophages into the subepithelial stromal tissue (Malaviya & Abraham, 2001; Marshall, 2004).

The stem cell factor receptor, *c-kit* (CD117) is expressed in hematopoietic stem cells and mast cells are the only terminally differentiated hematopoietic cells that are known to retain expression of the *c-kit* receptor. In order to determine whether mast cells were present in the teat-end tissues, cryosections were probed with a polyclonal antibody (A4502) against bovine CD117.

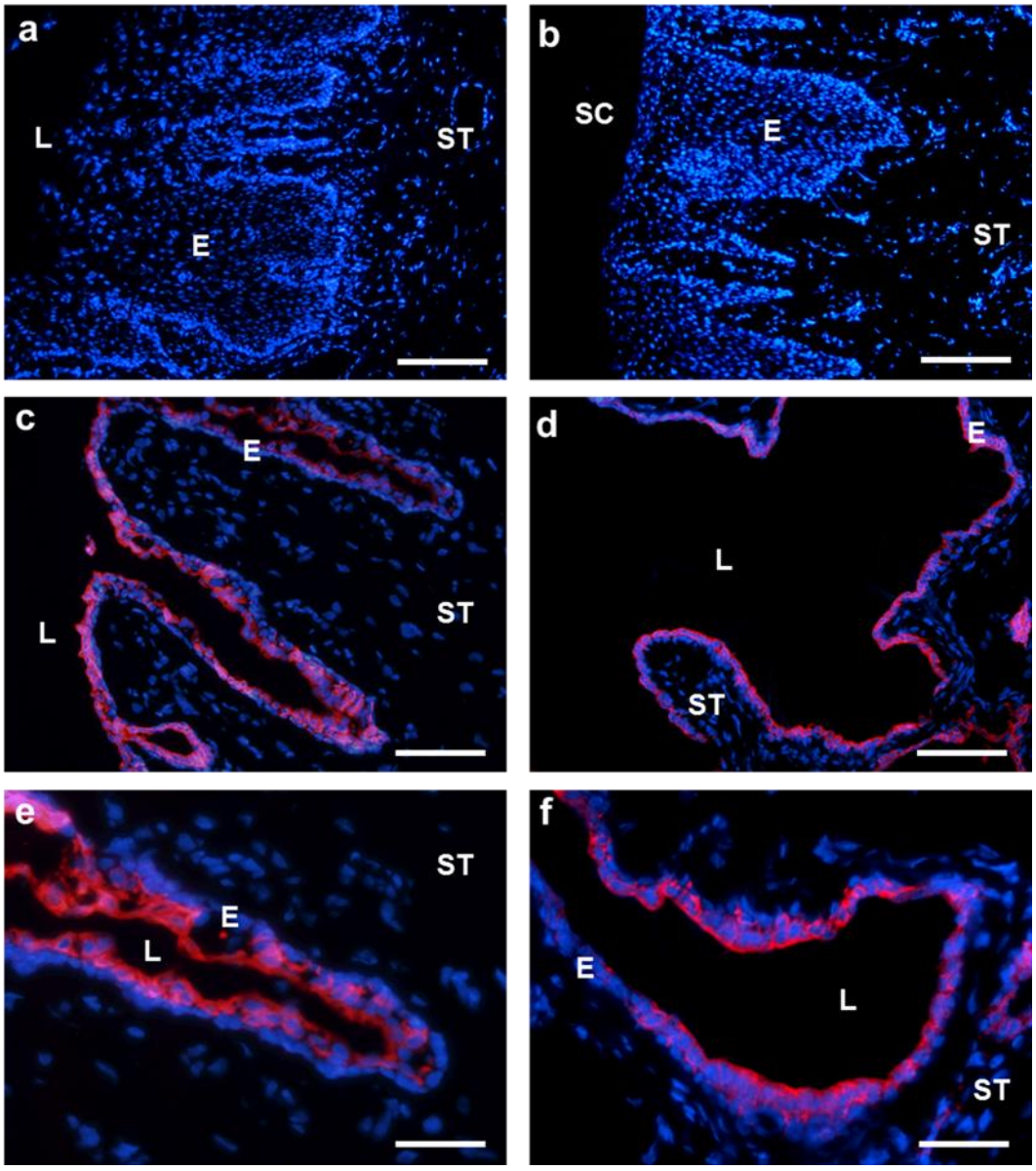

Figure 4.19: Keratin 18 labelled cells in teat-end tissues.
Representative micrographs from Cow #1048 of transverse cryosections. Sections of teat canal (a), teat skin (b), Fürstenberg's rosette (c, e) and teat sinus (d, f) were probed with anti-K18 monoclonal antibody (Alexa-fluor 594 IgG; red signal). **Note:** that there is no signal in the stratified epithelium of the teat canal and teat skin and that the K18 signal is restricted to the luminal layer of epithelial cells in the Fürstenberg's rosette and teat sinus. Each cryosection was counterstained with DAPI (blue signal). E, epidermis; SC, *stratum corneum*; ST, stromal tissue; L, lumen. Section thickness: 5 µm. Scale bar = 100 µm (a, b), 50 µm (c, d), 25 µm (e, f).

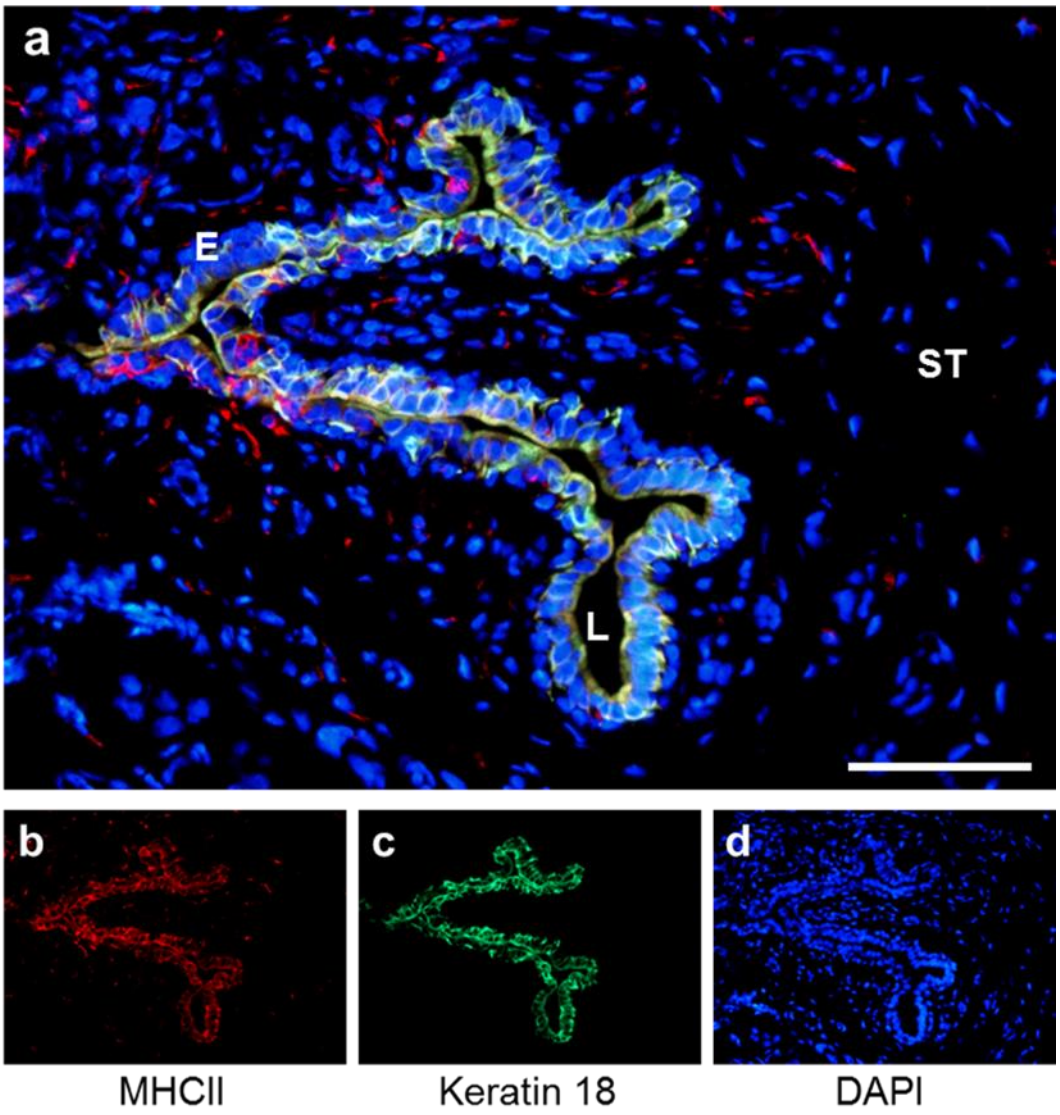

Figure 4.20: MHC class II and keratin 18 localisation in Fürstenberg's rosette.
Representative micrograph from Cow #05 of a transverse cryosection from Fürstenberg's rosette. The cryosection was probed with anti-MHC class II monoclonal antibody (b) (Alexa-fluor 594 IgG2a; red signal), anti-keratin 18 monoclonal antibody (c) (Alexa-fluor 488 IgG; green signal) and counterstained with DAPI (d), (blue signal). Cells expressing both MHC class II and CK18 antigen appear yellow and are restricted to the outer epithelial bilayer. E, epidermis; ST, stromal tissue; L, lumen. Section thickness: 5 µm. Scale bar = 50 µm.

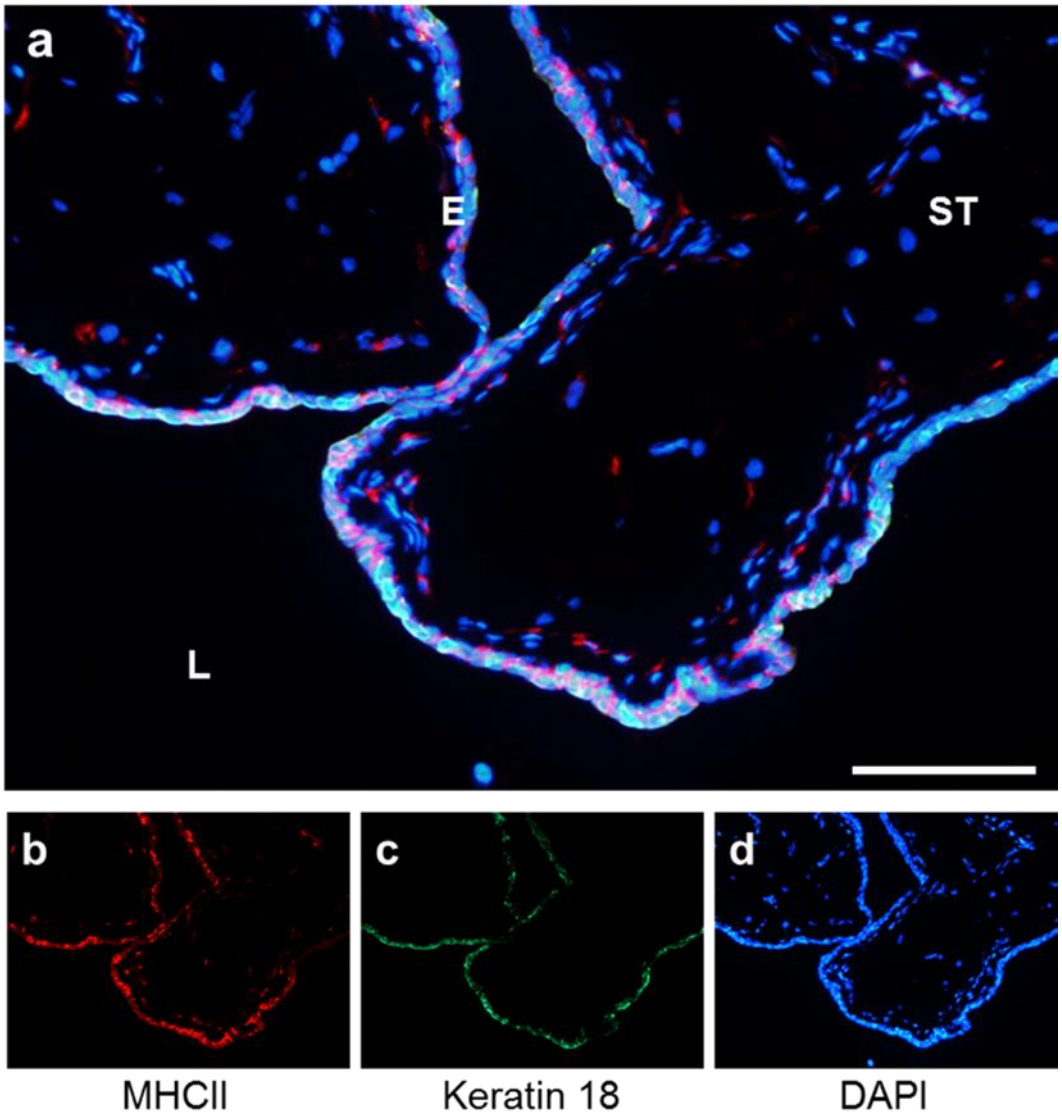

Figure 4.21: MHC class II and keratin 18 localisation in the teat sinus.
Representative micrograph from Cow #1048 of a transverse cryosection from the teat sinus. The cryosection was probed with anti-MHC class II monoclonal antibody (b) (Alexa-fluor 594 IgG2a; red signal), anti-keratin 18 monoclonal antibody (c) (Alexa-fluor 488 IgG; green signal) and counterstained with DAPI (d), (blue signal). Cells expressing both MHC class II and CK18 antigen appear yellow and are restricted to the outer layer of cells of the epithelial bilayer. E, epidermis; ST, stromal tissue; L, lumen. Section thickness: 5 µm. Scale bar = 50 µm.

$CD117^+$ cells (arrowed) were sparsely scattered among the subepithelial stromal tissue in teat canal and teat skin cryosections for all six cows examined (arrowed in Figure 4.22a, b). For the three-quarters of teat canal and teat skin cryosections (n = 6 each), $CD117^+$ cells were slightly more abundant in the stroma surrounding structures that resembled blood vessels (*data not shown*).

Semi-quantification of $CD117^+$ signal was performed by averaging the number of $CD117^+$ cells from seven nonadjacent fields per slide, from all six cows at 200 x magnification. Using Students paired *t*-test, there was no significant difference between the mean number of $CD117^+$ cells located in the stromal tissue of the teat canal, teat skin, and teat sinus (Figure 4.23). In contrast, there was approximately a three-fold greater abundance of $CD117^+$ cells in the stromal tissue underlying the epithelial bilayer of Fürstenberg's rosette ($p < 0.001$; Figure 4.23).

4.11. Abundance of granulocytes in teat-end tissues

Granulocytes, along with macrophages, are the principal phagocytic cells of the innate immune system (Alberts *et al.*, 2002). Neutrophils are by far the most abundant of the granulocytes and are rapidly recruited to sites of inflammation and infection (Paape *et al.*, 2002b). Consequently, neutrophils are part of the first line of cellular defence against invading pathogens (Smith, 1994).

In uninfected teat-end tissues, neutrophils have been identified by histological examination and electron microscopy in the Fürstenberg's rosette and teat sinus tissue regions (Nickerson & Pankey, 1983, 1984; Collins *et al.*, 1986). In this study, the bovine-specific anti-granulocyte monoclonal antibody, CH138A, was used to identify granulocytes such as neutrophils, basophils and eosinophils in the teat-end tissues.

The antibody has been mainly used to enrich for neutrophils in flow cytometry analysis, however, in a recently published paper, CH138A was used for IF staining to identify neutrophils in bovine skin (Constantinoiu *et al.*, 2010).

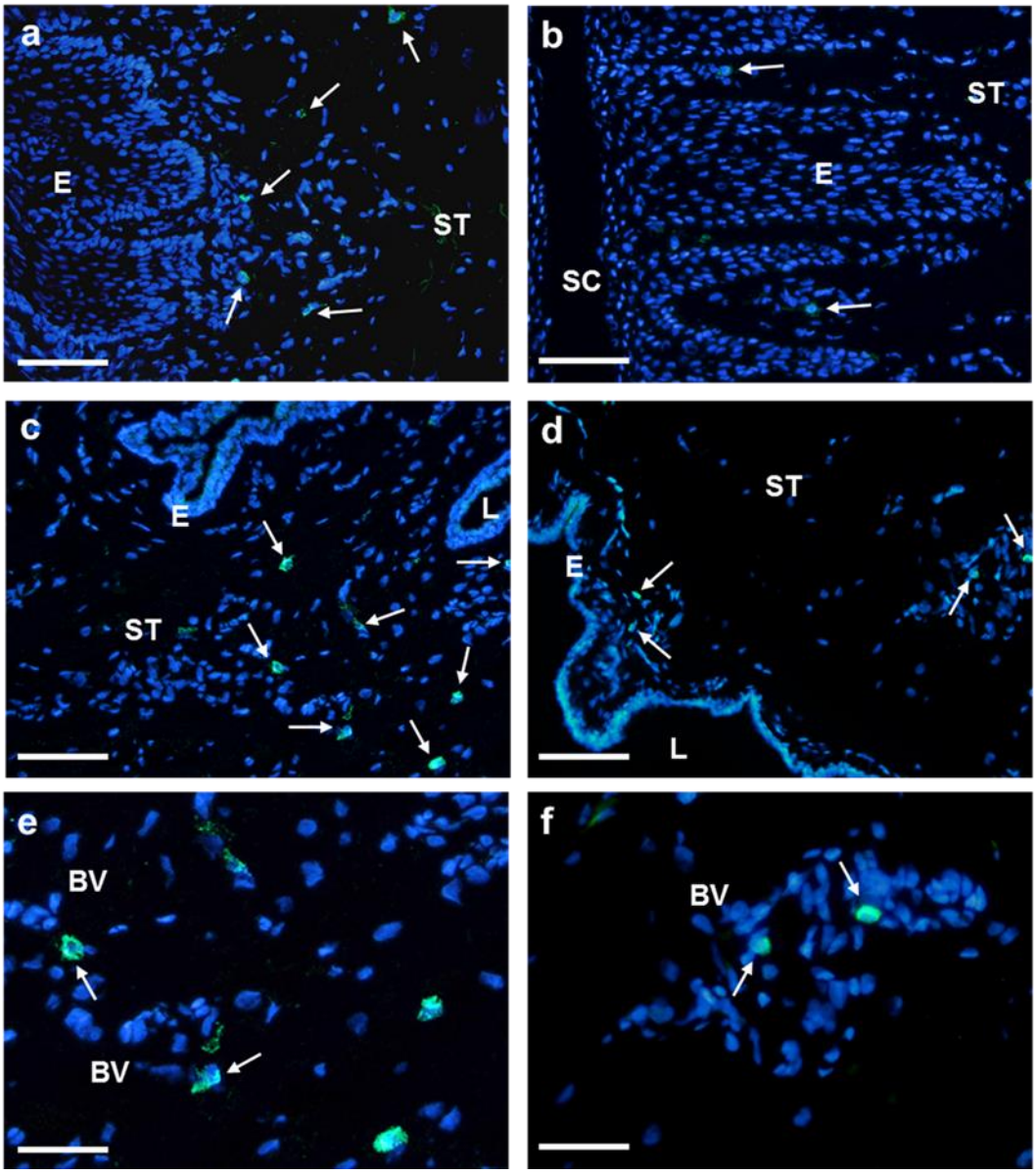

Figure 4.22: CD117 labelled cells in the teat-end tissues.
Representative micrographs from Cow #1048 of transverse cryosections. Sections of teat canal (a), teat skin (b), Fürstenberg's rosette (c, e) and teat sinus (d, f) were probed with anti-CD117 polyclonal antibody (Alexa-fluor 488 IgG; green signal) and counterstained with DAPI (blue signal). $CD117^{+}$ cells in the stroma are arrowed in all panels. Panel's e and f show $CD117^{+}$ cells (arrowed) located next to structures that resemble blood vessels. E, epidermis; SC, *stratum corneum*; ST, stromal tissue; L, lumen; BV, blood vessel. Section thickness: 5 µm. Scale bar = 50 µm (a-d), 25 µm (e, f).

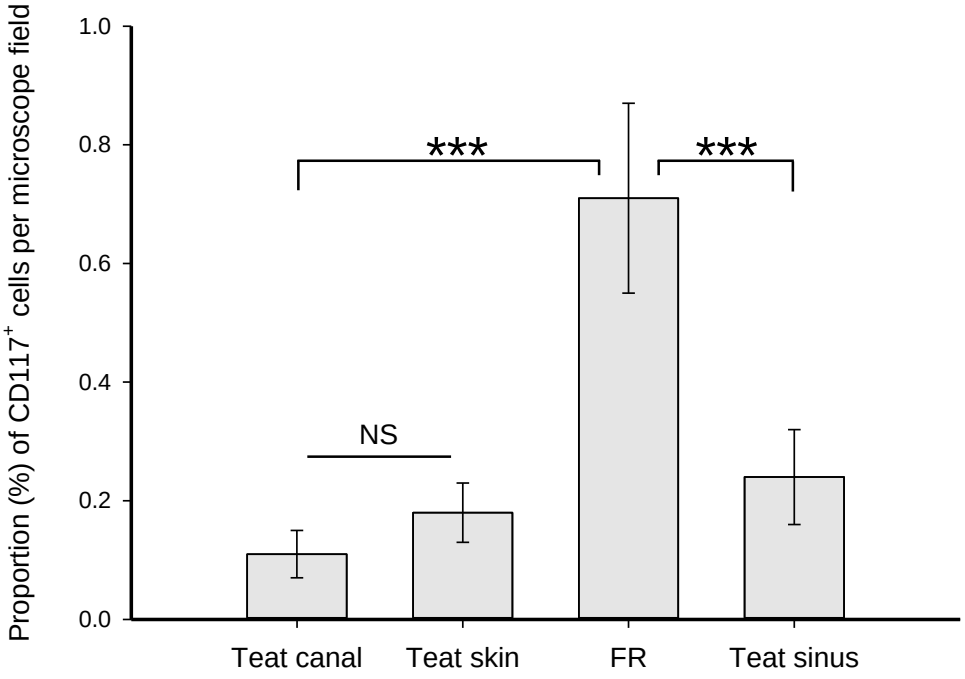

Figure 4.23: Relative abundance of CD117+ cells in teat-end tissues.
The numbers of positively stained CD117 expressing cells in the stromal tissue adjacent to the epithelial cell layer were counted from seven nonadjacent fields per slide at 100 x magnification and averaged. The results are cumulative data from six different cows. FR, Fürstenberg's rosette. Error bar: ± SEM. The asterisk *** indicates $p < 0.001$; NS, not significant

The exact epitope recognised by this antibody is currently unknown, so the human CD equivalent has not been determined (information sheet for monoclonal antibody CH138A, WSU Monoclonal Antibody Center, Pullman, USA).

In all four teat-end tissue areas examined, there was moderate to strong immunoreactivity with the CH138A antibody (Figure 4.24). In the teat canal and teat skin cryosections, cells reacting to the antibody were restricted to the stromal tissue, with more positive cells concentrated in the dermal papillae between the rete ridges (Figure 4.24a, b). Very little, if any, signal was observed within the stratified epithelium with the exception of the Marksäulchen in the teat canal (labelled M in Figure 4.24a & 4.25a).

The CH138A$^+$ cells were most abundant in the Fürstenberg's rosette and teat sinus tissue cryosections. This signal, however, was not always tightly associated with DAPI-stained nuclei (Arrowed in Figure 4.24f) and in the stroma of the Fürstenberg's rosette and the teat sinus, appeared to be pericellular to the epithelial bilayer (Figure 4.24c, d). The majority of the signal appeared to be localised just beneath the epidermal bilayer, suggesting an accumulation of granulocytes in this area. The occasional positive-staining cell could be seen in the epithelial bilayer (Arrowed in Figure 4.24e).

Under certain conditions, neutrophils can express MHC class II antigens on their cell surface (Gosselin *et al.*, 1993; Radsak *et al.*, 2000). To test the possibility that these CH138A$^+$ cells also contribute to the population of MHC class II$^+$ cells (See Figure 4.3), dual fluorescence IHC with CH138A and MHC class II antibodies were performed on cryosections from the Fürstenberg's rosette (Figure 4.26). Interestingly, some of the CH138A labelled cells also expressed low levels of MHC class II. Furthermore, these infrequently dual-labelled cells were only ever observed adjacent to the epithelial-stromal boundary and within the epithelial bilayer.

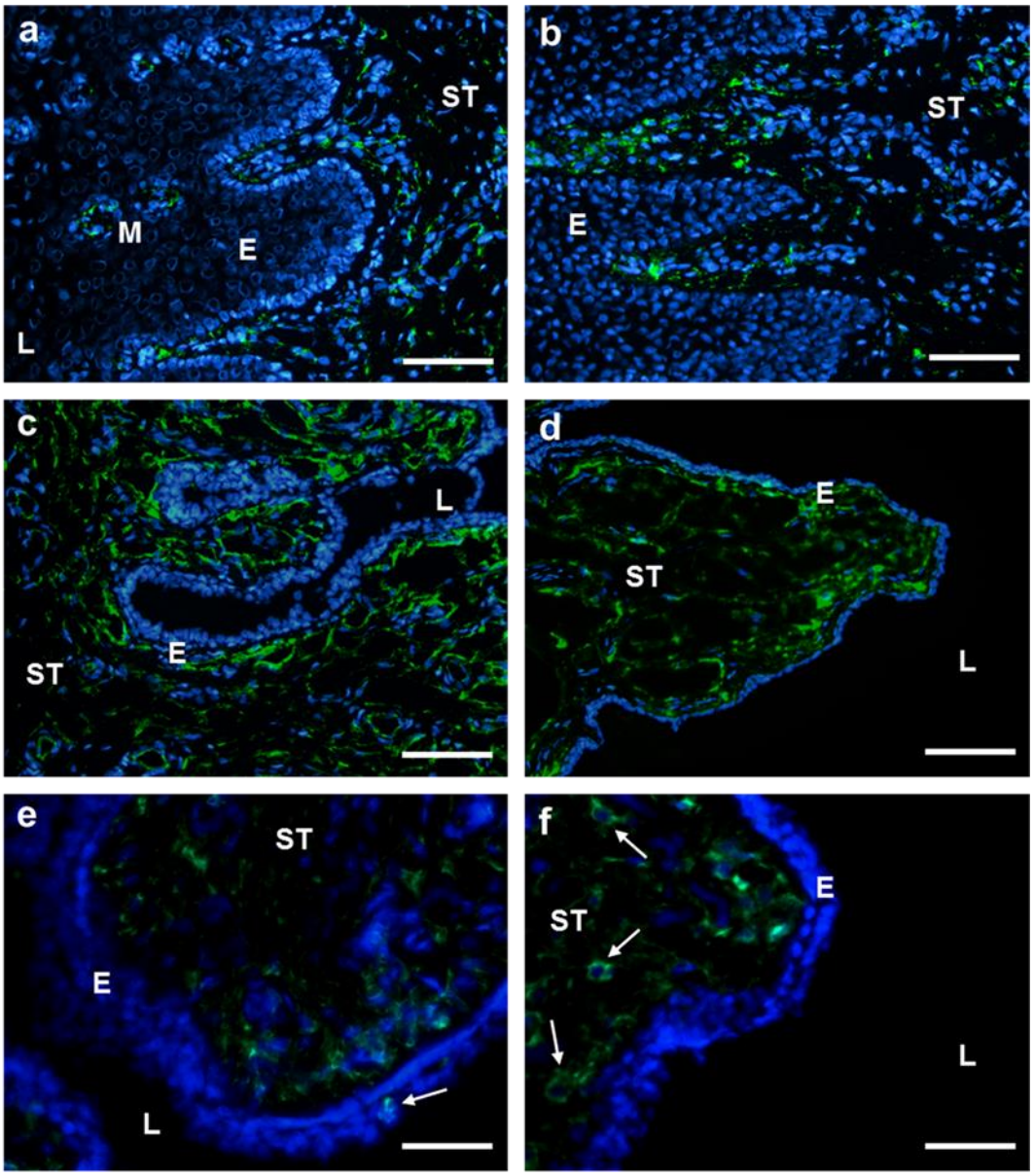

Figure 4.24: CH138A labelled cells in teat-end tissue sections.
Representative micrographs from Cow #1048 of transverse cryosections. Cryosections of teat canal (a), teat skin (b), Fürstenberg's rosette (c, e) and teat sinus (d, f) were probed with monoclonal CH138A antibody (Alexa-fluor 488 IgM; green signal). Infrequent CH138A$^+$ cells were observed in the Fürstenberg's rosette (e) epithelial bilayer (arrowed). In the teat sinus (f), CH138A$^+$ cells were detected only in the subepithelial stroma (arrowed). Each cryosection was counterstained with DAPI (blue signal). E, epidermis; M, Marksäulchen; ST, stromal tissue; L, lumen. Section thickness: 5 µm. Scale bar = 50 µm (a-d), 25 µm (e-f).

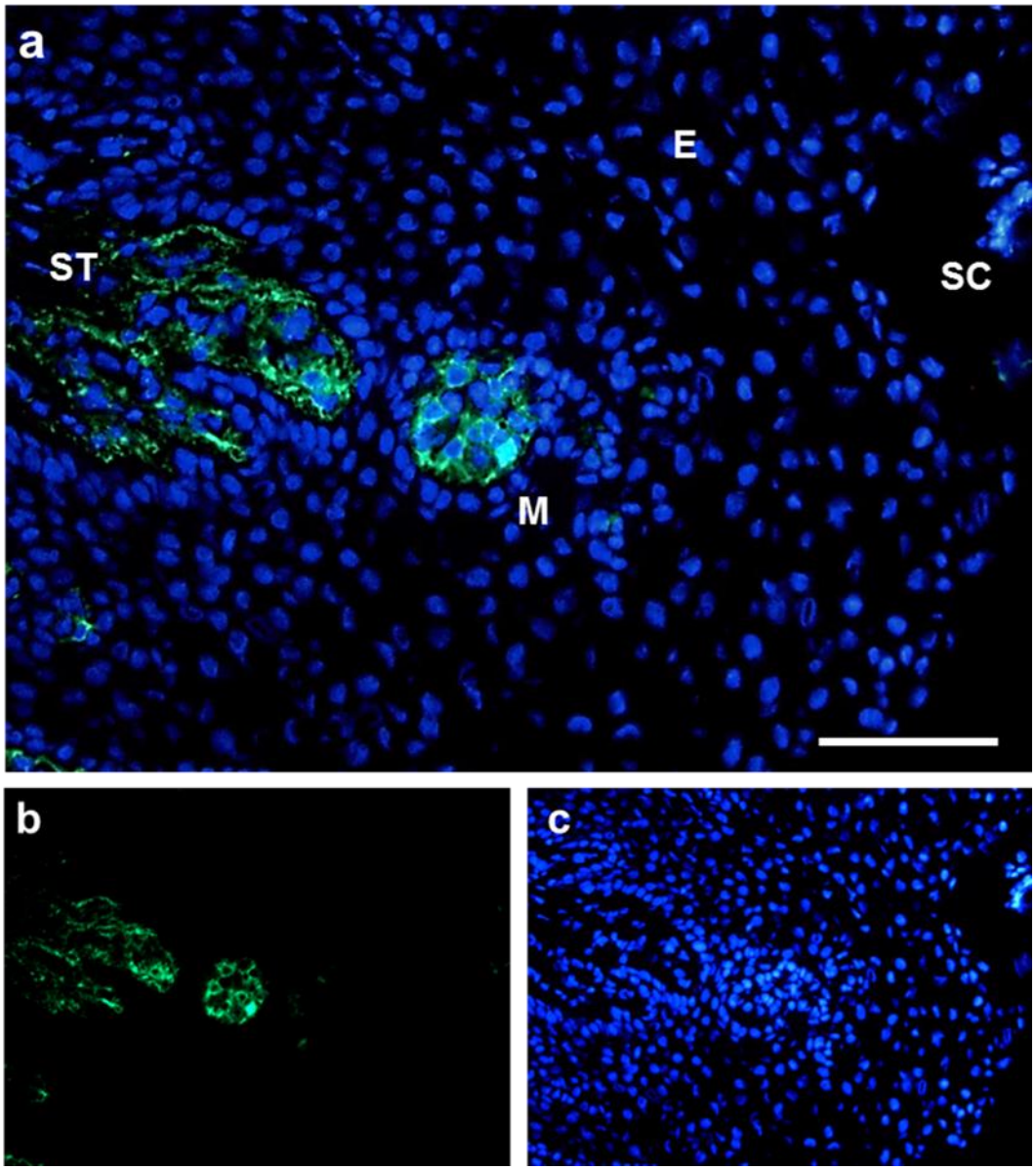

Figure 4.25: CH138A positive cells in the Marksäulchen of the teat canal epithelium.
Representative micrograph from Cow #452 of a transverse cryosection from the teat (a). The cryosection was probed with a monoclonal CH138A antibody (b) (Alexa-fluor 488 IgM; green signal) and counterstained with DAPI (c) (blue signal). **Note:** $CH138A^{+}$ cells were observed in the stroma and Marksäulchen but were absent in the stratified epithelium. E, epidermis; M, Marksäulchen; ST, stromal tissue; SC, *stratum corneum*. Section thickness: 5 µm. Scale bar = 50 µm (a-c).

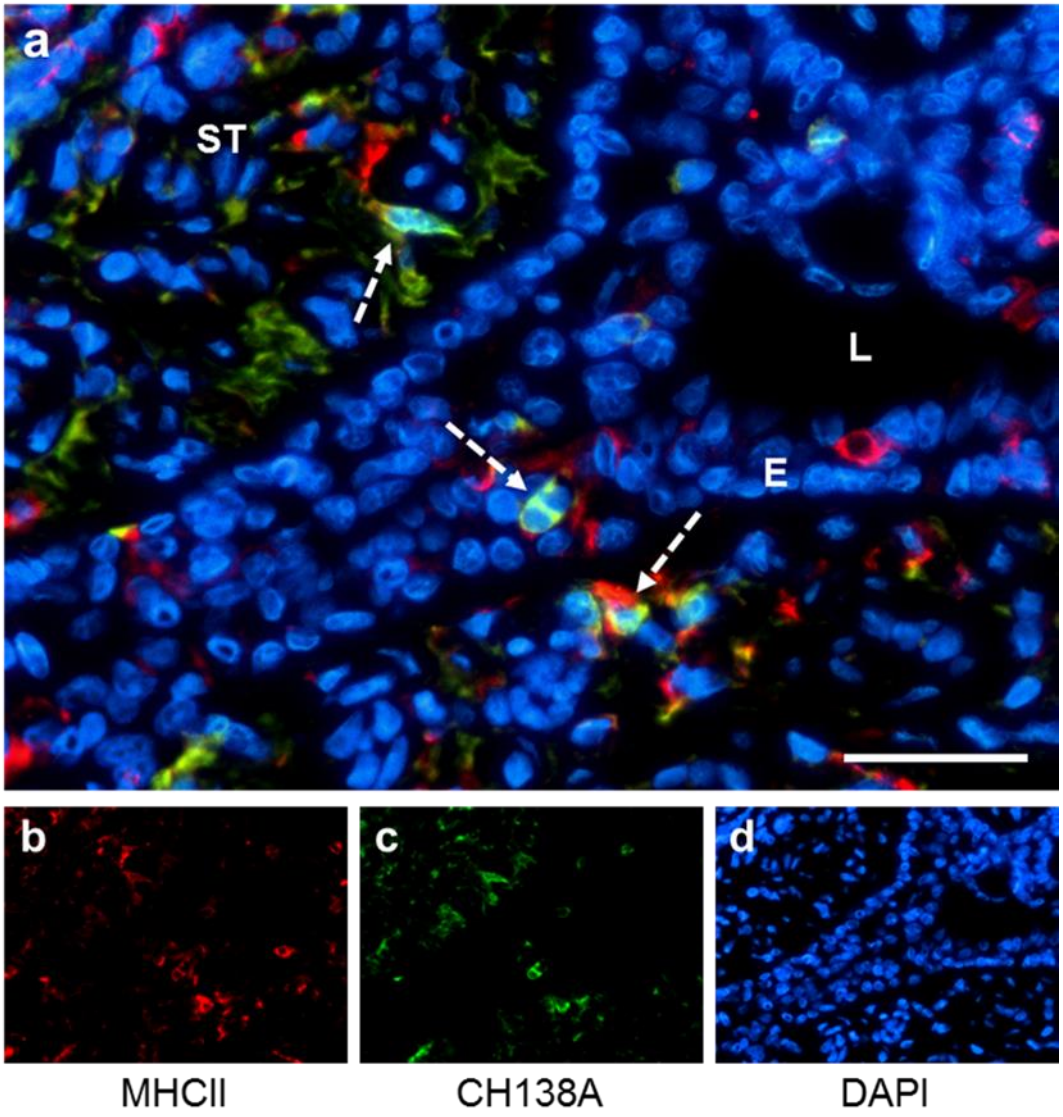

Figure 4.26: CH138A and MHC class II antigen positive cells in the Fürstenberg's rosette. Representative micrograph from Cow #1048 of a transverse cryosection from Fürstenberg's rosette. The cryosection was probed with anti-MHC class II monoclonal antibody (b) (Alexa-fluor 594 IgG2a; red signal), anti-granulocyte marker (CH138A) monoclonal antibody (c) (Alexa-fluor 488 IgM; green signal) and counterstained with DAPI (d), (blue signal). Cells expressing both CH138A and MHC class II antigen are shown as yellow (dashed arrows). E epidermis; ST, stromal tissue; L, lumen. Section thickness: 5 µm. Scale bar = 25 µm.

4.12. Discussion

The IHC analyses described in this chapter have established that the teat-end tissues contain significant numbers of cells important for innate immune functions. These include antigen-presenting cells, T lymphocytes, γδ T cells, macrophages and granulocytes with the distribution of these cells varying among the four tissues types examined. Fürstenberg's rosette and teat sinus were found to be comparatively rich in immune cells, while somewhat lesser numbers were observed in the differentiating keratinous epithelium of the teat canal and the teat skin. These differences in the abundance and distribution of immune cells, along with the differences in cellular morphology and microstructure of each of the tissues, suggest that each region may have a distinct innate immune functionality.

The keratinising epithelium of the teat canal, while being similar to, and having a common developmental origin as the teat skin, was found to contain a unique microstructure, as has been previously described (Fürstenberg, 1868; Mańkowski, 1903; Adams *et al.*, 1961; Paulrud, 2005). The thick keratin-rich *strateum corneum* presents an effective barrier to the environment, but also creates a barrier for the secretion of immune effector proteins and translocation of immune cells into the lumen. In the skin, the rapid differentiation of keratinocytes from the basal layer of cells creates a flux of cells towards the external environment with the constant shedding of the outermost layer of keratin. Immune cells are found in the epithelial and subepithelial stromal layer of skin, and many studies have established that they functional as a second line of defence in the event of a breach of the physical barrier to the environment (Mathers & Larregina, 2006; Bos & Luiten, 2009; Nestle *et al.*, 2009; Bangert *et al.*, 2011; Tay *et al.*, 2014).

A similar process appears to operate in the teat canal, based on the similarity of the morphology of the tissue and location of the immune cells. Analogous to the teat skin, MHC class II^+ cells, presumably antigen-presenting cells, were found in the subepithelial stroma, and it is reasonable to suppose that they have a similar function to those in the skin as a second line of defence. Similar to skin, a proportion of these cells appear to be dendritic cells, granulocytes and macrophages, based on their staining with the CD205, CD11c, CH138A, and

CD14 markers, and γδ T cells by virtue of them reacting with the CD3 and WC1 markers. A unique feature of the morphology of the teat canal are the numerous Marksäulchen, a structure with no equivalent within the skin epithelia. The morphology of the cells within these structures appears distinct from the surrounding tissue. Some of these cells stained strongly for the granulocyte marker CH138A. However, as this marker has yet to be fully characterised their full identity remains unresolved. Further studies using additional and novel cell type-specific markers may shed light on their identity.

The Fürstenberg's rosette, located at the distal end of the teat canal, has a high prevalence of immune cells. These two facts alone suggests it is important in the defence against pathogens. Presumptive antigen-presenting cells (MHC class II^+) are prevalent throughout the stroma as well as embedded within the epithelial bilayer. Based on the staining for CD11c, CD14 and CD205, a variety of subtypes of antigen-presenting cells may be present and most likely represents dendritic cells and macrophages. γδ T cells are also present, and are particularly abundant on the epithelial bilayer, further reinforcing the conclusion that the tissue-lumen surface is primed for sensing pathogens and responding to them. The subepithelial stroma of Fürstenberg's rosette contains moderate numbers of $CD3^+$ T cells and granulocytes, but surprisingly was found to contain very few B cells.

In the intestine, specialised epithelial cells called M-cells, overlay lymphoid follicles of Peyer's patches providing immunological surveillance of antigens. In this type of tissue keratin 18 has been identified as a specific marker of bovine and porcine M cells (Gebert *et al.*, 1994; Hondo *et al.*, 2011). However, the ubiquitous expression of this protein all through the apical layer of the Fürstenberg's rosette and the teat sinus epithelial bilayer, respectively, provides little similarity to these observations and therefore no conclusive evidence for discrete MALT-like structures in the teat-end tissues. Instead of discrete zones in these tissues, it is possible that the entire apical layer of epithelial cells allows for the transport and diffusion of small molecules, trans-epithelial migration of phagocytic cells and immune surveillance by innate immune cells. In support of this concept, evidence for antigen sampling of ferritin molecules in the Fürstenberg's rosette has been recently described (Aştı *et al.*, 2011).

Taken together, these analyses have established that Fürstenberg's rosette is a key site of immune surveillance among the teat-end tissues. The mucosal-like folds, which define the morphological structure of the Fürstenberg's rosette, provide a large surface contact area for immune cells to detect infiltrating pathogens. Along with its ability to restrict the flow of milk from the teat sinus, this strongly suggests that this region of the teat is crucial in preventing pathogens from migrating beyond the teat canal into the teat sinus.

Whether the Fürstenberg's rosette could be considered a lymphoid-like tissue is up for debate. In support of this idea, the high abundance of antigen-presenting cells and T lymphocytes in close proximity to each other would allow for the efficient induction of an effective immune response. However, there was no obvious microarchitecture typical of a classical lymphoid-like structures. Therefore, further investigation is required to determine if the Fürstenberg's rosette does possess lymphoid-like capabilities, similar to other secondary lymphoid tissues.

The morphological structure of the teat sinus, by light microscope, showed similarities to the Fürstenberg's rosette except for shallower epithelial folds and the presence of elongated nuclei in the subepithelial stroma. In this tissue, antigen-presenting cells were predominantly restricted to the epithelial bilayer; with very little signal observed in the subepithelial stroma. The apparent lower abundance of antigen-presenting cells scattered throughout the epithelial bilayer, along with a different ratio of CD205, CD14 and CD11c subtypes, and a higher proportion of γδ T cells would suggest that the teat sinus takes on a different role in antigen detection and immunological response compared to that of the Fürstenberg's rosette.

In summary, these results provide a useful characterisation of immune cells in the teat-end tissues of normal lactating cattle. The data obtained in this study will assist in future studies by providing a point of reference in response to normal physiological change – such as drying off, or an early infection model, in which a heightened immune defence is desirable.

5. Changes in the host-defence capacity of the teat-end tissues during mammary involution

5.1. Introduction:

The cessation of milk removal or drying-off of the lactating cow results in an accumulation of milk in the mammary gland. This build-up of milk brings about physiological changes to the mammary gland that initiates a complex process that ultimately halts milk production, allowing the gland to return to its non-lactating state (Capuco & Akers, 1999; Bachman & Schairer, 2003). This includes apoptosis of the secretory epithelium, remodelling of the stromal tissue and infiltration of immune cells into the gland (Singh *et al.*, 2005). This entire process is known as mammary involution and in the dairy cow, occurs over a period of three to four weeks after drying-off.

During the early stages of involution, the mammary gland is vulnerable to infection by invading pathogens (Oliver & Mitchell, 1983). There are many possible reasons for this increased susceptibility, including reduced physical barriers resulting from an altered morphology of the teat canal or a lack of flushing of the teat canal lining by milk. Alternatively, conditions within the mammary gland might be more suitable for the growth of bacteria already resident in the gland. Another likely reason and one that is within the scope of this study is that the host-defence mechanisms of the mammary gland and teat canal are suppressed during this period.

One physiological change that occurs during early involution is a decline in the rate of keratin production within the teat canal (Comalli *et al.*, 1984). This process eventually leads to the formation of the 'keratin plug' which provides an additional physical barrier to the entry of microorganisms into the involuting mammary gland. As involution progresses, it is possible that extra immune-related factors could be expressed to inhibit the growth of bacteria already residing within the teat canal, upstream of the keratin plug. Upregulation in the production of proteins with host-defence capabilities would provide another layer of protection in preventing new infections. To investigate this possibility, the

protein profile of the teat canal lining 14 days (14 d) after the cessation of milking was determined and compared with the protein profile obtained from healthy late-lactating cows (See Chapter 3).

The early involution period is also accompanied by a large influx of phagocytic immune cells, such as neutrophils and macrophages, into the lumen of the mammary gland (Nickerson, 1989; Tatarczuch *et al.*, 2000). As the environment of the teat canal and teat sinus lumen changes significantly during this period, it is conceivable that the spatial distribution, relative abundance and phenotype of the resident immune cells will change, as well as the protein repertoire. IHC using antibodies specific to antigen-presenting cells, mast cells, lymphocytes, and granulocytes will be employed to identify changes in their abundance and spatial organisation throughout four different regions of the 14 d involution teat-end tissues. Variations in the 14 d involution profiles will be compared with the immune cell profiles of healthy late-lactation cows (See Chapter 4). Overall, these analyses will characterise how the mucosal immune capacity of the teat end tissues is mobilised during involution, and thus contribute to a better understanding of how effective host defence is achieved during this crucial stage of the lactation cycle in cows.

5.2. Experimental design:

Twenty-eight late lactation dairy cows were assessed for intra-mammary infections by quarter milk SCC and microbiological analyses (See Section 3.1). From these 28 cows, 13 animals were found to be free of any clinical or subclinical intramammary infections in all four quarters. Seven of the 13 cows were randomly selected for drying-off over a 14 d period, and their individual characteristics detailed in Table 5.1.

No antibiotic dry therapy treatment or teat sealant was administered to the cows as this would interfere with the natural innate immune response of the teat as well as disrupting the accumulation and development of the teat canal lining. All seven cows were regularly monitored over the two-week period, and the teat-ends were sanitised daily with an iodine-based teat spray. This treatment reduced the chance of any new intra-mammary infection occurring before the keratin plug had formed. Both late-lactation and involution cows were managed as one husbandry herd on the dairy farm.

At the end of the 14 d period, the cows were slaughtered and the mammary glands collected for teat canal lining and tissue sampling. Teat canal lining collected from contralateral hindquarter and forequarter teats, from all seven cows, were processed to extract proteins (n = 14). The remaining pairs of contralateral teats from the seven cows were processed for IHC analyses with selected anti-bovine cell surface markers antibodies.

Table 5.1: Individual characteristics of cows in the 14 d involution trial

Cow #	Age (years)	Gestation status	Days in milk	Daily yield (L)[a]	SCC (x10^3 cells/mL)[b]
115	3	Pregnant	287	16.4	14
160	7	Empty	264	10.2	107
331	4	Pregnant	286	10.2	75
358	5	Empty	274	18.8	59
499	4	Pregnant	268	17.9	91
837	8	Empty	286	19.2	14
911	6	Pregnant	400	13.2	148
Average ± SD	*5.3 ± 1.8*		*295 ± 47*	*13.4 ± 2.2*	*72.6 ± 48.8*

a) Daily yield of milk in Litres (L).
b) Average somatic cell count (SCC) determined from milk collected from all four quarters before the cessation of milking.

5.3. Verification of the 14 d involution model

By 14 d, tissue remodelling has been initiated, cell loss through apoptosis and a considerable influx of leukocytes has occurred within the bovine mammary gland (Piantoni *et al.*, 2010). To verify the involution model used in this study, alveolar tissue and milk collected from two randomly selected 14 d involution cows (cow #331 and cow #358) were compared to equivalent tissue, and milk samples collected from two randomly selected late-lactating cows (cow #390 and cow #1048).

H&E staining were performed on Formaldehyde-fixed, paraffin-embedded tissues to characterise the structural changes occurring between late-lactating and 14 d involuting gland tissues. The alveolar tissue from late lactating cows displayed typical histology of a lactating gland, where the alveoli are made up of monolayers of epithelial cells surrounding each enlarged lumen (Figure 5.1a). Whereas, the 14 d alveolar tissues contained structures indicative of involution (Figure 5.1a). These included enlarged stromal areas, diminished lumenal spaces, and increased numbers of amyloid bodies in the mammary epithelial cells (arrowed) (Holst *et al.*, 1987).

SDS-PAGE analysis of the 14 d involuted milk demonstrated that it had been subjected to mild proteolysis through increased fragmentation and a reduction in the abundance of major milk proteins (*data not shown*). Western blot analyses of two known markers of involution were used to probe milk samples from each quarter of the gland to confirm that changes in the mammary gland physiology had been initiated. Very little lactoferrin and no chitinase-3-like protein-1 (CG-39) protein were observed in the late-lactation milk (Figure 5.1b). In contrast, the concentrations of both proteins were substantially increased in 14 d involution milk where an increase in lactoferrin and CG-39 was observed in all milk samples taken and was significantly higher ($p < 0.001$) than in milk collected from the same cows at the beginning of the drying-off process. These results are consistent with previously published observations by our laboratory (Boggs *et al.*, 2015) and the histological and biochemical changes observed provided confirmation that mammary involution had occurred.

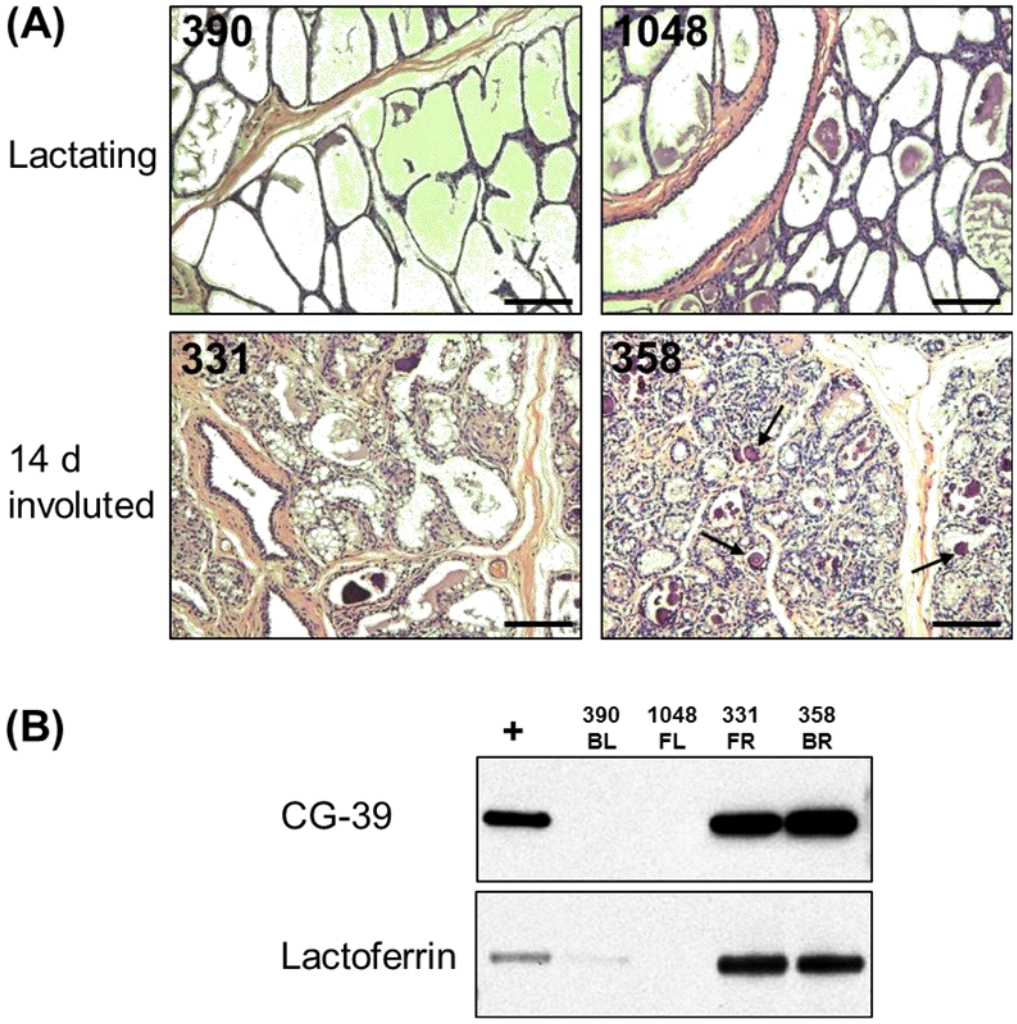

Figure 5.1: Verification of the involution model.
(A) Haematoxylin and eosin (H&E) staining of alveoli tissue sections from late lactation cows (#390 & #1048) and 14 d involution cows (#358 & #331). Representative micrographs of tissues from cows #390 & #1048 display the typical histology of a lactating gland, where the alveoli are made up of monolayers of epithelial cells surrounding each engorged lumen. Representative micrographs from 14 d involution cows #331 & #358 show collapsed alveoli with ruffled edges and cells within the lumen, consistent with involution. Almost all alveoli are showing signs of vesicle formation of coalescing milk fat and proteins, typical of a gland undergoing involution. Amyloid bodies, composed of dried out milk can be observed as dark purple spots within the lumens of some alveoli for cow #358 (arrowed). Section thickness 7 µm; Magnification 200 x; Scale bar = 100 µm. **(B)** Western blot analyses of 10 µg of late lactation and 14 d involution milks, probed with antibodies directed against bovine CG-39 and lactoferrin. Each involution milk sample was collected from a mammary gland quarter directly after teat removal. Lane 1 incorporates a 22 d involution positive (**+**) control sample. BL, left hindquarter; FL, left forequarter; FR, right forequarter; BR, right hindquarter.

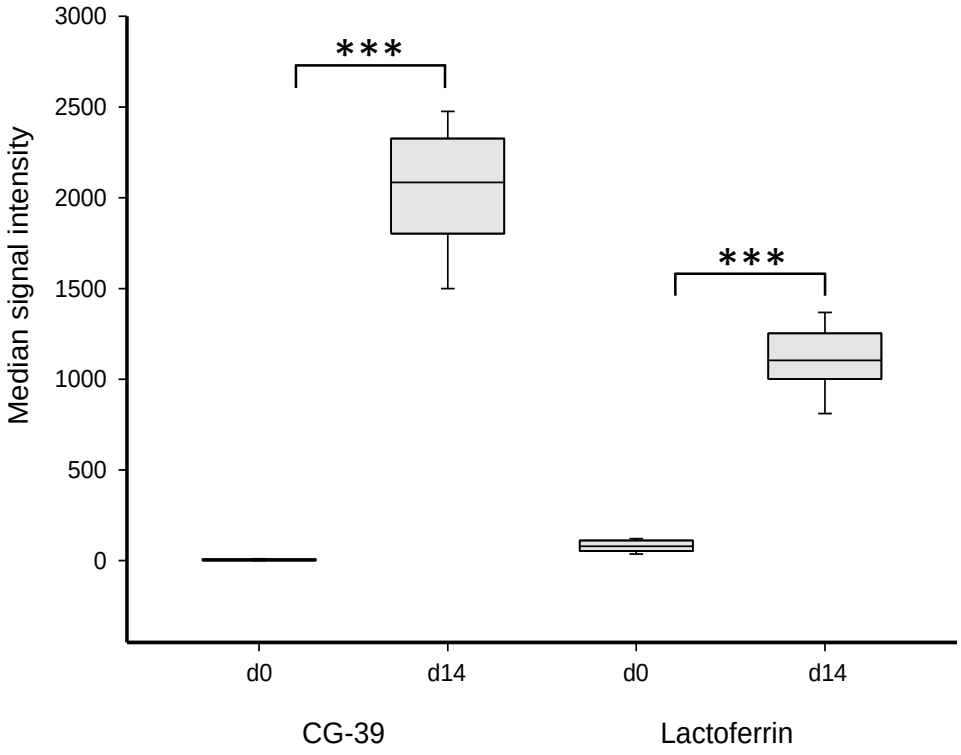

Figure 5.2: Increase in involution markers in milk 14 days after drying-off.
The presence of the involution markers CG-39 and lactoferrin were determined in 10 µg of milk protein by Western blot analyses. Milk from each quarter of the mammary gland from each of the seven cows was collected before (d0) and 14 days after drying-off (d14). The signal intensity values for the samples were normalised to a positive internal control. Horizontal lines within each box represent the median intensity value for each sample. The top and bottom of each box represent the 75th and 25th percentiles, respectively. Error bars above and below the boxes represent the 90th and 10th percentiles for the 28 samples. *** $p < 0.001$ as determined by two-tailed Students *t*-test.

5.4. Assessing the infection status of the teats after 14 d involution

For this study, the cows did not receive antibiotic dry cow therapy or internal teat sealing. Therefore, there was the possibility of intra-mammary infections occurring within the 14 d involution period. To test for signs of infection, milk samples were collected from each quarter immediately after the removal of the teats from the mammary glands, using sterile techniques. In addition, swabs of the teat sinus epithelial lining were performed to collect any bacteria that may have adhered to the epithelium. Additionally, a small aliquot of teat canal lining from each teat (n=28) was vortexed in 200 µL of sterile saline with 20 µL evenly spread out of a blood-agar plate. No obvious bacterial contamination was observed for all teat canal lining samples tested (*data not shown*).

For 18 of the 28 milk samples, no bacterial colonies were observed after 48 h incubation at 37 °C on blood agar plates and were classified as uninfected. Based on colony morphology, cleavage of esculin and haemolysis of the blood surrounding the colonies, one milk culture was positive for *Streptococcus uberis* (< 5 cfu), two milk cultures were positive for *Staphylococcus aureus*, and the remaining seven milk cultures were identified as being positive for *coagulase-negative Staphylococci* (CNS) (Table 5.2). To confirm that these *Staphylococcus* isolates were in fact *S. aureus* and CNS species, all isolates, along with five randomly selected isolates from the other two minor infections were subjected to a rabbit plasma coagulase test. All isolates from the colonies that had haemolytic activity on the blood agar plates produced solid coagulum after 48 h incubation. Based on these results and in addition to colony morphology, it is highly likely that the isolates are from a *S. aureus* infection. No visible coagulum mass was observed for the remaining picked isolates after 48 h incubation, suggesting that most of the minor bacterial infections in the milk were due to CNS.

Interestingly, all but one of the infected milk cultures contained *Staphylococcus* species. Bacteria, such as *S. uberis*, are known to adhere to and colonise mucosal surfaces (Almeida *et al.*, 1996), potentially limiting their appearance in milk. To investigate this possibility, samples were collected from the teat sinus epithelial

lining, using sterile cotton swabs. Only four of the 28 swabs had no colony growths after 48 h incubation on blood agar plates. The remaining 24 swabs all generated varying degrees of bacterial growth, with eleven teat sinus swabs consisting of mixed colonies of *Staphylococcus* and *Streptococcus* species and nine teat sinus swabs consisting of mixed colonies of *Staphylococcus* species. Three teat sinus swabs grew *Streptococcus* species only (presumably *S. uberis* due to the mucoid appearance of the colonies and cleavage of esculin) and one teat sinus swab cultivated a single colony of *Staphylococcus* (Table 5.2).

Representative examples of swabs are shown in Figure 5.3. A mixed population of bacteria was cultured from the left mammary hindquarter of cow #115, whereas samples from the right hindquarter of the same cow and the left hindquarter of cow #331 were devoid of any bacterial colonies. Samples from the right hindquarter of cow #331 and left hindquarter from cow #358 showed sparse growth of two types of *Staphylococcus* species. An example of a heavy bacterial load of *Staphylococcus* species is shown from the right hindquarter from cow #358. In this example, the predominant bacterial species appeared to be mixed *Staphylococcus* colonies with some minor coliform contamination. Of the 142 putative *Staphylococcus* colonies, 21 (15 %) showed haemolytic activity on the blood agar plates, typical of *S. aureus*. Coagulase testing was performed on 57 non-haemolytic, and two haemolytic *Staphylococcus* isolates from 19 different plates. Sampling ranged from two to five different isolates from each plate, depending on dissimilarities in morphology. A visible coagulum mass was only observed in the two isolates that showed haemolytic activity.

Just over a fifth (21.6 %) of the teat sinuses were clear of any signs of infection and the majority of bacteria present on the teat sinus epithelial lining were CNS species (68 %). Given that the milk from the teats was limited in growing bacterial colonies, the positive swabs of the epithelial lining probably represent microbial biofilms that have been kept in check by neighbouring host-defence mechanisms (Almeida & Oliver, 2001; Dego *et al.*, 2002; Melchior *et al.*, 2006). These findings are consistent with previously published research challenging mammary gland sterility of dairy cattle (Rainard, 2017).

Table 5.2: Cultures of *Streptococcus* and *Staphylococcus* strains isolated from quarter milk and epithelial lining of the teat sinus from 14 d involution cows.

Cow #	Quarter[a]	Milk Bacteriology[b]	Colony count[c]	Cotton swab Bacteriology[d]	Colony count
115	FL	*Staphylococcus sp.*	+	mixed Staph & Strep	++
	FR	NG		mixed Staph & Strep	+
	BL	NG		mixed Staph/Strep/coliforms	+
	BR	NG		NG	
160	FL	*S. uberis*	+	*S. uberis*	+
	FR	NG		mixed Staph & Strep	+
	BL	NG		mixed Staph & Strep	+
	BR	NG		mixed Staph & Strep	+
331	FL	*Staphylococcus sp.*	+	*Staphylococcus sp.*	+
	FR	NG		mixed Staph & Strep	+
	BL	NG		NG	
	BR	NG		Staph/coliforms	
358	FL	NG		mixed Staph & Strep	+
	FR	NG		NG	
	BL	NG		*Staphylococcus sp.*	+
	BR	NG		mixed Staph/coliforms	++
499	FL	*Staphylococcus sp.*	+	*Staphylococcus sp.*	+
	FR	*Staphylococcus sp.*	+	*Staphylococcus sp.*	+
	BL	*Staphylococcus sp.*	+	*Staphylococcus sp.*	+
	BR	NG		NG	
837	FL	NG		*S. uberis*	++
	FR	NG		*S. uberis*	++
	BL	NG		mixed Staph & Strep	+
	BR	NG		mixed Staph & Strep	+
911	FL	*Staphylococcus sp.*	++	*Staphylococcus sp.*	++
	FR	*S. aureus*	++	*Staphylococcus sp.*	++
	BL	*Staphylococcus sp.*	+	mixed Staph & Strep	++
	BR	*S. aureus*	+	*Staphylococcus sp.*	+

a) FL, left forequarter; FR, right forequarter, BL, left hindquarter; BR, right hindquarter.
b) NG, no growth; *Staphylococcus sp.*, mixed colonies of *Staphylococcus* species.
c) +, 1 – 10 colonies; ++, 10 – 50 colonies; +++, > 50 colonies.
d) mixed Staph & Strep, mixed colonies of *Staphylococcus* species and *Streptococcus* species.

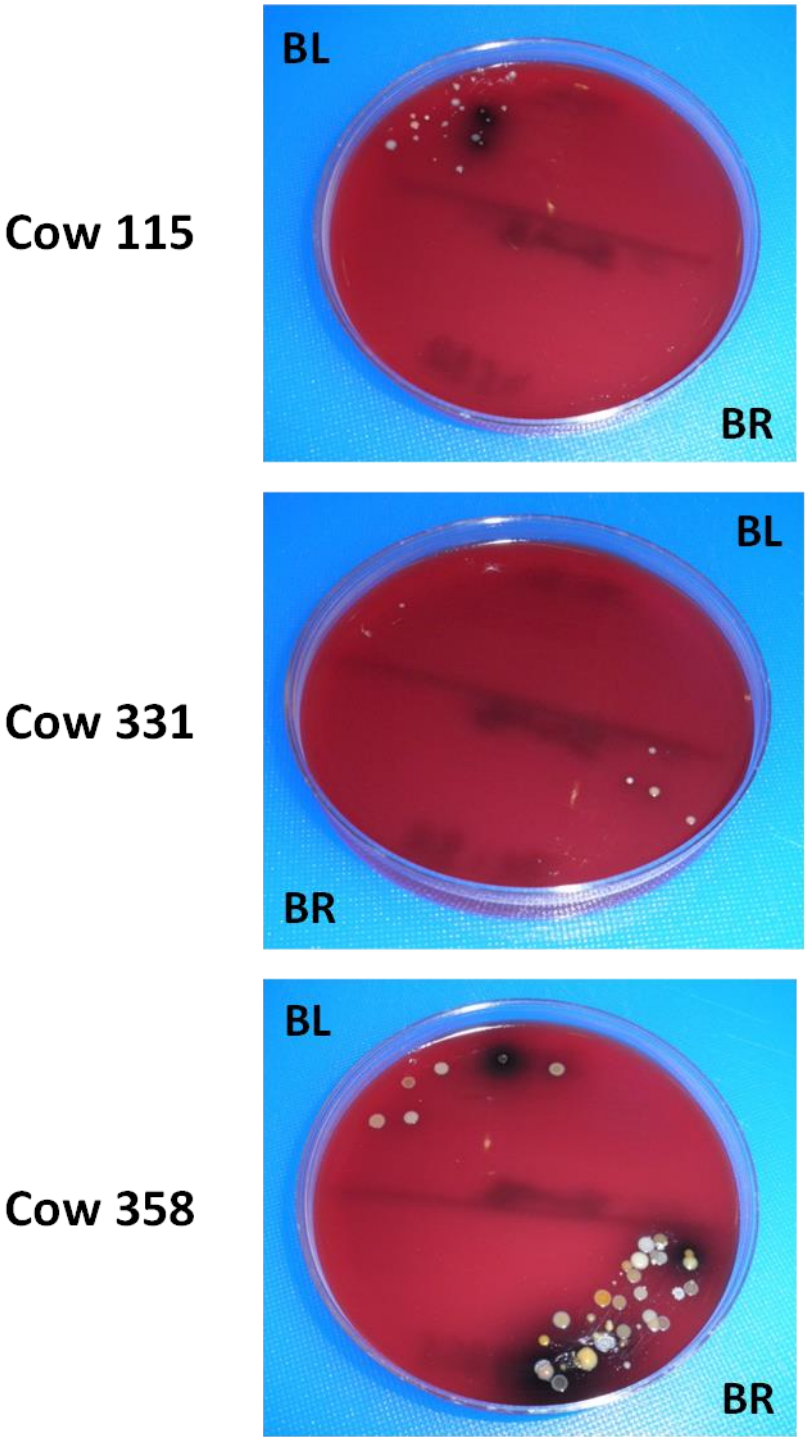

Figure 5.3: Cultures of bacteria isolated from cotton swabs of the teat sinus epithelial lining from 14 d involution cows.
Twenty microliters of sterile 0.85 % saline solution were added to one-half of a blood agar plate, and a swab was then rolled into the saline to transfer bacteria from the swab to the plate. This was repeated with another sample on the other half of the plate. The bacteria were then streaked across one-half of a blood agar plate using a sterile inoculation loop, and the plates were incubated at 37 °C for 24–48 h. The bacterial colonies were manually counted and visually assessed.

5.5. Comparative proteomic analyses of teat canal lining proteins after 14 days of involution

5.5.1. Comparative 2-DE analyses

Teat canal lining from seven adjacent pairs of forequarter and hindquarter teats were collected from seven cows 14 d after drying-off. Teat canal lining proteins were extracted using the 2D lysis buffer, using methods previously described (See Section 2.2.2). The total yield of teat canal lining (wet-weight) collected from each teat along with the total protein extracted out of each teat canal lining sample is summarised in Table 5.3. The average amount of extracted proteins per sample was 17.2 ± 2.5 mg which equated to approximately 14.6 % of the wet weight. This percentage of extractable protein was similar to that obtained from the late-lactating teat canal lining (See Table 3.2).

Approximately 2.1 mg of teat canal lining protein, evenly apportioned from four forequarter and three hindquarter teats, were mixed to create a pooled sample of 14 d involution teat canal lining proteins from the seven cows. Triplicate 2-DE gels of the pooled 14 d teat canal lining (350 µg total protein per gel) were generated (Figure 5.4), and the pattern of spots was compared with that of the pooled late-lactating teat canal lining proteome (See Section 3.3.2). PDQuest software was used to generate a late-lactating replicate gel-set (n = 3) and a 14 d involution replicate gel-set (n = 3) for protein spot quantification and statistical validation.

The number of resolved and matched spots was 429 for the late-lactating gel-set and 426 for the 14 d involution gel-set. Between the two gel-sets, 420 spots were matched between all six gels giving a matching rate of 98 %. A total of 16 protein spots, with an intensity value of ≥30, were shown to be altered by greater than two-fold between the two gel-sets (See Supplementary data, Figure C1). These 16 spots were excised and processed for protein identification by mass spectrometry. Confirmed amino acid sequence identity was obtained for all 16 spots (Table 5.4 & Figure 5.5).

Nine protein spots were found to be higher in abundance in the 14 d teat involution gel-set. Five of the nine protein spots were identified as type II keratin proteins (K3, K4, and K5) and a further two spots were identified as the type I keratin protein K14. The remaining two protein spots were identified as S100A7L. Both S100A7L protein spots were located in a more cationic position on the 2-DE gel compared with the equivalent protein spots in the late-lactating gel-set, suggesting that they may have been the target of further post-translational modifications. Additionally, seven protein spots were found to be less abundant in the 14 d involution gel-set than the late-lactating gel-set. These protein spots corresponded to the following proteins; type II keratin proteins K1 and K6A, S100A12, galactin-7 and the adipocyte-type fatty acid-binding protein (FABP4).

Table 5.3: Amount of solubilised protein obtained from teat canal lining 14 days after drying-off.

Cow#/Quarter[a]	SCC[b] (x10^3 cells/mL)	TCL[c] (mg wet weight)	Total yield of protein (mg)	% mg/wet weight
115/FL	20	14.7	2.085	14.2
115/BL	8	13.6	1.590	11.7
160/FL	145	16.4	2.660	16.2
160/BL	181	13.3	2.025	15.2
331/FL	70	16.3	2.445	15.0
331/BL	123	18.1	2.616	14.5
358/FL	125	18.3	2.556	14.0
358/BL	39	17.7	2.778	15.7
449/FL	87	16.1	2.545	15.8
449/BL	154	15.2	1.945	12.8
837/FL	10	20.8	3.216	15.5
837/BL	14	19.4	2.736	14.1
911/FL	165	19.1	2.712	14.2
911/BL	114	21.1	3.342	15.8
Average ± SD	*89 ± 62*	*17.2 ± 2.5*	*2.5 ± 0.5*	*14.6 ± 1.3*

a) FL, left forequarter; BL, left hindquarter.
b) SCC, milk somatic cell count immediately before drying-off.
c) TCL, teat canal lining

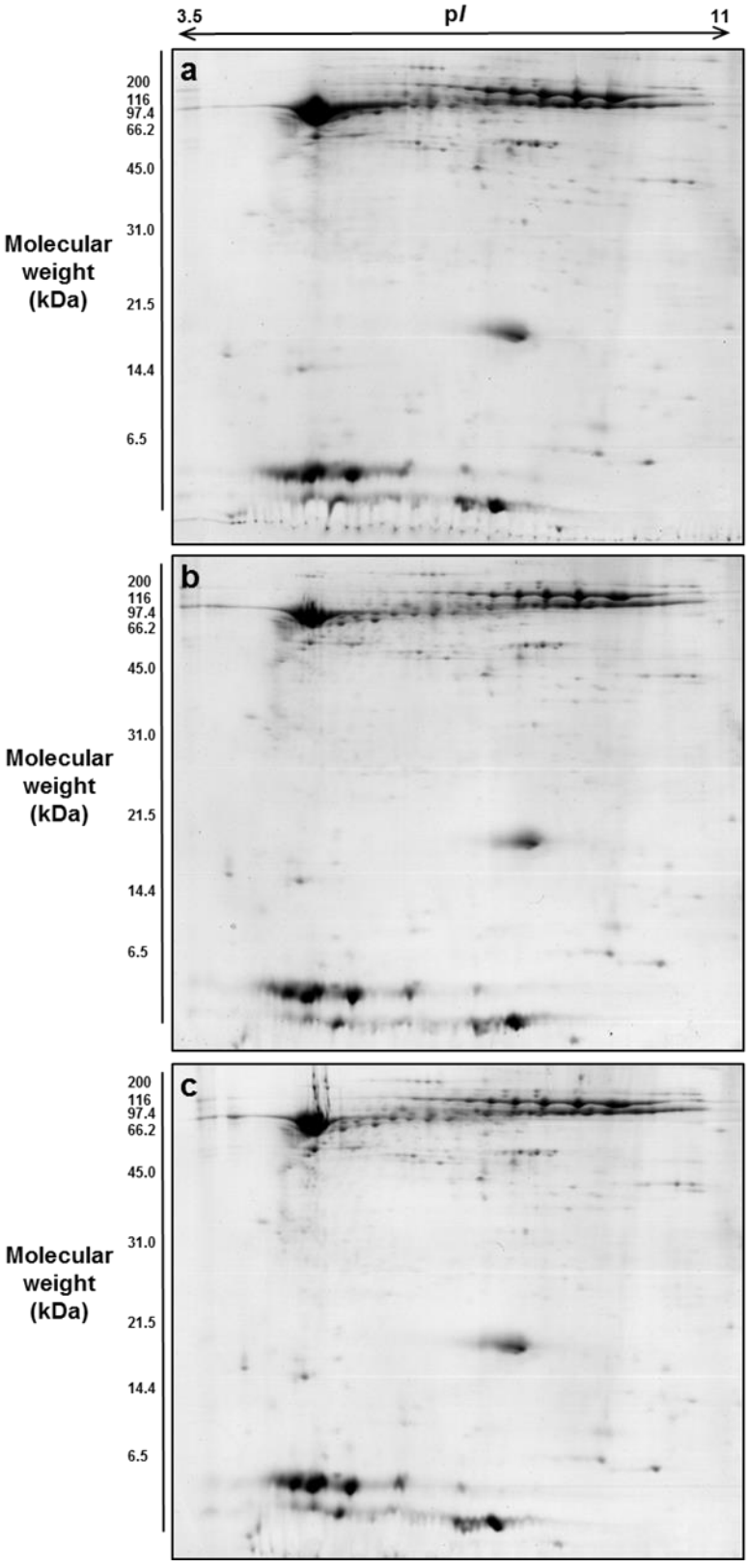

Figure 5.4: Colloidal Coomassie blue stained triplicate 2-DE gels of pooled 14 d teat canal lining proteins (350 µg total protein per gel).
Proteins were separated by IEF (pH 3-11) in the first dimension and by electrophoresis using 14 % SDS-PAGE in the second dimension (a-c).

Table 5.4: Identified protein spots with a ≥ 2-fold change in abundance ($p < 0.05$) between the late-lactating and 14 d involution gel-sets.

SSP[a]	Identified protein	Ave. LL TCL[b] spot intensity	Ave. 14 d TCL[c] spot intensity	Fold change[d]	*p*-value[e]
1006	fatty acid-binding protein, adipocyte	49.5	5.3	0.11	0.049
1304	keratin, type II cytoskeletal 4	35.4	75.6	2.13	0.048
2401	keratin, type I cytoskeletal 14	9.9	30.1	3.04	0.031
2406	keratin, type I cytoskeletal 14	13.4	41.6	3.10	0.047
3005	predicted S100A7-like	0.13	43.7	328	0.044
3603	keratin, type II cytoskeletal 5	19.3	45.4	2.35	0.031
4001	S100A12	289.4	132.4	0.46	0.003
4007	predicted S100A7-like	0.13	88.9	667.0	0.049
4103	galectin-7	30.9	4.0	0.13	0.049
4703	keratin, type II cytoskeletal 3	40.5	101.9	2.52	0.044
5505	keratin, type II cytoskeletal 5	39.2	109.6	2.80	0.011
5604	keratin, type II cytoskeletal 1	31.2	4.7	0.15	0.030
6501	keratin, type II cytoskeletal 4	9.0	38.8	4.32	0.027
8505	keratin, type II cytoskeletal 6A	80.4	24.9	0.31	0.044
8703	keratin, type II cytoskeletal 1	98.4	11.8	0.12	0.022
9701	keratin, type II cytoskeletal 1	105.9	11.0	0.10	0.006

a) SSP, Standard spot numbers assigned to each spot in PDQuest.
b) LL TCL, late-lactating teat canal lining.
c) 14 d TCL, 14 d involution teat canal lining.
d) Average spot intensity values from late-lactating teat canal lining gel-set were used as the denominator.
e) *p*-value determined using paired two-tailed Students *t*-test.

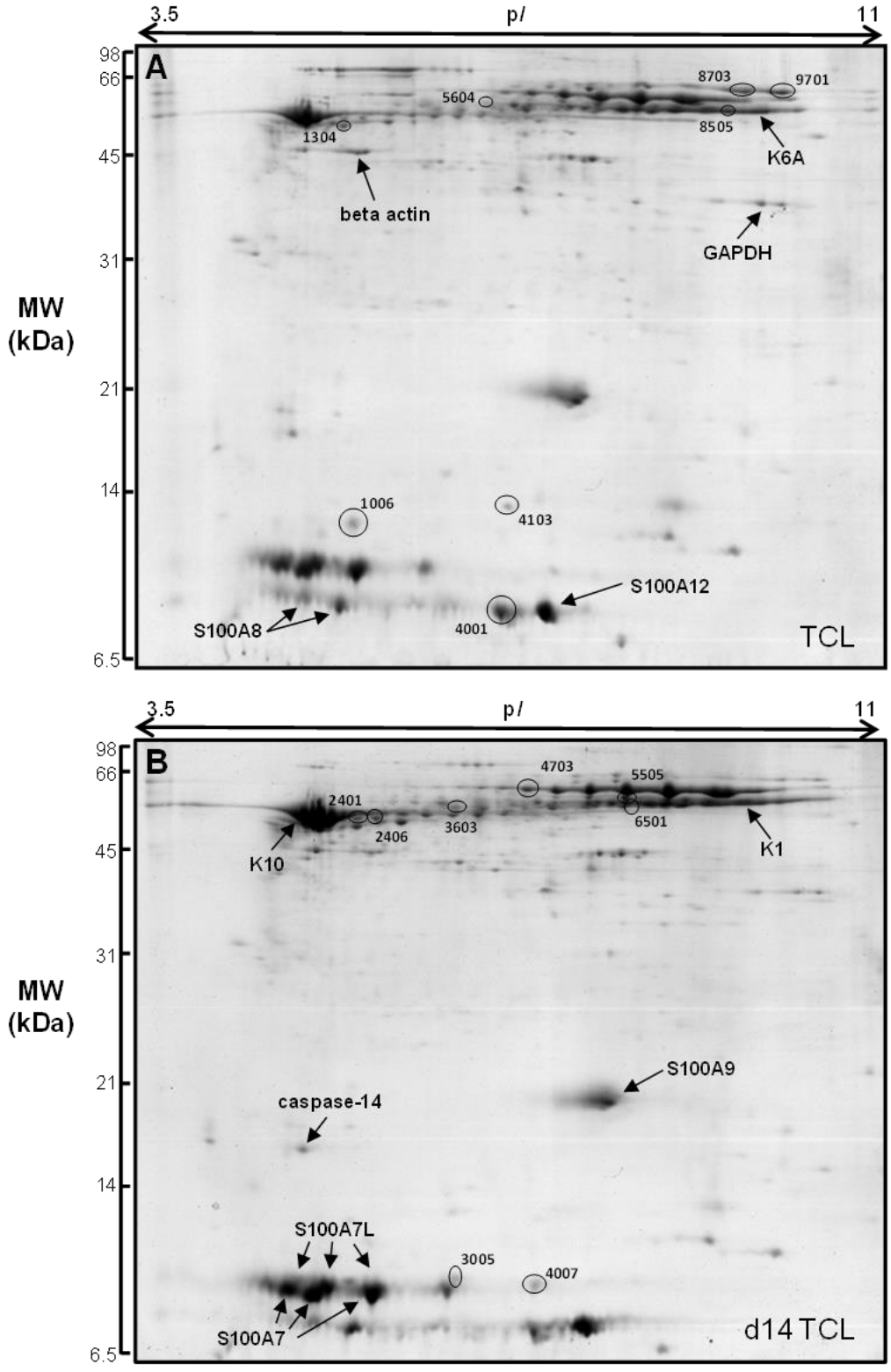

Figure 5.5: Representative 2-DE reference maps of pooled late-lactating teat canal lining (A) and pooled 14 d involution teat canal lining proteins (B).
Protein spots identified by circles were significantly changed in abundance ($p < 0.05$) between the two gel-sets. Each protein is annotated with its SSP number as specified by PDQuest. These spots are listed in Table 5.4. Several abundant proteins that were not altered between the two gel-sets are also labelled. K, keratin; TCL, teat canal lining.

5.5.2. Label-free quantification using GeLC-MS/MS and SpC

Previously, a qualitative "bottom-up" proteomic analyses of the teat canal lining was performed (See Chapter 3). This analysis provides an indirect measurement and characterisation of proteins through peptides derived from the proteolytic digestion of intact proteins (Zhang *et al.*, 2013). While this type of analyses is useful for identifying what proteins are present in the teat canal lining samples, it is non-quantitative for providing information on the relative abundance of proteins from cells or tissues undergoing biological change. Modern software and mass spectrometers can now be used to perform quantitative comparative proteomic analyses, using either stable isotope labelling or label-free quantification.

A label-free approach, called 'spectral counting' (SpC), was used to assess and compare the proteomes of late-lactating and 14 d involution teat canal lining. SpC is a semi-quantitative method for evaluating the relative abundance of proteins in a complex mixture (Schulze & Usadel, 2010). It is based on the observation that the more a given protein is present in a sample, the greater the number of precursor peptide ions detected. The sum of each precursor peptide fragment is calculated from the continuous analyses that occur during the liquid chromatography elution, allowing for different charge states of the same peptide. However, results should be viewed in context with the following sources of error: i) a protein with zero counts could still be present in the sample but at a low abundance; ii) larger proteins will generate more peptide fragments making it difficult to compare the absolute quantity of two different proteins; iii) the intensity of the MS signal is determined by numerous factors, such as fragmentation efficiency and its ability to ionise in electrospray, that will affect the number of matched spectra. To overcome some of this issues, researchers have developed methods using normalised spectra count that take into account the length of the protein (Florens *et al.*, 2006).

SpC has been shown to offer a wide dynamic range of quantification and is reasonably reproducible (Washburn *et al.*, 2001; Liu *et al.*, 2004; Old *et al.*, 2005; Usaite *et al.*, 2008). A number of strategies and statistical tools for analysing SpC data have been developed in recent years (Lundgren *et al.*, 2010) and are employed

in software searching algorithms such as Scaffold (Proteome Software, Inc), PEAKS (Bioinformatics Solutions, Inc), and Mascot (Matrix Science, Ltd).

5.5.2.1. SpC validation experiment

To verify that the GeLC methodology coupled with the maXis Impact Q/TOF would provide a reliable relative measurement of protein abundance from a complex protein mixture, a preliminary 'spiking experiment' was designed to validate the procedure. In GeLC-MS/MS, the protein sample is separated by SDS-PAGE, and each gel lane is cut into gel slices which, after in-gel tryptic digestion, are analysed by tandem mass spectrometry. For global analyses, the gel slices can be even or unequal in size depending on the sample being analysed. However, it is important that the whole lane is removed and processed.

In this experiment, an *E. coli* lysate solution was supplemented with specific quantities of four different mammalian proteins from chicken and cow (Figure 5.6). These proteins included conalbumin (75.7 kDa), ovalbumin (42.9 kDa), carbonic anhydrase (28.8 kDa) and lysozyme (14.4 kDa). Five different mixtures were created by two-fold serial dilution of the spiked lysate mixture with the original unadulterated *E. coli* lysate. In this manner, the same quantity of total protein (20 µg) was preserved. Each protein mixture was separated by SDS-PAGE, and four equal gel slices, encompassing the protein bands of each spiked protein, were independently digested using trypsin and then analysed in quadruplicate using LC-MS/MS (See Supplementary data Table C1). A 16-fold dynamic range between 12.5 and 200 fmol was chosen to define the lower limit of detection for this method.

All four proteins showed a linear correlation between SpC and their abundance, ranging from 200 fmol to 12.5 fmol, with regression coefficients ranging from 0.9895 to 0.9422 (See Supplementary data Figure C2). Below 12.5 fmol, the linear correlation was not maintained, and the average SpC values appeared to drop-off rapidly. At this concentration, an average of five spectral ions were detected for the four added mammalian proteins. This value is likely to represent the limit of detection using the current GeLC methodology and MS configuration and will, therefore, be used as the minimum cut-off value for analyses of the teat canal lining.

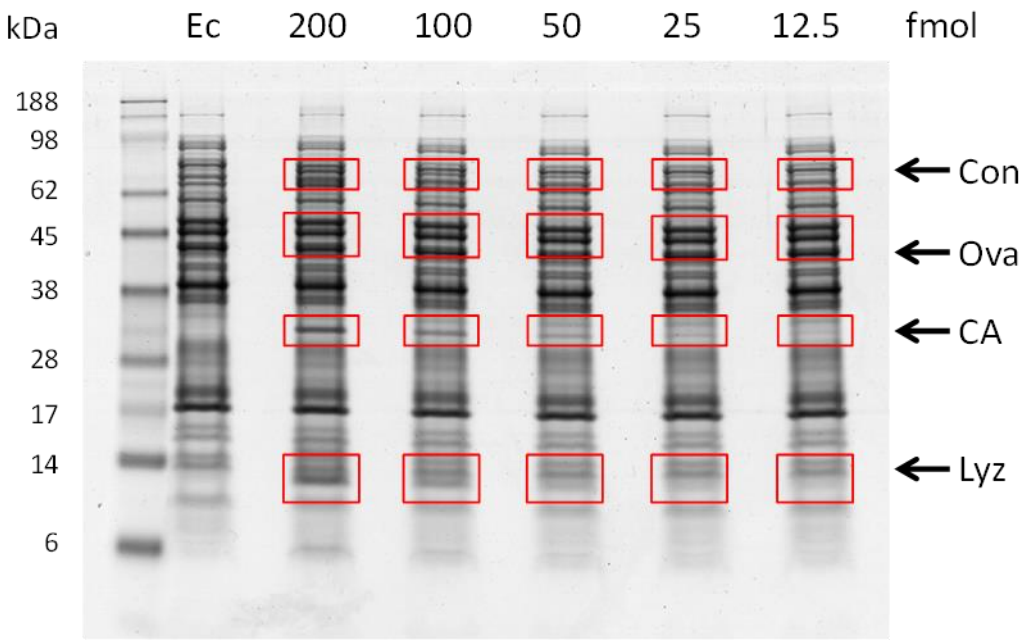

Figure 5.6: SDS-PAGE showing the separation of spiked *E. coli* lysates for SpC validation study.
Twenty micrograms of *E. coli* lysate (Ec) was spiked with 200 fmol of conalbumin (Con), ovalbumin (Ova), carbonic anhydrase (CA), and lysozyme (Lyz). Serial two-fold dilutions with *E. coli* lysate was performed down to 12.5 fmol. Red boxes show the area of the gel cut out for GeLC analyses and spiked proteins in each box are indicated on the right-hand side. The molecular sizes of the marker proteins are indicated on the left-hand side.

Table 5.5: Identified *E. coli* proteins used to validate the SpC model.

Gel Slice	Mammalian protein	Molecular mass (kDa)	*E. coli* protein	Molecular mass (kDa)
1	Conalbumin	75.7	pyruvate formate-lyase	85.2
			chaperone protein DnaK	69.1
2	Ovalbumin	42.9	phosphopyruvate hydratase	45.4
			translation elongation factor Tu	43.0
3	Carbonic anhydrase	28.8	outer membrane protein A	28.7
			oxidoreductase	26.5
4	Lysozyme	14.4	universal stress protein F	15.9
			global DNA-binding transcriptional dual regulator H-NS	15.5

Assuming that the total protein concentration of the lysate is the same for each protein mixture, it would be expected that the SpC and peptide count of *E. coli* proteins of similar molecular mass to the spiked mammalian proteins would be the same across each analogous gel slice. To test this assumption, *E. coli* proteins were identified in each of the gel slices for each of the different spiked protein concentrations. In each gel slice, the two most abundant *E. coli* proteins were examined (Table 5.5).

The data from this analysis (See Supplementary data Table C2) and SpC correlation coefficients (See Supplementary data Figure C3) showed no differences in peptide count or SpC over the dilution range of spiked proteins. This confirms that; i) there was no significant difference in the protein concentration of *E. coli* lysate in all the sample mixtures, and ii) the digestion and extraction methodology of the protocol was consistent and reproducible.

To test the technical reproducibility of the protocol, successive analyses of the four different protein slices were performed for each of the five different spiked protein concentrations. Each analysis set (n = 20) was repeated four times over four successive days. Very good reproducibility between samples was obtained with an average coefficient of variation (CV) of less than 15 % for all the proteins at all dilution ranges (See Supplementary data Table C2). This level of CV variation compares well with other gel-based quantitative assays, such as 1D and 2-DE gels, where technical variation can lead to CV ranges of 20-35 % (Molloy *et al.*, 2003). In comparison, ELISA assays and colorimetric assays generally have CVs below 10 % (Okutucu *et al.*, 2007; Selman *et al.*, 2012).

In summary, this validation study showed that the lower limit of detection for reliable quantitative data was approximately five spectral ions. Detection below this lower limit was achievable, but reliable relative quantitation would not always be attainable. These results suggest that this procedure could be applied with reasonable confidence to the relative quantitation of proteins in the teat canal lining samples if the SpC is five or greater.

5.5.2.2. SpC assessment of proteins in late-lactation versus 14 d involution teat canal lining

Changes in the abundance of teat canal lining proteins because of involution and the biological variability between individual cows were assessed. In this section of work, the six late-lactating teat canal lining samples (See Section 3.7), were compared with the seven individual 14 d involution teat canal lining samples (Figure 5.7).

For GeLC-MS/MS analyses, a preparative SDS-PAGE gel resolving 25 µg total protein/lane of 14 d involution teat canal lining proteins (n = 7) was run. A total of 70 fractions were processed by tryptic digestion and subjected to MS/MS analyses resulting in the generation of 63,660 fragment spectra (See Supplementary data Table C3). These spectra were submitted to analysis by Mascot, resulting in 3560 peptide assignments (5.6 %) from the bovine non-redundant database. A total of 86 distinct proteins with two or more unique peptides were identified in at least one of the seven 14 d involution biological replicates (See Supplementary data Table C4).

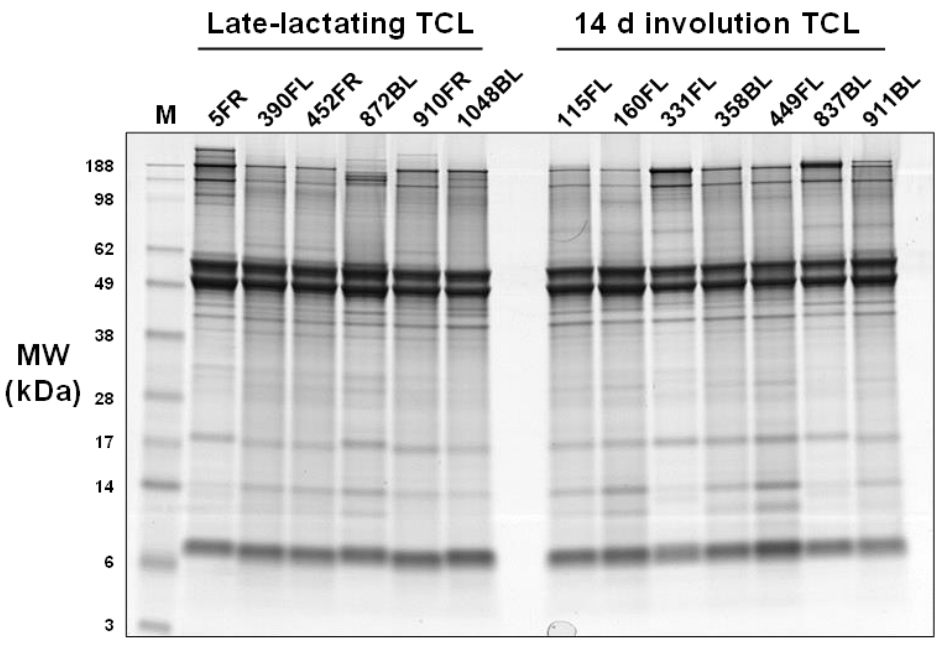

Figure 5.7: SDS-PAGE showing the separation of 10 µg of individual teat canal lining proteins from late-lactating cows and cows after 14 d involution.
The molecular weight sizes of the marker proteins are indicated on the left-hand side of the image and the cow number/quarter listed at the top of the image.

Both the late-lactating and 14 d involution teat canal lining datasets were subjected to a more stringent database search as part of the Scaffold software platform (See Section 2.2.14). In this analyses, the Mascot DAT result files were imported into Scaffold Q+ where another round of tandem MS searching was performed using the X!Tandem search algorithm (Craig & Beavis, 2004). The results from both search engines were combined resulting in a total of 96 proteins with two or more unique peptides identified across the two datasets of six (late-lactating) and seven (14 d involution) biological replicates. The peptide false discovery rate (FDR) at this level of stringency was calculated, by the Scaffold software, to be 0.2 %.

Label-free quantification by SpC was performed by Scaffold Q+, and the data were normalised for total SpC across each set of samples. Arbitrary fold change cut-offs of >2 and significance *p*-values of < 0.05 were chosen to determine up- and down-regulated proteins. This was due to the small number of biological replicates in each sample group.

Twenty-five proteins with differential abundance, supported by significance *p*-values of < 0.05 (See Supplementary data Table C5) were determined from the ratio of late-lactating and 14 d involution spectral ion counts. Of these 25 proteins, only 13 proteins had average SpC above the five-ion threshold (See Section 5.5.2.1) from all biological replicates (Table 5.6).

Besides normalised total SpC, Scaffold Q+ also provides another algorithm to identify proteins with differing abundances, called normalised spectral abundance factor (NSAF). Likewise, the Mascot search engine also provides an automated label-free quantitation algorithm known as the empirical protein abundance index (emPAI). For each of these approaches, relative quantitation, fold change comparison, and statistical significance (*p*-value) can be calculated. To evaluate if there is any search engine-induced bias due to the small number of biological replicates, it was preferable to perform the analyses with multiple algorithms and trust the results of only those identified using all approaches.

Table 5.6: S**ignificantly changed protein abundance by normalised SpC and statistical analyses between late-lactating and 14 d involution teat canal lining.**

			Total spectral count				EmPAI[a]				NSAF[b]			
Identified proteins	**Accession Number**	**Molecular Weight**	**LL[c] Ave**	**d14[d] Ave**	**Fc[e]**	***p*-value[f]**	**LL Ave**	**d14 Ave**	**Fc**	***p*-value**	**LL Ave**	**d14 Ave**	**Fc**	***p*-value**
14-3-3 protein zeta	gi|296475944	28 kDa	5.0	0.0	∞	0.0451	0.495	0.000	∞	0.0429	0.008	∞	0.00	0.0748
fatty acid-binding protein, adipocyte	gi|296480594	15 kDa	7.2	0.1	0.02	0.0452	0.809	0.029	0.04	0.0312	0.026	0.001	0.03	0.0194
beta-actin	gi|313507212	42 kDa	7.2	0.3	0.04	0.0009	0.320	0.015	0.05	0.0023	0.014	0.001	0.05	0.0035
heat shock protein beta-1	gi|529007450	22 kDa	6.0	0.3	0.05	0.0005	0.621	0.033	0.05	0.0032	0.025	0.002	0.08	0.0035
galectin-7-like	gi|296477713	15 kDa	5.7	0.3	0.05	0.0076	1.040	0.085	0.08	0.0069	0.030	0.002	0.07	0.0053
junction plakoglobin	gi|109658166	82 kDa	12.2	1.3	0.11	0.0008	0.560	0.081	0.15	0.0013	0.022	0.002	0.11	0.0007
14-3-3 protein sigma	gi|57163961	28 kDa	13.8	1.4	0.10	0.0130	1.290	0.173	0.13	0.0373	0.041	0.008	0.19	0.0290
nucleoside diphosphate kinase B	gi|115496892	17 kDa	7.3	1.1	0.16	0.0000	1.418	0.308	0.22	0.0005	0.041	0.010	0.24	0.0007
alpha-S2-casein precursor	gi|27806963	26 kDa	7.2	1.9	0.26	0.0467	0.839	0.238	0.28	0.0486	0.026	0.009	0.32	0.0585
desmoplakin	gi|300797856	332 kDa	7.0	2.3	0.33	0.0410	0.055	0.025	0.47	0.0823	0.002	0.001	0.45	0.0798
fatty acid-binding protein, epidermal	gi|1293786	15 kDa	10.7	3.7	0.35	0.0001	1.717	1.189	0.69	0.1840	0.065	0.038	0.59	0.0256
glyceraldehyde-3-phosphate dehydrogenase	gi|77404273	36 kDa	8.5	3.1	0.37	0.0136	0.447	0.278	0.62	0.2964	0.021	0.009	0.46	0.0622
lactoferrin	gi|163285	78 kDa	0.5	24.9	49.7	0.0006	0.039	1.255	32.5	0.0011	0.001	0.051	44.4	0.0002

a) EmPAI, empirical protein abundance index; b) NSAF, normalised spectral abundance factor; c) LL Ave, average late-lactating values; d) d14 Ave, average 14 d involution values; e) Fc, fold change, f) *p*-value determined using Students two-tailed *t*-test. Cells highlighted in grey have a *p*-value between 0.05 and 0.1 or were less than two-fold changed, according to the EmPAI and NSAF algorithms.

The three different label-free algorithms gave comparable results when comparing the proteins from late-lactating teat canal lining with 14 d involution teat canal lining. However, five of the 13 proteins identified by total normalised SpC failed the test for significance in either the EmPAI or NSAF calculations (highlighted grey cells in Table 5.6) at the set threshold values of $p < 0.05$ and two-fold change.

Lactoferrin was the only teat canal lining protein that was significantly increased in relative abundance (32- to 50-fold; $p < 0.001$) in all seven 14 d involution samples. This result is interesting in that an increase in lactoferrin was not observed in the 2-DE gel analyses of the teat canal lining. Also of note is that CG-39 and most of the major milk proteins were not detected by the GeLC analyses. Taken together, these results suggest that lactoferrin in the teat canal lining could be locally expressed by the teat canal keratinocytes and are not a contaminant from the involution milk.

Twelve proteins demonstrated reduced abundance in the 14 d involution teat canal lining samples compared to the late-lactating samples. These include six structural proteins associated with the plasma membrane (beta-actin, desmoplakin, junction plakoglobin, FABP4, FABP5), four cell signalling proteins involved in the transfer of phosphate groups to/from target proteins or in apoptosis (galactin-7, nucleoside diphosphate kinase B, 14-3-3-σ, 14-3-3-η), the metabolic enzyme GAPDH, and the major milk protein alpha-S2-casein. Remarkably, alpha-S2-casein was the only major milk protein to be detected in the 14 d involution teat canal lining. Based on the normalised SpC, alpha-S2-casein was 12-fold less abundant than lactoferrin in the same sample.

Furthermore, only two of the 13 proteins identified by GeLC-MS/MS were previously identified by 2-DE analyses. These were galectin-7 and fatty acid-binding protein, adipocyte (FABP4). The relative abundance of galectin-7 and FABP4 protein spots in the 14 d involution teat canal lining 2-DE gel-sets were found to be decreased 7.7-fold and 9-fold, respectively (Table 5.4). In comparison, the average fold-change, from all three label-free methods, estimated galectin-7 and FABP4 to be decreased approximately 15-fold and 33-fold, respectively. The fold-change estimates from the GeLC analysis and SpC were similar to the 2-DE PDQuest analysis.

5.5.3. Validation of proteomic results by Western blot analyses

To corroborate the previous MS identifications and to verify the quantitative differences observed by SpC, several proteins of interest were analysed, using Western blot analyses. These proteins of interest comprised the involution marker proteins lactoferrin, CG-39, and cathelicidin (Figure 5.8a), as well as the S100 proteins S100A7, S100A8, S100A9 and S100A12 (Figure 5.9a).

Lactoferrin was chosen as this was the most highly upregulated protein. Both CG-39 and cathelicidin were not detected by the GeLC analysis but were selected to provide additional evidence that there was no contamination of the teat canal lining proteins by the involuted milk. The label-free quantitation method showed no difference in the relative abundance of the four S100 proteins between late-lactating and 14 d involution teat canal lining. Although the four S100 proteins are abundant in the teat canal lining, they are small in mass, ranging from 11.5 kDa to 16.4 kDa. This could limit the number of SpC produced by these proteins relative to much larger proteins, biasing the final calculations.

To determine if the involution marker proteins were present in the 14 d involution teat canal lining samples, 10 µg of total protein in each lane were separated by SDS-PAGE, transferred to nitrocellulose membrane and probed for lactoferrin, CG-39, and cathelicidin. Strong signals were observed in all seven 14 d involution samples for lactoferrin, while very little, if any signal, was found in the six late-lactating samples (Figure 5.8a). Quantitation of the chemiluminescent signal by densitometric analysis ascertained that lactoferrin was, on average, 18-fold more abundant (Students t-test, $p < 0.001$) in the 14 d involution samples. In contrast, no signal for CG-39 was detected, and only the left hindquarter teat of cow# 911 gave a weak signal for cathelicidin. Although the size of this signal did not appear to match the positive control, this was an artefact due to the edge effect on the SDS-PAGE.

These observations support the GeLC-MS/MS and the SpC findings and provide additional confirmation that no involution milk has contaminated the 14 d involution teat canal lining.

To establish whether the lactoferrin found in the 14 d teat canal lining is expressed directly in the stratified epithelium of the teat canal or whether it is absorbed indirectly from the milk, IHC using a lactoferrin polyclonal antibody was performed on a series of late-lactation and 14 d involution teat canal cryosections. Representative micrographs show the lactoferrin signal was absent from the epithelium of the late-lactation cryosections whereas, in all fourteen 14 d involution cryosections, the lactoferrin signal was observed around nuclei located in the spinous and granular layers of the stratified epithelium (Figure 5.8b). As a result of the high level of background signal, observed in the 14 d involution Western blot, the IHC lactoferrin signal should be viewed with caution. However, the difference in signal seen between the two tissue groups is likely to be valid.

This observation, along with the absence of detectable CG-39 and cathelicidin, would imply that the source of the lactoferrin in the 14 d involution teat canal lining is from cells located within the stratified epithelium of the teat canal.

SpC demonstrated no significant difference in the relative abundance of S100A7, S100A8, S100A9 and S100A12 between the late-lactating and 14 d involution teat canal lining samples. To verify these observations, Western blots containing equal loadings of late-lactating and 14 d involution teat canal lining samples were probed in triplicate for S100A7/A7L, S100A8, S100A9 and S100A12. For each anti-S100 antibody, the amount of late-lactating and 14 d involution teat canal lining proteins loaded per lane for S100A7/A7L, S100A8, S100A9 and S100A12 was 0.8 µg, 10 µg, 10 µg and 4 µg, respectively. A representative Western blot for each S100 antibody shows no significant difference in the relative abundance of the S100 proteins between the two physiological states, consistent with results obtained from SpC analysis (Figure 5.9a). This is supported by the summary of the normalised triplicate analyses when shown as a box-plot (Figure 5.9b).

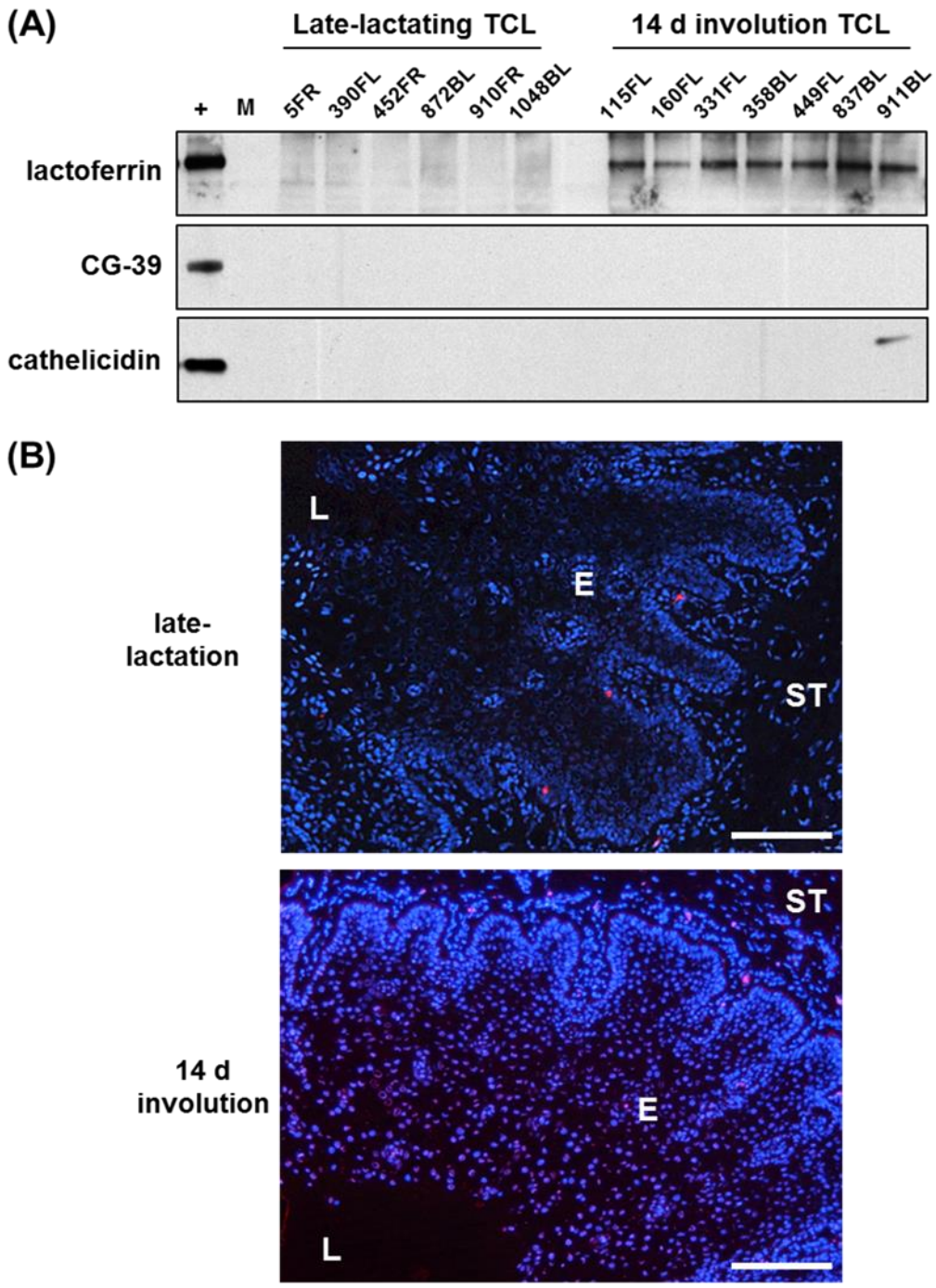

Figure 5.8: Relative abundance of involution markers in teat canal lining samples from late-lactating and 14 d involution cows.
(A) Western blot analyses of late-lactation and 14 d involution teat canal lining proteins from individual cows, probed with antibodies directed against lactoferrin, CG-39 and cathelicidin. **+,** positive control; M, molecular weight marker, TCL, teat canal lining. **(B)** Representative micrographs from cow #1048 (late-lactation) and cow #911 (14 d involution) of transverse cryosections probed with lactoferrin polyclonal antibody (Alexa Fluor-594 IgG; red signal). In the 14 d cryosections, lactoferrin appeared to be localised around nuclei in the upper spinous and granular layers. Each section was counterstained with DAPI (blue signal). E, epidermis; ST, stromal tissue; L, lumen. Sections thickness: 5 µm. Scale bar = 100 µm.

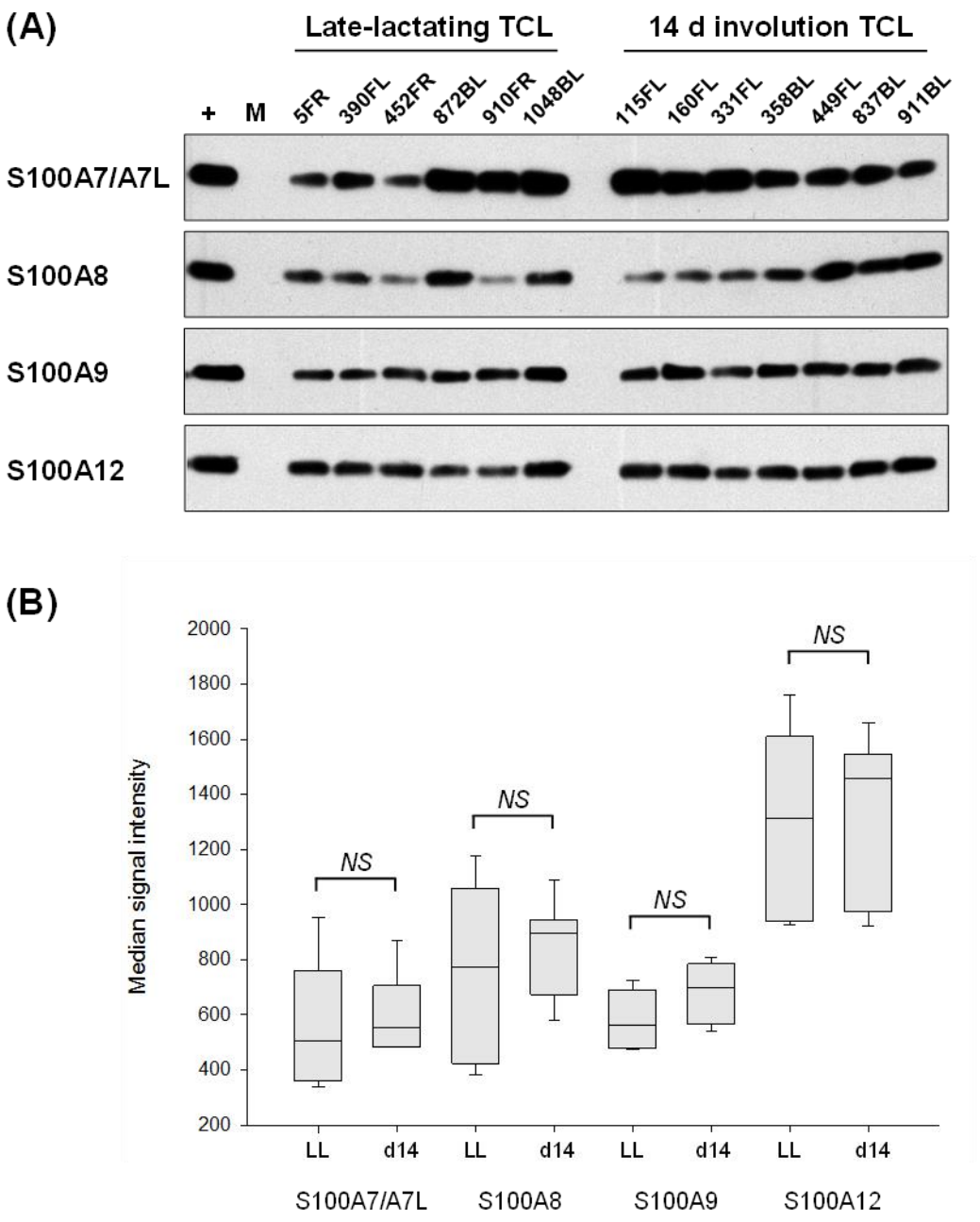

Figure 5.9: Relative abundance of S100 proteins in teat canal lining samples from late-lactating and 14 d involution cows.
(A) Western blot analyses of late-lactation and 14 d involution teat canal lining proteins from individual cows, probed with bovine specific antibodies directed against S100A7/A7L, S100A8, S100A9 and S100A12. +, positive control; M, molecular weight marker; TCL, teat canal lining. (B) Box-plot data shown are medians from triplicate analyses of Western blot signal intensity values, normalised to a positive internal control. Horizontal lines within each box represent the median intensity value for each S100 protein. The top and bottom of each box represent the 75th and 25th percentiles, respectively. Error bars above and below the boxes represent the 90th and 10th percentiles. LL, late-lactation teat canal lining, d14, 14 d involution teat canal lining. NS: non-significant difference, as determined by two-tailed Students t-test.

5.6. Changes in immune cell abundance in the teat-end tissues during early involution

Extensive physiological changes occur in the mammary gland during the first two weeks of drying-off. The protein profile of the milk changes dramatically as a result of programmed cell death (apoptosis) and hydrolysis of milk proteins by various proteases (Bonifaz *et al.*, 2002; Birkholz *et al.*, 2010; Maxymiv *et al.*, 2012). At the same time, the abundance of leukocytes in bovine milk secretions also increases substantially (Concha, 1985; Nickerson, 1989). What is unclear is how these physiological changes alter the immune cell profile and distribution of cells in the teat-end tissues.

In this section of work, the spatial and quantitative changes in immune cell populations during early involution were assessed by IHC. The localisation and abundance of these immune cells were then compared with analogous tissues obtained from late-lactating cows (See Chapter 4).

5.6.1. Expression of MHC class II is elevated in teat sinus sections from 14 d involution cows

As a first step in characterising the changes in immune cells within the teat-end tissues, sections of teat canal, Fürstenberg's rosette, and the teat sinus from all seven animals were examined for quantitative or spatial differences in the expression of the MHC class II cell surface molecule, which is expressed at high levels on antigen-presenting cells (Figure 5.10). The teat skin is also included in the analysis; however, as it is not directly involved in the involution process, the proportion of immune cells could be expected to be similar to that observed in skin from the late-lactating tissue.

There was no apparent difference in overall signal intensity for the MHC class II antigen in cryosections from 14 d involution teat canal, teat skin and Fürstenberg's rosette compared with equivalent late-lactation tissues (Table 5.7). Most of MHC class II signal in the 14 d involution teat canal and teat skin regions were localised within the stromal tissue in a pattern similar to that in the late-

lactating tissue. However, in four of the seven involution cows, there appeared to be an increased abundance of MHC class II signal within the teat canal epithelium, where it appeared to be expressed by cells located within or closely associated with the Marksäulchen structures (Figure 5.10b). Interestingly, for the Fürstenberg's rosette there was no apparent difference in the location of the MHC class II signal, the majority of which was seen in the epithelial bilayer of the primary and secondary mucosal folds (Figure 5.10e, f). There was also no apparent difference in the intensity of the MHC class II signal across all the cows analysed.

In contrast to the late-lactating tissue, a noticeable difference in signal intensity for MHC class II was observed in the 14 d involution teat sinus cryosections. In all seven involution tissues, there was an apparent increase in overall MHC class II abundance and most of this signal was localised to the epithelial bilayer (Figure 5.10g, h).

Table 5.7: Quickscore summary of MHC class II signal in teat-end tissue regions from late-lactating and 14 d involution cows.

Tissue region	Condition	
	Late-lactating	14 d involution
Teat canal	++	++
Teat skin	++	++
Fürstenberg's rosette	++++	++++
Teat sinus	++	+++

IF signal intensities in the cryosections were subjectively graded as negative (-), weakly positive (+), mildly positive (++), moderately positive (+++) and strongly positive (++++).

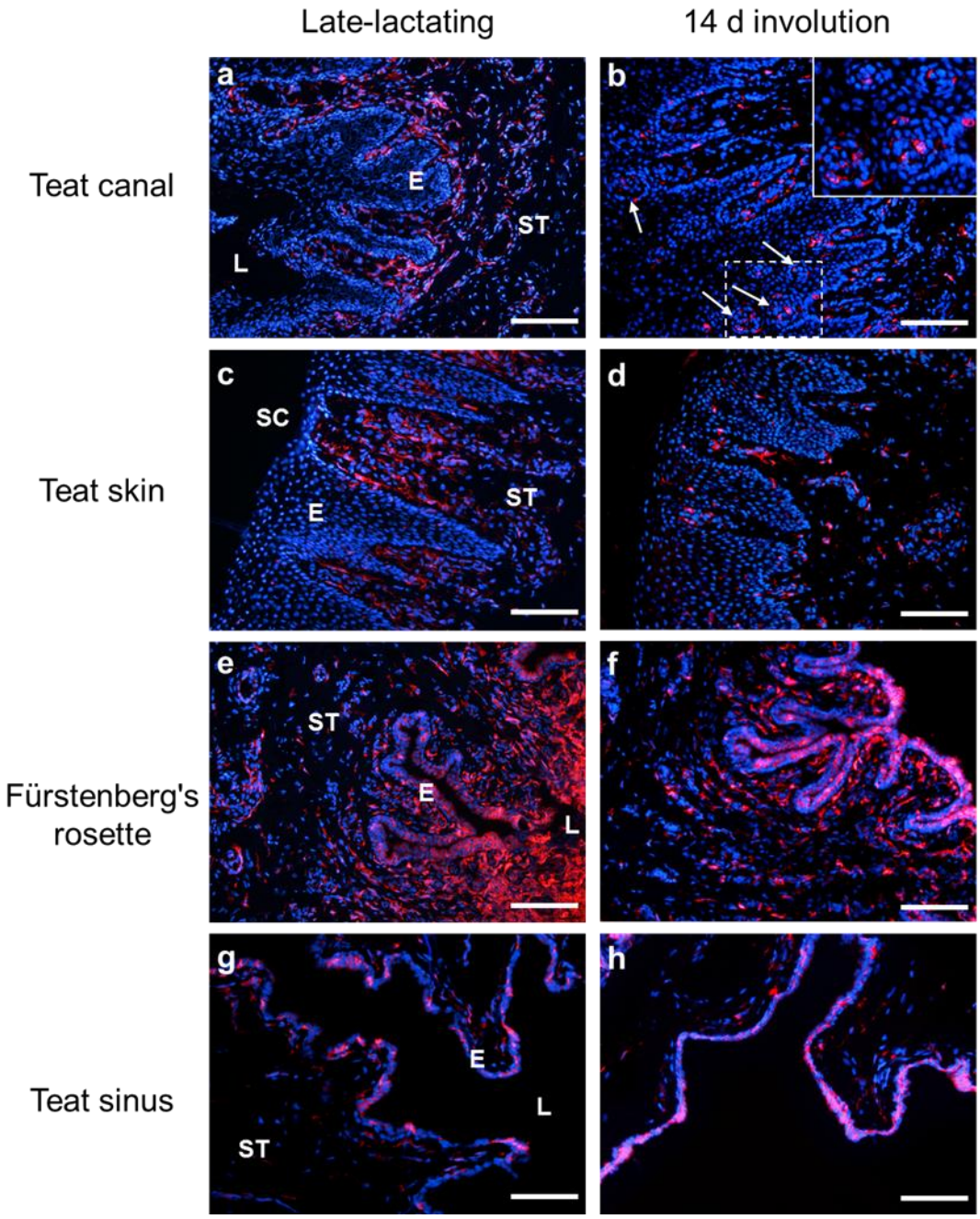

Figure 5.10: Comparison of MHC class II localisation in late-lactating and 14 d involuted teat-end tissues.
Representative immunofluorescence micrographs of transverse cryosections from Cow #005 (late-lactating) and Cow #115 (14 d involution). Cryosections of teat canal (a, b), teat skin (c, d), Fürstenberg's rosette (e, f), and teat sinus (g, h) were probed with anti-MHC class II monoclonal antibody (Alexa Fluor-594 IgG2a; red signal). Each cryosection was counterstained with DAPI (blue signal). The insert showing the Marksäulchen in micrograph b is indicated by a box with dashed lines. E, epidermis; SC, *stratum corneum*; ST, stromal tissue; L, lumen. Section thickness: 5 µm. Scale bar = 100 µm (a-d); 50 µm (e-h).

5.6.2. Antigen-presenting cells expressing the CD205 and CD14 cell surface receptors are increased in abundance in the Fürstenberg's rosette and teat sinus of 14 d involution cows

MHC class II molecules are primarily expressed by professional antigen presenting cells, such as dendritic cells, macrophages and B cells (Neefjes *et al.*, 2011). Thus, it is reasonable to presume that the increased intensity of MHC class II signal, observed in the 14 d involution sinus tissues, would also be consistent with an increased abundance of antigen-presenting cells. To examine this idea, teat-end sections from 14 d involution cows were probed for markers strongly expressed by antigen-presenting cells. These include the endocytic receptor CD205 (dendritic cells), the cell surface integrin molecule CD11c (epithelial bound dendritic cells), and the TLR4 co-receptor CD14 (macrophages). The localisation and signal intensity for each marker was compared with equivalent late-lactation tissues, examined previously in (See Sections 4.4.4 & 4.4.5).

Very little CD205 signal was observed in the epithelial and stromal tissues from 14 d involution cows for both the teat canal and teat skin cryosections. This level of expression was similar to that previously observed in the late-lactating tissues (Figure 4.12a, b). In contrast, the number of CD205 expressing cells occupying the space between the epithelial bilayer of both the Fürstenberg's rosette and teat sinus increased substantially when compared to analogous tissues from late-lactating cows. The increase in signal was determined by calculating the relative density of CD205 signal as a proportion of the total number of nuclei per microscope field. For the Fürstenberg's rosette, the relative proportion of CD205 signal was almost double that of the late-lactating tissue (85 % increase; $p < 0.001$) and in the teat sinus, the density of CD205 signal was almost quadruple (358 % increase; $p < 0.001$) that of the late-lactating tissue (Figure 5.14).

The high level of CD205 expression in the Fürstenberg's rosette and teat sinus, along with localisation of the signal between the epithelial bilayer, could indicate an increase in dendritic cell or macrophage populations in the 14 d involution tissues. To test this assumption, cryosections of 14 d involution teat-end tissue were probed for the cell surface integrin molecule, CD11c.

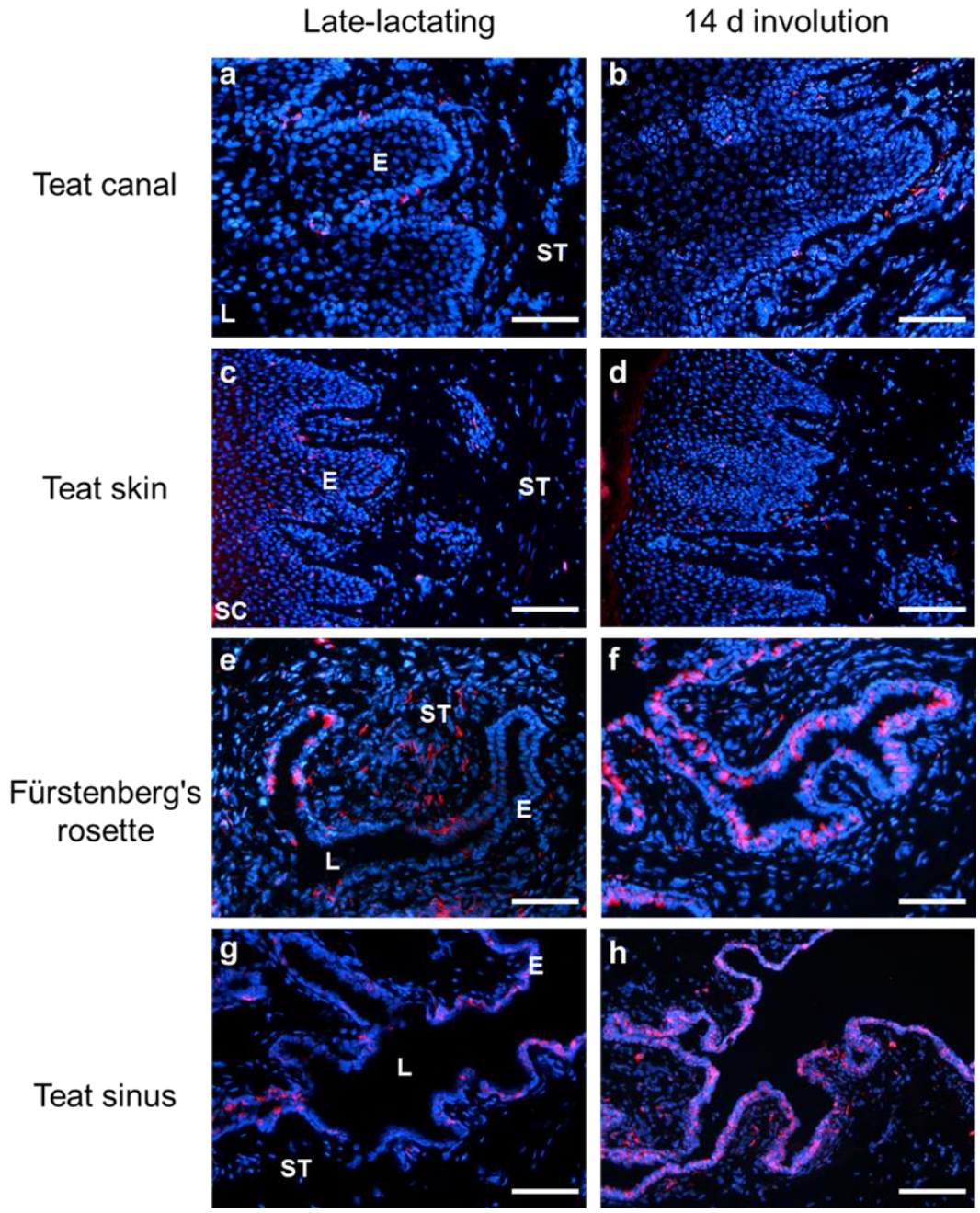

Figure 5.11: Comparison of the abundance of CD205 expressing cells in late-lactating and 14 d involuted teat-end tissues.
Representative immunofluorescence micrographs of transverse cryosections from Cow #452 (late-lactating) and Cow #331 (14 d involution). Cryosections of teat canal (a, b), teat skin (c, d), Fürstenberg's rosette (e, f), and teat sinus (g, h) were probed with anti-CD205 monoclonal antibody (Alexa Fluor-594 IgG; red signal). Each cryosection was counterstained with DAPI (blue signal). E, epidermis; SC, *stratum corneum*; ST, stromal tissue; L, lumen. Section thickness: 5 µm. Scale bar = 50 µm.

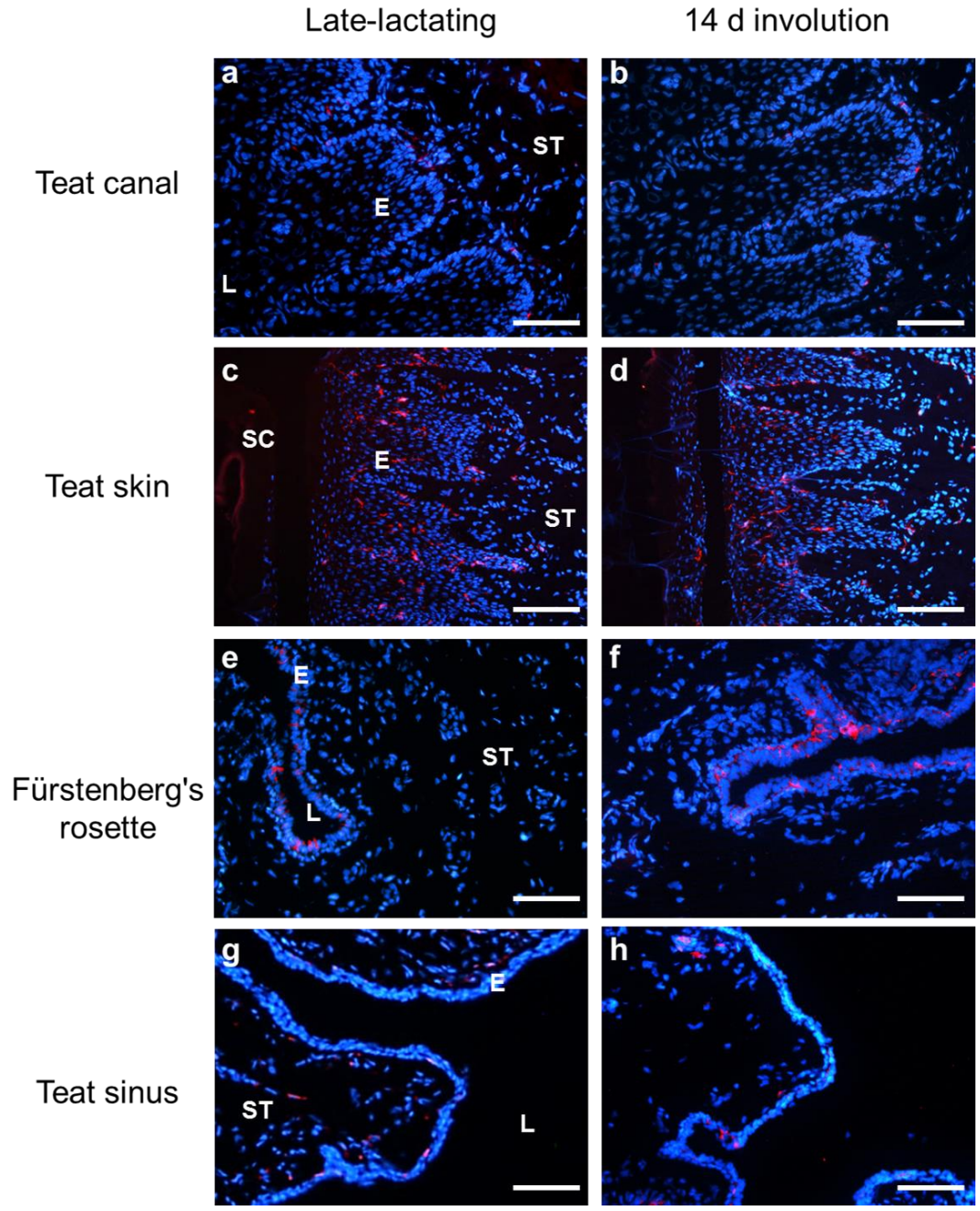

Figure 5.12: Comparison of the abundance of CD11c expressing cells in late-lactating and 14 d involuted teat-end tissues.
Representative immunofluorescence micrographs of transverse cryosections from Cow #452 (late-lactating) and Cow #358 (14 d involution). Cryosections of teat canal (a, b), teat skin (c, d), Fürstenberg's rosette (e, f), and teat sinus (g, h) were probed with anti-CD11c monoclonal antibody (Alexa Fluor-594 IgM; red signal). Each cryosection was counterstained with DAPI (blue signal). E, epidermis; SC, *stratum corneum*; ST, stromal tissue; L, lumen. Section thickness: 5 µm. Scale bar = 50 µm.

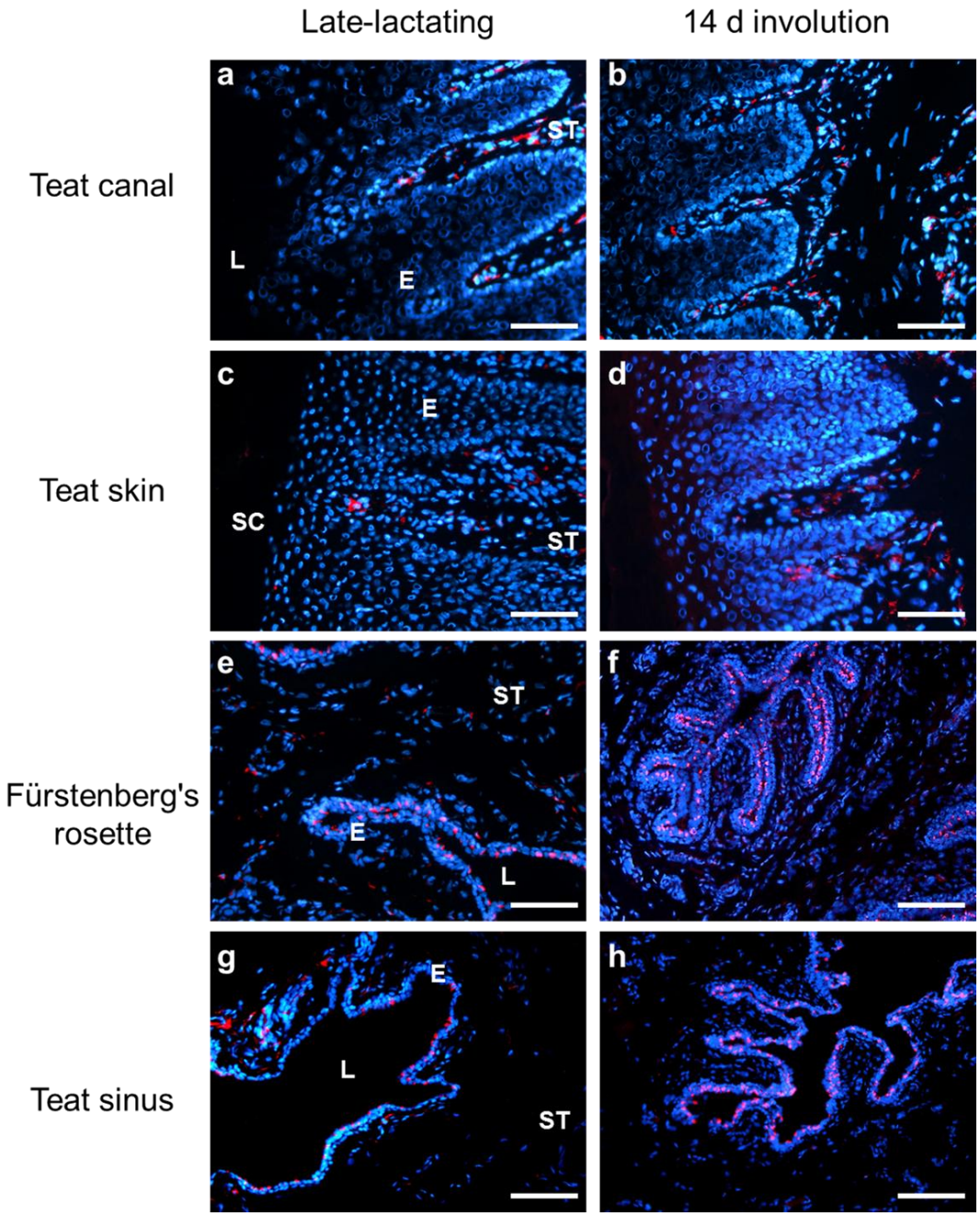

Figure 5.13: Comparison of the abundance of CD14 expressing cells in late-lactating and 14 d involuted teat-end tissues.
Representative immunofluorescence micrographs of transverse cryosections from Cow #910 (late-lactating) and Cow #837 (14 d involution). Cryosections of teat canal (a, b), teat skin (c, d), Fürstenberg's rosette (e, f), and teat sinus (g, h) were probed with anti-CD14 monoclonal antibody (Alexa Fluor-594 IgG; red signal). Each cryosection was counterstained with DAPI (blue signal). E, epidermis; SC, *stratum corneum*; ST, stromal tissue; L, lumen. Section thickness: 5 µm. Scale bar = 50 µm.

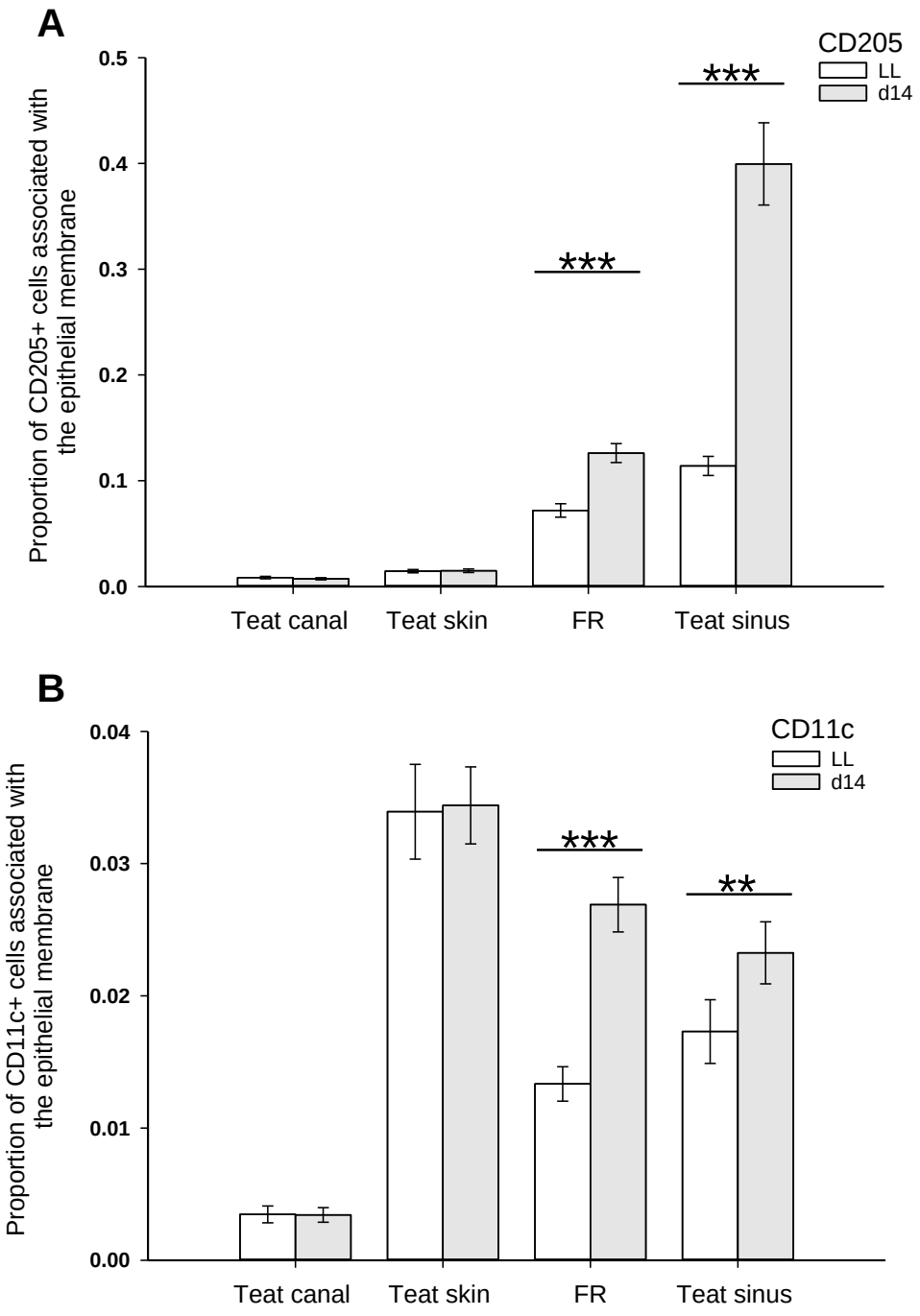

Figure 5.14: Semi-quantitative comparison of the proportion CD205$^+$ and CD11c$^+$ cells in late-lactating and 14 d involuted teat-end tissues.

Positively stained (A) CD205 expressing cells associated with the epithelial bilayer and (B), CD11c expressing cells located within the epithelial layer were counted from seven nonadjacent fields per slide at 200 x magnification and then averaged. The results are cumulative data from six late-lactating cows and seven 14 d involution cows (grey bars) and are expressed as a proportion of the total number of nuclei in each field. FR; Fürstenberg's rosette. Error bar: ± SEM. *** indicates $p < 0.001$, ** indicates $p < 0.01$

CD11c is primarily expressed by epithelial-bound dendritic cells and was previously shown to be co-expressed by epithelial-bound $CD205^+$ cells in the epithelial bilayer of the Fürstenberg's rosette (See Chapter 4; Figure 4.14). To examine this relationship after 14 days of involution, teat-end tissues were also probed for CD11c and compared to the analogous tissues in late-lactating tissue, with representative micrographs for CD11c shown (Figure 5.12). The average proportion of positively staining cells of all the nuclei in each microscopic field was calculated. In the 14 d involution tissue, there was a 66 % ($p < 0.001$) and 40 % ($p < 0.01$) increase in the proportion of cells expressing CD11c in the Fürstenberg's rosette and teat sinus, respectively, when compared with the late-lactating tissue (Figure 5.14b). No difference was observed between the 14 d and late-lactating samples in the teat canal and teat skin tissue sections.

In the Fürstenberg's rosette, the increase in CD11c signal (66 %) matched the increase in CD205 signal (85 %) with the majority of the signal for both antibodies localised to the epithelial bilayer. However, in the teat sinus tissue sections, there was a far greater increase in CD205 signal density (358 %) than CD11c signal density (40 %), indicating that there was a larger increase in a $CD205^+/CD11c^-$ population of cells in 14 d teat sinus tissues.

In humans, low to intermediate levels of CD205 have been found to be expressed by macrophage populations (Kato *et al.*, 2006). Unfortunately, there is little previous research describing CD205 in bovine macrophage populations, let alone bovine mammary tissues. The primary difficulty in distinguishing macrophages from dendritic cells is that they produce the same cell surface markers. However, in a recent study, bovine mammary dendritic cells were differentiated from macrophages by the difference in signal strength of CD14. Dendritic cells were characterised as $CD14^{lo}$ while macrophages were characterised as $CD14^{hi}$ (Maxymiv *et al.*, 2012).

To determine if macrophages were potentially responsible for the increased CD205 signal, the involution teat-end tissue sections were probed with the anti-bovine CD14 monoclonal antibody MM61A (Figure 5.13). In the teat canal and teat skin cryosections from the involution tissues, there was negligible difference in the abundance of CD14 signal compared to the equivalent late-lactating tissue sections. However, in both the Fürstenberg's rosette (331 %; $p < 0.001$) and teat sinus (338 %; $p < 0.001$) involution tissue sections there was an approximately three-fold increase in the density of CD14 signal, compared with the equivalent late-lactating tissue sections (Figure 5.15).

While this increase in the proportion of CD14 signal is similar to the increase in CD205 signal, especially for the teat sinus tissue sections, there was a lack of correlation with the proportion of $CD11c^+$ cells. CD11c has been previously shown to be present on bovine mammary macrophages as well as dendritic cells (Maxymiv *et al.*, 2012). Cells bearing both the markers CD205 and CD14 were not able to be identified in this study due to the monoclonal antibodies being of the same immunoglobulin isotype (IgG_1). This drawback could be overcome in future studies by labelling the primary antibodies with different fluorophores and performing direct immunofluorescence or by using different isotypes of CD205, CD11c, and CD14 to perform indirect immunofluorescence. Either technique could help to define the phenotype, distribution and density of cells containing a combination of these markers, especially in the teat sinus.

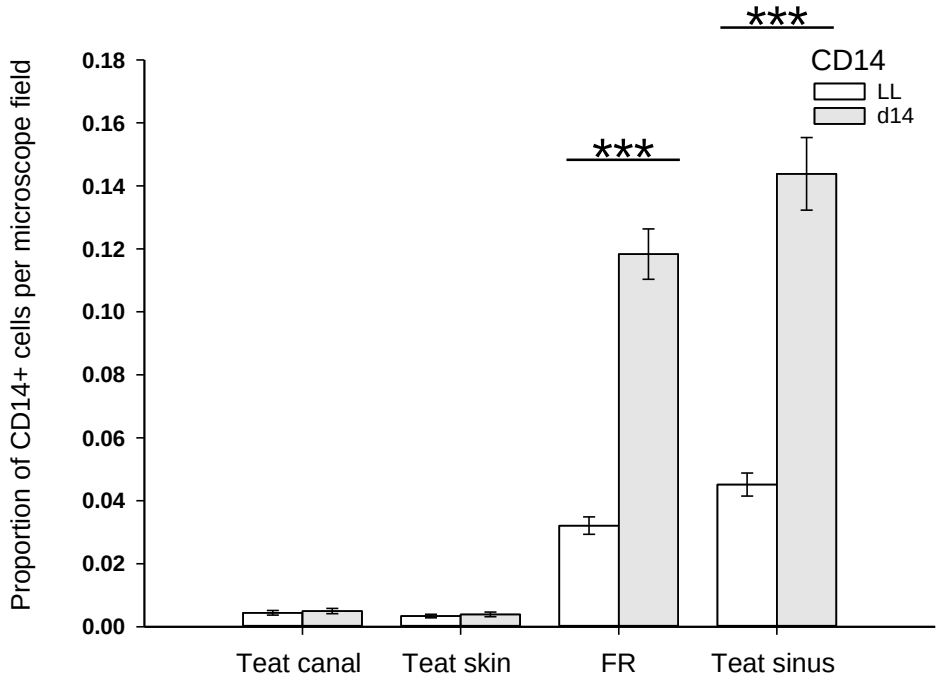

Figure 5.15: Semi-quantitative comparison of CD14+ cells in late-lactating and 14 d involuted teat-end tissues.
The relative proportion of positively stained CD14 cells associated with the epithelial layers were averaged from seven nonadjacent fields per slide at 200 x magnification. The results are cumulative data from six late-lactating cows and seven 14 d involution cows (grey bars). FR, Fürstenberg's rosette. Error bar ± SEM. *** indicates $p < 0.001$.

5.6.3. Increase in T lymphocyte abundance in the Fürstenberg's rosette and teat sinus of 14 d involution cows

Naïve T lymphocytes engage antigen-presenting cells in a stable interaction that results in efficient T cell stimulation and the initiation of adaptive immune responses (Davis & Chien, 1993). The magnitude and selectivity of the induced immune response are dependent on the concentration of the antigen as well as the maturation stage of the antigen-presenting cell, the expression of co-stimulatory molecules and the secretion of different cytokines. Given that there was an increase in the abundance of MHC class II expression in the teat sinus, most likely from an increase in the number of antigen-presenting cells, it is conceivable that there may also be an increase in the abundance of T lymphocytes in these tissues.

To examine the extent of the change involution has on the T lymphocyte populations, teat-end tissues were probed with the pan T lymphocyte marker CD3 (Figure 5.16) and compared to the analogous $CD3^+$ populations previously identified (See Chapter 4; section 4.4.2). There was no significant change in the T lymphocyte abundance surrounding the teat canal and teat skin epithelium. However, there was a slight increase in the proportion of T lymphocytes in the Fürstenberg's rosette (33%; $p < 0.001$) and teat sinus (21%; $p < 0.01$) (Figure 5.17). Interestingly, this increased T cell signal was due to more $CD3^+$ signal localised within the stroma of both tissue regions. For both the Fürstenberg's rosette and teat sinus, there was no difference in the number of $CD3^+$ cells associated with the epithelial bilayer between the involution and late-lactating tissues.

In the late-lactating tissues, the majority of epithelial-associated $CD3^+$ cells in the Fürstenberg's rosette and teat sinus also expressed the γδ T cell receptor - WC1 (See Chapter 4; Section 4.4.2). To determine if there was a change in the proportion of $WC1^+$ γδ T cells in 14 d involution compared with late-lactating tissues, teat-end cryosections were probed for the WC1 receptor marker (Figure 5.18). There was no significant difference in the average abundance of $WC1^+$ γδ T cells for either the Fürstenberg's rosette or teat sinus sections analysed when compared to the equivalent tissue regions from late-lactating cows (Figure 5.17b).

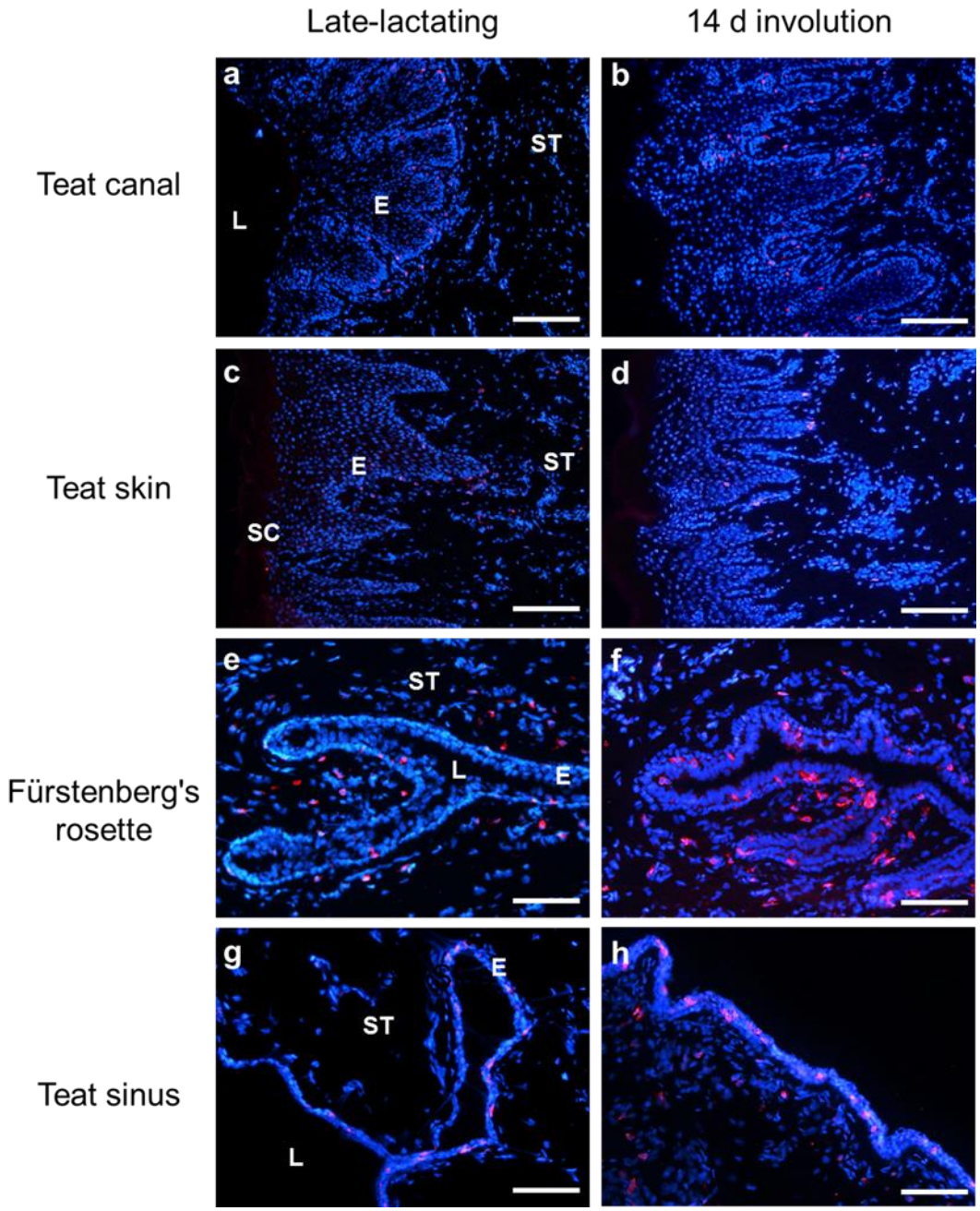

Figure 5.16: Comparison of the abundance of CD3 expressing cells in late-lactating and 14 d involuted teat-end tissues.
Representative immunofluorescence micrographs of transverse cryosections from Cow #1048 (late-lactating) and Cow #160 (14 d involution). Cryosections of teat canal (a, b), teat skin (c, d), Fürstenberg's rosette (e, f), and teat sinus (g, h) were probed with anti-CD3 monoclonal antibody (Alexa Fluor-594 labelled IgG; red signal). Each cryosection was counterstained with DAPI (blue signal). E, epidermis; SC, *stratum corneum*; ST, stromal tissue; L, lumen. Section thickness: 5 µm. Scale bar = 100 µm (a-d); 50 µm (e-h).

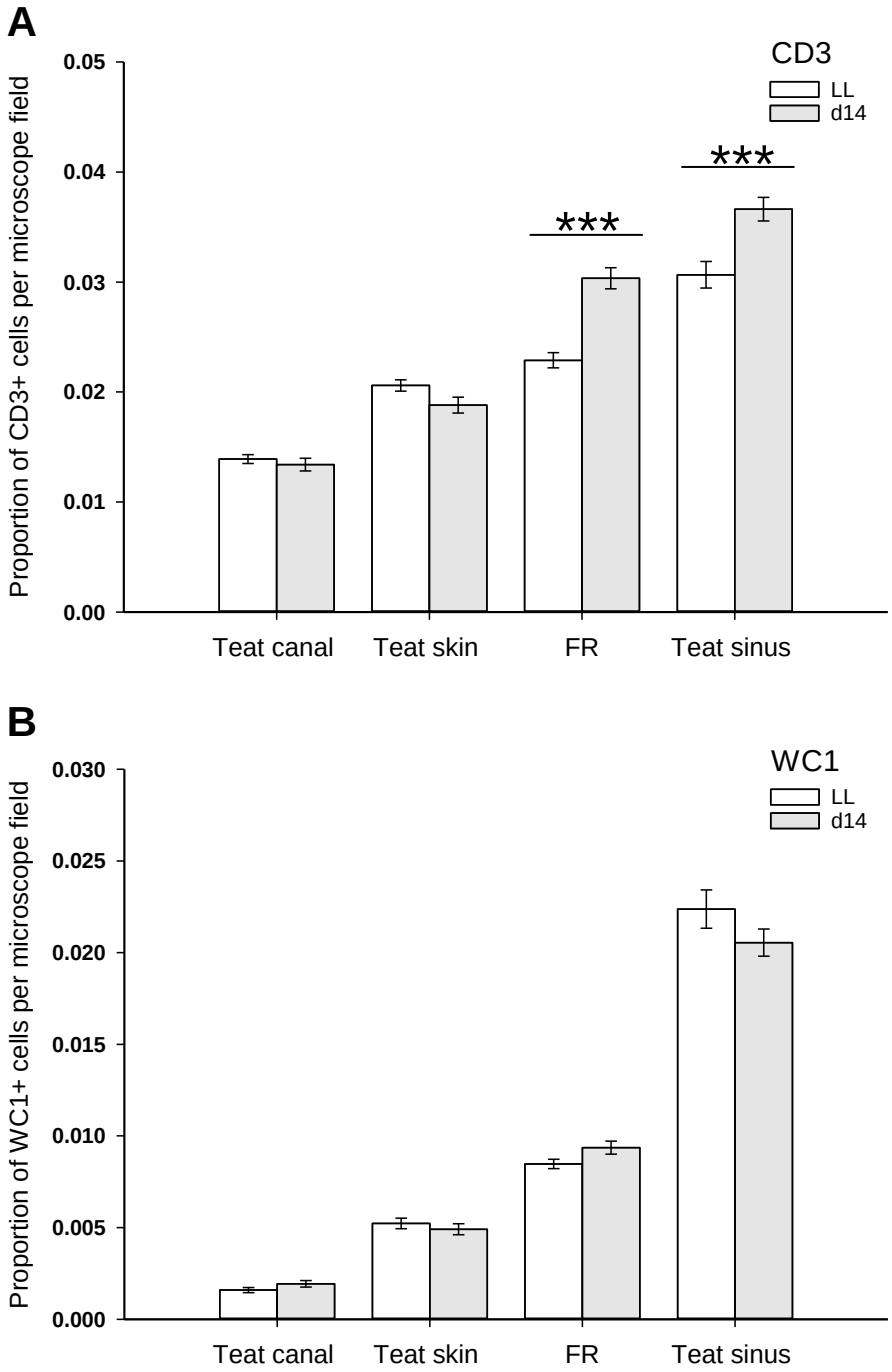

Figure 5.17: Semi-quantitative comparison of CD3+ and WC1+ cells in late-lactating and 14 d involuted teat-end tissues.
The proportion of positively stained (A) CD3 expressing cells and (B) WC1 expressing cells associated with the epithelial bilayer were estimated from seven nonadjacent fields per slide at 200 x magnification and then averaged. The results are cumulative data from six late-lactating cows and seven 14 d involution cows (grey bars). FR, Fürstenberg's rosette. Error bar ± SEM. *** indicates $p < 0.001$

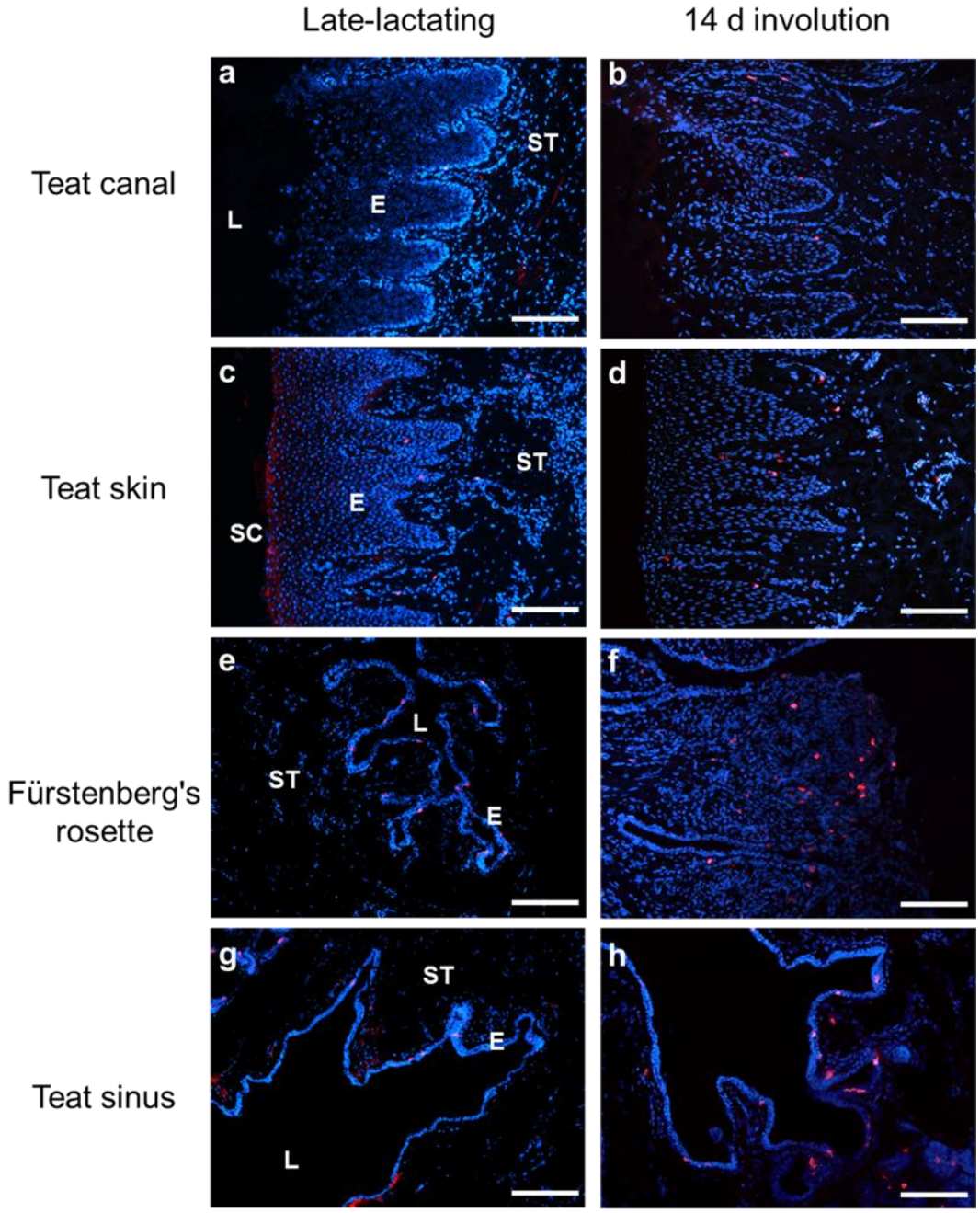

Figure 5.18: Comparison of the abundance of WC1 expressing cells in late-lactating and 14 d involuted teat-end tissues.
Representative immunofluorescence micrographs of transverse cryosections from Cow #390 (late-lactating) and Cow #911 (14 d involution). Cryosections of teat canal (a, b), teat skin (c, d), Fürstenberg's rosette (e, f), and teat sinus (g, h) were probed with anti-WC1 monoclonal antibody (Alexa Fluor-594 labelled IgG; red signal). Each cryosection was counterstained with DAPI (blue signal). E, epidermis; SC, *stratum corneum*; ST, stromal tissue; L, lumen. Section thickness: 5 µm. Scale bar = 100 µm.

5.6.4. Increased abundance of granulocytes in 14 d involution Fürstenberg's rosette and teat sinus stromal tissues compared to equivalent tissues from late-lactating cows

Like mastitis, early involution is characterised by an enormous influx of polymorphonuclear leukocytes from the circulation into the lumen of the teat sinus and mammary gland cistern (Monks *et al.*, 2002). The overwhelming majority of these granular white blood cells (granulocytes) are neutrophils.

The CH138A anti-granulocyte immunoreactive signal is shown on representative teat-end tissue sections from both late-lactating and 14 d involution cows (Figure 5.19). In all four tissue regions examined, most of the anti-granulocyte marker signal was localised to the stromal tissue for both the late-lactating and 14 d involution cows. There was no apparent difference in overall signal intensity for CH138A between late-lactating and 14 d involution cryosections from the teat canal and teat skin. In both groups of cows, low levels of signal were observed between the rete ridges for both the teat canal and teat skin sections in all cows (Figure 5.19a-d). Likewise, an equivalent level of signal was observed in the Marksäulchen for both the late-lactating and 14 d involution tissues. Signal to CH138A was more frequent and intense in the 14 d involution Fürstenberg's rosette (Figure 5.19e, f) when compared with the equivalent late-lactating tissue samples. This increase in signal intensity was consistent in all seven 14 d involution cows examined. In the teat sinus, a moderate increase in CH138A signal intensity was observed in the stroma of 14 d involution cows when compared with late-lactating cows (Figure 5.19g, h). The intensity of signal in the teat end tissue regions for granulocytes is summarised in Table 5.8.

Mast cells share many phenotypic and functional properties with basophils, which are a subset of granulocytes (Metcalfe *et al.*, 1997; Galli *et al.*, 2005). Mast cells are often located at sites exposed to the external environment and near blood vessels. Here, they can regulate vascular permeability and effector cell recruitment through the release of mediator molecules such as cytokines, chemokines and histamine.

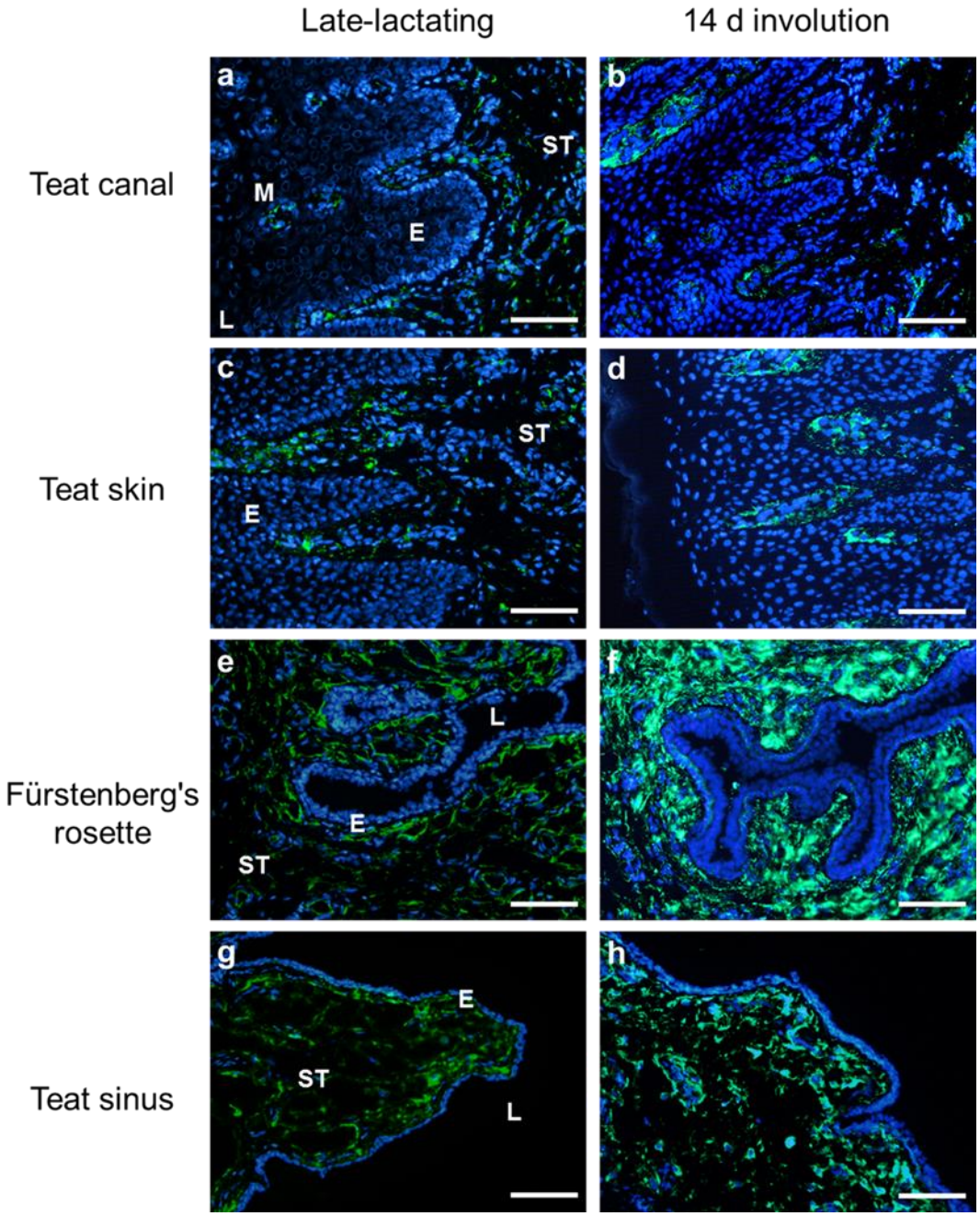

Figure 5.19: Comparison of CH138A+ cell abundance in late-lactating and 14 d involuted teat-end tissues.
Representative immunofluorescence micrographs of transverse cryosections from Cow #1048 (late-lactating) and Cow #115 (14 d involution). Cryosections of teat canal (a, b), teat skin (c, d), Fürstenberg's rosette (e, f), and teat sinus (g, h) were probed with monoclonal CH138A antibody (Alexa-fluor 488 IgM; green signal). In the 14 d involuted Fürstenberg's rosette and teat sinus stromal tissue, there is a substantial increase in signal intensity compared with late-lactating tissues. Each cryosection was counterstained with DAPI (blue signal). E, epidermis; M, Marksäulchen; ST, stromal tissue; L, lumen. Section thickness: 5 µm. Scale bar = 50 µm (a-h).

Table 5.8: Quickscore summary of CH138A anti-granulocyte signal in teat-end tissue regions from late-lactating and 14 d involution cows.

Tissue region	Condition	
	Late-lactating	14 d involution
Teat canal	++	++
Teat skin	++	++
Fürstenberg's rosette	+++	++++
Teat sinus	++	+++

The IF signal of labelled cells in each micrograph was subjectively graded as negative (-), weakly positive (+), mildly positive (++), moderately positive (+++) and strongly positive (++++).

Because of the marked increase in the abundance of apparent granulocytes in the Fürstenberg's rosette and teat sinus tissue regions, it is possible that there is also a discernible increase in the mast cell population during involution. To examine this possibility, the 14 d involution teat-end tissues were probed for *c-kit* (CD117) expression and compared with equivalent tissues from late-lactating cows (Figure 5.20).

The presence of $CD117^+$ mast cells was observed in the stromal tissue in proximity to structures resembling blood vessels in most of the tissues sections examined (Arrowed in Figure 5.20d, f, & h). Post-hoc comparisons of the relative abundance of $CD117^+$ cells in all four tissue regions showed a trend for a slight increase in 14 d involution tissues, but this change was not significantly different from the late-lactating tissues (Figure 5.21).

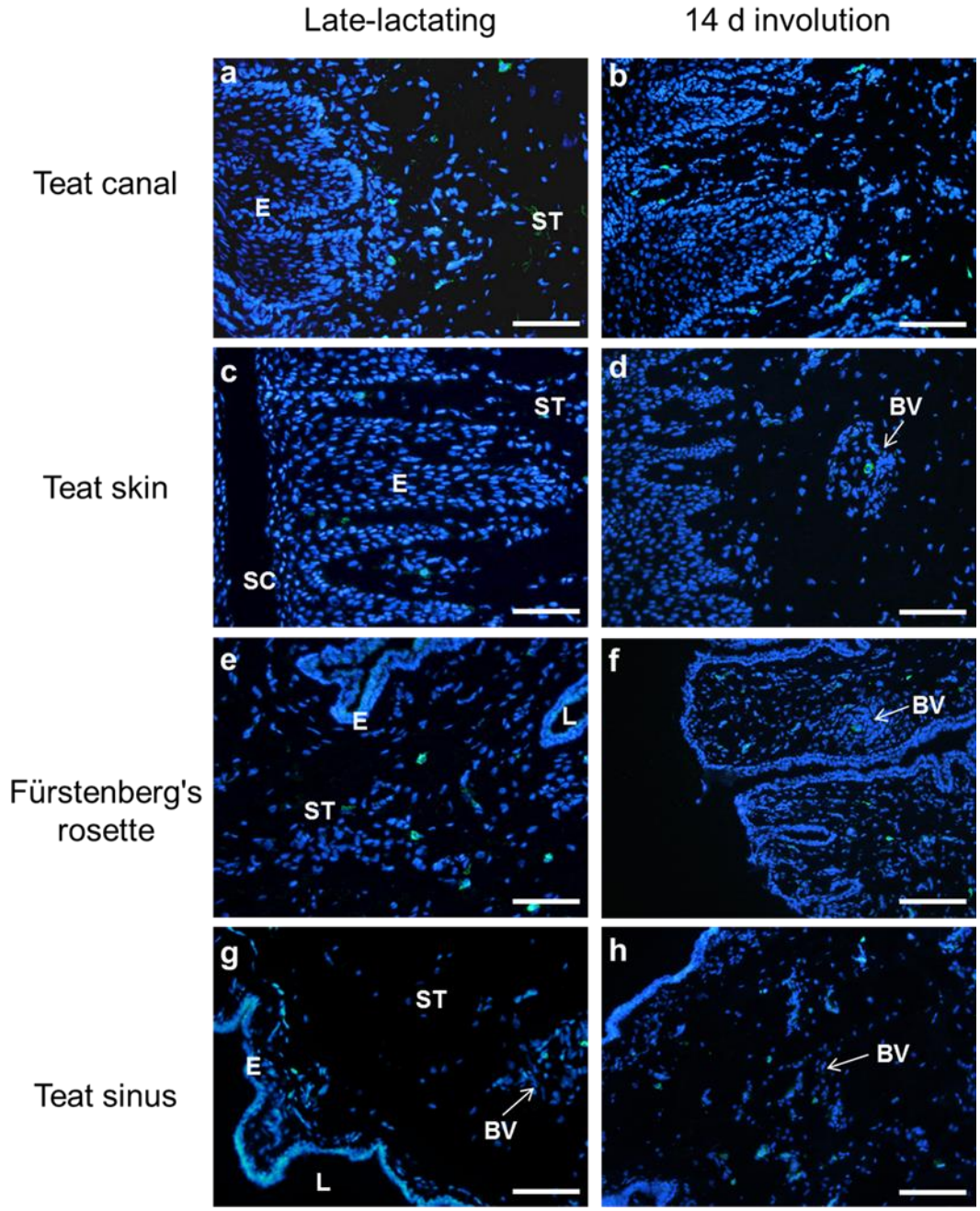

Figure 5.20: Comparison of CD117+ cell abundance in late-lactating and 14 d involuted teat-end tissues.
Representative immunofluorescence micrographs of transverse cryosections from Cow #1048 (late-lactating) and Cow #449 (14 d involution). Cryosections of teat canal (a, b), teat skin (c, d), Fürstenberg's rosette (e, f), and teat sinus (g, h) were probed with anti-CD117 polyclonal antibody (Alexa-fluor 488 IgG; green signal) and counterstained with DAPI (blue signal). Structures that resemble blood vessels are arrowed. E, epidermis; SC, *stratum corneum*; ST, stromal tissue; L, lumen; BV, blood vessel. Section thickness: 5 µm. Scale bar = 50 µm.

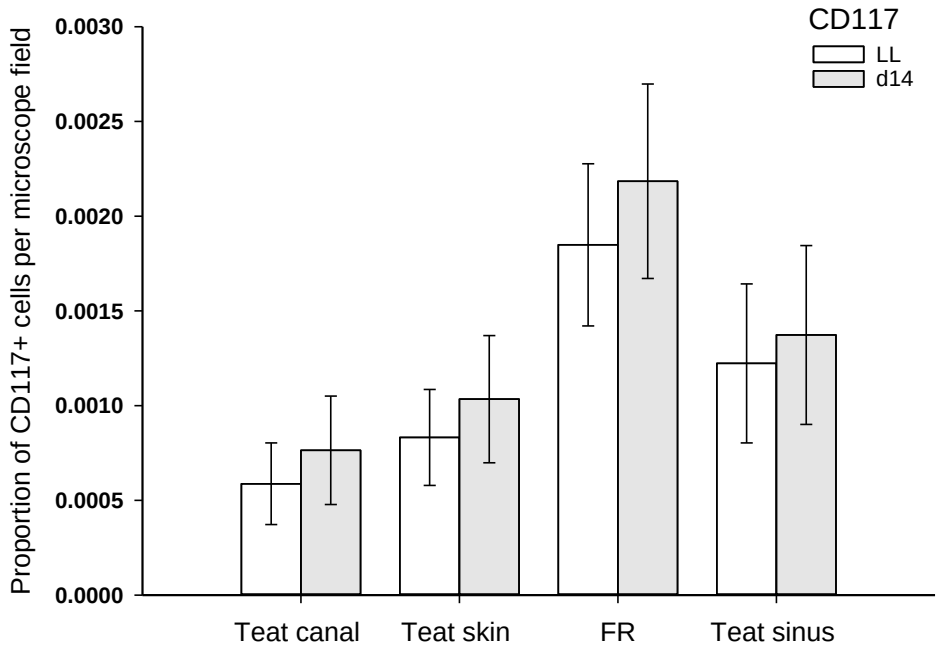

Figure 5.21: Semi-quantitative comparison of the proportion of CD117+ cells in late-lactating and 14 d involuted teat-end tissues.
The total number of positively stained CD117 expressing cells in the stromal tissue adjacent to the epithelial cell layer were counted from seven nonadjacent fields per slide at 200 x magnification, averaged and then expressed as a proportion of the total number of nuclei in the fields. The results are cumulative data from six late-lactating cows and seven 14 d involution cows (grey bars). FR, Fürstenberg's rosette. Error bar ± SEM.

5.7. Discussion:

The susceptibility of the bovine mammary gland to infection varies as involution progresses. The highest incidence of intramammary infection occurs during the early dry period as the mammary gland transitions from the lactating to the non-lactating state (Neave *et al.*, 1950; Oliver & Mitchell, 1983; Smith *et al.*, 1985; Nickerson, 1989). There are several schools of thought as to the cause of this increased susceptibility, including the teat canal being more readily penetrated by bacteria, or that the innate defences within the mammary gland are compromised in some fashion (Cousins *et al.*, 1980; Nonnecke & Smith, 1984; Nickerson, 1989). The analyses described in this chapter, detailing the biochemical and histological changes occurring in the teat-end tissues 14 d after drying-off, provide some insight into the merits of these schools of thought.

Inspection of the 14 d mammary tissue and cisternal milk confirmed that physiological and chemical changes associated with involution are well under way at this time interval for each animal. Moreover, there were no signs of infection by bacteria that would induce an inflammatory response not associated with the involution process, an otherwise potentially confounding factor. Proteomic analysis of the 14 d involution teat canal lining identified only subtle changes compared to teat canal lining from late-lactating cows. Most of the proteins/protein spots that were altered between 14 d involution and late-lactating teat canal lining were either keratins, proteins involved in keratinocyte differentiation, or energy metabolism. In addition to these changes, lactoferrin was found to be 25-fold more abundant in the 14 d involution teat canal lining by SpC analysis, and a small proportion of the S100A7L protein was found to migrate to a new position on the 2-DE gel, consistent with it being post-translationally modified. IHC analyses of Fürstenberg's rosette and teat sinus tissues after 14 d involution showed major changes in the abundance of several immune cell types compared to the equivalent late-lactating tissues. In contrast, very little if any difference was observed in the stratified epithelium of the teat canal and teat skin. These findings imply that lactoferrin may play a role in the host-defence of the teat canal lining during involution. Moreover, there is a significant increase in the abundance of immune cells in Fürstenberg's rosette and teat sinus tissue regions, confirming the importance of these tissue regions in protecting the mammary gland from infection.

Lactoferrin is a key innate immune component of mucosal secretions where it has been reported to perform both bacteriostatic and bactericidal functions (Ward *et al.*, 2002; Valenti & Antonini, 2005). These activities have been ascribed to be manifested through the sequestering of iron from the surrounding environment by apo-lactoferrin (Reiter & Oram, 1967; Rainard, 1986). Conceivably, this could occur in the teat canal lining. In addition, the suppression of bacterial growth has also been achieved by lactoferrin binding to the outer membrane of Gram-negative bacteria (Ellison *et al.*, 1988; Naidu *et al.*, 1993; Sallmann *et al.*, 1999), inhibition of bacterial biofilm formation (Singh *et al.*, 2002; Simojoki *et al.*, 2012), and by synergistically increasing the recognition and binding of immunoglobulin A

(Watanabe *et al.*, 1984). Antimicrobial activities of lactoferrin and lactoferrin fragments against mastitis pathogens have also been reported independent of its iron-binding function (Bellamy *et al.*, 1992; Nai-Yuan *et al.*, 2004).

Low levels of lactoferrin signal were observed surrounding the majority of nuclei located in the spinous and granular layers of the 14 d involution teat canal stratified epithelium. This is a very interesting observation worthy of further attention as the amount of lactoferrin expression could influence a cows' capacity to combat the initial stages of infection. Furthermore, the location of the lactoferrin signal is also intriguing. By surrounding the nucleus, the protein would seem to be performing functions other than host defence. Alternatively, the peri-nuclear lactoferrin could be in the process of being synthesised in the peri-nuclear rough ER and then secreted. The molecular mechanism by which lactoferrin expression is turned on is beyond the scope of this thesis but could be the subject of future investigation.

The function of S100A7L in the teat canal lining is unknown, but there is evidence that points towards a role in host-defence. It is present at very low levels in the teat skin, yet is expressed at equimolar levels to S100A7 in the teat canal, suggesting some significant biological function in this tissue. S100A7, otherwise known as psoriasin, is a potent killer of coliform bacteria with protective roles in the skin (Gläser *et al.*, 2005), eye (Garreis *et al.*, 2011), tongue (Meyer *et al.*, 2008), and urogenital tract (Mildner *et al.*, 2010). At higher concentrations, it exhibits bactericidal activity against several Gram-negative and Gram-positive mastitis causing bacteria (Gläser *et al.*, 2005; Lee & Eckert, 2007). The detection of two additional isoforms of S100A7L in the 14 d teat canal lining is indicative of a p*I* shift caused by a change in the net charge of the protein, typical of post-translational modification. One possibility is that the altered isoforms could enhance S100A7L's specificity and potency towards bacteria that are more resistant to the more usual form of S100A7, although supporting evidence is required to lift this idea beyond mere speculation. Future functional assays with purified or recombinant S100A7L should provide an insight into its possible role in the teat canal and host-defence.

There was very little difference in the abundance of MHC class II positive cells surrounding the stratified epithelium of the 14 d involution teat canal compared to the equivalent late-lactating tissues, but there were subtle differences in their location. More antigen-presenting cells appeared to be located within the teat canal epithelium in the involution samples compared with the lactation samples, the majority of which were associated with the Marksäulchen structures. The function of these structures is unknown, but it is conceivable that they provide MHC class II cells as well as granulocytes access to several layers of the teat canal epithelium, potentially allowing them to reach the *stratum corneum* and luminal surface. If true, this could provide an additional source of antimicrobial components to hinder the growth and passage of pathogens through the teat canal.

The complex immune cell repertoire of the Fürstenberg's rosette would suggest that it is actively involved in antigen/pathogen recognition and host-defence. Surprisingly, the antigen-presentation capacity of this tissue region, after 14 d involution, did not appear to be different from comparable late-lactating tissues. At first glance, this would suggest that the Fürstenberg's rosette is unresponsive to the physiological and biological changes occurring elsewhere in the mammary gland. However, a large influx of immune cells occurs into the alveolar luminal spaces after drying off, but the Fürstenberg's rosette appears to be shielded from these changes, possibly through the action of the sphincter muscle sealing off access of these cells and antigens. However, significant increases in immune cells with antigen-recognition capability (CD205 and CD14) and an increase in the abundance of T lymphocytes illustrate that the responses during involution are complex and defy a simple explanation. The results to date are sufficient to underscore the importance of this tissue in dividing the two distinct environments of the teat canal lumen and the teat sinus and maintaining the differences between them.

The 14 d involution teat sinus tissues showed the most dramatic changes in immune cell abundance of all the tissues examined. Not only was there a perceived increase in the intensity of MHC class II signal but there was also a dramatic increase in the abundance of immune cells expressing markers for CD205 and CD14. Interestingly, for both cell types, this increase was five-fold greater than the increase in CD11c positive cells. This difference in relative

proportion would indicate that there is a substantial population of $CD205^+/CD11c^-$ and $CD14^+/CD11c^-$ cells recruited into the teat sinus tissues during involution. While it is highly likely that these cells are immature myeloid cells, further studies using additional and novel cell-type-specific markers would provide more understanding on their identity and function. It is possible that these cells may simply differentiate to replace populations of epithelial bound macrophages and dendritic cells, but they could also be involved in other aspects of modulating localised immune response.

Several insights have been obtained into the composition and distribution of immune cells after 14 d involution. These will form the basis for future research. However, several outstanding questions remain, including: What is the role of lactoferrin in the teat canal and how does its relative abundance change during the involution cycle? Are the Marksäulchen a conduit for immune cells to access the teat canal lumen? What is the actual nature of the $CD205^+$ and $CD14^+$ cells in the teat sinus and what is their role during involution?

Although only a single time point (14 d) could be assessed in this study, the observations described raise several interesting questions with regards to host-defence. For example, do all cows have the same numbers of cells and do they all have the same degree of change with involution? Are all breeds of dairy cattle the same? Are there differences in the rate of change and is there a correlation with susceptibility to infection? Are the immune cells in the Fürstenberg's rosette and teat sinus fully active in a host defence capacity or are they compromised by the involution process?

In summary, these results demonstrate that the teat canal is somewhat inert as a host defence tissue during involution, with subtle changes in the biochemical composition of the teat canal lining and very little cellular response. On the other hand, the changes in abundance and composition of several immune cell types in the Fürstenberg's rosette and the teat sinus demonstrate that these tissues are more responsive to variations in the surrounding environment. The question of whether these changes increase the host-defence capacity of these tissues during involution is beyond the scope of this study, but worthy of future investigation.

6. Experimentally induced bacterial challenge of the bovine teat canal

6.1. Introduction:

The analyses described previously in Chapters 3 and 4 have shown that the stratified epithelium of the teat canal had a similar morphology, cellular architecture and proteomic profile to that of the surrounding teat skin. It would, therefore, be reasonable to presume that the teat canal epithelium functions in a similar manner to the epithelium of skin. One such function of the skin is to provide an antimicrobial and immunological barrier to environmental microbes (Bangert *et al.*, 2011; Harder *et al.*, 2013). This has been demonstrated in human and murine epithelial models where constitutively expressed antimicrobial proteins are found in healthy skin and when the cornified layer of the skin is breached, inducible antimicrobial proteins are expressed along with the release of signalling molecules to recruit effector immune cells (Schröder & Harder, 2006).

Studies into the host defences of the teat canal lining are limited and it remains unknown if the teat canal epithelium is capable of responding to the presence of microorganisms, similar to that of the skin. The aim of this chapter is to investigate the responses of the teat canal and teat-end tissues to the presence of bacterial pathogens in the teat canal, 24 h post-infection. We also wanted to determine if teat canal inoculation with a pathogen resulted in a localised cellular response or if the pathogenic bacteria could influence the cellular milieu in the teat-end tissues beyond the teat canal (i.e. in the Fürstenberg's rosette and the teat sinus tissue). Proteomics was used to identify inducible host-defence proteins in the teat canal lining in response to the presence of a pathogen and IHC was used to examine innate cellular responses within the teat-end tissues.

6.2. Experimental design:

6.2.1. Animal selection

A week before the start of the trial, the udder health of 17 late-lactation cows was evaluated by visual inspection, milk SCC and microbiological analysis of the milk samples. Cows that showed no signs of clinical mastitis, using the Rapid Mastitis Test, had SCCs of less than 200000 cells/mL in each quarter and returned clear milk cultures were included in the study. Eight cows met the study criteria, and their individual characteristics are listed in Table 6.1.

6.2.2. Experimental model and inoculation

The eight cows were randomly assigned into two groups of four cows (A and B). The two groups were inoculated two days apart to manage the handling of samples after slaughter better. Cows in group A (n = 4) were inoculated on day 1, and teat samples were collected 24 h later. Group B cows were similarly treated two days later (Figure 6.1). The use of the Newbould inoculator for the transfer of bacteria into the teat canal has previously been described (Newbould & Neave, 1965b; Prasad & Newbould, 1968; Grindal *et al.*, 1991; Lacy-Hulbert & Hillerton, 1995; Turner *et al.*, 2013). In each of the published studies, bacterial inoculations 2–4 mm proximal to the teat orifice, were performed immediately following milking (< 30 min). In these previous studies, the number of bacteria inoculated into the teat canals ranged from 17 – 1072 cfu for *S. aureus*, 200-500 cfu for *S. uberis*, and 5000 – 43000 cfu for *E. coli*. In some of these investigations, this treatment regime resulted in clinical intramammary infections in several cows.

To minimise the possibility of infection of the interior of the mammary gland, and possible confounding generalised inflammatory responses, teat canal inoculations were performed two hours post-milking. This delay ensured that the teat canal sphincter was completely closed before inoculation. The 24 h time interval between inoculation and sampling should only allow for the induction of an acute innate immune response and should not be enough time for any potential clinical mammary infection or antibody response to develop. Preparation of cultures for

teat canal inoculations consisted of 2500 cfu *S. uberis*, 2500 cfu *S. aureus* and 500,000 cfu *E. coli*. These are described in more detail in Supplementary data D1.

Table 6.1: Individual characteristics of cows in the bacterial challenge trial

Group[a]	Cow #	Quarter[b]	Age	Gestation status	Days in milk	Daily Yield (L)	SCC[c] (x10^3 cells/mL)
A	225	FL	11	Pregnant	214	14.6	118
		FR					198
		BL					73
		BR					40
	708	FL	7	Empty	283	15.5	79
		FR					146
		BL					76
		BR					111
	1193	FL	5	Pregnant	263	13.0	147
		FR					107
		BL					75
		BR					62
	1348	FL	4	Empty	272	16.2	21
		FR					14
		BL					37
		BR					22
B	428	FL	7	Empty	225	11.4	114
		FR					43
		BL					148
		BR					33
	862	FL	5	Pregnant	249	12.7	36
		FR					49
		BL					48
		BR					33
	1238	FL	4	Pregnant	254	15.1	40
		FR					77
		BL					44
		BR					47
	1312	FL	4	Pregnant	257	12.1	37
		FR					38
		BL					186
		BR					37
Ave. ± SD[d]			*4.0 ± 1.5*		*252 ± 23*	*13.8 ± 1.8*	*73.0 ± 49.4*

a) Trial groups for sample analysis
b) FL, left forequarter; FR, right forequarter; BL, left hindquarter; BR, right hindquarter
c) SCC, milk somatic cell count immediately before inoculations
d) Ave. ± SD, average ± standard deviation

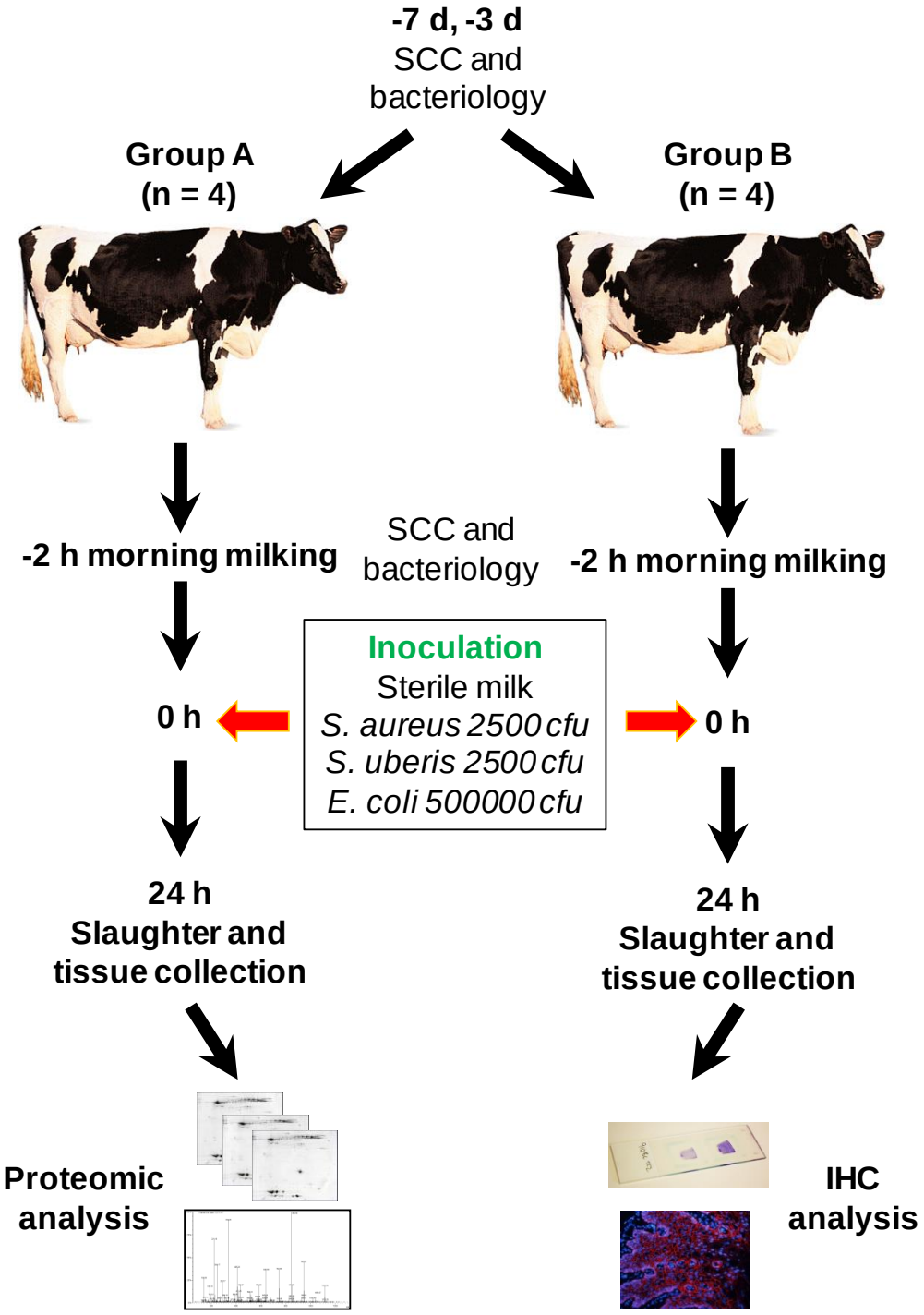

Figure 6.1: Schematic summary of the bacterial challenge experimental design.
Individual teats from two groups of cows were inoculated two hours after morning milking with one of three common mastitis causing bacteria. Control-treated teats with vehicle-only (sterile milk) served as internal controls for each animal. Teat canal lining and teat-end tissue were collected 24 h post-inoculation for proteomic and IHC analysis, respectively. TCL samples from Group A were collected for proteomic analysis with the Group B samples collected for IHC analysis.

6.2.3. Clinical examination and monitoring of animals

Temperature data loggers were inserted into the vaginal cavity of the cows to record core body temperature before the inoculation and at 10-minute intervals until just before slaughter. The cows were transported in a standardised manner to the abattoir for slaughter the following day. Before slaughter, the vaginal temperature loggers were removed, and the mammary glands examined.

6.2.4. Sample collection

Teats from Group A cows were selected for teat canal lining collection and proteomic analysis. Teats collected from Group B cows were frozen in liquid nitrogen for IHC analysis. Bacterial detection was performed, in a manner similar to that of the teat sinus (See Section 2.2.4). The teat canal was initially sliced open down its length, and a sterile swab (moistened in sterile 0.85 % (*w/v*) saline solution) was used to lightly touch the mid-point of the teat canal, approximately 3-4 mm proximal to the teat orifice (Figure 6.2). Bacteria recovered by the swabs were transferred to blood agar plates and colonies grown for 24 h at 37 °C for assessment. Unfortunately, this collection method does not allow for an accurate estimate of the total bacteria present in the teat canal and how it compares with the original number of bacteria introduced.

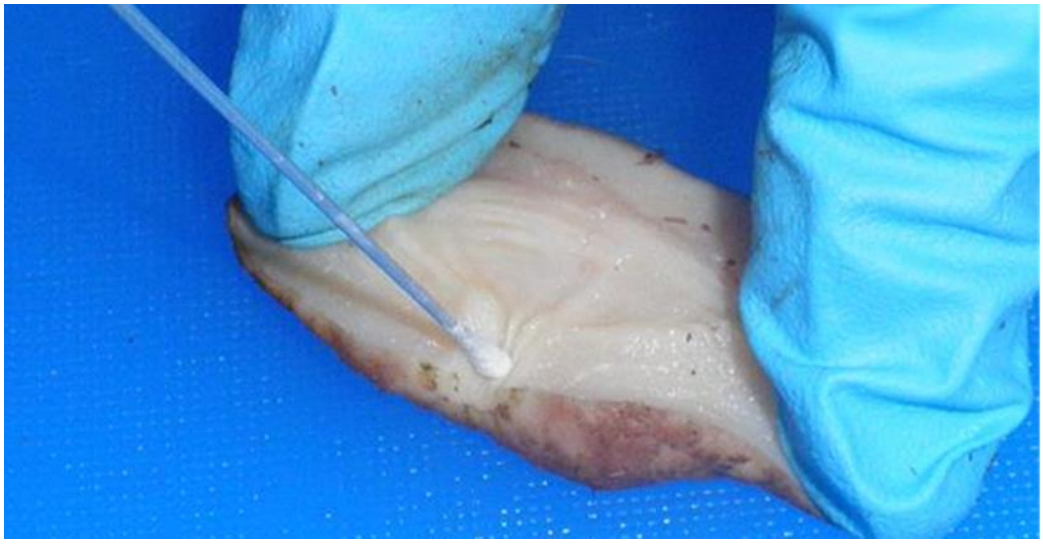

Figure 6.2: Assessment of teat canal infection by swab analysis.
A moistened sterile swab was used to collect bacteria from the lining near the midpoint of the teat canal 24 h post inoculation.

6.3. Physiological and physical responses to bacterial inoculations

Fever, as a consequence of an exaggerated inflammatory response to an infection, results in an increase in the core body temperature of an animal (Hasday *et al.*, 2000). Temperature loggers were inserted into the vaginal cavity of each cow to measure changes in core body temperature over the trial period. All cows were clinically healthy at the start of the trial, with vaginal temperatures less than 40 °C (average, 38.7 °C; range, 38.1 °C to 39.6 °C). At the end of the 24 h period, post-inoculation, the average vaginal temperature was 38.2 °C (range, 37.5 °C to 38.9 °C).

There was no evidence of an effect from the teat canal inoculations on the vaginal temperatures. Any differences in temperature that were observed were consistent with the known diurnal variation (McGee *et al.*, 2008). In addition, there were no other symptoms of mammary gland infection - such as swelling, heat, or soreness observed for any of the cows.

Milk SCC could not be utilised as a measure for infection due to the dramatic increase in somatic cells resulting from the tissue disturbance that occurs when the udder is removed from the cow at slaughter. Milking, prior to slaughter, was not an option as the milk would get contaminated by bacteria still present in the teat canal. Milking could also remove the teat canal lining limiting the amount of sample for proteomic analysis. To overcome this problem, two simple tests were performed to see if any of the bacteria had penetrated the teat canal barrier and established an infection in the mammary gland. Firstly, using aseptic technique, milk was collected from the 16 mammary gland cisterns directly after each teat had been removed from each of the four udders, to test for the presence of the inoculated bacteria. This test was performed similarly to the bacteriological assessment of quarter milk samples (See Section 2.2.4). Secondly, Western blot analysis was carried out on 1 µL (~35 µg total protein) of the 16 collected milk samples to look for known markers of infection. One such marker are the cathelicidin proteins released by infiltrating neutrophils into the milk (Smolenski *et al.*, 2011).

In both tests, there was no evidence of infection (*data not shown*). There was no growth of bacterial colonies on the blood agar plates from any of the 16 cisternal milk samples examined after 48 h incubation of the plates at 37 °C. Furthermore, there were no immunoreactive bands for cathelicidins in the Western blots of cisternal milk samples, even with longer exposure times.

To confirm that the inoculation method was successful in depositing a significant proportion of the bacteria into the teat canal, the bacterial load within the teat canal lining was assessed. For all eight cows examined, a sizeable number of bacterial colonies were grown from the *S. aureus* and *S. uberis* inoculated quarters. Colonies were provisionally identified by morphology, haemolysis patterns, coagulase activity and the cleavage of esculin. Two representative samples from Group A and Group B are shown in Figure 6.3. In these examples, two of the four control quarters, which received only the vehicle, showed minor bacterial contamination that resembled *Staphylococcus* species (Group B; #862 and #1238). Rabbit plasma coagulase testing of two randomly selected isolates from the control quarters showed no coagulation after 24 h incubation. It is likely that this infection is from a resident CNS species and not due to cross-infection from inoculation of *S. aureus* into the neighbouring teat. All other control quarters were assessed as uninfected.

Interestingly, the growth of *E. coli* on the blood agar plates was variable. For example, swabs taken from two Group A cows (#225 and #708) grew very few *E. coli* colonies (shown in Figure 6.3), whereas swabs from the remaining two Group A cows and all four Group B cows grew sizeable number of *E. coli* colonies.

There are three plausible explanations for this variation. Firstly, *E. coli* inoculation into different teat canals could have been unequal, resulting in fewer *E. coli* being transferred into the teat canal. Secondly, swabs may have been taken in the wrong place and did not accurately sample the infected area of the teat canal lining. Bacteria are motile and could spread along the teat canal during the 24 h incubation period and may not be restricted to where they were originally deposited. A third possibility is that the host-defence capability within the teat canal of some cows may be more effective at eliminating or restricting the growth of the *E. coli*. In support of this option, transient colonisation of *E. coli* within the teat canal has been

previously observed, with infection seldom persisting for more than four days (Bramley *et al.*, 1979).

In summary, the results of these analyses demonstrated that the inoculation was successful in depositing the bacteria into the teat canal and that the bacteria were still present 24 h post-inoculation in all the challenged teats. The results also showed that once closed, the teat canal effectively prevented the infiltration of bacteria into the teat sinus and the lower mammary gland, at least during the initial 24 h period post-inoculation.

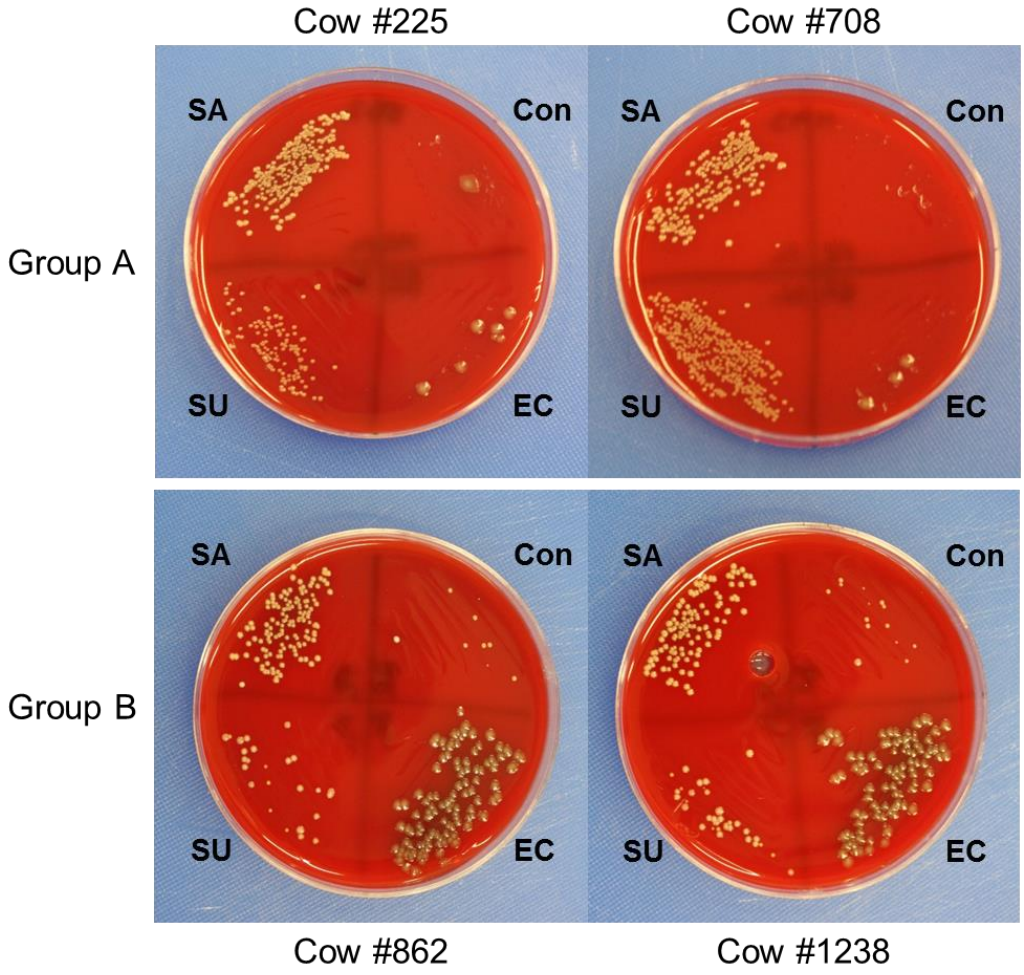

Figure 6.3: Teat canal swab samples from two selected Group A and Group B cows.
Swabs of teat canal lining, collected before tissue processing were rinsed with 10 µL 0.85 % sterile saline solution pre-spotted on blood agar plates and then streaked over one-quarter of the plate. The colonising species and colony density were assessed 24 h after incubation at 37 °C. **Note:** Cows #862 and #1238 showed a minor CNS infection in the control quarter, and cows #225 and #708 produced almost no *E. coli* colonies from the teat canal swabs. The dominant species cultured from each teat canal sample showed the morphological and biochemical characteristics of the inoculated bacteria.

6.4. Comparative proteomic analysis of teat canal lining proteins after inoculation with specific bacteria

6.4.1. Comparative 2-DE analysis using PDQuest

Teat canal lining proteins collected separately from 16 teats were extracted using the 2D lysis buffer, as previously described (See Section 2.2.2). The total yield of teat canal lining (wet-weight) collected from each teat, along with the amount of total protein extracted out of the individual teat canal lining samples are summarised in Table 6.2. The average amount of extracted proteins, as determined by the 2D-Quant assay, was 19 ± 0.6 % of the original wet weight and there was no significant difference in total recovery, based on inoculation treatment group. An SDS-polyacrylamide gel with 10 µg of teat canal lining protein per sample lane was stained with colloidal Coomassie blue and subjected to densitometry to confirm sample protein concentrations and equal protein loading (Figure 6.4).

Approximately 525 µg of teat canal lining protein, evenly apportioned from each teat within a treatment group, was combined to create four pooled samples totalling 2.1 mg of protein. Samples from each treatment group pool were subjected to 2-DE analysis in triplicate (350 µg per gel) (Figure 6.5). Replicate analysis sets for pooled control teat canal lining (Con), pooled *E. coli* infected teat canal lining (EC), pooled *S. aureus* infected teat canal lining (SA) and pooled *S. uberis* infected teat canal lining (SU), were compared using PDQuest. The pooled bacterial-infected samples were each compared with the pooled control sample.

Representative gels from each of the groups are shown in Figure 6.6. Twenty-five protein spots with greater than two-fold difference in abundance ($p < 0.05$) between the analysis sets were determined (Table 6.3) and are arrowed and labelled in Figure 6.6. Compared with the treatment control (Con) samples, all treatment groups showed some changes in the abundance of some protein spots. These protein spots were, for the most part, very low abundant proteins, that made MS identification of them difficult. However, of the more abundant proteins, some keratin protein isoforms showed changes in relative abundance. The normalised spot quantity data, calculated by PDQuest, is summarised in Supplementary data Tables D2-D4.

Table 6.2: Amount of solubilised protein obtained from teat canal lining 24 h after bacterial inoculations

Group[a]	Cow#/[b] Quarter	SCC[c] (x10^3 cells/mL)	TCL[d] (mg wet-weight)	Total yield of protein (mg)	% (mg/mg wet-weight)
Control	225/FL	108	6.8	1.40	20.6
S. aureus	225/FR	169	7.9	1.28	16.2
E coli	225/BL	113	6.9	1.40	20.3
S. uberis	225/BR	35	7.6	1.04	13.7
Control	708/FL	197	7.1	1.44	20.3
S. aureus	708/FR	159	4.5	1.00	22.2
S. uberis	708/BL	150	7.5	1.04	13.9
E coli	708/BR	98	6.0	0.76	12.7
S. aureus	1193/FL	174	6.1	1.68	27.5
Control	1193/FR	127	6.3	0.60	9.5
S. uberis	1193/BL	186	6.0	1.16	19.3
E coli	1193/BR	168	5.9	0.84	14.2
S. uberis	1348/FL	103	6.2	2.08	33.5
Control	1348/FR	76	6.6	1.60	24.2
S. aureus	1348/BL	123	5.9	1.04	17.6
E coli	1348/BR	62	6.1	1.12	18.4
	Ave. ± SD	*128 ± 47*	*6.5 ± 0.8*	*1.2 ± 0.4*	*19 ± 0.6*

a) Bacterial inoculation groups for pooled samples
b) FL, left forequarter; FR, right forequarter; BL, left hindquarter; BR, right hindquarter
c) SCC, milk somatic cell count immediately before inoculations
d) TCL, teat canal lining

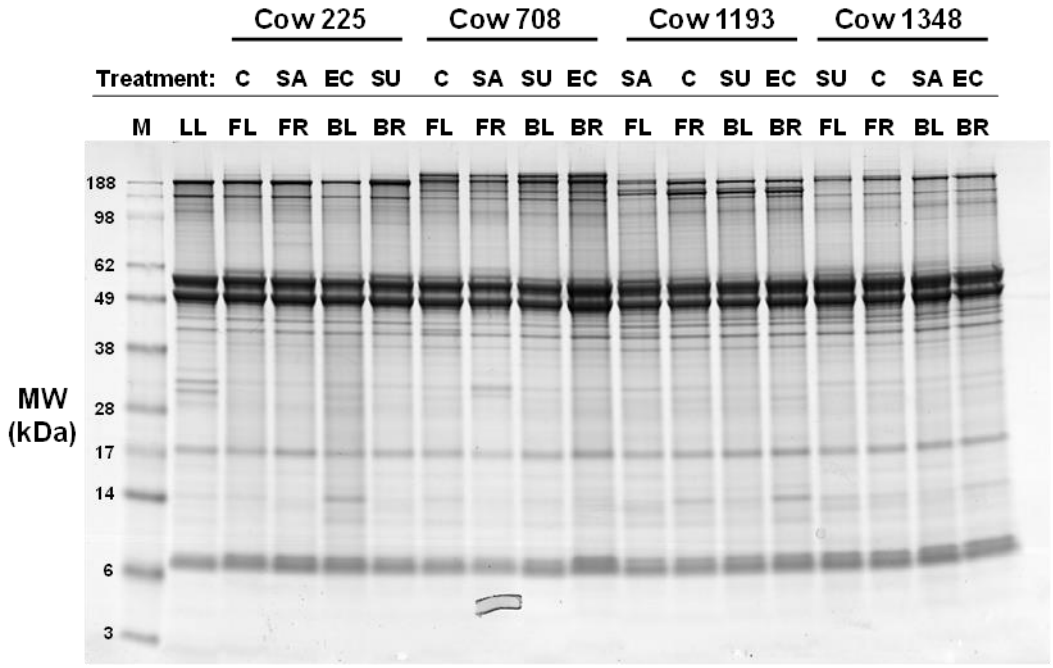

Figure 6.4: Extracts of teat canal lining proteins 24 h after bacterial challenge.
12 % Criterion Bis-Tris gel loaded with 10 µg of total protein per sample was stained with Coomassie blue G-250 to demonstrate equal loading. The late-lactating (LL) sample 5FR was loaded to show consistency between 2D-Quant assays performed previously on late-lactating and involution teat canal lining samples. M, SeeBlue Plus2 molecular weight marker; C, Control teat; EC, *E. coli* challenged teat; SA, *S. aureus* challenged teat; SU, *S. uberis* challenged teat; FL, left forequarter; FR, right forequarter; BL, left hindquarter; BR, right hindquarter.

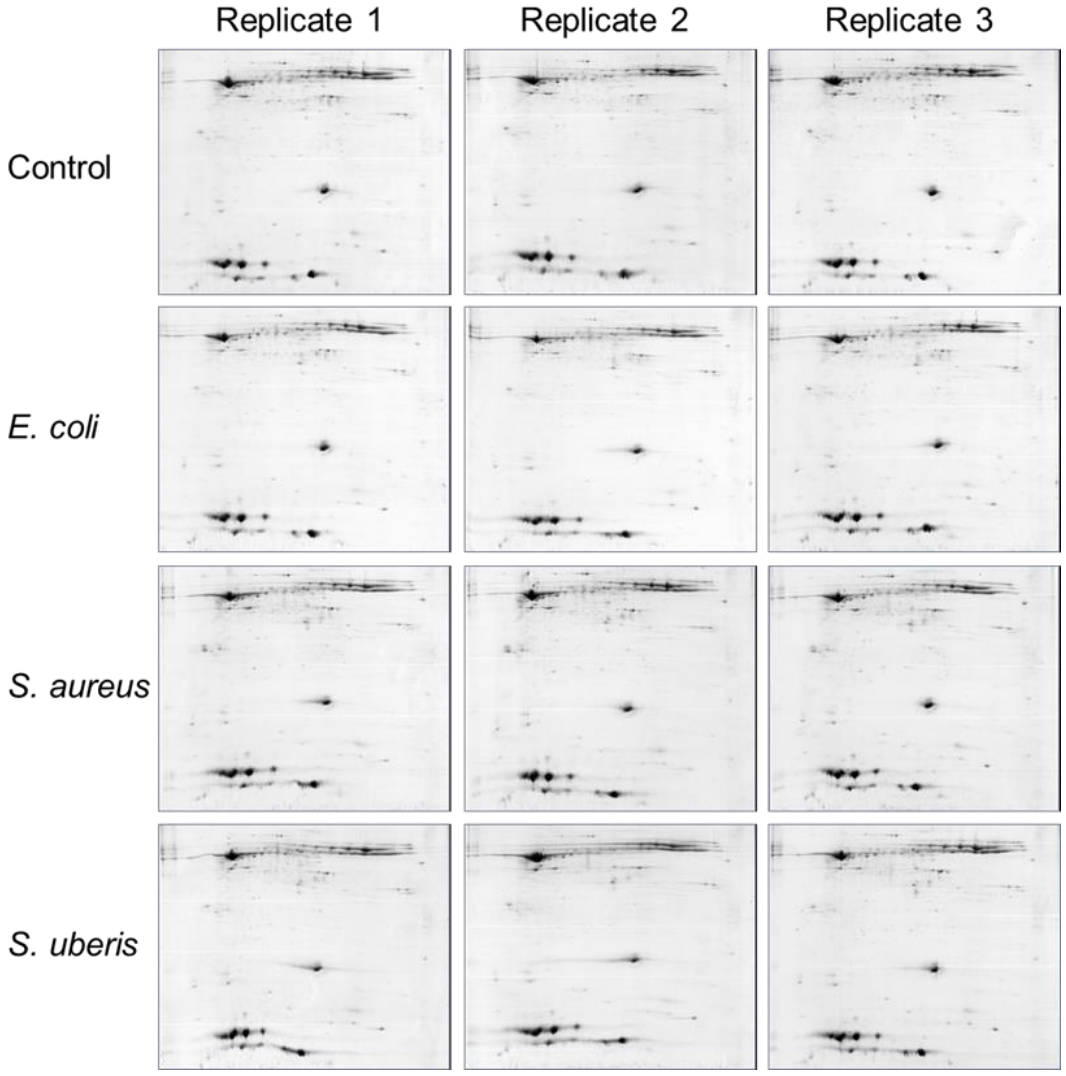

Figure 6.5: Coomassie-stained 2-DE gels (pH 3-11) of pooled teat canal lining proteins from experimentally infected and control teats.
Teat canal lining samples inoculated with *E. coli*, *S. aureus*, *S. uberis* and vehicle only (control) were pooled from four individual cows, and 350 µg of solubilised protein were separated by IEF and 14 % SDS-PAGE. Pooled samples were run in triplicate, and gel images were captured using a GS800 calibrated densitometer and Quantity One software.

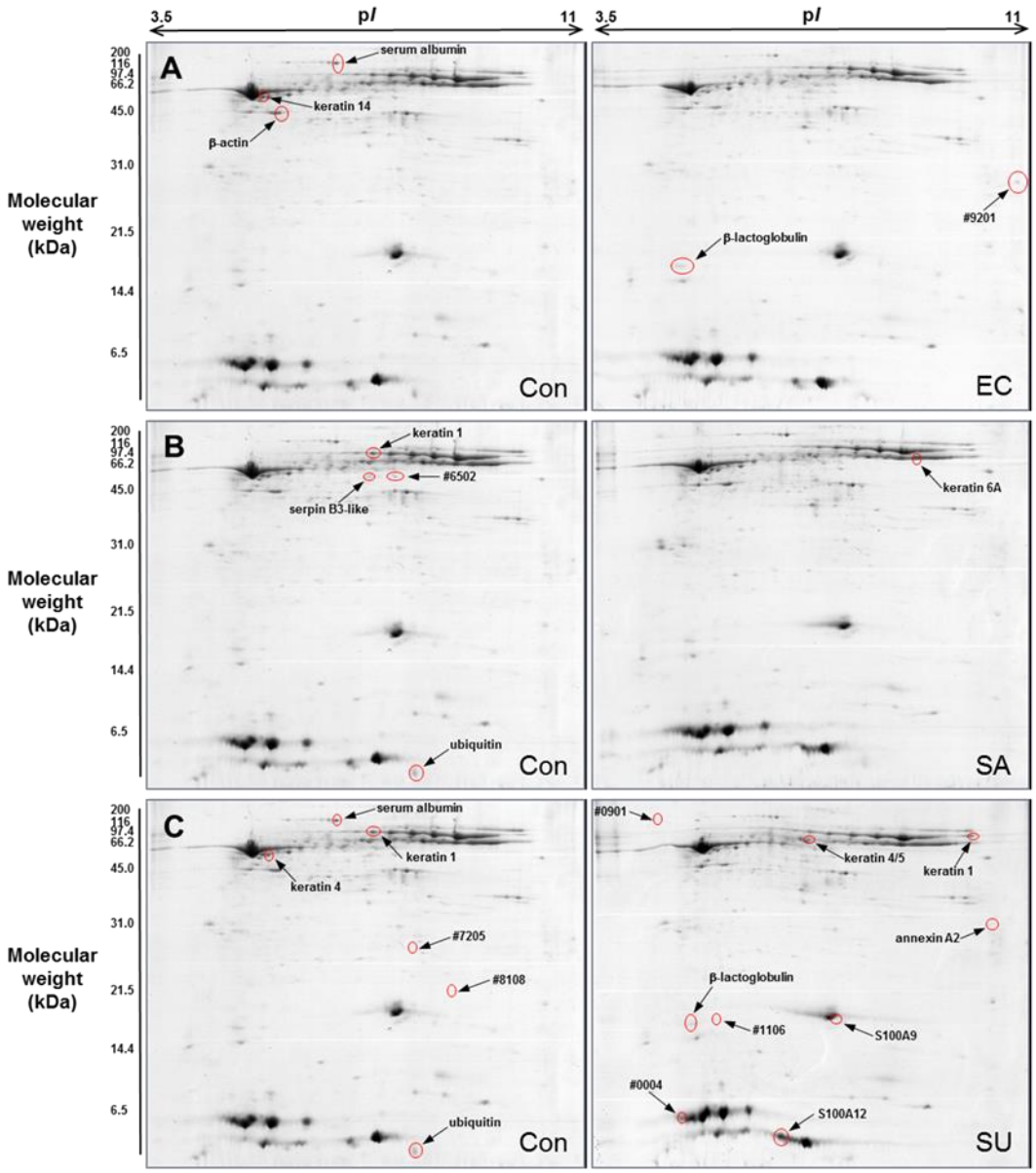

Figure 6.6: Representative 2-DE gels showing spot differences between infected teat canal lining versus uninfected (control) teat canal lining.

Twenty-five protein spots (circled and arrowed) were significantly changed in abundance ($p < 0.05$) between each comparative gel-set. These spots are listed in Table 6.4. Unidentified proteins are annotated with their SSP number specified by PDQuest. Con, Control; EC, *E. coli*; SA, *S. aureus*; SU, *S. uberis*.

Table 6.3: Summary of a ≥ two-fold abundance change in 2-DE protein spots ($p < 0.05$) for infected teat canal lining groups versus the uninfected control teat canal lining group.

E. coli	SSP[a]	Con (Ave.)[b]	SD[c]	*E. coli* (Ave.)[b]	SD	Fc[d]	*p*-value	Identified protein
	104	4.5	1.2	9.2	0.3	2.04	0.003	*spot not identified*
	1507	37.8	11.8	10.6	2.5	0.28	0.018	keratin 14
	2401	18.3	2.7	8.2	5.3	0.45	0.044	β-actin
	4901	20.8	4.2	7.5	1.5	0.36	0.007	serum albumin
	9201	3.7	2.2	11.0	1.8	2.98	0.011	*spot not identified*
S. aureus	**SSP**	**Con (Ave.)**	**SD**	***S. aureus* (Ave.)**	**SD**	**Fc**	***p*-value**	**Identified protein**
	6502	4.6	0.4	2.3	0.3	0.50	0.0013	*spot not identified*
	6504	11.1	4.1	1.6	0.5	0.14	0.0162	serpin B3-like
	6801	26.7	5.4	12.6	6.8	0.47	0.047	keratin 1
	7001	18.7	2.5	5.7	0.9	0.30	0.001	ubiquitin
	8708	27.8	4.0	89.7	15.4	3.22	0.003	keratin 6A
S. uberis	**SSP**	**Con (Ave.)**	**SD**	***S. uberis* (Ave.)**	**SD**	**Fc**	***p*-value**	**Identified protein**
	4	24.4	22.3	66.0	9.2	2.71	0.040	*spot not identified*
	901	0.7	0.6	2.4	0.4	3.65	0.016	*spot not identified*
	1106	3.0	2.8	8.2	1.4	2.70	0.044	*spot not identified*
	1110	2.3	1.6	10.9	2.2	4.81	0.005	β-lactoglobulin
	2501	26.5	5.4	12.4	2.1	0.47	0.013	keratin 4
	4002	78.1	33.5	165.7	38.8	2.12	0.041	S100A12
	4901	17.4	4.1	8.9	2.1	0.50	0.033	serum albumin
	5604	9.5	6.5	35.1	14.4	3.68	0.049	keratin 4/5
	5701	27.9	8.3	12.0	4.8	0.43	0.045	keratin 1
	7001	17.9	2.2	7.7	2.9	0.43	0.008	ubiquitin
	7104	4.7	2.9	10.0	0.7	2.11	0.036	S100A9
	7205	2.8	0.5	1.0	0.9	0.34	0.034	*spot not identified*
	8108	3.4	0.6	1.2	0.9	0.37	0.029	*spot not identified*
	8204	1.4	0.9	3.9	1.3	2.88	0.043	annexin A2
	9704	6.2	2.8	12.8	2.9	2.05	0.049	keratin 1

a) SSP, PDQuest protein spot identification number; b) Ave, average spot intensity (n = 3); c) SD, standard deviation; d) Fc, fold-change.

6.4.2. Label-free quantitation using GeLC-MS/MS and SpC

The large abundance of keratin proteins over the whole width of the 2-DE gel is an impediment for accurate quantitation of low abundance proteins migrating at a similar molecular mass and isoelectric point. To overcome this issue, label-free quantitation by SpC was used to assess changes in the relative protein abundance of teat canal lining proteins from each of the four treatment groups; Control (Con), *E. coli* (EC), *S. aureus* (SA) and *S. uberis* (SU).

A preparative SDS-PAGE gel, resolving 25 µg/lane of teat canal lining proteins from each individual teat of the four trial cows (n = 16) was run for GeLC-MS/MS analysis. A total of 128 fractions derived from 8 combinations of slices from each of the 16 gel lanes were subjected to GeLC-MS/MS analysis, resulting in the generation of 133,692 fragment spectra (See Supplementary data Table D5). These spectra were submitted to a Mascot database search using the identification criteria previously described (See Section 2.2.13) at an FDR of 5.0 %. A total of 137, 107, 141, and 114 distinct proteins with two or more unique peptides were identified in the Con, EU, SA and SU treatment groups, respectively. This represented a peptide assignment rate of 8.0 % from the bovine non-redundant database. The exported Mascot DAT files were then imported and consolidated into Scaffold Q+ for label-free quantitation. Bioinformatic analysis by Scaffold Q+, incorporating the XTandem! database searching algorithm resulted in the matching of 40701 spectra to peptides (at a 95 % confidence interval; 0.23 %. FDR) and the identification of 140 unique proteins (at a 99.9 % confidence interval; 0.0 %. FDR) with at least two peptides per protein (See Supplementary data Table D6). This second round of protein identification detected 123, 106, 134, and 118 distinct proteins with two or more unique peptides in the Con, EU, SA and SU treatment groups, respectively.

Combining the protein lists for all four treatments and removing redundancies resulted in a list of 140 unique proteins identified by two or more unique peptides. Among the 140 identified proteins, peptide spectra for 98 (70 %) proteins were observed to be common to all four treatment groups. Six unique proteins (4.3 %) were identified only in the *S. aureus* treatment group, and two unique proteins

(1.3 %) were identified in only the *S. uberis* treatment group (Figure 6.7). However, within both of the *S. aureus* and *S. uberis* treatment groups, none of these unique proteins were identified in all four animal samples, and all of the proteins exhibited low SpC (i.e. < 5). This result would suggest that the abundance of these proteins is at the limit of detection using the current GeLC and MS parameters.

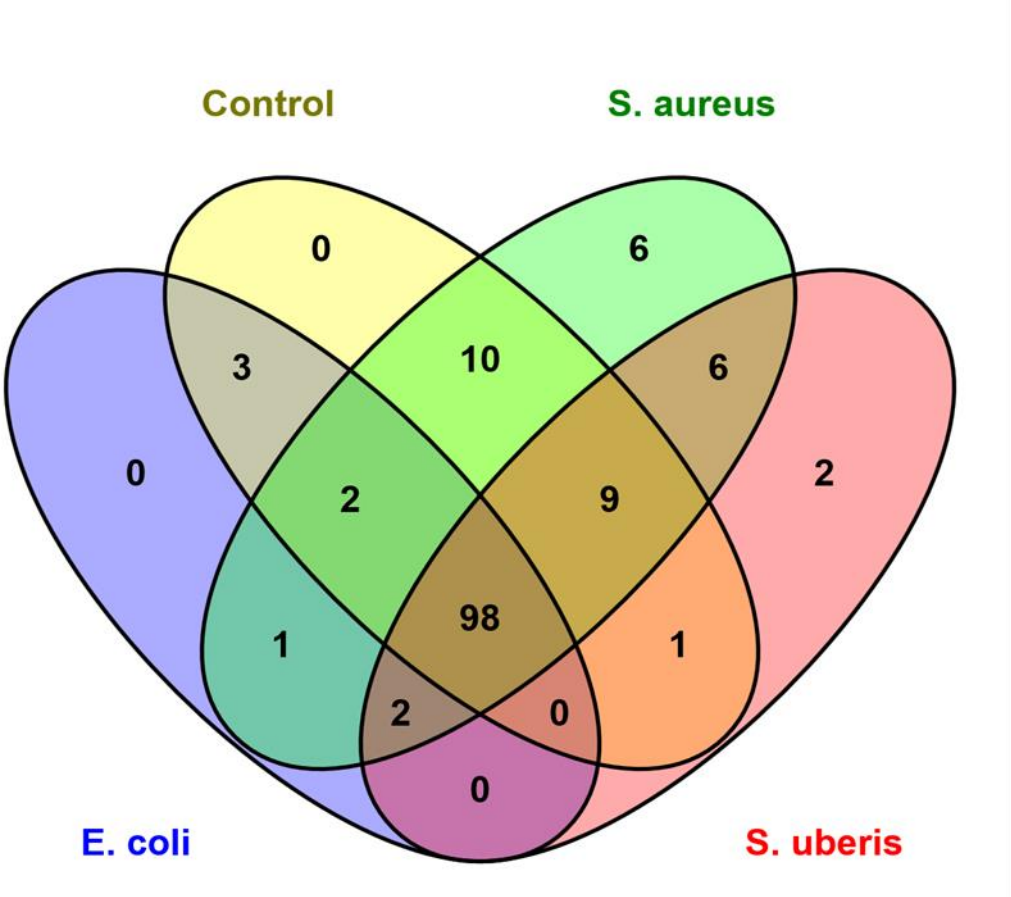

Figure 6.7: Venn diagram of total proteins found in common between each treatment group. Venn diagram was generated using VENNY (Oliveros, 2007-2015).

To identify proteins that were altered in abundance by the presence of bacteria, the relative abundance levels of 140 proteins detected in all 16 teat canal lining samples were determined by SpC-based quantitation (See Supplementary data Table D6). Fold change values for each protein was determined by dividing the average SpC of the protein in the bacterial challenge treatment group by that in the control group. A protein with a value two-fold or greater (≥ 2.0) than the control group value was deemed to be substantially increased in relative abundance, while proteins with a value less than half (≤ 0.5) of the control group value were considered to be markedly decreased in relative abundance. Abundance ratios and *p*-values for each treatment group were calculated from untransformed data.

Seven unique proteins were found to be significantly altered in relative abundance between the four treatment groups. For the *E. coli*, *S. aureus* and *S. uberis* treatment groups, a total of 4, 6 and 6 unique proteins were found to be increased in relative abundance, respectively, using the normalised total SpC. The identities of these proteins are listed in Table 6.4 together with the fold differences in abundance and *p*-values.

Table 6.4: Proteins altered in relative abundance with the bacterial challenge treatment and identified by SpC.

			Normalised Total SpC[c] ratio			***p*-value versus control[d]**		
Protein name	**#[b]**	**Accession[a] No.**	***E. coli* /Con**	***S. aureus* /Con**	***S. uberis* /Con**	***E. coli***	***S. aureus***	***S. uberis***
serum albumin	28	gi|30794280	2.89	4.57	3.00	0.047	0.065	0.028
GAPDH[e]	34	gi|77404273	0.55	0.49	0.64	0.004	0.016	0.088
HSP[f] beta-1	52	gi|529007450	0.75	6.00	2.25	0.822	0.001	0.128
PAUF[g]	64	gi|296473587	3.40	3.80	3.40	0.069	0.044	0.046
transferrin	82	gi|114326282	2.50	8.50	2.50	0.015	0.021	0.080
lactoferrin	97	gi|163285	4.60	14.20	14.80	0.006	0.050	0.049
apolipoprotein A-I	103	gi|162678	1.25	7.25	4.00	0.391	0.040	0.154

a) Accession No., gene index protein accession number from NCBI; b) protein number as listed in Supplementary data Table D5; c) SpC, spectral count; d) *p*-value determined using paired Student's *t*-test; e) GAPDH, glyceraldehyde-3-phosphate dehydrogenase; f) HSP, heat shock protein; g) PAUF, pancreatic adenocarcinoma upregulated factor-like protein.

A unique protein identified by GeLC-MS/MS analysis and found to be more abundant in teat canal lining from the three bacterial treatment groups was pancreatic adenocarcinoma upregulated factor-like protein (PAUF). Using the NCBI blast sequence analysis tool, PAUF is 100 % identical to another predicted bovine protein: zymogen granule protein 16 homolog B-like (XP_010823954.1). This protein contains a conserved Jacalin-like lectin binding domain that enables members of the Jacalin-like superfamily to bind to carbohydrate moieties (Kabir, 1998). PAUF has previously been identified as a minor protein component of mastitic cow's milk (Smolenski *et al.*, 2014).

PAUF was originally identified as a protein which is upregulated in pancreatic cancers, hence its name (Kim *et al.*, 2009). Recent research has demonstrated that PAUF is an endogenous ligand for TLR2 and TLR4 and stimulates inflammatory signalling (Kim *et al.*, 2011; Park *et al.*, 2011a). Furthermore, it has been shown that PAUF can act as an adjuvant, enhancing the immune response of dendritic cells to antigens. While these results establish that PAUF has immune modulating properties, its role in the teat canal is unknown.

Only one protein in the inoculated groups was found to be markedly decreased in relative abundance compared with the control group. Glyceraldehyde-3-phosphate dehydrogenase (GAPDH) was found to be two-fold less abundant in the *S. aureus* treatment group. In both the *E. coli* and *S. uberis* treatment groups, this protein also displayed a similar trend, with a 1.8-fold and a 1.6-fold decrease in relative abundance, respectively. The 1.8-fold reduction in the *E. coli* challenged sample was also found to be statistically significant ($p = 0.004$).

The samples from the *S aureus* treated teats showed the greatest response to inoculation of bacteria. In these samples, all seven significantly altered proteins showed the largest average fold-change in relative abundance, compared to corresponding proteins identified in the *E. coli* and *S. uberis* treatment samples. Interestingly, samples from *E. coli* challenged teat canals showed the least responsiveness to bacterial challenge. Limited colonisation of the teat canal by *E. coli* has been previously observed by Bramley and colleagues using up to 43000 cfu, indicating that *E. coli* might produce a weaker response (Bramley *et al.*,

1979). Therefore, in this study 500,000 cfu of *E. coli*, which was 11 times more than what Bramley applied and as much as 200 times more cfu used for both the *S. aureus* and *S. uberis* inoculum, were deposited into the teat canal. This observation, taken together with the variable growth of *E. coli* from the bacterial swabs (Figure 6.3), would suggest that the teat canal is effective at managing and eliminating *E. coli* infections.

Among these seven proteins that had a two-fold or more change in relative abundance, serum albumin, lactoferrin, transferrin, and pancreatic adenocarcinoma upregulated factor-like protein (PAUF) were found to be altered for all three bacterial challenge treatments. Five of the six proteins, which were increased in relative abundance, have been documented to have innate immune function. These include lactoferrin, transferrin, PAUF, heat shock protein beta-1 (HSP27) and apolipoprotein A-I.

In the data set of 140 unique proteins, there is the possibility that up to seven proteins could be altered by random chance or random sampling error (5 %), using the settings that were selected for the XTandem! analysis. To minimise the likelihood of this analytical error, the relative quantification of the bacterial challenge data set was performed using both the normalised total raw data and NSAF algorithms packaged with the Scaffold Q+ software as well as the EmPAI algorithm from Mascot (See Supplementary data Table D7). Comparison of all three algorithms revealed similar fold changes from the SpC of all seven proteins. However, the level of significance was reduced for some of the proteins, making their relevance less clear. For this reason, another validation method was required to confirm the SpC observations.

6.4.3. Validation of SpC results by Western blot analysis

To confirm the differences in relative protein abundance that was determined by SpC, Western blot analysis was performed on three of the four up-regulated proteins with likely host defence function. Bovine specific (lactoferrin and PAUF) and cross-reacting (anti-human transferrin) polyclonal antibodies were used to probe Western blots of the teat canal lining protein samples (n = 16). All analyses were performed in triplicate on independent gels, and representative images for each of the three different antibodies are shown (Figure 6.8). The mean intensity of lactoferrin, transferrin, and PAUF positive protein bands, relative to the positive control sample, was obtained for each of the triplicate Western blots.

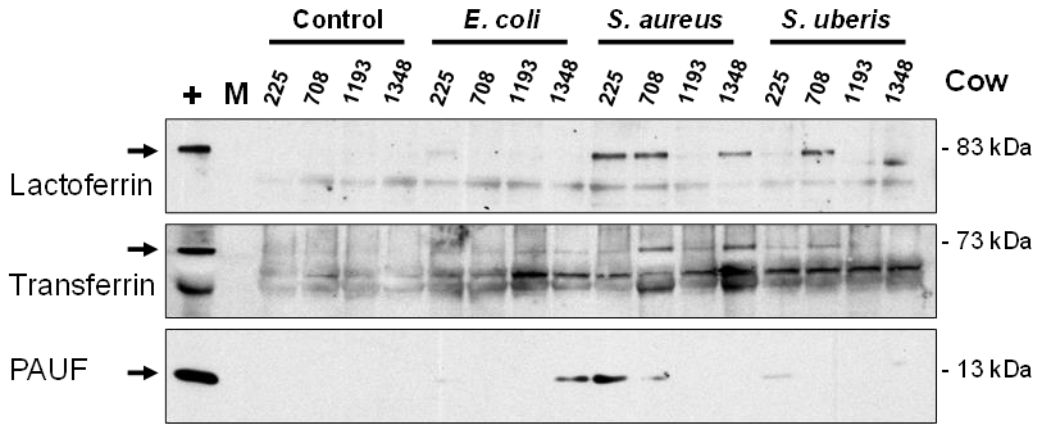

Figure 6.8: Proteins with reported host-defence properties are increased in abundance in response to 24 h bacterial challenge.
Western blots of teat canal lining samples containing 5 µg, 20 µg, and 30 µg, of total protein, separated by 12.5 % Bis-Tris SDS-PAGE, were probed with antibodies against lactoferrin, transferrin and PAUF, respectively. The signal was detected by chemiluminescence. Positive control for lactoferrin was 5 µg of cows' whey, with an exposure time of 3 min. Positive control for transferrin was 10 µg of cows' serum, with an exposure time of 4 min. Positive control for PAUF was 2 µg of Bali Cattle saliva, with an exposure time of 5 min. Positive control bands at the correct molecular weight are arrowed. M, SeeBlue Plus2 molecular weight marker.

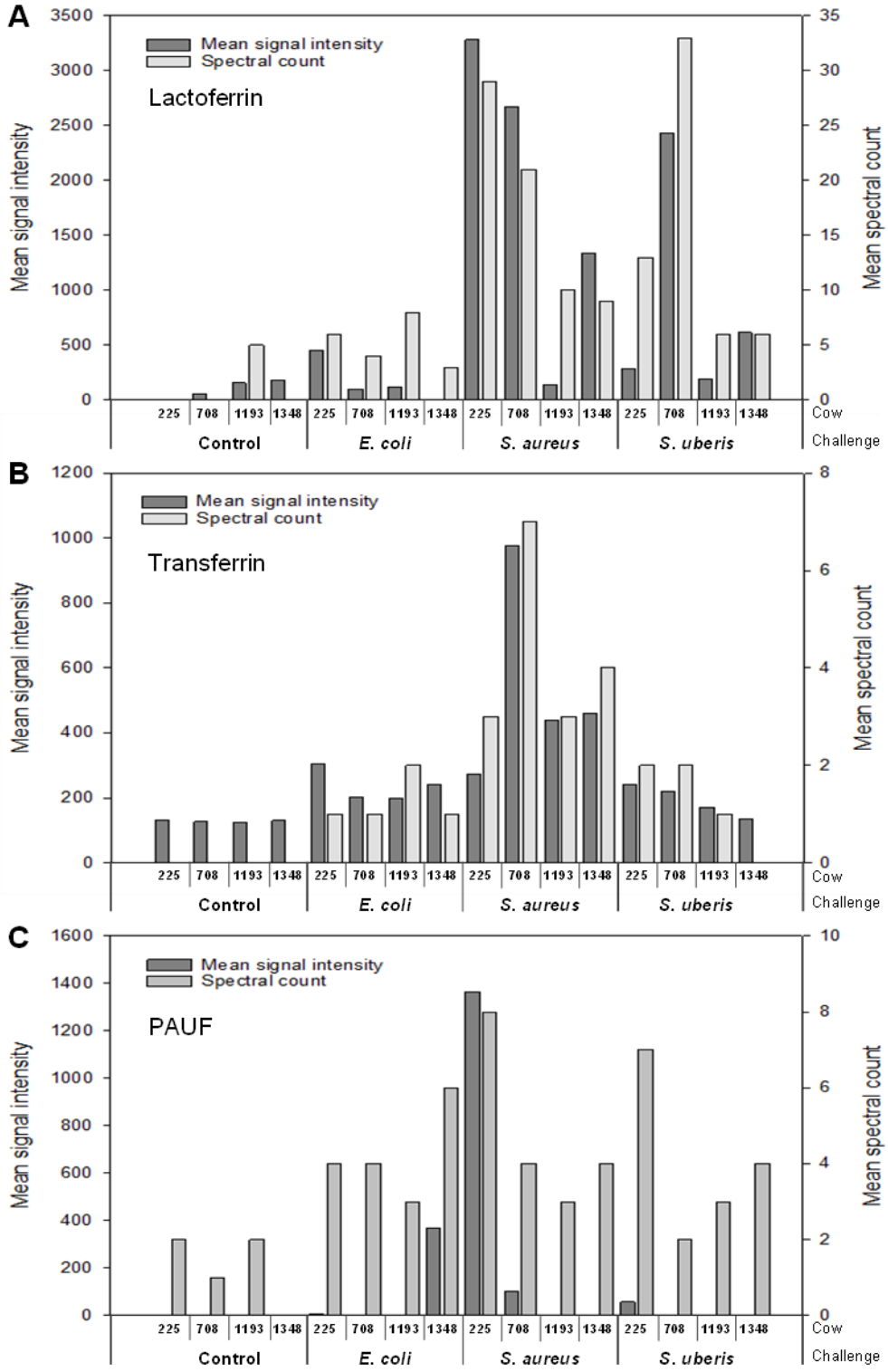

Figure 6.9: Mean densitometric intensities from Western blots versus mean SpC within teat canal lining samples.

Teat canal lining proteins were subjected to quantitative Western blotting using each positive control as an internal standard. The chemiluminescence signals were captured by a CCD camera and densitometry performed on the images. The mean densitometric values from three replicates for each sample were plotted against the mean SpC from triplicate GeLC-MS/MS analysis.

Comparisons were looked for between Western blot analysis results and SpC results for all samples (Figure 6.9). Calculated Pearson correlation coefficients between the two sets of data indicated strong positive correlations for lactoferrin (R^2 = 0.7991) and transferrin (R^2 = 0.8750), whereas the correlation between results from Western blot and SpC for PAUF (R^2 = 0.4409) was only moderate.

The anti-bovine lactoferrin antibody recognised several bands, including one at approximately 83 kDa, which corresponds to the predicted molecular mass of lactoferrin. The lower, less intense band at approximately 55 kDa appears evenly across all of the samples, which suggests that this signal is from a nonspecific cross-reacting species. In the four treatment control samples (lanes 3-6), no signal for lactoferrin was detected. This is in agreement with the previous proteomic findings. The lactoferrin band was detected in three of the four samples from the *S. aureus* challenge whereas only cow #708 showed a lactoferrin band after challenge by *S. uberis*. There was no obvious increase in lactoferrin in response to a challenge with *E. coli*. The samples that showed the greatest increase in lactoferrin abundance by Western blotting matched the samples with the highest mean SpC (Figure 6.9a). Because of the low sample number (n = 4) and wide variation in lactoferrin response from the *S. aureus* challenge, mean lactoferrin levels from this treatment group were not significantly different when compared with the treatment control samples (p = 0.099).

The anti-human transferrin antibody has been shown to cross-react with purified bovine transferrin in our laboratory (Ledgard, *personal communication*). However, when used on the teat canal lining samples, cross-reactivity was seen against proteins in the 50 kDa to 55 kDa region of the gel, where the keratin proteins are located. Nonetheless, transferrin in the teat canal lining samples appeared to migrate above this non-specific binding at approximately 73 kDa, as expected. This was the same molecular mass as the bovine transferrin found in the bovine serum positive control sample. Like lactoferrin, and in agreement with the previous proteomic findings, there was no observable transferrin protein band in the four treatment control samples. There was a slight increase in the mean levels of transferrin in the *E. coli* ($p < 0.05$) and *S. uberis* (p = 0.16) challenged samples. The largest increase in transferrin abundance was in the *S. aureus*

challenged samples, where a six-fold increase was observed ($p < 0.01$). The samples that showed the greatest increase in transferrin abundance by Western blotting matched the samples with the highest mean SpC (Figure 6.9b).

Unlike the lactoferrin and transferrin antibodies, the anti-bovine PAUF antibody gave clean, specific signals with the immunoreactive band for PAUF in the positive control sample migrating at approximately 13 kDa. This is smaller than the predicted molecular mass of 14.9 kDa for the annotated form of the protein in the NCBI database (DAA15702.1) and smaller than what had previously been reported in Bali Cattle saliva (Depamede, 2013). However, as the Bali Cattle saliva positive control also ran at the same molecular mass as the immunoreactive protein bands in the bacterial challenge samples, the difference in molecular weight could be due to the different SDS-PAGE resolving conditions and molecular weight markers used in this study.

Consistent with the previous proteomic findings, PAUF was not found in the treatment control teat canal lining samples. It was, however, only upregulated in a small number of samples from the challenged teat canals, with an irregular level of abundance compared to that of lactoferrin and transferrin. The samples that showed the greatest increase in PAUF abundance by Western blotting also corresponded well to the samples with the highest mean SpC (Figure 6.9c).

6.4.4. IHC localisation of lactoferrin, transferrin and PAUF in teat canal keratinocytes and teat canal lining

Serum albumin, transferrin and apolipoprotein A-I are well-known plasma proteins, and their increased abundance in the teat canal lining in response to a bacterial challenge is intriguing. Plasma exudation during inflammation has been well documented and is an important mucosal and epithelial defence mechanism (Persson *et al.*, 1991; Persson *et al.*, 1993; Linardi *et al.*, 2000). Alternatively, these proteins could be derived directly from the milk through leakage of the teat canal sphincter, or they may be expressed by the keratinocytes lining the lumen of the teat canal in response to the infection. Interestingly, proteomic analysis only identified low levels of casein proteins in the teat canal lining, so it is unlikely they came from the milk. However, in support of the later possibility, previous

investigations have shown that both lactoferrin and transferrin are expressed by skin and mucosal epithelial cells (Mason & Taylor, 1978).

To provide some insight into the likely source of the lactoferrin, transferrin, or PAUF proteins in the teat canal lining, IHC was performed on teat canal cryosections from each of the four different treatment groups. While IHC only shows where proteins are localised in the tissues, the concentration and distribution of these proteins may provide clues to their origin. Cows from Group B used for IHC analysis are listed Table 6.5.

Table 6.5: Group B cows and inoculation strategy used for IHC analysis from bacterial challenge study.

Cow #	Quarter	Bacterial challenge
428	Left forequarter	milk
	Right forequarter	*S. aureus*
	Left hindquarter	*E. coli*
	Right hindquarter	*S. uberis*
862	Left forequarter	*S. aureus*
	Right forequarter	milk
	Left hindquarter	*S. uberis*
	Right hindquarter	*E. coli*
1238	Left forequarter	*S. uberis*
	Right forequarter	milk
	Left hindquarter	*S. aureus*
	Right hindquarter	*E. coli*
1312	Left forequarter	milk
	Right forequarter	*S. aureus*
	Left hindquarter	*S. uberis*
	Right hindquarter	*E. coli*

6.4.4.1. Lactoferrin:

IHC analysis of teat canal sections from the bacterial challenge study revealed a strong signal for lactoferrin in the epidermal layer of the teat canal epithelium for *S. aureus, S. uberis* and *E. coli* challenged tissue samples (Figure 6.10). Some of the signal appeared to be localised around the keratinocyte nuclei. Lactoferrin signal was also concentrated in the cornified layer of the teat canal lining,

especially in the *S. aureus* infection model. A strong signal was observed in the basal epithelial cells in the boundary between the epidermis and the subepithelial stroma. No signal was detected in the epithelial tissues and the teat canal lining, using non-specific IgG isotype controls. Figure 6.10 is representative for all four cows analysed by IHC.

There was a strong signal for lactoferrin observed in the *stratum basale* layer of the epithelium. It could not be determined in this study whether the basal localisation of lactoferrin was a real result or an artefact due to nonspecific binding to keratin proteins. Western blotting showed the lactoferrin antibody binding to a faint band at approximately 50 kDa in all teat canal lining samples (Figure 6.8). It is possible that this could be the antibody cross-reacting with a keratin protein. However, it is important to note that this signal is absent in the treatment control samples, providing good evidence against this possibility. The selective binding of lactoferrin to heparin sulfate, a major component of the basement membrane which separates the epithelium from the underlying connective tissue, has been previously reported (Zou et al., 1992) which would also support this observation.

6.4.4.2. Transferrin:

IF with the anti-human transferrin antibody produced a strong signal in the cornified layer of the *S. aureus* challenged teat canals whereas the signal was less intense in the *S. uberis* and *E. coli* challenged teat canals (Figure 6.11). A minute amount of signal was also observed in the cornified layer of the control teat canal lining. Like lactoferrin, Western blotting (Figure 6.8) showed non-specific binding of the transferrin antibody with what appears to be keratin proteins, suggesting that some of the IF signal might be due to non-specific interaction. However, the transferrin signal was absent from the epithelial layer of the control teat canal tissues (Figure 6.11) and the treatment control samples in the Western blots (Figure 6.8), providing good evidence against this possibility. In all 12 of the bacterial-challenged tissue samples, especially the *S. aureus* samples, signals for transferrin were observed in the cytoplasm of the teat canal keratinocytes. The intensity of the signal was more noticeable in the *S. aureus* sections while both the

E. coli and *S. uberis* sections had a similar signal of lesser intensity. The pattern of staining and the cellular localisation for transferrin was different to that for lactoferrin. No signal was detected in the epithelial tissues and the teat canal lining using non-specific IgG isotype controls.

Although there remains some doubt upon the reliability of the cross-reactive transferrin antibody, there was no signal in the treatment control samples and the transferrin staining was restricted to specific areas of the epithelium rather than just generalised staining. Future use of a transferrin antibody derived from a bovine antigen may provide a clearer picture of transferrin abundance and distribution in the teat canal lining and epithelium.

6.4.4.3. PAUF:

The fluorescent signal obtained with the anti-PAUF antibody was weaker than that observed for lactoferrin and transferrin, requiring the exposure time to be increased from 600-800 ms to 2500 ms. The micrographs presented provide the strongest signal with the *S. aureus* challenge when probed with the PAUF polyclonal antibody (Figure 6.12). In the treatment control teat canal of these images, a faint signal for PAUF was observed throughout the epidermal layer of the teat canal. However, a noticeable increase in PAUF signal in the epidermal layer was observed for teat canals infected with *E. coli* and *S. aureus*, although the intensity of the signal was variable between individual cows. Cows with the strongest PAUF signal in the epithelium also tended to have the strongest signal in the cornified layer, which was especially evident for the *S. aureus* infected teat canals. In contrast, the *S. uberis* infected teat canal only showed a slight increase in PAUF signal compared to the treatment control tissues. No signal was detected in the epithelial tissues and the teat canal lining using non-specific IgG isotype controls.

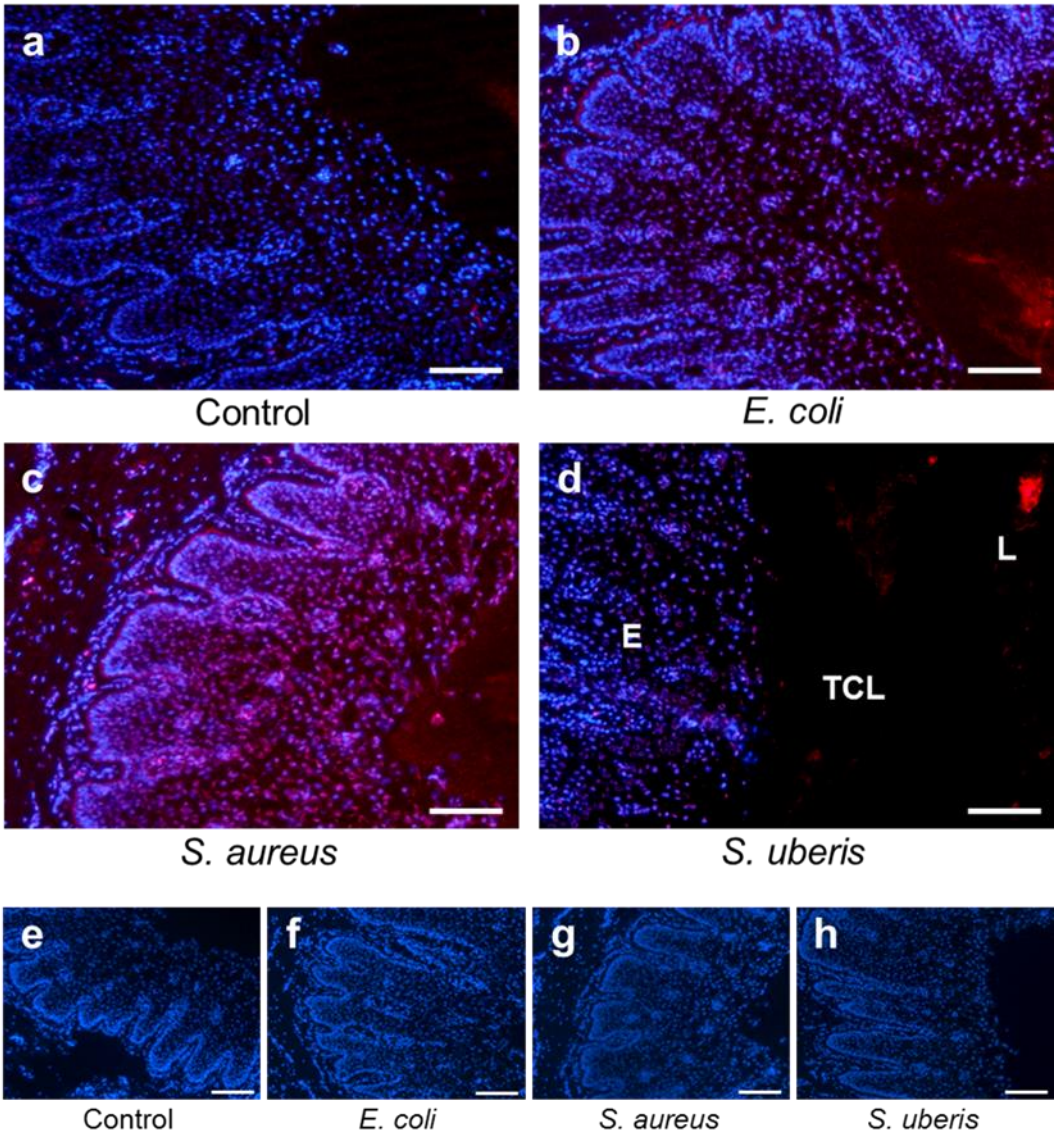

Figure 6.10: Distribution of lactoferrin signal in cryosections of teat canal tissues after the 24h bacterial challenge.
Representative micrographs from Cow #1312 of transverse cryosections of teat canal challenged with (a) vehicle only (control), (b) *E. coli*, (c) *S. aureus*, and (d) *S. uberis*. Sections were probed with an anti-lactoferrin polyclonal antibody, and bound antibody was detected with Alexa Fluor-594 labelled secondary antibody (red signal) using fluorescence microscopy. Isotype-matched control antibody shows negative staining for lactoferrin (e-h). Each cryosection was counterstained with DAPI (blue signal). E, epidermis; L, lumen; TCL, teat canal lining. Section thickness: 5 µm. Scale bar = 100 µm.

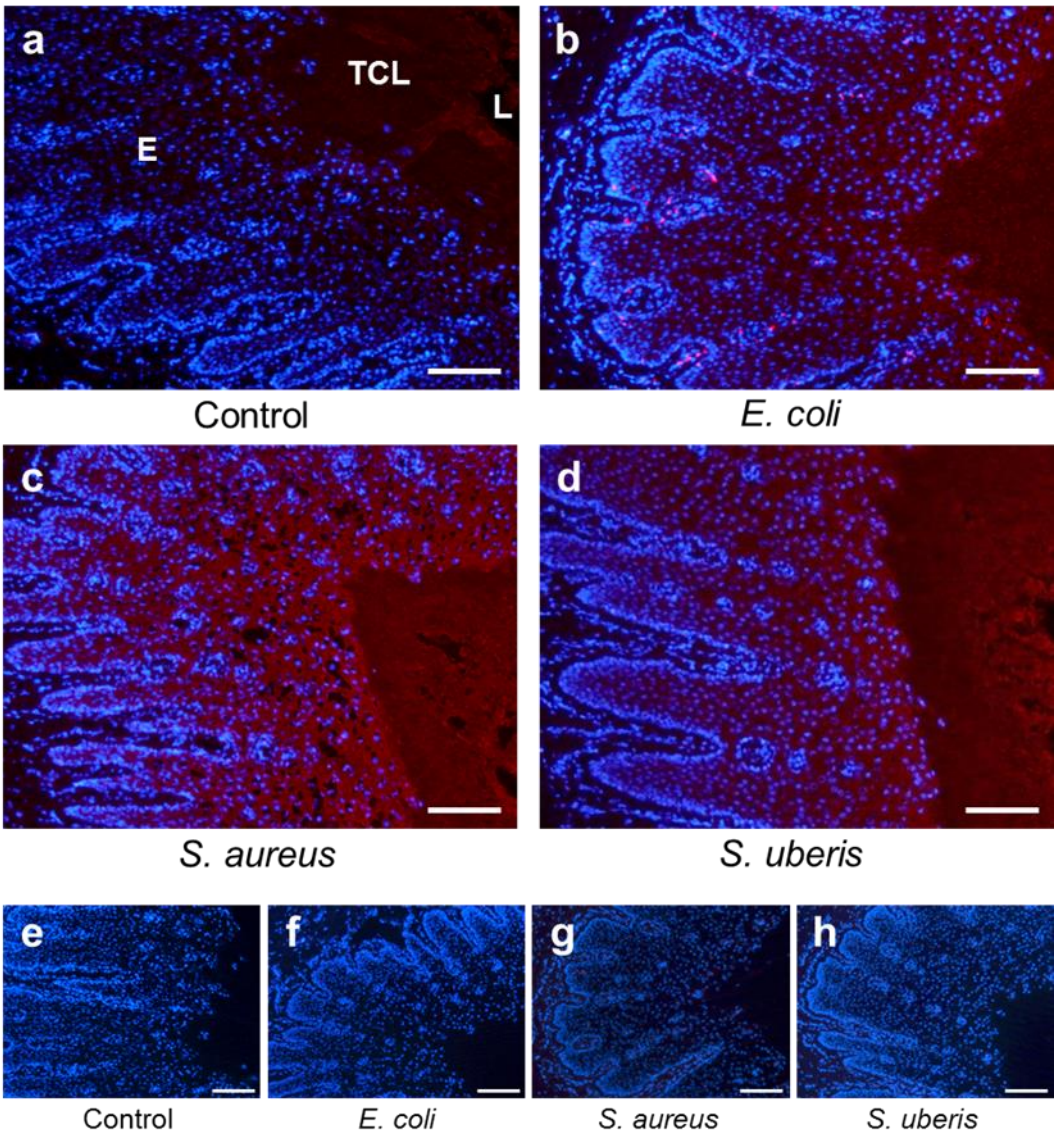

Figure 6.11: Distribution of transferrin signal in cryosections of teat canal tissues after the 24h bacterial challenge.
Representative micrographs from Cow #1238 of transverse cryosections of teat canal challenged with (a) vehicle only (control), (b) *E. coli*, (c) *S. aureus*, and (d) *S. uberis*. Sections were probed with an anti-human transferrin goat polyclonal antibody. Bound antibody was detected with Alexa Fluor-568 labelled secondary antibody (red signal) using fluorescence microscopy. Isotype-matched control antibody shows negative staining for transferrin (e-h). Each cryosection was counterstained with DAPI (blue signal). E, epidermis; L, lumen; TCL, teat canal lining. Section thickness: 5 µm. Scale bar = 100 µm.

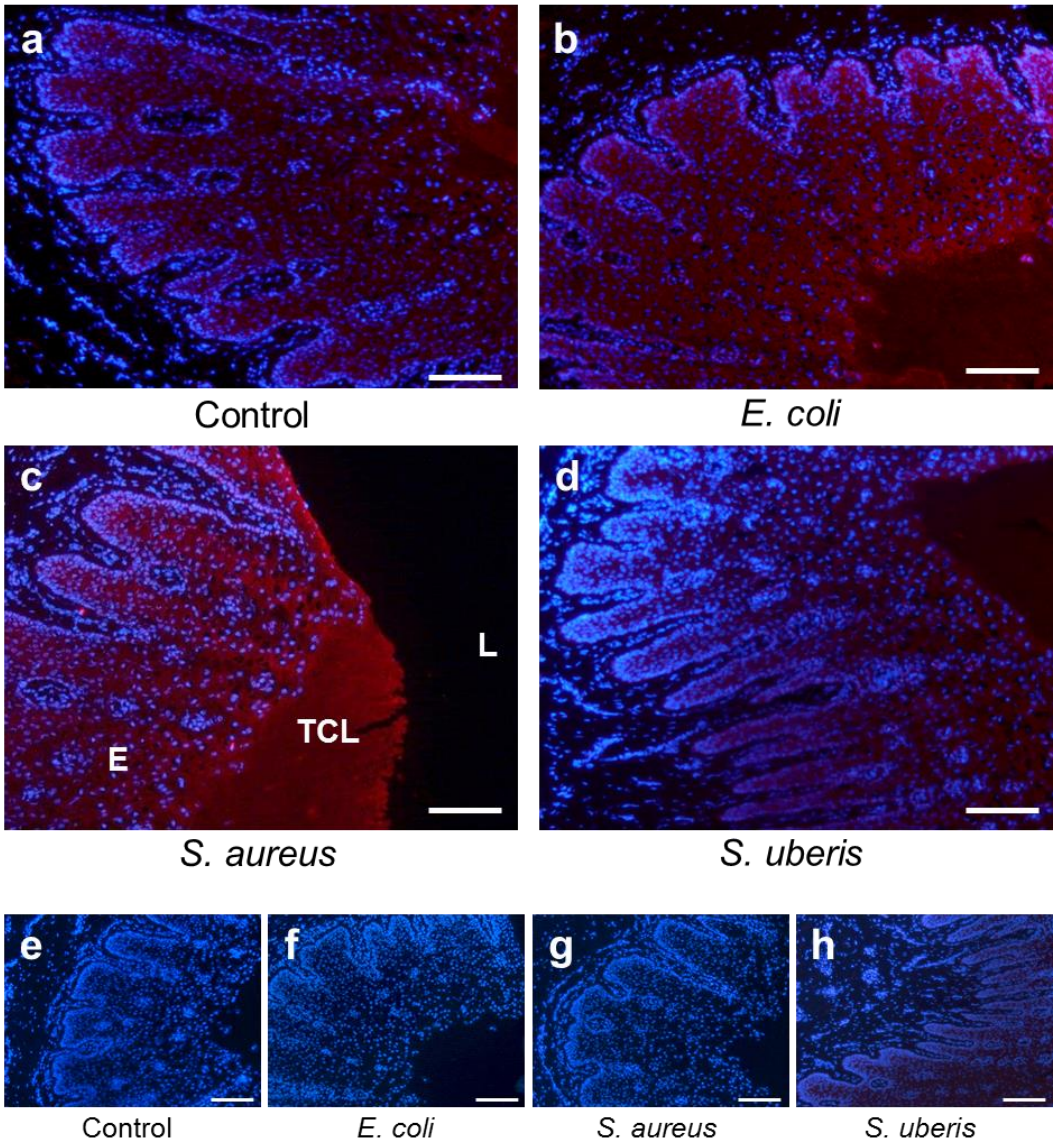

Figure 6.12: Distribution of PAUF signal in cryosections of teat canal tissues after the 24h bacterial challenge.
Micrographs from Cow #862 of transverse cryosections of teat canal challenged with (a) vehicle only (control), (b) *E. coli*, (c) *S. aureus*, and (d) *S. uberis*. Sections were probed with an anti-PAUF polyclonal antibody, and bound antibody was detected with Alexa Fluor-594 labelled secondary antibody (red signal) using fluorescence microscopy. Isotype-matched control antibody shows negative staining for PAUF (e-h). Each cryosection was counterstained with DAPI (blue signal). E, epidermis; L, lumen; TCL, teat canal lining. Section thickness: 5 µm. Scale bar = 100 µm.

6.5. Changes in immune cell abundance in the teat-end tissues after experimentally-induced teat canal infection

Along with an increase in abundance of lactoferrin, transferrin and PAUF, other changes may have occurred, resulting in alterations in the distribution and types of immune cells that are present in the teat-end tissues in response to an acute bacterial challenge. Although the bacteria were inoculated midway along the length of the teat canal, it is possible that signalling molecules may be released from this site, which attract and recruit cells, altering the immune cell profiles in adjacent teat-end tissues, such as Fürstenberg's rosette and teat sinus.

To investigate this, sections of teat canal, Fürstenberg's rosette and teat sinus from this experiment were probed for changes in the abundance of antigen-presenting cells (MHC class II^+ and $CD205^+$), T lymphocytes ($CD3^+$) and granulocytes, using antibodies to cell surface antigens. Sections from bacterial-challenged teats were compared with the in-cow control teats that received the vehicle-only (Control).

6.5.1. Detection of antigen-presenting cells in the teat canal

Compared with the control inoculation tissues, semi-quantitative analysis of IF intensities by Quickscore analysis (See Section 2.2.20.3) showed no detectable differences in the overall signal intensities for the MHC class II antigen in cryosections from the teat canal, Fürstenberg's rosette, and teat sinus for all three bacterial challenges for all four cows (See Supplementary data Table D8). Furthermore, regardless of treatment condition there appeared to be no variance in MHC class II signal distribution between the subepithelial stroma and the epithelial bilayer in both the Fürstenberg's rosette and teat sinus tissue sections (Figure 6.13).

For the antigen capture receptor CD205, similar patterns of distribution were observed to that of the MHC class II signal. For these sections, the majority of CD205 labelled cells were located in the subepithelial stroma of the teat canal and

the epithelial bilayer in the Fürstenberg's rosette, and teat sinus tissues (Figure 6.14). There was no statistically significant difference in the proportion of CD205 expressing cells in cryosections from the teat canal, Fürstenberg's rosette, and teat sinus for all three bacterial infections, compared across treatments and between each treatment and the control inoculation for all four cows (See Supplementary data Figure D2).

6.5.2. Detection of T lymphocytes

Migrating lymphocytes are essential for mounting an effective host defence response. To establish if T cells are recruited to the teat-end tissues in response to the inoculation of bacteria, cryosections of tissue from each of the three infected teats (*E. coli*, *S. aureus*, and *S. uberis*) were probed with the pan T lymphocyte marker CD3 and compared to the equivalent tissues from the control inoculation for each cow (Figure 6.15). Analysis of cryosections from all four cows showed that there was no statistically significant difference in the proportion of CD3 expressing cells in the epithelial and stromal tissue sections from the teat canal, Fürstenberg's rosette, and teat sinus compared across treatments and between each treatment and the control inoculation (See Supplementary data Figure D2).

6.5.3. Detection of granulocytes

The active recruitment of granulocytes to sites of injury and infection is a fundamental step in the innate immune system. Chemoattractants released by host cells sensing pathogens or pathogen-derived factors mobilise and recruit polymorphonuclear leukocytes, such as neutrophils, from the circulation to sites of infection. Teat-end tissues from *E. coli*, *S. aureus* and *S. uberis* challenged teat canals, along with the control inoculation, were probed with the antibody CH138A to identify granulocytes (Figure 6.16). Signals from this bound antibody were localised to the stromal tissue between the rete ridges and Marksäulchen in all challenged teat canals as well as in control inoculated teats. For both the Fürstenberg's rosette and teat sinus tissue sections there was also no appreciable difference in signal intensity and localisation of $CH138A^{+}$ cells between teat sections from the same animal and generally amongst sections from cows in each of the four treatment groups (See Supplementary data Table D9).

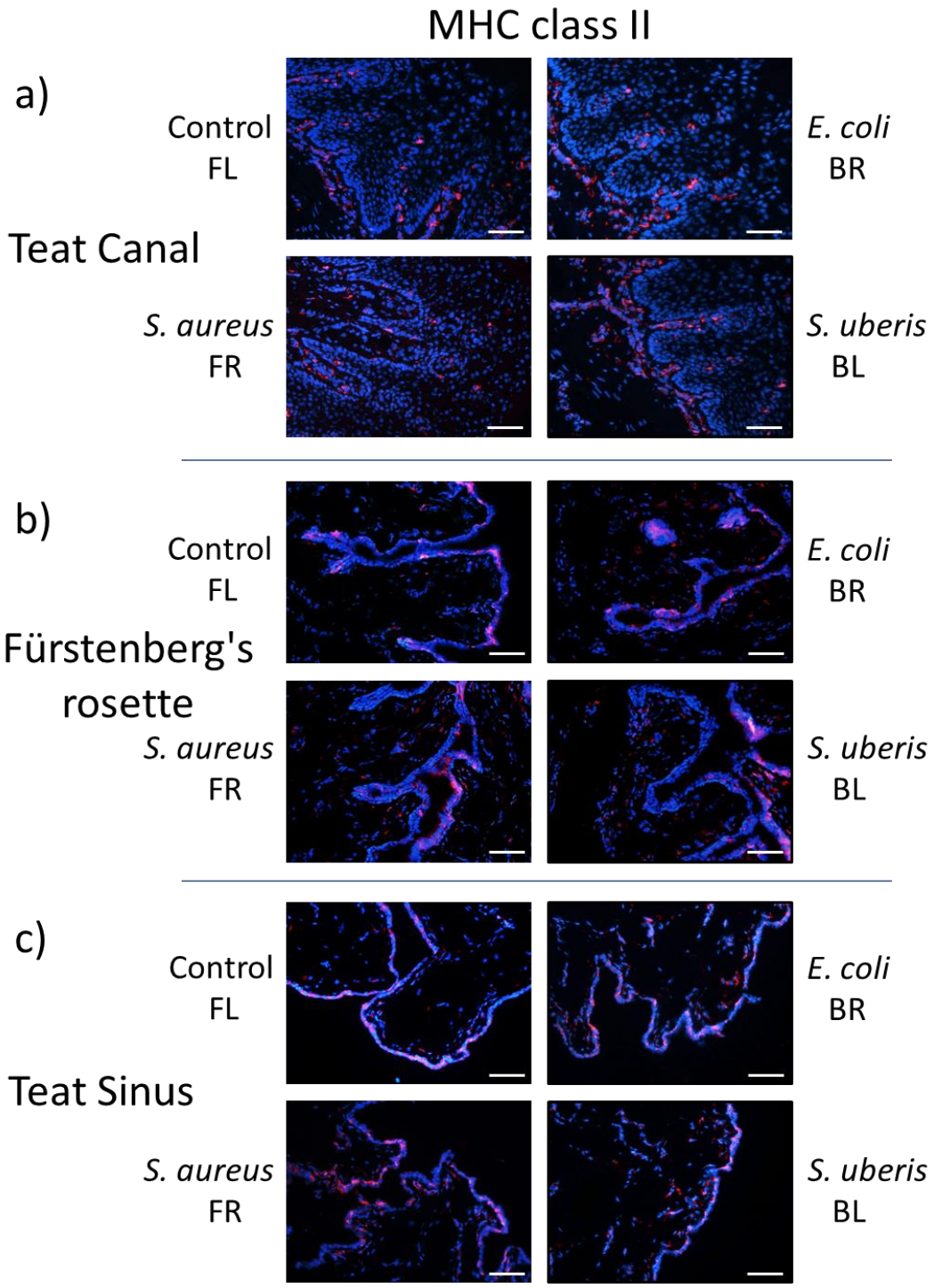

Figure 6.13: Distribution of MHC class II positive cells in cryosections of the teat-end tissues infected with *E. coli, S. aureus* and *S. uberis*.
Representative micrographs from Cow #1312 of transverse cryosections of teat canal (a), Fürstenberg's rosette (b), and teat sinus (c) were probed with anti-MHC class II monoclonal antibody (Alexa Fluor-594 IgG2a; red signal). Each cryosection was counterstained with DAPI (blue signal). Inoculum was administered to each teat as listed in Table 6.5. Control, vehicle only; FR, right forequarter; FL, left forequarter; BR, right hindquarter; BL, left hindquarter. Section thickness: 5 µm. Scale bar = 100 µm.

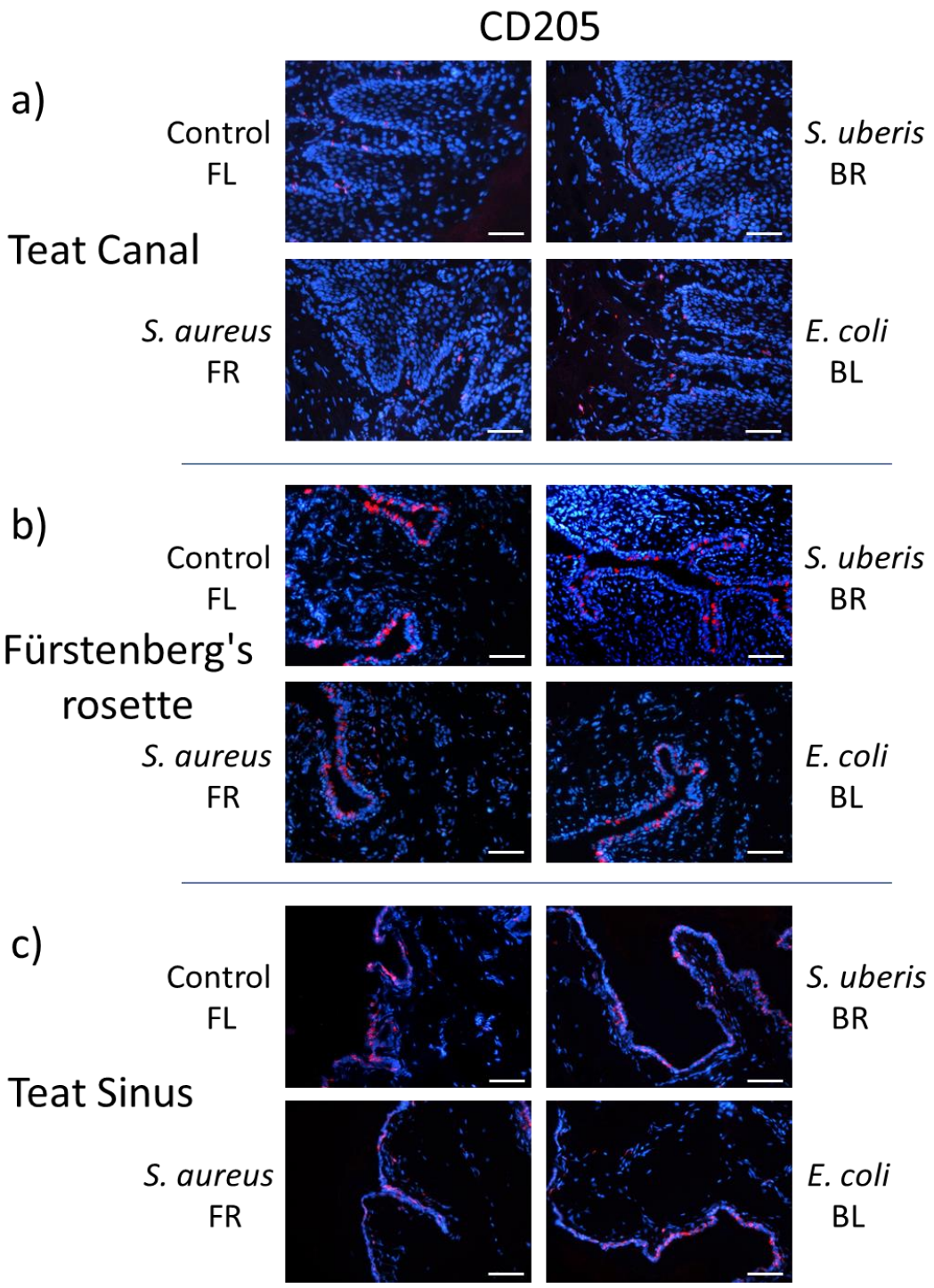

Figure 6.14: Distribution of CD205 positive cells in cryosections of the teat-end tissues infected with *E. coli*, *S. aureus* and *S. uberis*.
Representative micrographs from Cow #428 of transverse cryosections of teat canal (a), Fürstenberg's rosette (b), and teat sinus (c) were probed with an anti-CD205 monoclonal antibody (Alexa Fluor-594 IgG; red signal). Each cryosection was counterstained with DAPI (blue signal). Inoculum was administered to each teat as listed in Table 6.5. Control, vehicle only; FR, right forequarter; FL, left forequarter; BR, right hindquarter; BL, left hindquarter. Section thickness: 5 µm. Scale bar = 100 µm

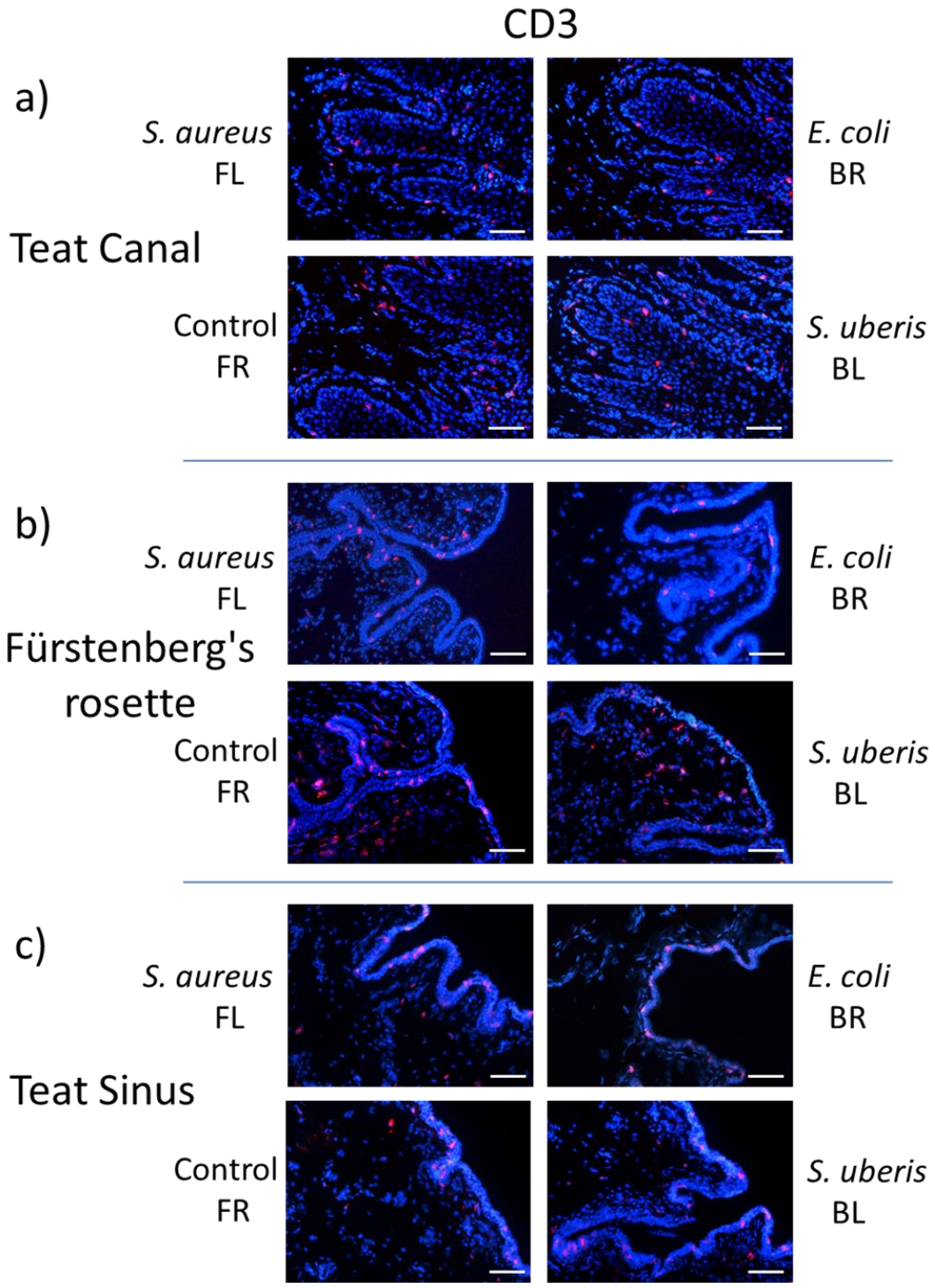

Figure 6.15: Distribution of CD3 positive cells in cryosections of the teat-end tissues infected with *E. coli*, *S. aureus* and *S. uberis*.
Representative micrographs from Cow #862 of transverse cryosections of teat canal (a), Fürstenberg's rosette (b), and teat sinus (c) were probed with an anti-CD3 monoclonal antibody (Alexa Fluor-594 IgG; red signal). Each cryosection was counterstained with DAPI (blue signal). Inoculum was administered to each teat as listed in Table 6.5. Control, vehicle only; FR, right forequarter; FL, left forequarter; BR, right hindquarter; BL, left hindquarter. Section thickness: 5 µm. Scale bar = 100 µm.

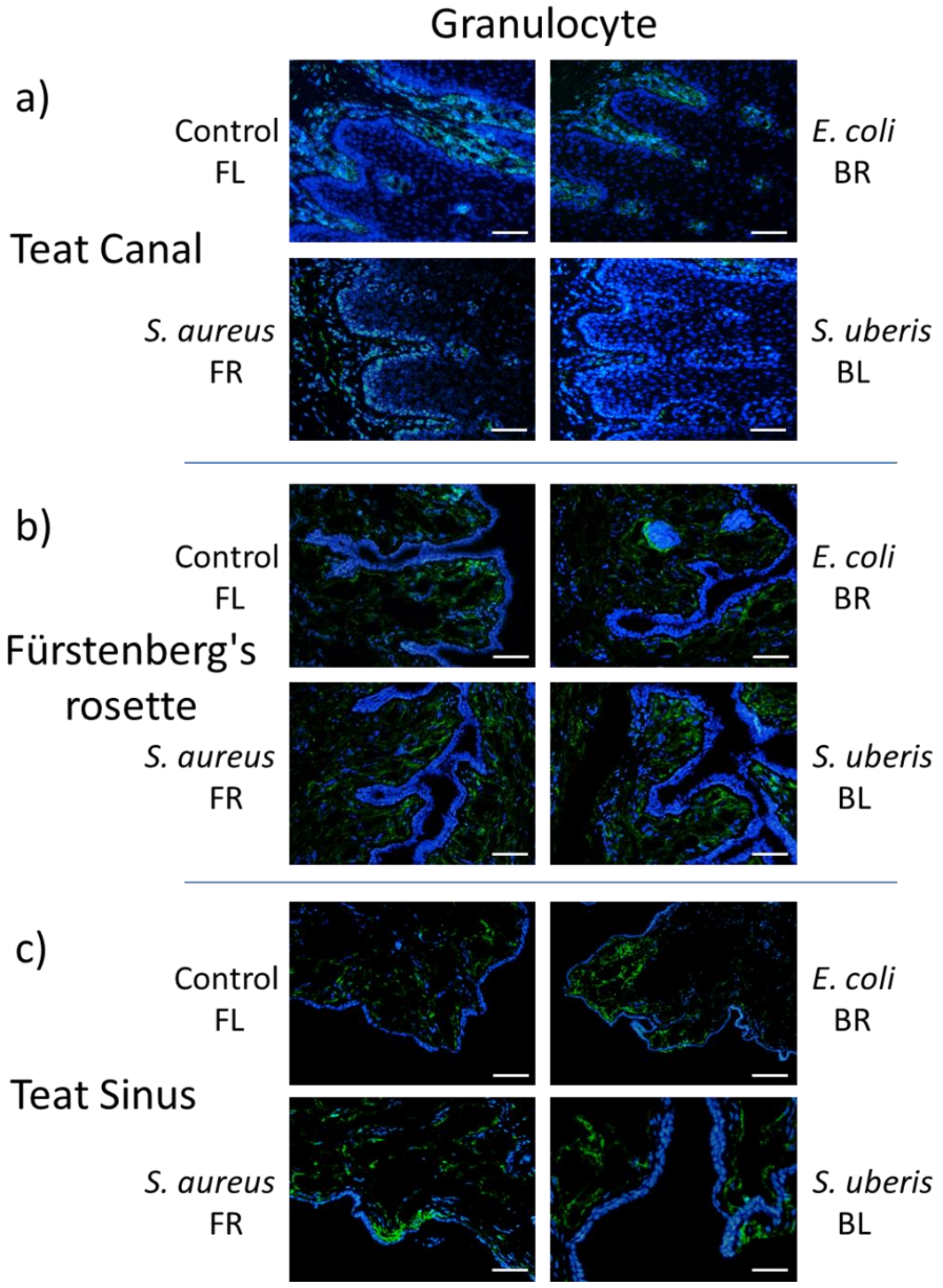

Figure 6.16: Distribution of CH138A labelled cells in cryosections of the teat-end tissues infected with *E. coli*, *S. aureus* and *S. uberis*.
Representative micrographs from Cow #1312 of transverse cryosections of teat canal (a), Fürstenberg's rosette (b), and teat sinus (c) were probed with an anti-CH138A monoclonal antibody (Alexa Fluor-488 IgM; green signal). Each cryosection was counterstained with DAPI (blue signal). Inoculum was administered to each teat as listed in Table 6.5. Control, vehicle only; FR, right forequarter; FL, left forequarter; BR, right hindquarter; BL, left hindquarter. Section thickness: 5 µm. Scale bar = 100 µm.

6.6. Discussion:

Like healthy skin, the bovine teat canal has been found to be inhabited by a diverse population of resident microorganisms (Gill *et al.*, 2006; Falentin *et al.*, 2016). Despite the presence of these resident microbes, the teat canal is not normally overwhelmed by an inflammatory response, suggesting that a host-pathogen equilibrium within the teat canal is maintained. Although not completely understood, this balance is sustained through complex interactions between the host tissue, resident commensals and potential pathogens. The pathogen challenges examined in this chapter were designed to maximise the likelihood of perturbing the local homoeostasis, thereby generating an immunological response, such as the upregulation of effector molecules and possibly the influx of innate immune cells.

The proteomic and IHC analyses described in this chapter have established that the teat canal is a highly tolerant tissue that can resist a heavy bacterial burden without bringing about an inflammatory response typical of mastitis. This is very different from the teat sinus where low numbers of introduced bacteria can generate an intramammary infection leading to clinical symptoms (Boehmer *et al.*, 2008; Smolenski *et al.*, 2014). The data suggests that there was very little localised innate immune response to the bacterial inoculations, at least in the first 24 h after the introduction of the bacteria. Nonetheless, several teat canal lining proteins with antimicrobial and immune modulating properties were elevated in abundance, especially when the teat canal was exposed to *S. aureus*. Furthermore, there were no obvious signs of a systemic response to the infections through changes in the abundance and distribution of immune cells in the teat-end tissues regardless, of the pathogenic agent.

Over the past few decades, it has become apparent that the skin provides, in addition to a physical barrier, an 'immune barrier' based on the release of antimicrobial proteins that inhibits the growth of microorganisms. Effector molecules such as defensins, cathelicidins, proteinase inhibitors, RNases, and S100 proteins have been shown to play a role in host-defence protection of the skin. Some of these antimicrobial proteins are constitutively expressed by

keratinocytes while other antimicrobial proteins are upregulated at sites of infection and inflammation. In the teat canal lining, the major constitutively expressed proteins that fit this category are the S100 proteins and the serpin proteinase inhibitors. GeLC-MS/MS analysis of the teat canal lining from the infection models detected a small increase in abundance of lactoferrin, transferrin, and PAUF. These upregulated proteins also respond in a similar manner during the process of involution (See Chapter 5). In addition to these three proteins, heat shock protein beta-1 (HSPB1; also known as HSP-27) and apolipoprotein A-I were also upregulated during the experimental infection. Unexpectedly, there was no detection of other inducible skin antimicrobial proteins such as defensins, cathelicidins, or RNase 7, suggesting possible differences between the organisation of the teat canal epithelium and that of the skin. However, it should be noted that parallel pathogen challenges were not performed on teat skin itself.

Of the three inoculated bacteria, *S. aureus* elicited the greatest immune response in the teat canal lining, with the highest increase in abundance of HSPB1, PAUF, transferrin, apolipoprotein A-I and an equal elevation of lactoferrin with *S. uberis* infection. The potential antimicrobial roles of lactoferrin, transferrin, and PAUF in limiting the passage and growth of bacteria have already been discussed (See Chapter 5) and will not be covered here. However, the evidence from the challenge data adds weight towards a local origin of production for these proteins as there were no other observations supporting an inflammatory response that would transport these proteins from other sources. Moreover, the *S. aureus* challenge model highlighted two new proteins that may potentially modulate the immune response of the teat canal to infection.

Heat shock proteins are molecular chaperones found ubiquitously in intracellular compartments where they are involved in processes like protein folding and protein trafficking. However, during stress conditions, heat shock proteins are released to extracellular compartments where some can perform other roles. Some heat shock proteins have been shown to function as pro-inflammatory signalling molecules while others have an anti-inflammatory capacity, reducing excessive inflammation (Calderwood *et al.*, 2007). Monocytes exposed to HSPB1 generate substantial amounts of the anti-inflammatory cytokine IL-10, which

supresses the immune response of macrophages and dendritic cells (De *et al.*, 2000; Miller-Graziano *et al.*, 2008). The source and effect of HSPB1 in the teat canal lining remains unknown. However, the host could be utilising the production of HSPB1 to limit the effect of inflammation, preventing damage to the surrounding tissues. This is important as the site of infection within the teat canal itself is difficult to get to, and an unnecessary and continual influx of immune cells through the stratified epithelial layer could cause more damage to the teat tissue than the bacteria themselves.

Apolipoprotein A-I is a negative acute phase protein mainly found in plasma (Mahley *et al.*, 1984) whose concentration decreases in response to inflammation. It has previously been identified at low levels in normal milk and shown to increase in abundance in mastitic milk (Smolenski *et al.*, 2014). In addition to transport functions, there is evidence to suggest that lipoproteins may also play an important role in host defence as part of the innate immune system (Khovidhunkit *et al.*, 2004). One of the key functions of lipoproteins is to bind and inactivate lipopolysaccharide from Gram-negative bacteria, neutralising its toxic effects (Ma *et al.*, 2004). In this study, the increase in abundance of apolipoprotein A-I in the teat canal is noteworthy as it may be acting as a positive acute phase protein during Gram-positive bacterial infection. However, to complicate the issue, lipoproteins from *S. aureus* lipoteichoic acid fractions have been shown to activate immune cells through stimulation of toll-like receptor 2 (Hashimoto *et al.*, 2006). It is possible that the upregulation of apolipoprotein A-I in the teat canal may help signal other components of the immune response. With this in mind, its role as a positive acute phase protein during teat canal infection should be examined further to better understand its role in host defence of dairy cows.

Another interesting observation from the teat canal challenge trial was that infection by *S. aureus* produced a greater response compared to the infection by *E. coli*, which elicited the least. In three of the four *S. aureus* infected cows examined, increases in the relative abundance of lactoferrin, transferrin, and to a lesser extent PAUF, were detected by mass spectrometry and confirmed by Western blot analysis. The extent of the immune response not only provides some insight into animal-to-animal variability but also into the ability of the cow to

respond to different pathogens, assuming that all cows received the same dose of inoculum. It is possible that *E. coli* may have been effectively managed by the anti-coliform properties of S100A7, thus inducing a limited response, whereas the *S. aureus* infection was harder to eliminate, requiring a more complex response with additional innate immune components.

The challenge model would have benefited from a larger sample set of animals but unfortunately due to the selection criteria, was limited to four cows per analysis group. Another limitation of this study was that it only looked at a single time point (i.e. 24 h post inoculation). The study did not investigate how long the immune response took for the teat canal to clear the pathogenic bacteria and re-establish equilibrium with the mix of 'regular' commensal microbes or whether the extent of the response influenced the speed of recovery. To what extent these five inducible proteins can provide protection to the teat canal and influence other innate immune components should be explored in further studies. In addition, further investigation of this inflammatory response on a larger number of cows over successive milking seasons is required to show if there is a correlation between low responders and susceptibility to naturally occurring mastitis.

There was scarcely any change in the relative abundance of immune cells surrounding the stratified epithelium of the teat canal or in the stromal and epithelial layers of the Fürstenberg's rosette and teat sinus, regardless of pathogenic agent, suggesting little cellular immunity involvement in response to the pathogen challenge. However, this lack of response could be because the bacterial load may not have been large enough to initiate an immune response in the teat canal. Also, the 24 h period may not have been long enough for the colonising bacteria to cause enough damage to the teat canal epithelium to initiate a signalling cascade. Lastly, and in the case of *E. coli*, the bacteria might have been effectively killed off or incapacitated by the constitutively produced antimicrobial proteins. However, this is not to mean that certain innate immune signalling pathways have not been activated. It is conceivable that microorganisms could be detected in the teat canal without creating a local inflammatory response. This sensing could result in cytokines being released that then stimulate immune cells in the Fürstenberg's rosette or teat sinus, priming

them for an immediate response without necessarily causing proliferation. The expression of pro-inflammatory cytokines and signalling molecules from the teat canal keratinocytes is an area that should be explored further to determine whether their expression is upregulated during infection and to determine if there are systemic changes in the other teat-end tissues, especially the Fürstenberg's rosette.

Another possibility to consider is that the bacteria may not have been able to effectively colonise the teat canal lining due to the resident microflora occupying preferential binding sites. Mammalian barrier surfaces, such as the skin, the vagina, upper respiratory and gastrointestinal tracts, are usually colonised by commensal microbial communities (Tlaskalová-Hogenová *et al.*, 2004; Honda & Littman, 2012) as is the teat canal (Gill *et al.*, 2006; Falentin *et al.*, 2016). Therefore, under steady state conditions, the innate immune response must find a balance between tolerance and immunity. In fact, in these studies, the commensal bacteria have been found to provide signals that calibrate the activation threshold and sensitivity of the innate immune system. If a similar arrangement was present in the teat canal, this might provide an explanation for the level of tolerance observed with the teat canal inoculations, particularly to the presence of *E. coli*.

Taken together, these results have established that the teat canal is a highly resistant tissue that can withstand significant challenge by mastitis causing bacteria. The proteomic analysis has offered some insight into the biological response to bacterial infection in the teat canal while the IHC analysis established a lack of inflammatory response at the cellular level. Despite the limited response, the analysis was able to highlight the presence of several novel proteins in the teat canal lining that could play a role in both signalling and limiting infection and inflammation. A lot more work needs to be performed to fully understand the processes operating on the teat canal mucosa to maintain a robust host defence capability.

7. Summary

The overall aims of this study were to: i) Characterise the protein constituents of the teat canal lining (**Chapter 3**), ii) Identify key immune-related cells in the teat-end tissues (**Chapter 4**), iii) Assess changes associated with mammary involution (**Chapter 5**), and iv) Determine the teat canal responses to pathogen challenge (**Chapter 6**). During this study, a range of host-defence associated proteins have been identified in the teat canal lining, and their responses to physiological and environmental challenge characterised. Many immune-related cell types have been identified in the teat-end tissues, and changes in their relative abundance and distribution characterised. Thus, the overall stated aims of the investigation have been achieved.

The results generated and described in Chapters 3 to 6 have characterised some key elements of the bovine teat-end tissues. The structure of the teat canal is superficially like skin but has several distinct differences, including anatomical structure and response to bacterial challenge. Notably, the presence of bacteria in the teat canal lumen does not result in a typical, observable inflammatory response. However, the teat canal lining does contain a unique mixture of proteins, some of which, have been linked to antimicrobial functionality. These include the constitutively produced Serpin protease inhibitors and the S100A7-like protein, which by contrast are almost absent from skin. Anatomically the makeup of the Fürstenberg's rosette is very different from that of the teat canal, comprising two layers of epithelial cells and no cornified keratin layer. The prevalence of antigen-presenting cells in the Fürstenberg's rosette strongly suggests an active cell-mediated host-defence functionality, which is likely to form a significant barrier to the ingress of microbial pathogens into the gland. The teat sinus also appears to have a similar cell-mediated host-defence functionality, although the numbers and types of immune cells are distinct compared to Fürstenberg's rosette.

These observations lead us to the following conclusions. Firstly, the teat canal appears to be remarkably unresponsive to bacterial challenge, at least in the models used in this study. The bacterial challenges outlined in this study utilised

four to five times more bacteria than had been previously inoculated into teat canals, with only very limited inflammatory responses detected. The fact that the teat canal can tolerate the presence of bacteria at the loadings described in this study would suggest that it can also tolerate lower levels of bacteria during a natural physiological challenge. Secondly, the presence of granulocytes in the Marksäulchen implies a mechanism for delivery of these immune cells and their antimicrobial constituents into the teat canal lumen, thereby contributing to an antimicrobial environment. To date, this type of structure has not been described in any other tissue. Lastly, the Fürstenberg's rosette appears to play a key role in the host-defence of the mammary gland. This tissue has by far the highest density of immune cells of any of the teat-end tissues investigated. While this implies a function similar to known mucosa-associated lymphoid tissues, it does not appear to contain any of the well-defined secondary lymphoid follicles, such as germinal centres, typical of these types of structures. Nevertheless, this tissue seems likely to recognise the presence of pathogens and facilitate an inflammatory response.

The above findings suggest that effective host-defence is achieved through a compartmentalised multifactorial process. Previous reports using PCR-based approaches have indicated that a range of microbial species already inhabits the teat canal lining even in the absence of overt signs of infection (Gill *et al.*, 2006; Falentin *et al.*, 2016). When a pathogen first encounters the teat canal lining its fate is determined by the interaction with these commensal organisms as well as with antimicrobial substances produced within the tissue. It appears that an inflammatory response is not the predominant means of suppressing the potential infection at this stage. However, if the pathogen survives this environment, its next obstacle to establishing an intra-mammary infection is the physical barrier of the closed teat canal sphincter as well as the epithelial surface of the Fürstenberg's rosette. It seems reasonable that the immune cells within the Fürstenberg's rosette are equipped to sense any pathogens that are present in this region of the teat and mount a local inflammatory response to them. Any pathogens surviving this response would enter the teat sinus where they would still be subject to the host-defence activity of the teat sinus epithelium and innate immune components of the milk. Thus, it is likely that the environment, including the commensal microbes

present, is very different in the teat sinus compared with the teat canal, and is probably similar to that of the more distal regions of the mammary gland, i.e. the cisternal, ductal and alveolar lumen. A number of previous investigations have shown that once pathogens gain entry to the teat sinus, a clinical intra-mammary infection is more likely to occur, (Bannerman *et al.*, 2004; Bannerman *et al.*, 2005; Smolenski *et al.*, 2014). However, in some cases infection does not develop after intra-sinus inoculation, leading to high between-animal variability in the clinical outcome (Notcovich *et al.*, 2016). This could be because the infection is effectively suppressed in some animals through the initial innate immune response.

Despite our investigations, a lot still remains to be discovered. Firstly, the microbiome present in the teat-end tissues has not been fully characterised. Although the microbiome of the teat canal has been previously investigated, the dynamics of constituent bacteria including their quantitative aspects and differences among the various teat-end environments has not been examined. Secondly, the functional role played by the host-defence associated proteins identified in this study remains unknown. The existent literature leads to questions as to their role in this environment. Thirdly, the function of the Fürstenberg's rosette is only partially understood, and this study, therefore, presents additional information and knowledge of this tissue. A previous study has shown that Fürstenberg's rosette has some of the functionality expected for lymphoid tissue (Aştı *et al.*, 2011), while this study demonstrated for the first time the prevalence of antigen-presenting cells. However, the pathways through which the tissue senses pathogens and elicits an inflammatory response is unknown. In particular, there have been no experiments conducted to determine changes in molecular pathways occurring in response to pathogen-associated substances.

These knowledge gaps need to be addressed through future investigations. The role of the putative antimicrobial proteins could be determined through experiments using purified recombinant proteins and testing their antimicrobial function *in vitro*. Also, they could be used in cell culture experiments to test their ability to act as adaptor proteins in recognition of pathogen-derived substances by innate immune receptors. For example, both the calprotectin complex

(S100A8/SA9) and S100A12 have been shown to activate TLR4 and RAGE receptors (Ehrchen *et al.*, 2009; Foell *et al.*, 2013; Narumi *et al.*, 2015), while PAUF has been shown to be an endogenous ligand for TLR2 and TLR4 in HEK293T cell lines (Park *et al.*, 2011a). Also of particular interest would be how these proteins act on the cells present in the Fürstenberg's rosette and teat sinus. A second area for further investigation would be a fuller characterisation of the microbiomes of the teat-end tissues and how each microbial species interact with each other and the tissue and what role this has in maintaining homoeostasis. A third area is the identity and roles of the immune cells within the epithelia of the teat end tissues. For example, it is not clear from this investigation whether the teat end tissues contain Langerhans-type dendritic cells and what the wider implications of the Marksäulchen are with respect to the transport of innate immune cells. Lastly, what is the role that the Fürstenberg's rosette plays in determining the susceptibility of a cow to mastitis? To this end, the structure and function of the Fürstenberg's rosette could be characterised in cows selected for high and low susceptibility to mastitis and any differences further investigated for their role in determining susceptibility to mastitis. This work could lead to the identification of novel biomarkers for mastitis resistance.

Overall the data presented in this thesis provides experimental evidence to support the original hypothesis that the teat canal and associated teat-end tissues play an important role in the immune surveillance and defence of the bovine mammary gland. The variance in abundance of the S100 proteins and the response of proteins such as lactoferrin to infection may impact the level of resistance to infection shown by some animals. In addition, the number of immune cells with antigen recognition and antigen presentation capability identified in the epithelial tissues of the Fürstenberg's rosette and teat sinus suggest that these two locations, in the teat, are important sites for the detection and prevention of infection from invading microorganisms.

In summary, the findings presented in this thesis lay important foundations for future research that could result in the development of novel tools and animal management practices to minimise the impact of mastitis on the dairy industry.

8. References

Aboud, L., Ball, T. B., Tjernlund, A., & Burgener, A. (2014). The role of serpin and cystatin antiproteases in mucosal innate immunity and their defense against HIV. *American Journal of Reproductive Immunology, 71*(1), 12-23.

Abraham, S. N., & John, A. L. S. (2010). Mast cell-orchestrated immunity to pathogens. *Nature Reviews in Immunology, 10*(6), 440-452.

Adams, E., & Rickard, C. G. (1963). The antistreptococcic activity of bovine teat canal keratin. *American Journal of Veterinary Research, 24*, 122-135.

Adams, E. W., Rickard, C. G., & Murphy, J. (1961). Some histological and histochemical observations on bovine teat epithelium. *The Cornell Veterinarian, 51*, 124-154.

Aderem, A., & Underhill, D. M. (1999). Mechanisms of phagocytosis in macrophages. *Annual Review of Immunology, 17*(1), 593-623.

Akers, R. M., & Nickerson, S. C. (2011). Mastitis and its impact on structure and function in the ruminant mammary gland. *Journal of Mammary Gland Biology and Neoplasia, 16*(4), 275-289.

Albanesi, C., Scarponi, C., Giustizieri, M. L., & Girolomoni, G. (2005). Keratinocytes in inflammatory skin diseases. *Current Drug Targets. Inflammation and Allergy, 4*(3), 329-34.

Alberts, B., Johnson, A., Lewis, J., Raff, M., Roberts, K., & Walter, P. (2002). Innate immunity. In *Molecular Biology of the Cell. 4th edition* Garland Science, New York. Retrieved from http://www.ncbi.nlm.nih.gov/books/NBK26846/.

Aldridge, G. M., Podrebarac, D. M., Greenough, W. T., & Weiler, I. J. (2008). The use of total protein stains as loading controls: an alternative to high-abundance single-protein controls in semi-quantitative immunoblotting. *Journal of Neuroscience Methods, 172*(2), 250-254.

Almeida, R., Luther, D., Kumar, S., Calvinho, L., Bronze, M., & Oliver, S. (1996). Adherence of *Streptococcus uberis* to bovine mammary epithelial cells and to extracellular matrix proteins. *Journal of Veterinary Medicine, Series B, 43*(1-10), 385-392.

Almeida, R. A., & Oliver, S. P. (2001). Interaction of coagulase-negative *Staphylococcus* species with bovine mammary epithelial cells. *Microbial Pathogenesis, 31*(5), 205-212.

Aranami, T., Miyake, S., & Yamamura, T. (2006). Differential expression of CD11c by peripheral blood NK cells reflects temporal activity of multiple sclerosis. *Journal of Immunology, 177*(8), 5659-5667.

Aştı, R., Kurtdede, N., Altunay, H., Alabay, B., Özen, A., & Bayraktaroğlu, A. (2011). Histological and immunohistochemical studies on the Furstenberg's rosette in cows. *Kafkas Üniversitesi Veteriner Fakültesi Dergisi, 17*(2), 223-228.

Bachman, K., & Schairer, M. (2003). Invited review: Bovine studies on optimal lengths of dry periods. *Journal of Dairy Science, 86*(10), 3027-3037.

Banchereau, J., Briere, F., Caux, C., Davoust, J., Lebecque, S., Liu, Y.-J., Pulendran, B., & Palucka, K. (2000). Immunobiology of dendritic cells. *Annual Review of Immunology, 18*(1), 767-811.

Bangert, C., Brunner, P. M., & Stingl, G. (2011). Immune functions of the skin. *Clinics in Dermatology, 29*(4), 360-376.

Bannerman, D. D., Chockalingam, A., Paape, M. J., & Hope, J. C. (2005). The bovine innate immune response during experimentally-induced *Pseudomonas aeruginosa* mastitis. *Veterinary Immunology and Immunopathology, 107*(3), 201-215.

Bannerman, D. D., Paape, M. J., Lee, J.-W., Zhao, X., Hope, J. C., & Rainard, P. (2004). *Escherichia coli* and *Staphylococcus aureus* elicit differential innate immune responses following intramammary infection. *Clinical and Diagnostic Laboratory Immunology, 11*(3), 463-472.

Beagley, K., & Husband, A. J. (1998). Intraepithelial lymphocytes: origins, distribution, and function. *Critical Review in Immunology, 18*(3).

Bellamy, W., Takase, M., Wakabayashi, H., Kawase, K., & Tomita, M. (1992). Antibacterial spectrum of lactoferricin B, a potent bactericidal peptide derived from the N-terminal region of bovine lactoferrin. *Journal of Applied Bacteriology, 73*(6), 472-479.

Belz, G. T., Heath, W. R., & Carbone, F. R. (2002). The role of dendritic cell subsets in selection between tolerance and immunity. *Immunology and Cell Biology, 80*(5), 463-468.

Bennett, R. (2011). Anatomy and Physiology of the Skin. I. D. Papel (Ed.), In *Facial Plastic and Reconstructive Surgery* (3rd ed., pp. 3-14) Thieme Medical Publishers. Inc., New York.

Bernerd, F., Sarasin, A., & Magnaldo, T. (1999). Galectin-7 overexpression is associated with the apoptotic process in UVB-induced sunburn keratinocytes. *Proceedings of the National Academy of Sciences, 96*(20), 11329-11334.

Bilzer, M., Roggel, F., & Gerbes, A. L. (2006). Role of Kupffer cells in host defense and liver disease. *Liver International, 26*(10), 1175-1186.

Birbeck, M. S., Breathnach, A. S., & Everall, J. D. (1961). An electron microscope study of basal melanocytes and high-level clear cells (Langerhans cells) in vitiligo[1]. *Journal of Investigative Dermatology, 37*(1), 51-64.

Birkholz, K., Schwenkert, M., Kellner, C., Gross, S., Fey, G., Schuler-Thurner, B., Schuler, G., Schaft, N., & Dörrie, J. (2010). Targeting of DEC-205 on human dendritic cells results in efficient MHC class II–restricted antigen presentation. *Blood, 116*(13), 2277-2285.

Bitman, J., Wood, D., Bright, S., & Miller, R. (1988). Lipid composition of bovine teat canal keratin. *Journal of Dairy Science, 71*(5), 1389-1395.

Bitman, J., Wood, D., Bright, S., Miller, R., Capuco, A., Roche, A., & Pankey, J. (1991). Lipid composition of teat canal keratin collected before and after milking from Holstein and Jersey cows. *Journal of Dairy Science, 74*(2), 414-420.

Boehmer, J., Bannerman, D., Shefcheck, K., & Ward, J. (2008). Proteomic analysis of differentially expressed proteins in bovine milk during experimentally induced *Escherichia coli* mastitis. *Journal of Dairy Science, 91*(11), 4206-4218.

Boggs, I., Hine, B., Smolenski, G., Hettinga, K., Zhang, L., & Wheeler, T. T. (2015). Changes in the repertoire of bovine milk proteins during mammary involution. *EuPA Open Proteomics, 9*, 65-75.

Boman, H. G. (2000). Innate immunity and the normal microflora. *Immunological Reviews, 173*(1), 5-16.

Bonifaz, L., Bonnyay, D., Mahnke, K., Rivera, M., Nussenzweig, M. C., & Steinman, R. M. (2002). Efficient targeting of protein antigen to the dendritic cell receptor DEC-205 in the steady state leads to antigen presentation on major histocompatibility complex class I products and peripheral CD8+ T cell tolerance. *The Journal of Experimental Medicine, 196*(12), 1627-1638.

Bonneville, M., O'Brien, R. L., & Born, W. K. (2010). γδ T cell effector functions: a blend of innate programming and acquired plasticity. *Nature Reviews in Immunology, 10*(7), 467-478.

Borregaard, N., Sørensen, O. E., & Theilgaard-Mönch, K. (2007). Neutrophil granules: a library of innate immunity proteins. *Trends in Immunology, 28*(8), 340-345.

Bos, J. D., & Luiten, R. M. (2009). Skin immune system. In *Skin Cancer after Organ Transplantation* (pp. 45-62) Springer.

Boyce, J. A. (2007). Mast cells and eicosanoid mediators: a system of reciprocal paracrine and autocrine regulation. *Immunological reviews, 217*(1), 168-185.

Bramley, A., King, J., Higgs, T., & Neave, F. (1979). Colonization of the bovine teat duct following inoculation with *Staphylococcus aureus* and *Escherichia coli*. *British Veterinary Journal*.

Brandon, M., Watson, D., & Lascelles, A. (1971). The mechanism of transfer of immunoglobulin into mammary secretion of cows. *Australian Journal of Experimental Biology and Medical Science, 49*, 613-623.

Brandtzaeg, P. (1989). Overview of the mucosal immune system. In *New Strategies for Oral Immunization* (pp. 13-25) Springer.

Brandtzaeg, P. (2009). Mucosal immunity: induction, dissemination, and effector functions. *Scandinavian Journal of Immunology, 70*(6), 505-515.

Brandtzaeg, P., & Pabst, R. (2004). Let's go mucosal: communication on slippery ground. *Trends in Immunology, 25*(11), 570-577.

Brandtzaeg, P., Baekkevold, E. S., Farstad, I. N., Jahnsen, F. L., Johansen, F.-E., Nilsen, E. M., & Yamanaka, T. (1999). Regional specialization in the mucosal immune system: what happens in the microcompartments? *Immunology Today, 20*(3), 141-151.

Brinkmann, V., Reichard, U., Goosmann, C., Fauler, B., Uhlemann, Y., Weiss, D. S., Weinrauch, Y., & Zychlinsky, A. (2004). Neutrophil extracellular traps kill bacteria. *Science, 303*(5663), 1532-1535.

Broadhurst, M., Beddis, K., Black, J., Henderson, H., Nair, A., & Wheeler, T. (2015). Effect of gestation length on the levels of five innate defence proteins in human milk. *Early Human Development, 91*(1), 7-11.

Brogden, K. A. (2005). Antimicrobial peptides: pore formers or metabolic inhibitors in bacteria? *Nature Reviews in Microbiology, 3*(3), 238-250.

Broome, A.-M., Ryan, D., & Eckert, R. L. (2003). S100 protein subcellular localization during epidermal differentiation and psoriasis. *Journal of Histochemistry & Cytochemistry, 51*(5), 675-685.

Brunelli, L., Crow, J. P., & Beckman, J. S. (1995). The comparative toxicity of nitric oxide and peroxynitrite to *Escherichia coli*. *Archives of Biochemistry and Biophysics, 316*(1), 327-334.

Burton, J. L., & Erskine, R. J. (2003). Immunity and mastitis some new ideas for an old disease. *Veterinary Clinics: Food Animal Practice, 19*(1), 1-45.

Burvenich, C., Van Merris, V., Mehrzad, J., Diez-Fraile, A., & Duchateau, L. (2003). Severity of *E. coli* mastitis is mainly determined by cow factors. *Veterinary Research, 34*(5), 521-564.

Bussard, K. M., & Smith, G. H. (2011). The mammary gland microenvironment directs progenitor cell fate in vivo. *International journal of cell biology, 2011*.

Butcher, G., King, G., & Dyke, K. (1976). Sensitivity of *Staphylococcus aureus* to unsaturated fatty acids. *Journal of General Microbiology, 94*(2), 290-296.

Butler, M., Morel, A.-S., Jordan, W. J., Eren, E., Hue, S., Shrimpton, R. E., & Ritter, M. A. (2007). Altered expression and endocytic function of CD205 in human dendritic cells, and detection of a CD205–DCL-1 fusion protein upon dendritic cell maturation. *Immunology, 120*(3), 362-371.

Cairns, J. A., & Walls, A. F. (1996). Mast cell tryptase is a mitogen for epithelial cells. Stimulation of IL-8 production and intercellular adhesion molecule-1 expression. *Journal of Immunology, 156*(1), 275-283.

Calderwood, S. K., Mambula, S. S., Gray, P. J., & Theriault, J. R. (2007). Extracellular heat shock proteins in cell signaling. *FEBS letters, 581*(19), 3689-3694.

Campbell, N., Yio, X. Y., So, L. P., Li, Y., & Mayer, L. (1999). The intestinal epithelial cell: processing and presentation of antigen to the mucosal immune system. *Immunological Reviews, 172*(1), 315-324.

Candi, E., Schmidt, R., & Melino, G. (2005). The cornified envelope: a model of cell death in the skin. *Nature Reviews in Molecular Cell Biology, 6*(4), 328-340.

Capuco, A., Wood, D., Bright, S., Miller, R., & Bitman, J. (1990). Regeneration of teat canal keratin in lactating dairy cows. *Journal of Dairy Science, 73*(7), 1745-1750.

Capuco, A., Bright, S., Pankey, J., Wood, D., Miller, R., & Bitman, J. (1992). Increased susceptibility to intramammary infection following removal of teat canal keratin. *Journal of Dairy Science, 75*(8), 2126-2130.

Capuco, A. V., & Akers, R. M. (1999). Mammary involution in dairy animals. *Journal of Mammary Gland Biology and Neoplasia, 4*(2), 137-144.

Carlén, L. M., Sánchez, F., Bergman, A.-C., Becker, S., Hirschberg, D., Franzén, B., Coffey, J., Jörnvall, H., Auer, G., & Alaiya, A. A. (2005). Proteome analysis of skin distinguishes acute guttate from chronic plaque psoriasis. *Journal of Investigative Dermatology, 124*(1), 63-69.

Cerf-Bensussan, N., & Guy-Grand, D. (1991). Intestinal intraepithelial lymphocytes. *Gastroenterology Clinics of North America, 20*(3), 549-576.

Cesta, M. F. (2006). Normal structure, function, and histology of mucosa-associated lymphoid tissue. *Toxicologic Pathology, 34*(5), 599-608.

Champaiboon, C., Sappington, K. J., Guenther, B. D., Ross, K. F., & Herzberg, M. C. (2009). Calprotectin S100A9 calcium-binding loops I and II are essential for keratinocyte resistance to bacterial invasion. *The Journal of Biological Chemistry, 284*(11), 7078-90.

Chandler, R., Lepper, A., & Wilcox, J. (1969). Ultrastructural observations on the bovine teat duct. *Journal of Comparative Pathology, 79*(3), 315-319.

Chang, C., Winter, A., & Norcross, N. (1981). Immune response in the bovine mammary gland after intestinal, local, and systemic immunization. *Infection and Immunity, 31*(2), 650-659.

Chen, G. Y., & Nuñez, G. (2010). Sterile inflammation: sensing and reacting to damage. *Nature Reviews Immunology, 10*(12), 826-837.

Cheng, L., Cui, Y., Shao, H., Han, G., Zhu, L., Huang, Y., O'Brien, R. L., Born, W. K., Kaplan, H. J., & Sun, D. (2008). Mouse gammadelta T cells are capable of expressing MHC class II molecules, and of functioning as antigen-presenting cells. *Journal of Neuroimmunology, 203*(1), 3-11.

Chetty, R., & Gatter, K. (1994). CD3: structure, function, and role of immunostaining in clinical practice. *The Journal of Pathology, 173*(4), 303-307.

Christ, F. (1905). *Untersuchungen über die Muskulatur und das elastische Gewebe in der Milchdrüse der Haussäugetiere.* thesis, Von Münchow'sche Hof-und Universitäts-Druckerei (O. Kindt).

Cogen, A., Nizet, V., & Gallo, R. (2008). Skin microbiota: a source of disease or defence? *British Journal of Dermatology, 158*(3), 442-455.

Cole, A. M., Kim, Y. H., Tahk, S., Hong, T., Weis, P., Waring, A. J., & Ganz, T. (2001). Calcitermin, a novel antimicrobial peptide isolated from human airway secretions. *FEBS Letters, 504*(1-2), 5-10.

Coleman, J. (2002). Nitric oxide: a regulator of mast cell activation and mast cell-mediated inflammation. *Clinical & Experimental Immunology, 129*(1), 4-10.

Collins, R. A., Parsons, K. R., & Bland, A. P. (1986). Antibody-containing cells and specialised epithelial cells in the bovine teat. *Research in Veterinary Science, 41*(1), 50-55.

Collins, R. A., Parsons, K. R., Field, T. R., & Bramley, A. J. (1988). Histochemical localization and possible antibacterial role of xanthine oxidase in the bovine mammary gland. *Journal of Dairy Research, 55*(1), 25-32.

Collins, R. A., Werling, D., Duggan, S. E., Bland, A. P., Parsons, K. R., & Howard, C. J. (1998). Gammadelta T cells present antigen to CD4+ alphabeta T cells. *Journal of Leukocyte Biology, 63*(6), 707-714.

Comalli, M., Eberhart, R., Griel Jr, L., & Rothenbacher, H. (1984). Changes in the microscopic anatomy of the bovine teat canal during mammary involution. *American Journal of Veterinary Research, 45*(11), 2236-2242.

Concha, C. (1985). Cell types and their immunological functions in bovine mammary tissues and secretions-a review of the literature. *Nordisk Veterinaermedicin, 38*(5), 257-272.

Constantinoiu, C., Jonsson, N., Jorgensen, W., Jackson, L., Piper, E., & Lew-Tabor, A. (2013). Immuno-fluorescence staining patterns of leukocyte subsets in the skin of taurine and indicine cattle. *Research in Veterinary Science, 95*(3), 854-860.

Constantinoiu, C., Jackson, L., Jorgensen, W., Lew-Tabor, A., Piper, E., Mayer, D., Venus, B., & Jonsson, N. (2010). Local immune response against larvae of *Rhipicephalus* (*Boophilus*) *microplus* in *Bos taurus indicus* and *Bos taurus taurus* cattle. *International Journal for Parasitology, 40*(7), 865-875.

Coulombe, P. A., & Omary, M. B. (2002). 'Hard' and 'soft' principles defining the structure, function and regulation of keratin intermediate filaments. *Current Opinion in Cell Biology, 14*(1), 110-122.

Couper, K. N., Blount, D. G., & Riley, E. M. (2008). IL-10: the master regulator of immunity to infection. *Journal of Immunology, 180*(9), 5771-5777.

Cousins, C. L., Higgs, T. M., Jackson, E. R., Neave, F. K., & Dodd, F. H. (1980). Susceptibility of the bovine udder to bacterial infection in the dry period. *Journal of Dairy Research, 47*(1), 11-18.

Craig, R., & Beavis, R. C. (2004). TANDEM: matching proteins with tandem mass spectra. *Bioinformatics, 20*(9), 1466-1467.

Craig, S. W., & Cebra, J. J. (1971). Peyer's patches: an enriched source of precursors for IgA-producing immunocytes in the rabbit. *Journal of Experimental Medicine, 134*(1), 188-200.

Cua, D. J., & Tato, C. M. (2010). Innate IL-17-producing cells: the sentinels of the immune system. *Nature Reviews in Immunology, 10*(7), 479-489.

Cumberbatch, M., Dearman, R., Griffiths, C., & Kimber, I. (2000). Langerhans cell migration. *Clinical and Experimental Dermatology, 25*(5), 413-418.

Cunningham, A., Zhang, J.-G., Moy, J., Ali, S., & Kirby, J. (1997). A comparison of the antigen-presenting capabilities of class II MHC-expressing human lung epithelial and endothelial cells. *Immunology, 91*(3), 458-463.

Czerkinsky, C., Prince, S. J., Michalek, S. M., Jackson, S., Russell, M. W., Moldoveanu, Z., McGhee, J. R., & Mestecky, J. (1987). IgA antibody-producing cells in peripheral blood after antigen ingestion: evidence for a common mucosal immune system in humans. *Proceedings of the National Academy of Sciences, 84*(8), 2449-2453.

Dahlen, J. R., Foster, D. C., & Kisiel, W. (1997). Human proteinase inhibitor 9 (PI9) is a potent inhibitor of subtilisin A. *Biochemical and Biophysical Research Communications, 238*(2), 329-333.

Dale, B. A., Salonen, J., & Jones, A. H. (1990). New approaches and concepts in the study of differentiation of oral epithelia. *Critical Reviews in Oral Biology & Medicine, 1*(3), 167-190.

Daly, C. H. (1982). Biomechanical properties of dermis. *Journal of Investigative Dermatology, 79*, 17-20.

Davis, M. M., & Chien, Y.-h. (1993). Topology and affinity of T-cell receptor mediated recognition of peptide-MHC complexes. *Current Opinion in Immunology, 5*(1), 45-49.

Davis, W., Heirman, L., Hamilton, M., Parish, S., Barrington, G., Loftis, A., & Rogers, M. (2000). Flow cytometric analysis of an immunodeficiency disorder affecting juvenile llamas. *Veterinary Immunology and Immunopathology, 74*(1), 103-120.

Davis, W. C., & Hamilton, M. J. (2006). Use of flow cytometry to characterize immunodeficiency syndromes in camelids. *Small Ruminant Research, 61*(2), 187-193.

Davis, W. C., Brown, W. C., Hamilton, M. J., Wyatt, C. R., Orden, J. A., Khalid, A. M., & Naessens, J. (1996). Analysis of monoclonal antibodies specific for the gamma delta TcR. *Veterinary Immunology and Immunopathology, 52*(4), 275-283.

De, A. K., Kodys, K. M., Yeh, B. S., & Miller-Graziano, C. (2000). Exaggerated human monocyte IL-10 concomitant to minimal TNF-α induction by heat-shock protein 27 (Hsp27) suggests Hsp27 is primarily an antiinflammatory stimulus. *The Journal of Immunology, 165*(7), 3951-3958.

Dego, O. K., Van Dijk, J., & Nederbragt, H. (2002). Factors involved in the early pathogenesis of bovine *Staphylococcus aureus* mastitis with emphasis on bacterial adhesion and invasion. A review. *Veterinary Quarterly, 24*(4), 181-198.

del Rio, M. L., Rodriguez-Barbosa, J. I., Kremmer, E., & Forster, R. (2007). CD103- and CD103+ bronchial lymph node dendritic cells are specialized in presenting and cross-presenting innocuous antigen to CD4+ and CD8+ T cells. *Journal of Immunology, 178*(11), 6861-6866.

Depamede, S. N. (2013). Proteomic analysis of a 14.2 kDa protein isolated from Bali cattle (Bos sondaicus/javanicus) saliva using 1-D SDS-PAGE gel and MALDITOF-TOF mass spectrometer. *Italian Journal of Animal Science, 12*(3), 59-62.

Detre, S., Jotti, G. S., & Dowsett, M. (1995). A" quickscore" method for immunohistochemical semiquantitation: validation for oestrogen receptor in breast carcinomas. *Journal of Clinical Pathology, 48*(9), 876-878.

Donato, R. (2003). Intracellular and extracellular roles of S100 proteins. *Microscopy Research and Technique, 60*(6), 540-551.

Dosogne, H., Vangroenweghe, F., Mehrzad, J., Massart-Leen, A., & Burvenich, C. (2003). Differential leukocyte count method for bovine low somatic cell count milk. *Journal of Dairy Science, 86*(3), 828-834.

Doymaz, M., Sordillo, L., Oliver, S., & Guidry, A. (1988). Effects of *Staphylococcus aureus* mastitis on bovine mammary gland plasma cell populations and immunoglobulin concentrations in milk. *Veterinary Immunology and Immunopathology, 20*(1), 87-93.

Drake, D. R., Brogden, K. A., Dawson, D. V., & Wertz, P. W. (2008). Thematic review series: skin lipids. Antimicrobial lipids at the skin surface. *Journal of Lipid Research, 49*(1), 4-11.

Düvel, A., Frank, C., Schnapper, A., Schuberth, H.-J., & Sipka, A. (2012). Classically or alternatively activated bovine monocyte-derived macrophages in vitro do not resemble CD163/Calprotectin biased macrophage populations in the teat. *Innate Immunity, 18*(6), 886-896.

Eckert, R. L., Broome, A.-M., Ruse, M., Robinson, N., Ryan, D., & Lee, K. (2004). S100 proteins in the epidermis. *Journal of Investigative Dermatology, 123*(1), 23-33.

Ehrchen, J. M., Sunderkötter, C., Foell, D., Vogl, T., & Roth, J. (2009). The endogenous Toll-like receptor 4 agonist S100A8/S100A9 (calprotectin) as innate amplifier of infection, autoimmunity, and cancer. *Journal of Leukocyte Biology, 86*(3), 557-566.

Elgharably, H., Roy, S., Khanna, S., Abas, M., DasGhatak, P., Das, A., Mohammed, K., & Sen, C. K. (2013). A modified collagen gel enhances healing outcome in a preclinical swine model of excisional wounds. *Wound Repair and Regeneration, 21*(3), 473-481.

Ellison, R. D., Giehl, T. J., & LaForce, F. M. (1988). Damage of the outer membrane of enteric gram-negative bacteria by lactoferrin and transferrin. *Infection and Immunity, 56*(11), 2774-2781.

Elsbach, P., & Weiss, J. (1985). Oxygen-dependent and oxygen-independent mechanisms of microbicidal activity of neutrophils. *Immunology Letters, 11*(3), 159-163.

Eversole, L., Miyasaki, K. T., & Christensen, R. E. (1993). Keratinocyte expression of calprotectin in oral inflammatory mucosal diseases. *Journal of Oral Pathology & Medicine, 22*(7), 303-307.

Falentin, H., Rault, L., Nicolas, A., Bouchard, D. S., Lassalas, J., Lamberton, P., Aubry, J.-M., Marnet, P.-G., Le Loir, Y., & Even, S. (2016). Bovine teat microbiome analysis revealed reduced alpha diversity and significant changes in taxonomic profiles in quarters with a history of mastitis. *Frontiers in Microbiology, 7*, Article 480.

Faurschou, M., & Borregaard, N. (2003). Neutrophil granules and secretory vesicles in inflammation. *Microbes and Infection, 5*(14), 1317-1327.

Figdor, C. G., van Kooyk, Y., & Adema, G. J. (2002). C-type lectin receptors on dendritic cells and Langerhans cells. *Nature Reviews in Immunology, 2*(2), 77-84.

Fithian, E., Kung, P., Goldstein, G., Rubenfeld, M., Fenoglio, C., & Edelson, R. (1981). Reactivity of Langerhans cells with hybridoma antibody. *Proceedings of the National Academy of Sciences, 78*(4), 2541-2544.

Fitzpatrick, J., Cripps, P., Hill, A., Bland, P., & Stokes, C. (1992). MHC class II expression in the bovine mammary gland. *Veterinary Immunology and Immunopathology, 32*(1), 13-23.

Florens, L., Carozza, M. J., Swanson, S. K., Fournier, M., Coleman, M. K., Workman, J. L., & Washburn, M. P. (2006). Analyzing chromatin remodeling complexes using shotgun proteomics and normalized spectral abundance factors. *Methods, 40*(4), 303-311.

Flotte, T. J., Springer, T., & Thorbecke, G. (1983). Dendritic cell and macrophage staining by monoclonal antibodies in tissue sections and epidermal sheets. *The American Journal of Pathology, 111*(1), 112-124.

Foell, D., Wittkowski, H., Vogl, T., & Roth, J. (2007). S100 proteins expressed in phagocytes: a novel group of damage-associated molecular pattern molecules. *Journal of Leukocyte Biology, 81*(1), 28-37.

Foell, D., Wittkowski, H., Kessel, C., Lüken, A., Weinhage, T., Varga, G., Vogl, T., Wirth, T., Viemann, D., & Björk, P. (2013). Proinflammatory S100A12 can activate human monocytes via Toll-like receptor 4. *American Journal of Respiratory and Critical Care Medicine, 187*(12), 1324-1334.

Forbes, D. (1968). *Studies of the infection of bovine teat canals, their epidemiology and role in the pathogenesis of mastitis.* Ph.D thesis, University of Reading.

Forbes, D. (1970). The survival of *Micro-coccaceae* in bovine teat canal keratin. *British Veterinary Journal, 126*, 268-274.

Fragkou, I., Dagleish, M., Papaioannou, N., Cripps, P., Boscos, C., Ververidis, H., Orfanou, D., Solomakos, N., Finlayson, J., & Govaris, A. (2010). The induction of lymphoid follicle-like structures in the ovine teat duct following experimental infection with *Mannheimia haemolytica*. *Veterinary Journal, 184*(2), 194-200.

Franke, W. W., Schiller, D. L., Moll, R., Winter, S., Schmid, E., Engelbrecht, I., Denk, H., Krepler, R., & Platzer, B. (1981). Diversity of cytokeratins: differentiation specific expression of cytokeratin polypeptides in epithelial cells and tissues. *Journal of Molecular Biology, 153*(4), 933-959.

Frey, A., Giannasca, K. T., Weltzin, R., Giannasca, P. J., Reggio, H., Lencer, W. I., & Neutra, M. R. (1996). Role of the glycocalyx in regulating access of microparticles to apical plasma membranes of intestinal epithelial cells: implications for microbial attachment and oral vaccine targeting. *The Journal of Experimental Medicine, 184*(3), 1045-1059.

Fries, P., Popowych, Y. I., Guan le, L., Beskorwayne, T., Potter, A., Babiuk, L., & Griebel, P. J. (2011). Mucosal dendritic cell subpopulations in the small intestine of newborn calves. *Developmental & Comparative Immunology, 35*(10), 1040-1051.

Fries, P. N., & Griebel, P. J. (2011). Mucosal dendritic cell diversity in the gastrointestinal tract. *Cell and Tissue Research, 343*(1), 33-41.

Fürstenberg, M. (1868). *Die Milchdrüsen der Kuh: Ihre Anatomie, Physiologie und Pathologie unter besonderer Berücksichtigung der Haltung, Pflege, Fütterung und Zucht der Milchkühe.* Doctoral thesis, Munich, Wilhelm. Engelmann, Leipzig.

Galli, S. J., Kalesnikoff, J., Grimbaldeston, M. A., Piliponsky, A. M., Williams, C. M., & Tsai, M. (2005). Mast cells as "tunable" effector and immunoregulatory cells: recent advances. *Annual Review of Immunology, 23*, 749-786.

Garreis, F., Gottschalt, M., Schlorf, T., Gläser, R., Harder, J., Worlitzsch, D., & Paulsen, F. P. (2011). Expression and regulation of antimicrobial peptide psoriasin (S100A7) at the ocular surface and in the lacrimal apparatus. *Investigative Ophthalmology & Visual Science, 52*(7), 4914-4922.

Gebert, A., Rothkötter, H.-J., & Pabst, R. (1994). Cytokeratin 18 is an M-cell marker in porcine Peyer's patches. *Cell and Tissue Research, 276*(2), 213-221.

Giesecke, W., Gerneke, W., & van Rensburg, I. (1972). The morphology of the bovine teat canal: a preliminary report. *Journal of the South African Veterinary Medical Association, 43*(4), 351-354.

Gill, J. J., Sabour, P. M., Gong, J., Yu, H., Leslie, K. E., & Griffiths, M. W. (2006). Characterization of bacterial populations recovered from the teat canals of lactating dairy and beef cattle by 16S rRNA gene sequence analysis. *FEMS Microbiology Ecology, 56*(3), 471-481.

Girardi, M. (2006). Immunosurveillance and immunoregulation by γδ T cells. *Journal of Investigative Dermatology, 126*(1), 25-31.

Gläser, R., Harder, J., Lange, H., Bartels, J., Christophers, E., & Schröder, J.-M. (2005). Antimicrobial psoriasin (S100A7) protects human skin from *Escherichia coli* infection. *Nature Immunology, 6*(1), 57-64.

Gliddon, D. R., Hope, J. C., Brooke, G. P., & Howard, C. J. (2004). DEC-205 expression on migrating dendritic cells in afferent lymph. *Immunology, 111*(3), 262-272.

Godber, B. L., Doel, J. J., Durgan, J., Eisenthal, R., & Harrison, R. (2000a). A new route to peroxynitrite: a role for xanthine oxidoreductase. *FEBS Letters, 475*(2), 93-96.

Godber, B. L., Doel, J. J., Sapkota, G. P., Blake, D. R., Stevens, C. R., Eisenthal, R., & Harrison, R. (2000b). Reduction of nitrite to nitric oxide catalyzed by xanthine oxidoreductase. *Journal of Biological Chemistry, 275*(11), 7757-7763.

González-Cano, P., Arsic, N., Popowych, Y. I., & Griebel, P. J. (2014). Two functionally distinct myeloid dendritic cell subpopulations are present in bovine blood. *Developmental & Comparative Immunology, 44*(2), 378-388.

Gonzalez, L. F., Krawczyk, W. S., & Wilgram, G. F. (1976). Ultrastructural observations on the enzymatic activity of keratinosomes. *Journal of Ultrastructure Research, 55*(2), 203-211.

Goodman, T., & Lefrancois, L. (1988). Expression of the γδ T-cell receptor on intestinal CD8+ intraepithelial lymphocytes. *Nature, 333*(6176), 855-858.

Goodwin, C. (2011). Anatomy and Physiology of the Skin. *Journal of the Dermatology Nurses' Association, 3*(4), 203-213.

Goossens, K., Tesfaye, D., Rings, F., Schellander, K., Hölker, M., Van Poucke, M., Van Zeveren, A., Lemahieu, I., Van Soom, A., & Peelman, L. J. (2010). Suppression of keratin 18 gene expression in bovine blastocysts by RNA interference. *Reproduction, Fertility and Development, 22*(2), 395-404.

Gosselin, E., Wardwell, K., Rigby, W., & Guyre, P. (1993). Induction of MHC class II on human polymorphonuclear neutrophils by granulocyte/macrophage colony-stimulating factor, IFN-gamma, and IL-3. *Journal of Immunology, 151*(3), 1482-1490.

Gottsch, J. D., Eisinger, S. W., Liu, S. H., & Scott, A. L. (1999). Calgranulin C has filariacidal and filariastatic activity. *Infection and Immunity, 67*(12), 6631-6636.

Granger, D. N., Rutili, G., & McCord, J. M. (1981). Superoxide radicals in feline intestinal ischemia. *Gastroenterology, 81*(1), 22-29.

Gray, P. (1954). *The Microtomist's Formulary and Guide* The Microtomist's Formulary and Guide. Philadelphia: Constable and Co Limited

Green, S. J., Crawford, R. M., Hockmeyer, J. T., Meltzer, M. S., & Nacy, C. A. (1990). Leishmania major amastigotes initiate the L-arginine-dependent killing mechanism in IFN-gamma-stimulated macrophages by induction of tumor necrosis factor-alpha. *Journal of Immunology, 145*(12), 4290-4297.

Grindal, R. J., Walton, A. W., & Hillerton, J. E. (1991). Influence of milk flow rate and streak canal length on new intramammary infection in dairy cows. *Journal of Dairy Research, 58*(4), 383-388.

Guidry, A., Ost, M., Mather, I., Shainline, W., & Weinland, B. (1983). Sequential response of milk leukocytes, albumin, immunoglobulins, monovalent ions, citrate, and lactose in cows given infusions of *Escherichia coli* endotoxin into the mammary gland. *American Journal of Veterinary Research, 44*(12), 2262-2267.

Guilliams, M., Ginhoux, F., Jakubzick, C., Naik, S. H., Onai, N., Schraml, B. U., Segura, E., Tussiwand, R., & Yona, S. (2014). Dendritic cells, monocytes and macrophages: a unified nomenclature based on ontogeny. *Nature Reviews Immunology*, *14*(8), 571-578.

Gupta, R., & Ramnani, P. (2006). Microbial keratinases and their prospective applications: an overview. *Applied Microbiology and Biotechnology*, *70*(1), 21-33.

Guzman, E., Price, S., Poulsom, H., & Hope, J. (2011). Bovine γδ T cells: Cells with multiple functions and important roles in immunity. *Veterinary Immunology and Immunopathology*, *148*(1-2), 161-167.

Gyorki, D. E., Asselin-Labat, M.-L., van Rooijen, N., Lindeman, G. J., & Visvader, J. E. (2009). Resident macrophages influence stem cell activity in the mammary gland. *Breast Cancer Research, 11*(4), R62.

Hamada, H., Hiroi, T., Nishiyama, Y., Takahashi, H., Masunaga, Y., Hachimura, S., Kaminogawa, S., Takahashi-Iwanaga, H., Iwanaga, T., & Kiyono, H. (2002). Identification of multiple isolated lymphoid follicles on the antimesenteric wall of the mouse small intestine. *Journal of Immunology, 168*(1), 57-64.

Hamada, S., Umemura, M., Shiono, T., Tanaka, K., Yahagi, A., Begum, M. D., Oshiro, K., Okamoto, Y., Watanabe, H., & Kawakami, K. (2008). IL-17A produced by γδ T cells plays a critical role in innate immunity against *Listeria monocytogenes* infection in the liver. *Journal of Immunology*, *181*(5), 3456-3463.

Hampton, M. B., Kettle, A. J., & Winterbourn, C. C. (1998). Inside the neutrophil phagosome: oxidants, myeloperoxidase, and bacterial killing. *Blood, 92*(9), 3007-3017.

Harder, J., & Schroder, J. M. (2002). RNase 7, a novel innate immune defense antimicrobial protein of healthy human skin. *Journal of Biological Chemistry, 277*(48), 46779-46784.

Harder, J., Schröder, J.-M., & Gläser, R. (2013). The skin surface as antimicrobial barrier: present concepts and future outlooks. *Experimental Dermatology, 22*(1), 1-5.

Harmon, R., & Heald, C. (1982). Migration of polymorphonuclear leukocytes into the bovine mammary gland during experimentally induced *Staphylococcus aureus* mastitis. *American Journal of Veterinary Research, 43*(6), 992-998.

Hasday, J. D., Fairchild, K. D., & Shanholtz, C. (2000). The role of fever in the infected host. *Microbes and Infection, 2*(15), 1891-1904.

Hashimoto, M., Tawaratsumida, K., Kariya, H., Aoyama, K., Tamura, T., & Suda, Y. (2006). Lipoprotein is a predominant Toll-like receptor 2 ligand in *Staphylococcus aureus* cell wall components. *International Immunology, 18*(2), 355-362.

Hayday, A., & Viney, J. L. (2000). The ins and outs of body surface immunology. *Science, 290*(5489), 97-100.

Hayday, A., Theodoridis, E., Ramsburg, E., & Shires, J. (2001). Intraepithelial lymphocytes: exploring the third way in immunology. *Nature Immunology, 2*(11), 997-1003.

Heczko, P., Lütticken, R., Hryniewicz, W., Neugebauer, M., & Pulverer, G. (1979). Susceptibility of *Staphylococcus aureus* and group A, B, C, and G streptococci to free fatty acids. *Journal of Clinical Microbiology, 9*(3), 333-335.

Hell, W., Essig, A., Bohnet, S., Gatermann, S., & Marre, R. (1993). Cleavage of tumor necrosis factor-α by *Legionella* exoprotease. *Apmis, 101*(1-6), 120-126.

Hershberg, R. M., Framson, P. E., Cho, D. H., Lee, L. Y., Kovats, S., Beitz, J., Blum, J. S., & Nepom, G. T. (1997). Intestinal epithelial cells use two distinct pathways for HLA class II antigen processing. *Journal of Clinical Investigation, 100*(1), 204-215.

Hettinga, K., Van Valenberg, H., De Vries, S., Boeren, S., Van Hooijdonk, T., van Arendonk, J., & Vervoort, J. (2011). The host defense proteome of human and bovine milk. *PloS one, 6*(4), e19433.

Hibbitt, K., Cole, C., & Reiter, B. (1969). Antimicrobial proteins isolated from the teat canal of the cow. *Journal of General Microbiology, 56*(3), 365-371.

Hibbs, R. G., & Clark, W. H. (1959). Electron microscope studies of the human epidermis: The cell boundaries and topography of the stratum malpighii. *The Journal of Biophysical and Biochemical Cytology, 6*(1), 71-76.

Hogan, J., Duthie, A., & Pankey, J. (1986). Fatty acid composition of bovine teat canal keratin. *Journal of Dairy Science, 69*(9), 2424-2427.

Hogan, J., Pankey, J., & Duthie, A. (1987). Growth inhibition of mastitis pathogens by long-chain fatty acids. *Journal of Dairy Science, 70*(5), 927-934.

Hogan, J. S. (1999). *Laboratory handbook on bovine mastitis: In diagnostic procedures*. National Mastitis Council Inc: National Mastitis Council.

Holderness, J., Hedges, J. F., Ramstead, A., & Jutila, M. A. (2013). Comparative biology of γδ T cell function in humans, mice, and domestic animals. *Annual Review of Animal Biosciences, 1*(1), 99-124.

Holst, B., Hurley, W., & Nelson, D. (1987). Involution of the bovine mammary gland: histological and ultrastructural changes. *Journal of Dairy Science, 70*(5), 935-944.

Honda, K., & Littman, D. R. (2012). The microbiome in infectious disease and inflammation. *Annual Review of Immunology, 30*, 759-795.

Hondo, T., Kanaya, T., Takakura, I., Watanabe, H., Takahashi, Y., Nagasawa, Y., Terada, S., Ohwada, S., Watanabe, K., & Kitazawa, H. (2011). Cytokeratin 18 is a specific marker of bovine intestinal M cell. *American Journal of Physiology-Gastrointestinal and Liver Physiology, 300*(3), G442-G453.

Howard, C., Morrison, W., Bensaid, A., Davis, W., Eskra, L., Gerdes, J., Hadam, M., Hurley, D., Leibold, W., & Letesson, J. (1991). Summary of workshop findings for leukocyte antigens of cattle. *Veterinary Immunology and Immunopathology, 27*(1), 21-27.

Huang, C.-M., Elmets, C. A., van Kampen, K. R., DeSilva, T. S., Barnes, S., Kim, H., & Tang, D.-c. C. (2005). Prospective highlights of functional skin proteomics. *Mass Spectrometry Reviews, 24*(5), 647-660.

Hurley, W. (1987). Mammary function during the nonlactating period: enzyme, lactose, protein concentrations, and pH of mammary secretions. *Journal of Dairy Science, 70*(1), 20-28.

Inaba, K., Swiggard, W. J., Inaba, M., Meltzer, J., Miryza, A., Sasagawa, T., Nussenzweig, M. C., & Steinman, R. U. (1995). Tissue distribution of the DEC-205 protein that is detected by the monoclonal antibody NLDC-145 I. Expression on dendritic cells and other subsets of mouse leukocytes. *Cellular Immunology, 163*(1), 148-156.

Ip, W. K., Takahashi, K., Ezekowitz, R. A., & Stuart, L. M. (2009). Mannose-binding lectin and innate immunity. *Immunological Reviews, 230*(1), 9-21.

Itohara, S., Farr, A. G., Lafaille, J. J., Bonneville, M., Takagaki, Y., Haas, W., & Tonegawa, S. (1990). Homing of a γδ thymocyte subset with homogeneous T-cell receptors to mucosal epithelia. *Nature, 343*(6260), 754-757.

Iwasaki, A. (2007). Mucosal dendritic cells. *Annual Review of Immunology, 25*, 381-418.

Janeway, C. A., Jr. (1989). Approaching the asymptote? Evolution and revolution in immunology. *Cold Spring Harbor Symposia on Quantitative Biology, 54*(1), 1-13.

Jensen, D., & Eberhart, R. (1975). Macrophages in bovine milk. *American Journal of Veterinary Research, 36*(5), 619-624.

Jensen, D. L., & Eberhart, R. J. (1981). Total and differential cell counts in secretions of the nonlactating bovine mammary gland. *American Journal of Veterinary Research, 42*(5), 743-7.

Jenssen, H., & Hancock, R. E. (2009). Antimicrobial properties of lactoferrin. *Biochimie, 91*(1), 19-29.

John, A. L. S., & Abraham, S. N. (2013). Innate immunity and its regulation by mast cells. *Journal of Immunology, 190*(9), 4458-4463.

Jung, C., Hugot, J. P., & Barreau, F. (2010). Peyer's Patches: The Immune Sensors of the Intestine. *International Journal of Inflammation 2010*, 823710.

Kabelitz, D., Wesch, D., & He, W. (2007). Perspectives of γδ T Cells in Tumor Immunology. *Cancer Research, 67*(1), 5-8.

Kabir, S. (1998). Jacalin: a jackfruit (*Artocarpus heterophyllus*) seed-derived lectin of versatile applications in immunobiological research. *Journal of Immunological Methods, 212*(2), 193-211.

Kamada, N., Chen, G. Y., Inohara, N., & Núñez, G. (2013). Control of pathogens and pathobionts by the gut microbiota. *Nature Immunology, 14*(7), 685-690.

Kanitakis, J. (2002). Anatomy, histology and immunohistochemistry of normal human skin. *European Journal of Dermatology, 12*(4), 390-401.

Kato, M., McDonald, K. J., Khan, S., Ross, I. L., Vuckovic, S., Chen, K., Munster, D., MacDonald, K. P., & Hart, D. N. (2006). Expression of human DEC-205 (CD205) multilectin receptor on leukocytes. *International Immunology, 18*(6), 857-869.

Kehl-Fie, T. E., Chitayat, S., Hood, M. I., Damo, S., Restrepo, N., Garcia, C., Munro, K. A., Chazin, W. J., & Skaar, E. P. (2011). Nutrient metal sequestration by calprotectin inhibits bacterial superoxide defense, enhancing neutrophil killing of *Staphylococcus aureus*. *Cell Host & Microbe, 10*(2), 158-164.

Kehrli, M. E., & Shuster, D. E. (1994). Factors affecting milk somatic cells and their role in health of the bovine mammary gland. *Journal of Dairy Science, 77*(2), 619-627.

Keller, A., Nesvizhskii, A. I., Kolker, E., & Aebersold, R. (2002). Empirical statistical model to estimate the accuracy of peptide identifications made by MS/MS and database search. *Analytical Chemistry, 74*(20), 5383-92.

Kemper-Krämer, G. (1983). *Untersuchungen über das Keratin des Strichkanals von Kühen unter Berücksichtigung morphologischer Zitzenmerkmale [Investigations on keratin of the teat canal in cows with special regard to morphological properties of the teats]*. thesis, Justus-Liebig-Universität, Gießen.

Keresztes, G., Takacs, L., Vilmos, P., Kurucz, E., & Ando, I. (1996). Monoclonal antibodies detecting components of the bovine immune system in formaldehyde-fixed paraffin-embedded tissue specimens. *Veterinary Immunology and Immunopathology, 52*(4), 383-392.

Khovidhunkit, W., Kim, M.-S., Memon, R. A., Shigenaga, J. K., Moser, A. H., Feingold, K. R., & Grunfeld, C. (2004). Effects of infection and inflammation on lipid and lipoprotein metabolism: mechanisms and consequences to the host. *The Journal of Lipid Research, 45*(7), 1169-1196.

Kilian, M., Reinholdt, J., Lomholt, H., Poulsen, K., & Frandsen, E. V. G. (1996). Biological significance of IgA1 proteases in bacterial colonization and pathogenesis: critical evaluation of experimental evidence. *Apmis, 104*(1-6), 321-338.

Kim, S. A., Lee, Y., Jung, D. E., Park, K. H., Park, J. Y., Gang, J., Jeon, S. B., Park, E. C., Kim, Y. G., & Lee, B. (2009). Pancreatic adenocarcinoma up-regulated factor (PAUF), a novel up-regulated secretory protein in pancreatic ductal adenocarcinoma. *Cancer Science, 100*(5), 828-836.

Kim, S. J., Min, J.-K., Lee, Y., & Koh, S. S. (2011). Pancreatic adenocarcinoma upregulated factor promotes angiogenesis and vascular permeability through modulation of endothelial cell activation. *Cancer Research, 71*(8 Supplement), 5137-5137.

Klechevsky, E., Morita, R., Liu, M., Cao, Y., Coquery, S., Thompson-Snipes, L., Briere, F., Chaussabel, D., Zurawski, G., & Palucka, A. K. (2008). Functional specializations of human epidermal Langerhans cells and CD14+ dermal dendritic cells. *Immunity, 29*(3), 497-510.

Klein, L. M., Lavker, R. M., Matis, W. L., & Murphy, G. F. (1989). Degranulation of human mast cells induces an endothelial antigen central to leukocyte adhesion. *Proceedings of the National Academy of Sciences, 86*(22), 8972-8976.

Knoop, K. A., & Newberry, R. D. (2012). Isolated Lymphoid Follicles are Dynamic Reservoirs for the Induction of Intestinal IgA. *Frontiers in Immunology, 3*, 84.

Koay, M. A., Delbeck, T., Mack, M., Ermert, M., Ermert, L., Blackwell, T. S., Christman, J. W., Schlöndorff, D., Seeger, W., & Lohmeyer, J. (2002). Role of resident alveolar macrophages in leukocyte traffic into the alveolar air space of intact mice. *American Journal of Physiology-Lung Cellular and Molecular Physiology, 282*(6), L1245-L1252.

Kobayashi, M., Yoshiki, R., Sakabe, J., Kabashima, K., Nakamura, M., & Tokura, Y. (2009). Expression of toll-like receptor 2, NOD2 and dectin-1 and stimulatory effects of their ligands and histamine in normal human keratinocytes. *British Journal of Dermatology, 160*(2), 297-304.

Kobayashi, S. D., Voyich, J. M., Burlak, C., & DeLeo, F. R. (2005). Neutrophils in the innate immune response. *Archivum Immunologiae et Therapiae Experimentalis, 53*(6), 505-517.

Kolarsick, P. A., Kolarsick, M. A., & Goodwin, C. (2011). Anatomy and Physiology of the Skin. *Journal of the Dermatology Nurses' Association, 3*(4), 203-213.

Komiyama, T., Grøn, H., Salvesen, G. S., & Pemberton, P. A. (1996). Interaction of subtilisins with serpins. *Protein Science, 5*(5), 874-882.

Korhonen, H., Marnila, P., & Gill, H. (2000). Milk immunoglobulins and complement factors. *British Journal of Nutrition, 84*(S1), 75-80.

Kraal, G., Breel, M., Janse, M., & Bruin, G. (1986). Langerhans' cells, veiled cells, and interdigitating cells in the mouse recognized by a monoclonal antibody. *The Journal of Experimental Medicine, 163*(4), 981-997.

Kraehenbuhl, J.-P., & Neutra, M. R. (2000). Epithelial M cells: differentiation and function. *Annual Review of Cell and Developmental Biology, 16*(1), 301-332.

Krisanaprakornkit, S., Weinberg, A., Perez, C. N., & Dale, B. A. (1998). Expression of the peptide antibiotic human β-defensin-1 in cultured gingival epithelial cells and gingival tissue. *Infection and Immunity, 66*(9), 4222-4228.

Kuehn, J. S., Gorden, P. J., Munro, D., Rong, R., Dong, Q., Plummer, P. J., Wang, C., & Phillips, G. J. (2013). Bacterial community profiling of milk samples as a means to understand culture-negative bovine clinical mastitis. *PloS one, 8*(4), e61959.

Kumar, H., Kawai, T., & Akira, S. (2011). Pathogen recognition by the innate immune system. *International Reviews of Immunology, 30*(1), 16-34.

Kupper, T. S., & Fuhlbrigge, R. C. (2004). Immune surveillance in the skin: mechanisms and clinical consequences. *Nature Reviews in Immunology, 4*(3), 211-222.

Lacy-Hulbert, S. J., & Hillerton, J. E. (1995). Physical characteristics of the bovine teat canal and their influence on susceptibility to *streptococcal* infection. *Journal of Dairy Research, 62*(3), 395-404.

Lambris, J. D., Ricklin, D., & Geisbrecht, B. V. (2008). Complement evasion by human pathogens. *Nature Reviews in Microbiology, 6*(2), 132-142.

Leclerc, E., Fritz, G., Vetter, S. W., & Heizmann, C. W. (2009). Binding of S100 proteins to RAGE: an update. *Biochimica et Biophysica Acta, 1793*(6), 993-1007.

Lee, K. C., & Eckert, R. L. (2007). S100A7 (Psoriasin)–mechanism of antibacterial action in wounds. *Journal of Investigative Dermatology, 127*(4), 945-957.

Leigh, I., Navsaria, H., Purkis, P., McKay, I., Bowden, P., & Riddle, P. (1995). Keratins (Kl6 and Kl7) as markers of keratinocyte hyperproliferation in psoriasis in vivo and in vitro. *British Journal of Dermatology, 133*(4), 501-511.

Levashina, E. A., Langley, E., Green, C., Gubb, D., Ashburner, M., Hoffmann, J. A., & Reichhart, J.-M. (1999). Constitutive activation of toll-mediated antifungal defense in serpin-deficient *Drosophila*. *Science, 285*(5435), 1917-1919.

Linardi, A., Costa, S. K., da Silva, G. R., & Antunes, E. (2000). Involvement of kinins, mast cells and sensory neurons in the plasma exudation and paw oedema induced by staphylococcal enterotoxin B in the mouse. *European Journal of Pharmacology, 399*(2), 235-242.

Lind, M., Sipka, A. S., Schuberth, H.-J., Blutke, A., Wanke, R., Sauter-Louis, C., Duda, K. A., Holst, O., Rainard, P., & Germon, P. (2015). Location-specific expression of chemokines, TNF-α and S100 proteins in a teat explant model. *Innate Immunity*, 1753425914539820.

Liu, H., Sadygov, R. G., & Yates, J. R. (2004). A model for random sampling and estimation of relative protein abundance in shotgun proteomics. *Analytical Chemistry, 76*(14), 4193-4201.

Liu, Y.-J. (2001). Dendritic cell subsets and lineages, and their functions in innate and adaptive immunity. *Cell, 106*(3), 259-262.

Lominadze, G., Powell, D. W., Luerman, G. C., Link, A. J., Ward, R. A., & McLeish, K. R. (2005). Proteomic analysis of human neutrophil granules. *Molecular & Cellular Proteomics, 4*(10), 1503-1521.

Lundberg, K. C., Fritz, Y., Johnston, A., Foster, A. M., Baliwag, J., Gudjonsson, J. E., Schlatzer, D., Gokulrangan, G., McCormick, T. S., & Chance, M. R. (2015). Proteomics of Skin Proteins in Psoriasis: From Discovery and Verification in a Mouse Model to Confirmation in Humans. *Molecular & Cellular Proteomics, 14*(1), 109-119.

Lundgren, D. H., Hwang, S.-I., Wu, L., & Han, D. K. (2010). Role of spectral counting in quantitative proteomics. *Expert Review of Proteomics, 7*(1), 39-53.

Lundqvist, C., Baranov, V., Hammarstrom, S., Athlin, L., & Hammarstrom, M. L. (1995). Intra-epithelial lymphocytes. Evidence for regional specialization and extrathymic T cell maturation in the human gut epithelium. *International Immunology, 7*(9), 1473-87.

Lytinas, M., Kempuraj, D., Huang, M., Boucher, W., Esposito, P., & Theoharides, T. C. (2003). Acute stress results in skin corticotropin-releasing hormone secretion, mast cell activation and vascular permeability, an effect mimicked by intradermal corticotropin-releasing hormone and inhibited by histamine-1 receptor antagonists. *International Archives of Allergy and Immunology, 130*(3), 224-231.

Ma, J., Liao, X.-L., Lou, B., & Wu, M.-P. (2004). Role of apolipoprotein AI in protecting against endotoxin toxicity. *Acta Biochimica et Biophysica Sinica, 36*(6), 419-424.

MacDonald, T. T. (2003). The mucosal immune system. *Parasite Immunology, 25*(5), 235-246.

Mackie, D., & Logan, E. (1986). Changes in immunoglobulin levels in whey during experimental *Streptococcus agalactiae* mastitis. *Research in Veterinary Science, 40*(2), 183-188.

Magert, H.-J., Drogemuller, K., & Raghunath, M. (2005). Serine proteinase inhibitors in the skin: role in homeostasis and disease. *Current Protein and Peptide Science, 6*(3), 241-254.

Mahley, R. W., Innerarity, T. L., Rall, S. C., & Weisgraber, K. H. (1984). Plasma lipoproteins: apolipoprotein structure and function. *Journal of Lipid Research, 25*(12), 1277-1294.

Malaviya, R., & Abraham, S. N. (2001). Mast cell modulation of immune responses to bacteria. *Immunological Reviews, 179*(1), 16-24.

Mańkowski, H. (1903). *Der histologische Bau des Strichkanals der Kuhzitze.* Doctoral thesis, Drukarnia Ludowa.

Marshall, J. S. (2004). Mast-cell responses to pathogens. *Nature Reviews in Immunology, 4*(10), 787-799.

Martin, B., Hirota, K., Cua, D. J., Stockinger, B., & Veldhoen, M. (2009). Interleukin-17-producing γδ T cells selectively expand in response to pathogen products and environmental signals. *Immunity, 31*(2), 321-330.

Martin, H. M., Hancock, J. T., Salisbury, V., & Harrison, R. (2004). Role of xanthine oxidoreductase as an antimicrobial agent. *Infection and Immunity, 72*(9), 4933-9.

Mason, D., & Taylor, C. (1978). Distribution of transferrin, ferritin, and lactoferrin in human tissues. *Journal of Clinical Pathology, 31*(4), 316-327.

Mathers, A. R., & Larregina, A. T. (2006). Professional antigen-presenting cells of the skin. *Immunologic Research, 36*(1-3), 127-136.

Matoltsy, A. (1976). Keratinization. *Journal of Investigative Dermatology, 67*(1), 20-25.

Mauri, C., & Bosma, A. (2012). Immune regulatory function of B cells. *Annual Review of Immunology, 30*, 221-241.

Mavrogianni, V., Cripps, P., Brooks, H., Taitzoglou, I., & Fthenakis, G. (2007). Presence of subepithelial lymphoid nodules in the teat of ewes. *Anatomia, Histologia, Embryologia, 36*(3), 168-171.

Maxymiv, N. G., Bharathan, M., & Mullarky, I. K. (2012). Bovine mammary dendritic cells: A heterogeneous population, distinct from macrophages and similar in phenotype to afferent lymph veiled cells. *Comparative Immunology, Microbiology and Infectious Diseases, 35*(1), 31-38.

McAleer, M. A., & Irvine, A. D. (2013). The multifunctional role of filaggrin in allergic skin disease. *Journal of Allergy and Clinical Immunology, 131*(2), 280-291.

McClellan, K. (1997). Mucosal defense of the outer eye. *Survey of Ophthalmology, 42*(3), 233-246.

McDermott, M. R., & Bienenstock, J. (1979). Evidence for a common mucosal immunologic system. I. Migration of B immunoblasts into intestinal, respiratory, and genital tissues. *Journal of Immunology, 122*(5), 1892-1898.

McGee, D. A., Rasby, R. J., Nielsen, M. K., & Mader, T. L. (2008). *Effects of summer climatic conditions on body temperature in beef cows.* University of Nebraska, Lincoln. 14-16p.

Medzhitov, R., & Janeway Jr, C. A. (1997). Innate immunity: impact on the adaptive immune response. *Current Opinion in Immunology, 9*(1), 4-9.

Méhul, B., Bernard, D., & Schmidt, R. (2001). Calmodulin-like skin protein: a new marker of keratinocyte differentiation. *Journal of Investigative Dermatology, 116*(6), 905-909.

Melchior, M., Vaarkamp, H., & Fink-Gremmels, J. (2006). Biofilms: a role in recurrent mastitis infections? *The Veterinary Journal, 171*(3), 398-407.

Menon, G., & Elias, P. (2001). The epidermal barrier and strategies for surmounting it: an overview. U. R. Hengge & B. Volc-Platzer (Eds.), In *The Skin and Gene Therapy* (pp. 3-26) Springer-Verlag Berlin Heidelberg.

Menon, G. K., Cleary, G. W., & Lane, M. E. (2012). The structure and function of the stratum corneum. *International Journal of Pharmaceutics, 435*(1), 3-9.

Menzies, M., & Ingham, A. (2006). Identification and expression of Toll-like receptors 1-10 in selected bovine and ovine tissues. *Veterinary Immunology and Immunopathology, 109*(1-2), 23-30.

Metcalfe, D. D., Baram, D., & Mekori, Y. A. (1997). Mast cells. *Physiological Reviews, 77*(4), 1033-1079.

Metz, M., Siebenhaar, F., & Maurer, M. (2008). Mast cell functions in the innate skin immune system. *Immunobiology, 213*(3), 251-260.

Meyer-Hoffert, U. (2009). Reddish, scaly, and itchy: how proteases and their inhibitors contribute to inflammatory skin diseases. *Archivum Immunologiae et Therapiae Experimentalis, 57*(5), 345-354.

Meyer, J. E., Harder, J., Sipos, B., Maune, S., Klöppel, G., Bartels, J., Schröder, J. M., & Gläser, R. (2008). Psoriasin (S100A7) is a principal antimicrobial peptide of the human tongue. *Mucosal Immunology, 1*(3), 239-243.

Michalek, M., Gelhaus, C., Hecht, O., Podschun, R., Schröder, J. M., Leippe, M., & Grötzinger, J. (2009). The human antimicrobial protein psoriasin acts by permeabilization of bacterial membranes. *Developmental & Comparative Immunology, 33*(6), 740-746.

Mikesh, L. M., Aramadhaka, L. R., Moskaluk, C., Zigrino, P., Mauch, C., & Fox, J. W. (2013). Proteomic anatomy of human skin. *Journal of Proteomics, 84*, 190-200.

Mildner, M., Stichenwirth, M., Abtin, A., Eckhart, L., Sam, C., Gläser, R., Schröder, J. M., Gmeiner, R., Mlitz, V., & Pammer, J. (2010). Psoriasin (S100A7) is a major *Escherichia coli*-cidal factor of the female genital tract. *Mucosal Immunology, 3*(6), 602-609.

Miller-Graziano, C. L., De, A., Laudanski, K., Herrmann, T., & Bandyopadhyay, S. (2008). *HSP27: an anti-inflammatory and immunomodulatory stress protein acting to dampen immune function*. Novartis Foundation Symposium: Chichester; New York; John Wiley; 1999.

Miller, L. S., & Modlin, R. L. (2007). *Toll-like receptors in the skin*. Seminars in Immunopathology: Springer.

Mizumoto, N., & Takashima, A. (2004). CD1a and langerin: acting as more than Langerhans cell markers. *Journal of Clinical Investigation, 113*(5), 658-660.

Mogensen, T. H. (2009). Pathogen recognition and inflammatory signaling in innate immune defenses. *Clinical Microbiology Reviews, 22*(2), 240-273.

Moll, R., Divo, M., & Langbein, L. (2008). The human keratins: biology and pathology. *Histochemistry and Cell Biology, 129*(6), 705-733.

Molloy, M. P., Brzezinski, E. E., Hang, J., McDowell, M. T., & VanBogelen, R. A. (2003). Overcoming technical variation and biological variation in quantitative proteomics. *Proteomics, 3*(10), 1912-1919.

Monks, J., Geske, F. J., Lehman, L., & Fadok, V. A. (2002). Do inflammatory cells participate in mammary gland involution? *Journal of Mammary Gland Biology and Neoplasia, 7*(2), 163-176.

Montgomery, P., Cohn, J., & Lally, E. (1974). The induction and characterization of secretory IgA antibodies. In *The immunoglobulin A system* (pp. 453-462) Springer.

Montilla, N. A., Blas, M. P., Santalla, M. L., & Villa, J. M. (2004). Mucosal immune system: A brief review. *Immunologia, 23*, 207-16.

Mosaad, A. A., Elbagory, A. R., Khalid, A. M., Waters, W., Tibary, A., Hamilton, M. J., & Davis, W. C. (2006). Identification of monoclonal antibody reagents for use in the study of the immune response to infectious agents in camel and water buffalo. *Journal of Camel Practice and Research, 13*(2), 91-101.

Mosmann, T. R., & Sad, S. (1996). The expanding universe of T-cell subsets: Th1, Th2 and more. *Immunology Today, 17*(3), 138-146.

Mueller, S. N., Gebhardt, T., Carbone, F. R., & Heath, W. R. (2013). Memory T cell subsets, migration patterns, and tissue residence. *Annual Review of Immunology, 31*, 137-161.

Murdough, P., Martus, N., Mazzola, G., Salamun, D., Scudder, P., Urbano, M., & Pankey, J. (1991). In vitro growth studies of mastitis pathogens on teat canal keratin. *Journal of Dairy Science, 74* (Suppl 1), 204.

Murphy, J. (1959). The effect of certain mild stresses to the bovine teat canal on infection with *Streptococcus agalactiae*. *The Cornell Veterinarian, 49*(3), 411.

Murray, P. J., & Wynn, T. A. (2011). Protective and pathogenic functions of macrophage subsets. *Nature Reviews in Immunology, 11*(11), 723-737.

Murthy, A. R., Lehrer, R. I., Harwig, S. S., & Miyasaki, K. T. (1993). In vitro candidastatic properties of the human neutrophil calprotectin complex. *Journal of Immunology, 151*(11), 6291-301.

Naessens, J., & Hopkins, J. (1996). Introduction and summary of workshop findings. *Veterinary Immunology and Immunopathology, 52*(4), 213-235.

Naessens, J., Nthale, J. M., & Muiya, P. (1996). Biochemical analysis of preliminary clusters in the non-lineage panel. *Veterinary Immunology and Immunopathology, 52*(4), 347-356.

Nai-Yuan, L. E. E., Kawai, K., Nakamura, I., Tanaka, T., Kumura, H., & Shimazaki, K.-i. (2004). Susceptibilities against bovine lactoferrin with microorganisms isolated from mastitic milk. *Journal of Veterinary Medical Science, 66*(10), 1267-1269.

Naidu, S., Svensson, U., Kishore, A. R., & Naidu, A. S. (1993). Relationship between antibacterial activity and porin binding of lactoferrin in *Escherichia coli* and *Salmonella typhimurium*. *Antimicrobial Agents and Chemotherapy, 37*(2), 240-245.

Narumi, K., Miyakawa, R., Ueda, R., Hashimoto, H., Yamamoto, Y., Yoshida, T., & Aoki, K. (2015). Proinflammatory proteins S100A8/S100A9 activate NK cells via interaction with RAGE. *The Journal of Immunology, 194*(11), 5539-5548.

Neave, F., Dodd, F., & Henriques, E. (1950). 408. Udder infections in the 'dry period'. I. *Journal of Dairy Research, 17*(1), 37-49.

Neefjes, J., Jongsma, M. L., Paul, P., & Bakke, O. (2011). Towards a systems understanding of MHC class I and MHC class II antigen presentation. *Nature Reviews Immunology, 11*(12), 823-836.

Nestle, F. O., Di Meglio, P., Qin, J.-Z., & Nickoloff, B. J. (2009). Skin immune sentinels in health and disease. *Nature Reviews in Immunology, 9*(10), 679-691.

Nesvizhskii, A. I., Keller, A., Kolker, E., & Aebersold, R. (2003). A statistical model for identifying proteins by tandem mass spectrometry. *Analytical Chemistry, 75*(17), 4646-58.

Neutra, M. R., Mantis, N. J., & Kraehenbuhl, J.-P. (2001). Collaboration of epithelial cells with organized mucosal lymphoid tissues. *Nature Immunology, 2*(11), 1004-1009.

Newbould, F., & Neave, F. (1965a). The response of the bovine mammary gland to an infusion of *staphylococci*. *Journal of Dairy Research, 32*(02), 163-170.

Newbould, F., & Neave, F. (1965b). The effect of inoculating the bovine teat duct with small numbers of *Staphylococcus aureus*. *Journal of Dairy Research, 32*(2), 171-179.

Nickerson, S. (1989). Immunological aspects of mammary involution[1]. *Journal of Dairy Science, 72*(6), 1665-1678.

Nickerson, S., & Pankey, J. (1983). Cytologic observations of the bovine teat end. *American Journal of Veterinary Research, 44*(8), 1433-1441.

Nickerson, S., & Pankey, J. (1984). Neutrophil Migration Through Teat End Tissues of Bovine Mammary Quarters Experimentally Challenged with *Staphylococcus aureus*. *Journal of Dairy Science, 67*(4), 826-834.

Nickerson, S., & Boddie, R. (1994). Effect of naturally occurring coagulase-negative *Staphylococcal* infections on experimental challenge with major mastitis pathogens[1]. *Journal of Dairy Science, 77*(9), 2526-2536.

Nickerson, S. C., & Heald, C. (1982). Cells in local reaction to experimental *Staphylococcus aureus* infection in bovine mammary gland. *Journal of Dairy Science, 65*(1), 105-116.

Nickerson, S. C., Pankey, J. W., & Boddie, N. T. (1984). Distribution, location, and ultrastructure of plasma cells in the uninfected, lactating bovine mammary gland. *Journal of Dairy Research, 51*(2), 209-217.

Nisapakultorn, K., Ross, K. F., & Herzberg, M. C. (2001). Calprotectin expression inhibits bacterial binding to mucosal epithelial cells. *Infection and Immunity, 69*(6), 3692-3696.

Nonnecke, B. J., & Smith, K. L. (1984). Biochemical and antibacterial properties of bovine mammary secretion during mammary involution and at parturition[1]. *Journal of Dairy Science, 67*(12), 2863-2872.

Notcovich, S., deNicolo, G., Williamson, N., Grinberg, A., Lopez-Villalobos, N., & Petrovski, K. (2016). The ability of four strains of *Streptococcus uberis* to induce clinical mastitis after intramammary inoculation in lactating cows. *New Zealand Veterinary Journal*, *64*(4), 218-223.

Obland, G. F. (1958). The fine structure of the interrelationship of cells in the human epidermis. *The Journal of Biophysical and Biochemical Cytology*, *4*(5), 529-538.

Ochoa, M. T., Loncaric, A., Krutzik, S. R., Becker, T. C., & Modlin, R. L. (2008). "Dermal Dendritic Cells" Comprise Two Distinct Populations: $CD1^+$ Dendritic Cells and $CD209^+$ Macrophages. *Journal of Investigative Dermatology*, *128*(9), 2225-2231.

Oikonomou, G., Machado, V. S., Santisteban, C., Schukken, Y. H., & Bicalho, R. C. (2012). Microbial diversity of bovine mastitic milk as described by pyrosequencing of metagenomic 16s rDNA. *PLoS One, 7*(10), e47671.

Oikonomou, G., Bicalho, M. L., Meira, E., Rossi, R. E., Foditsch, C., Machado, V. S., Teixeira, A. G. V., Santisteban, C., Schukken, Y. H., & Bicalho, R. C. (2014). Microbiota of cow's milk; distinguishing healthy, sub-clinically and clinically diseased quarters. *PloS one, 9*(1), e85904.

Okabe, Y., & Medzhitov, R. (2014). Tissue-specific signals control reversible program of localization and functional polarization of macrophages. *Cell, 157*(4), 832-844.

Okutucu, B., Dınçer, A., Habib, Ö., & Zıhnıoglu, F. (2007). Comparison of five methods for determination of total plasma protein concentration. *Journal of Biochemical and Biophysical Methods, 70*(5), 709-711.

Old, W. M., Meyer-Arendt, K., Aveline-Wolf, L., Pierce, K. G., Mendoza, A., Sevinsky, J. R., Resing, K. A., & Ahn, N. G. (2005). Comparison of label-free methods for quantifying human proteins by shotgun proteomics. *Molecular & Cellular Proteomics*, *4*(10), 1487-1502.

Oliaro, J., Dudal, S., Liautard, J., Andrault, J.-B., Liautard, J.-P., & Lafont, V. (2005). Vγ9Vδ2 T cells use a combination of mechanisms to limit the spread of the pathogenic bacteria *Brucella*. *Journal of Leukocyte Biology*, *77*(5), 652-660.

Oliver, S., & Mitchell, B. (1983). Susceptibility of bovine mammary gland to infections during the dry period. *Journal of Dairy Science, 66*(5), 1162-1166.

Oliveros, J. C. (2007-2015). *Venny. An interactive tool for comparing lists with Venn's diagrams*. from http://bioinfogp.cnb.csic.es/tools/venny/index.html.

Oviedo-Boyso, J., Valdez-Alarcón, J. J., Cajero-Juárez, M., Ochoa-Zarzosa, A., López-Meza, J. E., Bravo-Patino, A., & Baizabal-Aguirre, V. M. (2007). Innate immune response of bovine mammary gland to pathogenic bacteria responsible for mastitis. *Journal of Infection*, *54*(4), 399-409.

Paape, M., Schultze, W., Desjardins, C., & Miller, R. (1974). Plasma corticosteroid, circulating leukocyte and milk somatic cell responses to *Escherichia coli* endotoxin-induced mastitis. *Proceedings of the Society for Experimental Biology and Medicine, 145*(2), 553-559.

Paape, M., Mehrzad, J., Zhao, X., Detilleux, J., & Burvenich, C. (2002a). Defense of the bovine mammary gland by polymorphonuclear neutrophil leukocytes. *Journal of Mammary Gland Biology and Neoplasia, 7*(2), 109-121.

Paape, M. J., Bannerman, D. D., Zhao, X., & Lee, J.-W. (2003). The bovine neutrophil: Structure and function in blood and milk. *Veterinary Research, 34*(5), 597-627.

Paape, M. J., Shafer-Weaver, K., Capuco, A. V., Van Oostveldt, K., & Burvenich, C. (2002b). Immune surveillance of mammary tissue by phagocytic cells. In *Biology of the Mammary Gland* (pp. 259-277) Springer.

Palmer, R. M. J., Ferrige, A. G., & Moncada, S. (1987). Nitric oxide release accounts for the biological activity of endothelium-derived relaxing factor. *Nature, 327*(6122), 524-526.

Panja, A., Blumberg, R. S., Balk, S. P., & Mayer, L. (1993). CD1d is involved in T cell-intestinal epithelial cell interactions. *The Journal of Experimental Medicine, 178*(3), 1115-1119.

Pankey, J., Nickerson, S., Boddie, R., & Hogan, J. (1985). Effects of *Corynebacterium bovis* infection on susceptibility to major mastitis pathogens. *Journal of Dairy Science, 68*(10), 2684-2693.

Park, H. D., Lee, Y., Oh, Y. K., Jung, J. G., Park, Y. W., Myung, K., Kim, K. H., Koh, S. S., & Lim, D. S. (2011a). Pancreatic adenocarcinoma upregulated factor promotes metastasis by regulating TLR/CXCR4 activation. *Oncogene, 30*(2), 201-211.

Park, S. H., Jiang, R., Piao, S., Zhang, B., Kim, E.-H., Kwon, H.-M., Jin, X. L., Lee, B. L., & Ha, N.-C. (2011b). Structural and functional characterization of a highly specific serpin in the insect innate immunity. *Journal of Biological Chemistry, 286*(2), 1567-1575.

Patel, G. K., Wilson, C. H., Harding, K. G., Finlay, A. Y., & Bowden, P. E. (2006). Numerous keratinocyte subtypes involved in wound re-epithelialization. *Journal of Investigative Dermatology, 126*(2), 497-502.

Paulrud, C. O. (2005). Basic concepts of the bovine teat canal. *Veterinary Research Communications, 29*(3), 215-245.

Paulrud, C. O., & Rasmussen, M. D. (2004). How teat canal keratin depends on the length and diameter of the teat canal in dairy cows. *Journal of Dairy Research, 71*(2), 253-255.

Persson, C., Gustafsson, B., Erjefalt, J., & Sundler, F. (1993). Mucosal exudation of plasma is a noninjurious intestinal defense mechanism. *Allergy, 48*(8), 581-586.

Persson, C., Erjefält, I., Alkner, U., Baumgarten, C., Greiff, L., Gustafsson, B., Luts, A., Pipkorn, U., Sundler, F., & Svensson, C. (1991). Plasma exudation as a first line respiratory mucosal defence. *Clinical & Experimental Allergy, 21*(1), 17-24.

Piantoni, P., Wang, P., Drackley, J. K., Hurley, W. L., & Loor, J. J. (2010). Expression of metabolic, tissue remodeling, oxidative stress, and inflammatory pathways in mammary tissue during involution in lactating dairy cows. *Bioinformatics and Biology Insights, 4*, 85.

Platt, N., da Silva, R. P., & Gordon, S. (1998). Recognizing death: the phagocytosis of apoptotic cells. *Trends in Cell Biology, 8*(9), 365-372.

Politis, I., Zhao, X., McBride, B., & Burton, J. (1992). Function of bovine mammary macrophages as antigen-presenting cells. *Veterinary Immunology and Immunopathology, 30*(4), 399-410.

Postigo, A., Corbi, A., Sanchez-Madrid, F., & De Landazuri, M. (1991). Regulated expression and function of CD11c/CD18 integrin on human B lymphocytes. Relation between attachment to fibrinogen and triggering of proliferation through CD11c/CD18. *The Journal of Experimental Medicine, 174*(6), 1313-1322.

Prasad, L., & Newbould, F. (1968). Inoculation of the bovine teat duct with *Staph. Aureus*: the relationship of teat duct length, milk yield and milking rate to development of intramammary infection. *The Canadian Veterinary Journal, 9*(5), 107.

Pudney, J., & Anderson, D. J. (1995). Immunobiology of the human penile urethra. *The American Journal of Pathology, 147*(1), 155-165.

Qin, G., Mao, H., Zheng, J., Sia, S. F., Liu, Y., Chan, P. L., Lam, K. T., Peiris, J. S., Lau, Y. L., & Tu, W. (2009). Phosphoantigen-expanded human gammadelta T cells display potent cytotoxicity against monocyte-derived macrophages infected with human and avian influenza viruses. *Journal of Infectious Diseases, 200*(6), 858-865.

Radsak, M., Iking-Konert, C., Stegmaier, S., Andrassy, K., & Hänsch, G. (2000). Polymorphonuclear neutrophils as accessory cells for T-cell activation: major histocompatibility complex class II restricted antigen-dependent induction of T-cell proliferation. *Immunology, 101*(4), 521-530.

Rainard, P. (1986). Bacteriostatic activity of bovine milk lactoferrin against mastitic bacteria. *Veterinary Microbiology, 11*(4), 387-392.

Rainard, P. (2003). The complement in milk and defense of the bovine mammary gland against infections. *Veterinary Research, 34*(5), 647-670.

Rainard, P. (2017). Mammary microbiota of dairy ruminants: fact or fiction? *Veterinary Research, 48*(25), 1-10.

Rainard, P., & Riollet, C. (2006). Innate immunity of the bovine mammary gland. *Veterinary Research, 37*(3), 369-400.

Raj, D., Brash, D. E., & Grossman, D. (2006). Keratinocyte apoptosis in epidermal development and disease. *Journal of Investigative Dermatology, 126*(2), 243-257.

Reece, W. O. (2013). *Functional anatomy and physiology of domestic animals*: John Wiley & Sons.

Regenhard, P., Petzl, W., Zerbe, H., & Sauerwein, H. (2010). The antibacterial psoriasin is induced by *E. coli* infection in the bovine udder. *Veterinary Microbiology, 143*(2), 293-298.

Regenhard, P., Leippe, M., Schubert, S., Podschun, R., Kalm, E., Grotzinger, J., & Looft, C. (2009). Antimicrobial activity of bovine psoriasin. *Veterinary Microbiology, 136*(3-4), 335-40.

Reiter, B. (1978). Antimicrobial systems in milk. *Journal of Dairy Research, 45*(1), 131-147.

Reiter, B., & Oram, J. (1967). Bacterial inhibitors in milk and other biological fluids. *Nature, 216*(5113), 328-330.

Reynolds, H. Y., Atkinson, J. P., Newball, H. H., & Frank, M. M. (1975). Receptors for immunoglobulin and complement on human alveolar macrophages. *Journal of Immunology, 114*(6), 1813-1819.

Rinaldi, M., Li, R. W., Bannerman, D. D., Daniels, K. M., Evock-Clover, C., Silva, M. V., Paape, M. J., Van Ryssen, B., Burvenich, C., & Capuco, A. V. (2010). A sentinel function for teat tissues in dairy cows: dominant innate immune response elements define early response to *E. coli* mastitis. *Functional & Integrative Genomics, 10*(1), 21-38.

Romani, N., Clausen, B. E., & Stoitzner, P. (2010). Langerhans cells and more: langerin-expressing dendritic cell subsets in the skin. *Immunological Reviews, 234*(1), 120-141.

Romani, N., Brunner, P. M., & Stingl, G. (2012). Changing views of the role of Langerhans cells. *Journal of Investigative Dermatology, 132*, 872-881.

Rossi, C., & Kiesel, G. (1977). Bovine immunoglobulin G subclass receptor sites on bovine macrophages. *American Journal of Veterinary Research, 38*(7), 1023-1025.

Sallmann, F. R., Baveye-Descamps, S., Pattus, F., Salmon, V., Branza, N., Spik, G., & Legrand, D. (1999). Porins OmpC and PhoE of *Escherichia coli* as specific cell-surface targets of human lactoferrin: Binding characteristics and biological effects. *Journal of Biological Chemistry, 274*(23), 16107-16114.

Sarikaya, H., Prgomet, C., Pfaffl, M., & Bruckmaier, R. (2004). Differentiation of leukocytes in bovine milk. *Milchwissenschaft, 59*(11-12), 586-589.

Sato, S., & Kiyono, H. (2012). The mucosal immune system of the respiratory tract. *Current Opinion in Virology, 2*(3), 225-232.

Schauber, J., & Gallo, R. L. (2008). Antimicrobial peptides and the skin immune defense system. *The Journal of Allergy and Clinical Immunology, 122*(2), 261-6.

Schittek, B., Hipfel, R., Sauer, B., Bauer, J., Kalbacher, H., Stevanovic, S., Schirle, M., Schroeder, K., Blin, N., & Meier, F. (2001). Dermcidin: a novel human antibiotic peptide secreted by sweat glands. *Nature Immunology, 2*(12), 1133-1137.

Schröder, J., & Harder, J. (2006). Antimicrobial skin peptides and proteins. *Cellular and Molecular Life Sciences, 63*(4), 469-486.

Schroder, K., Hertzog, P. J., Ravasi, T., & Hume, D. A. (2004). Interferon-γ: an overview of signals, mechanisms and functions. *Journal of Leukocyte Biology, 75*(2), 163-189.

Schukken, Y., Leslie, K., Barnum, D., Mallard, B., Lumsden, J., Dick, P., Vessie, G., & Kehrli, M. (1999). Experimental *Staphylococcus aureus* intramammary challenge in late lactation dairy cows: quarter and cow effects determining the probability of infection. *Journal of Dairy Science, 82*(11), 2393-2401.

Schultze, W., & Bright, S. (1983). Changes in penetrability of bovine papillary duct to endotoxin after milking. *American Journal of Veterinary Research, 44*(12), 2373-2375.

Schulze, W. X., & Usadel, B. (2010). Quantitation in mass-spectrometry-based proteomics. *Annual Review of Plant Biology, 61*, 491-516.

Schutyser, E., Struyf, S., & Van Damme, J. (2003). The CC chemokine CCL20 and its receptor CCR6. *Cytokine & Growth Factor Reviews, 14*(5), 409-26.

Schweizer, J., Bowden, P. E., Coulombe, P. A., Langbein, L., Lane, E. B., Magin, T. M., Maltais, L., Omary, M. B., Parry, D. A., Rogers, M. A., & Wright, M. W. (2006). New consensus nomenclature for mammalian keratins. *Journal of Cell Biology, 174*(2), 169-74.

Searle, B. C. (2010). Scaffold: a bioinformatic tool for validating MS/MS-based proteomic studies. *Proteomics, 10*(6), 1265-9.

Segal, A. W. (2005). How neutrophils kill microbes. *Annual Review of Immunology, 23*, 197.

Seguin, M. C., Klotz, F. W., Schneider, I., Weir, J. P., Goodbary, M., Slayter, M., Raney, J. J., Aniagolu, J. U., & Green, S. J. (1994). Induction of nitric oxide synthase protects against malaria in mice exposed to irradiated *Plasmodium berghei* infected mosquitoes: involvement of interferon gamma and CD8+ T cells. *The Journal of Experimental Medicine, 180*(1), 353-358.

Selman, L., Henriksen, M., Brandt, J., Palarasah, Y., Waters, A., Beales, P., Holmskov, U., Jørgensen, T., Nielsen, C., & Skjodt, K. (2012). An enzyme-linked immunosorbent assay (ELISA) for quantification of human collectin 11 (CL-11, CL-K1). *Journal of Immunological Methods, 375*(1), 182-188.

Senft, B., Meyer, F., & Hartmann, M. (1990). The importance of proteins of teat canal keratin as a complex defence system of the bovine mammary gland. *Milchwissenschaft, 45*(5), 295-298.

Seykora, A. J., & McDaniel, B. T. (1985). Udder and teat morphology related to mastitis resistance: a review. *Journal of Dairy Science, 68*(8), 2087-2093.

Sharma, R., & Gupta, R. (2010). Extracellular expression of keratinase Ker P from *Pseudomonas aeruginosa* in *E. coli*. *Biotechnology Letters, 32*(12), 1863-1868.

Sheldrake, R., Husband, A., & Watson, D. (1988). Origin of antibody-containing cells in the ovine mammary gland following intraperitoneal and intramammary immunisation. *Research in Veterinary Science, 45*(2), 156-159.

Simojoki, H., Hyvönen, P., Ferrer, C. P., Taponen, S., & Pyörälä, S. (2012). Is the biofilm formation and slime producing ability of coagulase-negative *staphylococci* associated with the persistence and severity of intramammary infection? *Veterinary Microbiology, 158*(3), 344-352.

Singh, K., Dobson, J., Phyn, C., Davis, S., Farr, V., Molenaar, A., & Stelwagen, K. (2005). Milk accumulation decreases expression of genes involved in cell–extracellular matrix communication and is associated with induction of apoptosis in the bovine mammary gland. *Livestock Production Science, 98*(1), 67-78.

Singh, P. K., Parsek, M. R., Greenberg, E. P., & Welsh, M. J. (2002). A component of innate immunity prevents bacterial biofilm development. *Nature, 417*(6888), 552-555.

Slade, H. B., & Schwartz, S. A. (1987). Mucosal immunity: the immunology of breast milk. *Journal of Allergy and Clinical Immunology, 80*(3), 348-358.

Smith, J. A. (1994). Neutrophils, host defense, and inflammation: a double-edged sword. *Journal of Leukocyte Biology, 56*(6), 672-686.

Smith, K. L., Todhunter, D., & Schoenberger, P. (1985). Environmental pathogens and intramammary infection during the dry period [1, 2]. *Journal of Dairy Science, 68*(2), 402-417.

Smolenski, G., Wieliczko, R., Pryor, S., Broadhurst, M., Wheeler, T., & Haigh, B. (2011). The abundance of milk cathelicidin proteins during bovine mastitis. *Veterinary Immunology and Immunopathology, 143*(1), 125-130.

Smolenski, G. A., Broadhurst, M. K., Stelwagen, K., Haigh, B. J., & Wheeler, T. T. (2014). Host defence related responses in bovine milk during an experimentally induced *Streptococcus uberis* infection. *Proteome Science, 12*(19), 1-14.

Sohnle, P. G., Hunter, M. J., Hahn, B., & Chazin, W. J. (2000). Zinc-reversible antimicrobial activity of recombinant calprotectin (migration inhibitory factor—related proteins 8 and 14). *Journal of Infectious Diseases, 182*(4), 1272-1275.

Sordillo, L., & Nickerson, S. (1988). Morphologic changes in the bovine mammary gland during involution and lactogenesis. *American Journal of Veterinary Research, 49*(7), 1112-1120.

Sordillo, L., Shafer-Weaver, K., & DeRosa, D. (1997). Immunobiology of the mammary gland. *Journal of Dairy Science, 80*(8), 1851-1865.

Sordillo, L. M., & Streicher, K. L. (2002). Mammary gland immunity and mastitis susceptibility. *Journal of Mammary Gland Biology and Neoplasia, 7*(2), 135-146.

Spencer, J., Isaacson, P. G., Diss, T. C., & MacDonald, T. T. (1989). Expression of disulfide-linked and non-disulfide-linked forms of the T cell receptor gamma/delta heterodimer in human intestinal intraepithelial lymphocytes. *European Journal of Immunology, 19*(7), 1335-8.

Spitznagel, J. K., & Shafer, W. M. (1985). Neutrophil killing of bacteria by oxygen-independent mechanisms: a historical summary. *Review of Infectious Diseases, 7*(3), 398-403.

Stacker, S. A., & Springer, T. A. (1991). Leukocyte integrin P150, 95 (CD11c/CD18) functions as an adhesion molecule binding to a counter-receptor on stimulated endothelium. *Journal of Immunology, 146*(2), 648-655.

Stefater, J. A., Ren, S., Lang, R. A., & Duffield, J. S. (2011). Metchnikoff's policemen: macrophages in development, homeostasis and regeneration. *Trends in Molecular Medicine, 17*(12), 743-752.

Steinbakk, M., Naess-Andresen, C., Fagerhol, M., Lingaas, E., Dale, I., & Brandtzaeg, P. (1990). Antimicrobial actions of calcium binding leucocyte L1 protein, calprotectin. *The Lancet, 336*(8718), 763-765.

Steinman, R., Hoffman, L., & Pope, M. (1995). Maturation and migration of cutaneous dendritic cells. *Journal of Investigative Dermatology, 105*(Suppl.), 2S-7S.

Stelwagen, K., Carpenter, E., Haigh, B., Hodgkinson, A., & Wheeler, T. (2009). Immune components of bovine colostrum and milk. *Journal of Animal Science, 87*(13 Suppl), 3-9.

Stout, R. D., & Suttles, J. (2004). Functional plasticity of macrophages: reversible adaptation to changing microenvironments. *Journal of Leukocyte Biology, 76*(3), 509-513.

Suh, H. J., & Lee, H. K. (2001). Characterization of a keratinolytic serine protease from *Bacillus subtilis* KS-1. *Journal of Protein Chemistry, 20*(2), 165-169.

Suzuki, T., Chow, C. W., & Downey, G. P. (2008). Role of innate immune cells and their products in lung immunopathology. *International Journal of Biochemistry and Cell Biology, 40*(6-7), 1348-61.

Takeichi, M. (1990). Cadherins: a molecular family important in selective cell-cell adhesion. *Annual Review of Biochemistry, 59*(1), 237-252.

Tam, C., Mun, J. J., Evans, D. J., & Fleiszig, S. M. (2012). Cytokeratins mediate epithelial innate defense through their antimicrobial properties. *Journal of Clinical Investigation, 122*(10), 3665-3677.

Tang, A., Amagai, M., Granger, L. G., Stanley, J. R., & Uddy, M. C. (1993). Adhesion of epidermal Langerhans cells to keratinocytes mediated by E-cadherin. *Nature, 361*, 82-85.

Tatarczuch, L., Philip, C., Bischof, R., & Lee, C. (2000). Leucocyte phenotypes in involuting and fully involuted mammary glandular tissues and secretions of sheep. *Journal of Anatomy, 196*(3), 313-326.

Tay, S. S., Roediger, B., Tong, P. L., Tikoo, S., & Weninger, W. (2014). The skin-resident immune network. *Current Dermatology Reports, 3*(1), 13-22.

Taylor, B. C., Choi, K. Y., Scibienski, R. J., Moore, P., & Stott, J. L. (1993). Differential expression of bovine MHC class II antigens identified by monoclonal antibodies. *Journal of Leukocyte Biology, 53*(5), 479-489.

Tetens, J., Friedrich, J. J., Hartmann, A., Schwerin, M., Kalm, E., & Thaller, G. (2010). The spatial expression pattern of antimicrobial peptides across the healthy bovine udder. *Journal of Dairy Science, 93*(2), 775-783.

Theander, T., Kharazmi, A., Pedersen, B., Christensen, L. D., Tvede, N., Poulsen, L., Odum, N., Svenson, M., & Bendtzen, K. (1988). Inhibition of human lymphocyte proliferation and cleavage of interleukin-2 by *Pseudomonas aeruginosa* proteases. *Infection and Immunity, 56*(7), 1673-1677.

Thewes, M. s., Stadler, R., Korge, B., & Mischke, D. (1991). Normal psoriatic epidermis expression of hyperproliferation-associated keratins. *Archives of Dermatological Research, 283*(7), 465-471.

Tlaskalová-Hogenová, H., Štěpánková, R., Hudcovic, T., Tučková, L., Cukrowska, B., Lodinová-Žádnıková, R., Kozáková, H., Rossmann, P., Bártová, J., & Sokol, D. (2004). Commensal bacteria (normal microflora), mucosal immunity and chronic inflammatory and autoimmune diseases. *Immunology Letters, 93*(2), 97-108.

Toulon, A., Breton, L., Taylor, K. R., Tenenhaus, M., Bhavsar, D., Lanigan, C., Rudolph, R., Jameson, J., & Havran, W. L. (2009). A role for human skin–resident T cells in wound healing. *The Journal of Experimental Medicine, 206*(4), 743-750.

Travis, J., Potempa, J., & Maeda, H. (1995). Are bacterial proteinases pathogenic factors? *Trends in Microbiology, 3*(10), 405-407.

Turner, C. W. (1952). *The mammary gland. I. The anatomy of the udder of cattle and domestic animals*. Columbia, Missouri: Lucas Brothers.

Turner, S.-A., Williamson, J. H., Lacy-Hulbert, S. J., & Hillerton, J. E. (2013). Relationship between previous history of *Streptococcus uberis* infection and response to a challenge model. *Journal of Dairy Research, 80*(3), 360-366.

Urmacher, C. (1990). Histology of normal skin. *The American Journal of Surgical Pathology, 14*(7), 671-686.

Usaite, R., Wohlschlegel, J., Venable, J. D., Park, S. K., Nielsen, J., Olsson, L., & Yates Iii, J. R. (2008). Characterization of global yeast quantitative proteome data generated from the wild-type and glucose repression *Saccharomyces cerevisiae* strains: The comparison of two quantitative methods. *Journal of Proteome Research, 7*(1), 266-275.

Valenti, P., & Antonini, G. (2005). Lactoferrin. *Cellular and Molecular Life Sciences, 62*(22), 2576.

Valladeau, J., & Saeland, S. (2005). *Cutaneous dendritic cells*. Seminars in Immunology: Elsevier.

Valladeau, J., Ravel, O., Dezutter-Dambuyant, C., Moore, K., Kleijmeer, M., Liu, Y., Duvert-Frances, V., Vincent, C., Schmitt, D., Davoust, J., Caux, C., Lebecque, S., & Saeland, S. (2000). Langerin, a novel C-type lectin specific to Langerhans cells, is an endocytic receptor that induces the formation of Birbeck granules. *Immunity, 12*(1), 71-81.

Van der Merwe, N. (1985). Some observations on the morphology of the bovine teat canal (*Ductus papillaris mammae*). *Journal of the South African Veterinary Association, 56*(1), 13-16.

van Hooijdonk, A., Kussendrager, K., & Steijns, J. (2000). In vivo antimicrobial and antiviral activity of components in bovine milk and colostrum involved in non-specific defence. *British Journal of Nutrition, 84*(S1), 127-134.

Van Nguyen, A., & Pollard, J. W. (2002). Colony stimulating factor-1 is required to recruit macrophages into the mammary gland to facilitate mammary ductal outgrowth. *Developmental Biology, 247*(1), 11-25.

van Zuijlen, P. P., Lamme, E. N., van Galen, M. J., van Marle, J., Kreis, R. W., & Middelkoop, E. (2002). Long-term results of a clinical trial on dermal substitution.: A light microscopy and Fourier analysis based evaluation. *Burns, 28*(2), 151-160.

Vangroenweghe, F., Dosogne, H., & Burvenich, C. (2002). Composition and milk cell characteristics in quarter milk fractions of dairy cows with low cell count. *Veterinary Journal, 164*(3), 254-260.

Vangroenweghe, F., Dosogne, H., Mehrzad, J., & Burvenich, C. (2001). Effect of milk sampling techniques on milk composition, bacterial contamination, viability and functions of resident cells in milk. *Veterinary Research, 32*(6), 565-579.

Veniaminova, N. A., Vagnozzi, A. N., Kopinke, D., Do, T. T., Murtaugh, L. C., Maillard, I., Dlugosz, A. A., Reiter, J. F., & Wong, S. Y. (2013). Keratin 79 identifies a novel population of migratory epithelial cells that initiates hair canal morphogenesis and regeneration. *Development, 140*(24), 4870-4880.

Venus, M., Waterman, J., & McNab, I. (2011). Basic physiology of the skin. *Surgery, 29*(10), 471-474.

Venzke, C. E. (1940). A histological study of the teat and gland cistern of the bovine mammary gland. *Journal of the American Veterinary Medical Association, 96*, 170-175.

Vesterinen, H. M., Corfe, I. J., Sinkkonen, V., Iivanainen, A., Jernvall, J., & Laakkonen, J. (2015). Teat morphology characterization with 3D imaging. *The Anatomical Record, 298*(7), 1359-1366.

Vignali, D. A., Collison, L. W., & Workman, C. J. (2008). How regulatory T cells work. *Nature Reviews in Immunology, 8*(7), 523-532.

Wagter, L., Mallard, B., Wilkie, B., Leslie, K., Boettcher, P., & Dekkers, J. (2000). A quantitative approach to classifying Holstein cows based on antibody responsiveness and its relationship to peripartum mastitis occurrence. *Journal of Dairy Science, 83*(3), 488-498.

Wallace, J. L., & Miller, M. J. (2000). Nitric oxide in mucosal defense: a little goes a long way. *Gastroenterology, 119*(2), 512-20.

Wang, Y., Sui, Y., Steel, J., Morris, J., & Berzofsky, J. (2013). Vaginal type-II mucosa acts as an inductive site during the generation of primary CD8+ T cell mucosal immune responses (P3186). *Journal of Immunology, 190*, 124.4.

Ward, P. P., Uribe-Luna, S., & Conneely, O. M. (2002). Lactoferrin and host defense. *Biochemistry and Cell Biology, 80*(1), 95-102.

Waseem, A., Dogan, B., Tidman, N., Alam, Y., Purkis, P., Jackson, S., Lalli, A., Machesney, M., & Leigh, I. M. (1999). Keratin 15 expression in stratified epithelia: downregulation in activated keratinocytes. *Journal of Investigative Dermatology, 112*(3), 362-369.

Washburn, M. P., Wolters, D., & Yates, J. R. (2001). Large-scale analysis of the yeast proteome by multidimensional protein identification technology. *Nature Biotechnology, 19*(3), 242-247.

Watanabe, T., Nagura, H., Keiichi, W., & Brown, W. R. (1984). The binding of human milk lactoferrin to immunoglobulin A. *FEBS letters, 168*(2), 203-207.

Watson, D., & Lascelles, A. (1973). Mechanisms of transfer of immunoglobulins into mammary secretion of ewes. *Australian Journal of Experimental Biology and Medical Science, 52*, 247-254.

Watt, F. (1989). Terminal differentiation of epidermal keratinocytes. *Current Opinion in Cell Biology, 1*(6), 1107-1115.

Wedemeyer, J., Tsai, M., & Galli, S. J. (2000). Roles of mast cells and basophils in innate and acquired immunity. *Current Opinion in Immunology., 12*(6), 624-31.

Weiss, T., Weber, L., Scharffetter-Kochanek, K., & Weiss, J. M. (2005). Solitary cutaneous dendritic cell tumor in a child: role of dendritic cell markers for the diagnosis of skin Langerhans cell histiocytosis. *Journal of the American Academy of Dermatology, 53*(5), 838-844.

Weisz-Carrington, P., Roux, M. E., McWilliams, M., Phillips-Quagliata, J. M., & Lamm, M. E. (1979). Organ and isotype distribution of plasma cells producing specific antibody after oral immunization: evidence for a generalized secretory immune system. *The Journal of Immunology, 123*(4), 1705-1708.

Wershil, B. K., & Furuta, G. T. (2008). Gastrointestinal mucosal immunity. *Journal of Allergy and Clinical Immunology, 121*(2 S2), S380-383.

Wessel, D., & Flügge, U. (1984). A method for the quantitative recovery of protein in dilute solution in the presence of detergents and lipids. *Analytical Biochemistry, 138*(1), 141-143.

Wheeler, T., Ledgard, A., Smolenski, G., Backmann, E., McDonald, R., & Lee, R. S.-F. (2012a). *Innate immune proteins as biomarkers for mastitis and endometritis*. Proceedings of the 5th Australasian Dairy Science Symposium. http://www.adssymposium.com.au/inewsfiles/ADSS_Final_Proceedings.pdf.

Wheeler, T., Smolenski, G., Harris, D., Gupta, S., Haigh, B., Broadhurst, M., Molenaar, A., & Stelwagen, K. (2012b). Host-defence-related proteins in cows' milk. *Animal, 6*(3), 415-422.

Whelehan, C. J., Meade, K. G., Eckersall, P. D., Young, F. J., & O'Farrelly, C. (2011). Experimental *Staphylococcus aureus* infection of the mammary gland induces region-specific changes in innate immune gene expression. *Veterinary Immunology and Immunopathology, 140*(3-4), 181-189.

Wijngaard, P., Metzelaar, M., MacHugh, N., Morrison, W., & Clevers, H. (1992). Molecular characterization of the WC1 antigen expressed specifically on bovine CD4-CD8-gamma delta T lymphocytes. *Journal of Immunology, 149*(10), 3273-3277.

Williams, D. M. D. (1984). *A study of the epithelium of the bovine teat canal.* Doctoral thesis, University of Melbourne.

Williams, T., & Morley, J. (1973). Prostaglandins as potentiators of increased vascular permeability in inflammation. *Nature, 246*(5430), 215.

Williamson, J., Woolford, M., & Day, A. (1995). The prophylactic effect of a dry-cow antibiotic against *Streptococcus uberis*. *New Zealand Veterinary Journal, 43*(6), 228-234.

Wynn, T. A., Chawla, A., & Pollard, J. W. (2013). Macrophage biology in development, homeostasis and disease. *Nature, 496*(7446), 445-455.

Xiong, X., Wu, T., & He, S. (2013). Physical forces make rete ridges in oral mucosa. *Medical Hypotheses, 81*(5), 883-886.

Xuan, W., Qu, Q., Zheng, B., Xiong, S., & Fan, G.-H. (2015). The chemotaxis of M1 and M2 macrophages is regulated by different chemokines. *Journal of Leukocyte Biology, 97*(1), 61-69.

Yoo, B.-C., Aoki, K., Xiang, Y., Campbell, L. R., Hull, R. J., Xoconostle-Cázares, B., Monzer, J., Lee, J.-Y., Ullman, D. E., & Lucas, W. J. (2000). Characterization of *Cucurbita maxima* Phloem Serpin-1 (CmPS-1): A developmentally regulated elastase inhibitor. *Journal of Biological Chemistry, 275*(45), 35122-35128.

Zambare, V., Nilegaonkar, S., & Kanekar, P. (2007). Production of an alkaline protease by *Bacillus cereus* MCM B-326 and its application as a dehairing agent. *World Journal of Microbiology and Biotechnology, 23*(11), 1569-1574.

Zhang, Y., Fonslow, B. R., Shan, B., Baek, M.-C., & Yates III, J. R. (2013). Protein analysis by shotgun/bottom-up proteomics. *Chemical Reviews, 113*(4), 2343-2394.

Zhao, X., & Lacasse, P. (2008). Mammary tissue damage during bovine mastitis: causes and control. *Journal of Animal Science, 86*(13_suppl), 57-65.

Zou, S., Magura, C., & Hurley, W. (1992). Heparin-binding properties of lactoferrin and lysozyme. *Comparative Biochemistry and Physiology Part B: Comparative Biochemistry*, *103*(4), 889-895.

Zwadlo, G., Bröcker, E., Von Bassewitz, D., Feige, U., & Sorg, C. (1985). A monoclonal antibody to a differentiation antigen present on mature human macrophages and absent from monocytes. *Journal of Immunology*, *134*(3), 1487-1492.